**DAVID BARBOSA MEDEIROS**

# ON THE ROLES OF ORGANIC ACIDS TRANSPORT AND SUCROSE METABOLISM CONTROLLING STOMATAL MOVEMENTS

Thesis presented to the Federal University of Viçosa as part of the requirements of the Plant Physiology Graduate Program for obtaining the *Doctor Scientiae* degree.

**VIÇOSA**
**MINAS GERAIS – BRASIL**
**2017**

**Ficha catalográfica preparada pela Biblioteca Central da Universidade Federal de Viçosa - Campus Viçosa**

T

M488o
2017

Medeiros, David Barbosa, 1989-
On the roles of organic acids transport and sucrose metabolism controlling stomatal movements : . / David Barbosa Medeiros. - Viçosa, MG, 2017.
x, 130f. : il. (algumas color.) ; 29 cm.

Orientador: Wagner Luiz Araújo.
Tese (doutorado) - Universidade Federal de Viçosa.
Inclui bibliografia.

1. Plantas - Metabolismo. 2. *Arabidopsis*. 3. Estômatos. 4. Sacarose. 5. Fisiologia vegetal. I. Universidade Federal de Viçosa. Departamento de Biologia Vegetal. Programa de Pós-graduação em Fisiologia Vegetal. II. Título.

CDD 22 ed. 572.472

**DAVID BARBOSA MEDEIROS**

# ON THE ROLES OF ORGANIC ACIDS TRANSPORT AND SUCROSE METABOLISM CONTROLLING STOMATAL MOVEMENTS

Thesis presented to the Federal University of Viçosa as part of the requirements of the Plant Physiology Graduate Program for obtaining the *Doctor Scientiae* degree.

APPROVED: July 19th, 2017.

Dimas Mendes Ribeiro

Samuel Cordeiro Vitor Martins

Danilo de Menezes Daloso

Adriano Nunes Nesi
(Co-advisor)

Wagner Luiz Araújo
(Advisor)

## ACKNOWLEDGMENTS

I would like to thank the Universidade Federal de Viçosa (UFV), mainly to the Plant Physiology Graduate Program, for the support and for providing me all conditions required during the development of my research. I am also grateful to the scholarships provided by CAPES (Coordination for the Improvement of Higher Level Personnel) and FAPEMIG (Foundation for Research Assistance of the Minas Gerais State).

I sincerely thank my supervisor Prof. Wagner Araújo for his guidance and support. Wagner, I was very lucky to be part of your starting team at the UFV. I need to say thank you very much for your supervision and friendship always encouraging me to be a better scientist.

I also want to thank Prof. Dr. Alisdair R. Fernie for his great support and for giving me the opportunity to spend one year in his lab at the Max-Planck-Institut für Molekulare Pflanzenphysiologie – MPI-MP (Potsdam, Germany), where I was able to deepen my knowledge in plant metabolism and molecular biology.

I am also grateful to Prof. Danilo Daloso for his amazing support and help during the development of this work.

I would like to thank Prof. Adriano Nunes Nesi and Prof. Fábio DaMatta for their co-supervision and for helping me with discussions and advices for this thesis.

I want to thank the other members of my evaluation committee Prof. Dimas Ribeiro and Prof. Samuel Martins which all the criticisms were invaluable to improve this work.

To all my colleagues from the "UCP group", former and current members, for the pleasant working atmosphere and for all the help provided in the lab. Special thanks go to Ítalo Antunes, Ivan Corrêa, Jéssica Barros, Joao Henrique Cavalcanti, Jorge Condori, Luiz Valente, Rebeca Omena, and William Silva for their friendship and assistance in this work.

To people at the MPI-MP, mainly those at AG Fernie for including me in this incredible group. Special thanks to Ina Krahnert, Dr. Leonardo Perez, Regina Wenderburg, Dr. Saleh Alseekh, Prof. Takayuki Tohge, Prof. Toshihiro Obata, and Dr. Youjun Zhang for all support in the lab and help during data analysis. I am indebted to Dr. Laíse Rosado who friendship made my days in Germany lighter. Thanks Laíse for all the help during my stay and for listening patiently my "comments" about life during our afternoon breaks. Also, thanks to Dr. Stéphanie Arrivault (AG Stitt) for her friendship and help in the lab. I also would like to thank members of the Green team at the MPI-MP, especially Sven Roigk for being always helpful and for their amazing work on producing high-quality plant material for my experiments.

I also express here my gratitude to all the professors, technicians, and colleagues at the Plant Physiology Graduate Program for the support. I would like to say very special thanks to my friends who started together in the master course, always supporting each other. Namely, Adinan Alves, Amanda Ávila, Fernanda Vidal, and Rebeca Omena. I am sure without these wonderful people my time throughout this graduate journey would be harder. We made it folks!

Many thanks for all other people who in some way had ever helped or supported me during my doctoral studies and whose names are not mentioned here.

Last, but by no means least, I sincerely would like to express my gratitude to my family. My parents Fátima and João Gualberto de Medeiros and my siblings Cláudia, Paula, and Tiago which although more than 2,000 km far away from me were always supportive, believing in my capacity sometimes even more than I did.

## BIOGRAPHY

David Barbosa Medeiros, son of João Gualberto de Medeiros Neto and Maria de Fátima Barbosa Medeiros, was born in Aracati, Ceará state, Brazil, on July 28$^{th}$, 1989.

In 2006, he started the undergraduate course in Agronomy at the Federal Rural University of Pernambuco, Recife, Pernambuco state, Brazil and achieved the bachelor degree in December 2011. In March 2012, he started his Master course at the Federal University of Viçosa (UFV), achieving the Master degree in Plant Physiology in July 2013. In the same year, he started his doctoral studies at the UFV. From July 2016 to June 2017 he developed part of his research as a guest PhD student at the Max-Planck-Institut für Molekulare Pflanzenphysiologie, Potsdam, Brandenburg state, Germany, under the supervision of Prof. Dr. Alisdair R. Fernie before finishing his doctoral studies in Plant Physiology at UFV under the supervision of Prof. Wagner L. Araújo.

## TABLE OF CONTENTS

## ABSTRACT

MEDEIROS, David Barbosa, D.Sc., Universidade Federal de Viçosa, July, 2017. **On the roles of organic acids transport and sucrose metabolism controlling stomatal movements**. Advisor: Wagner L. Araújo. Co-advisors: Adriano Nunes Nesi and Fábio Murilo da Matta.

Regulation of the stomatal movements by osmotic control is a well-documented mechanism that is associated to the transport of solutes coupled with changes in the guard cell metabolism. Potassium and chloride are the main inorganic ions whereas malate and sucrose (Suc) are the main organic osmolytes involved in stomatal movements. Despite the growing body of information concerning the control of stomatal movements, there are, however, several gaps regarding the stomata regulation to be fully elucidated. Thus, understanding stomatal behaviour represents an important step towards enhancement of water use efficiency in plants. Several efforts have been performed to fully characterize the events that occur in guard cells. Experimental data describing distinct aspects of stomatal behaviour have been presented, providing significant insights into guard cell transcriptome, proteome, and metabolome. In this thesis I, initially, revisited the current available omics studies and modelling in guard cells. By doing that, it was possible to demonstrate that the current modelling approaches describe the stomatal conductance in terms of relatively few easy-to-measure variables being unsuitable for *in silico* design of genetic manipulation. Therefore, we discuss that system biology approach combining modelling and high-throughput assays may be used to elucidate the mechanisms underlying stomatal control allowing a better prediction of phenotypes in the field. Additionally, to obtain a more comprehensive picture of the function of organic acid transport and sucrose metabolism during stomatal movements, three independent but complementary experimental approaches were used to: (*i*) characterise mutant plants lacking the organic acids channel located at the guard cell plasma membrane (*At*QUAC1); (*ii*) analyse the effects on stomatal behaviour, photosynthetic capacity, and the metabolism due to impaired malate and fumarate accumulation in Arabidopsis leaves; (*iii*) to investigate the effects of sucrose on the stomatal aperture and the carbon flux during stomatal opening by using stomatal aperture assays and isotope labelling kinetic experiments. Briefly, the results presented here provided several novel findings. Firstly, the inefficient stomatal closure via the repression of *At*QUAC1 culminates in higher growth and photosynthetic rates through increased mesophyll and stomatal conductance, followed by changes in organic acids and sugars accumulation in leaves. Secondly, impaired malate and fumarate accumulation throughout the diel cycle in *attdt* mutants strongly affected mitochondrial metabolism but not plant growth without any impact in both stomata kinetics and photosynthesis. Thirdly, the role

of sucrose during stomatal opening was demonstrated to be dose-dependent whilst sucrose is degraded within guard cells during light-induced stomatal opening. Collectively, the results obtained here demonstrate the complex interaction between guard cells and mesophyll and also highlight the role of the mesophyll metabolism as an important player controlling guard cell movements. I further discuss these observations in the context of the current knowledge concerning the metabolic control of stomatal movements, central carbon metabolism, and plant performance.

## RESUMO

MEDEIROS, David Barbosa, D.Sc., Universidade Federal de Viçosa, julho de 2017. **Papeis do transporte de ácidos orgânicos e do metabolismo de sacarose controlando os movimentos estomáticos**. Orientador: Wagner L. Araújo. Coorientadores: Adriano Nunes Nesi e Fábio Murilo da Matta.

A regulação dos movimentos estomáticos devido ao controle osmótico das células-guarda é um mecanismo bem caracterizado e associado com transporte de solutos e alterações no metabolismo dessas células. Potássio e cloreto são os principais íons inorgânicos, enquanto malato e sacarose são os principais osmólitos orgânicos envolvidos nos movimentos estomáticos. No entanto, apesar do aumento de informações referentes ao controle dos estômatos, ainda existem questões sem respostas sobre a regulação estomática. Assim, o entendimento do comportamento estomático representa um passo importante para aumentar a eficiência no uso da água em plantas. Muitos esforços vêm sendo feitos para caracterizar completamente os eventos que ocorrem durante os movimentos estomáticos. Dados experimentais sobre diferentes aspectos das células-guarda têm sido apresentados e o conhecimento do transcriptoma, proteoma e metaboloma dessas células aumentado consideravelmente. Nesta tese, inicialmente, apresenta-se uma revisão dos estudos utilizando tecnologias de ômicas e modelagem em células-guarda. Foi possível demonstrar que os estudos de modelagem atuais descrevem condutância estomática em termos de variáveis medidas de forma relativamente simples, não sendo usuais para a manipulação genética de modo geral. Portanto, acredita-se que uma abordagem de biologia de sistema combinada com modelagem e utilização de tecnologia de ômicas pode ser utilizada para elucidar os mecanismos subjacentes ao controle dos estômatos e predizer melhor fenótipos em condições de campo. Para compreender melhor as funções do transporte de ácidos orgânicos e do metabolismo de sacarose durante os movimentos estomáticos, três abordagens experimentais foram adotadas para: (*i*) caracterizar plantas perdendo um canal de ácidos orgânicos localizado na membrana plasmática de células-guarda (*At*QUAC1); (*ii*) analisar os efeitos no comportamento estomático, capacidade fotossintética e metabolismo devido ao prejuízo no acúmulo de malato e fumarato em folhas de Arabidopsis; (*iii*) investigar os efeitos da sacarose na abertura estomática e o fluxo de carbono durante a abertura dos estômatos, usando ensaios de abertura estomática e de cinética de marcação isotópica. Brevemente, os resultados apresentados fornecem novas descobertas, primeiro, a ineficiência do fechamento estomático via repressão de *At*QUAC1 resulta em maior crescimento e atividade fotossintética devido à aumentos nas condutâncias estomática e mesofílica. Segundo, prejuízos no acúmulo de malato e fumarato durante o ciclo diurno em mutantes *attdt* afeta o metabolismo mitocondrial, porém

sem consequências para o movimento dos estômatos e fotossíntese. Terceiro, o efeito da sacarose na abertura dos estômatos é dose dependente e a mesma é degradada durante a abertura estomática induzida por luz. Coletivamente, os resultados demonstram a complexidade das interações células-guarda/mesofilo e destacam o papel do metabolismo do mesofilo como um fator importante controlando células-guarda. Essas observações são discutidas no contexto do conhecimento atual acerca do controle metabólico dos movimentos estomáticos, metabolismo central do carbono e performance vegetal.

# Chapter 1

# General introduction

## 1. General introduction

Stomata, microscopic pores surrounded by two specialized cells known as guard cells in the epidermis of leaves, control the essential exchange of $CO_2$ concomitantly with transpiration in land plants. Although plants are in constant need of sufficient quantities of $CO_2$ to maintain their photosynthetic rates, the water losses associated with the $CO_2$ entry must be also strictly regulated to prevent dehydration and the subsequent unfavourable changes of the metabolic state that it invokes. Accordingly, the majority of the water lost via transpiration and $CO_2$ absorption for that matter, occurs through stomatal pores rendering the stomata as the main control point, which regulates the flow of gases between plants and atmosphere (Schroeder et al., 2001; Lawson et al., 2014).

For over a century, guard cells have been extensively studied and considerable efforts have been made to better understand their structure, development, physiology, and metabolism (Bergmann and Sack, 2007; Mott, 2009; Berry et al., 2010; Casson and Hetherington, 2010; Kim et al., 2010; Dow and Bergmann, 2014; Daloso et al., 2016; Santelia and Lawson, 2016). In addition, the relative ease of guard cells isolation has facilitated experimental interrogation contributing to the increase in their understanding much more than other plant cell types. These advances have rendered the guard cell as one of the best studied plant cell models for membrane transport, signalling, and homeostasis (Blatt, 2000; Hetherington and Brownlee, 2004; Israelsson et al., 2006; Hills et al., 2012; Engineer et al., 2016).

It has been recently demonstrated that the relationship between stomatal aperture and photosynthesis/transpiration is linear over a wide range of environmental conditions (Gago et al., 2016). Moreover, it has been suggested that improvement of C3 photosynthesis can be achieved by modifying stomatal behaviour (Lawson et al., 2014; Flexas, 2016). Therefore, a better understanding of stomatal regulation and how it is influenced by the surrounding mesophyll cells and environmental stimuli represents an important step for developing plants in which water use efficiency (WUE) is enhanced (Gago et al., 2014; Lawson et al., 2014; Flexas, 2016; Nunes-Nesi et al., 2016).

Although stomatal pores are structurally simple, the surrounding guard cells are one of the most specialized cell in land plants (Bergmann and Sack, 2007). They are morphologically distinguished from other epidermal cells and possess a complex signal transduction network, tightly regulated membrane ion system, and specialized metabolic pathways, modulating guard cell turgor, subsequently, promoting the stomatal opening and closure (Santelia and Lawson, 2016). Generally speaking, the stomatal pores open in response to increases in guard cell volume driven by decreases in the water potential of the guard cell as result of the

osmolytes accumulation and subsequently water influx. Conversely, during stomatal closure, an efflux of osmolytes from guard cells is required with an associated increase in guard cell water potential and in turn efflux of water (Assmann and Wang, 2001). Potassium ($K^+$) and chloride ($Cl^-$) act as the main inorganic ions, while malate$^{2-}$ and sucrose (Suc) are considered as the main organic osmolytes during stomatal movements (Roelfsema and Hedrich, 2005; Vavasseur and Raghavendra, 2005; Kollist et al., 2014). The main aim of this thesis is focused on better understanding the roles of organic acids and Suc on the stomatal regulation, thus in the following two sections I briefly review the current knowledge regarding the transport and metabolism of malate and sucrose in guard cells and to which extent it affects stomatal movements.

### *1.1.Roles of the malate transport and metabolism for stomatal function*

Organic acids, mainly malate, have long been suggested as key regulators mechanistically involved in the guard cell response to environmental stimuli (Van Kirk and Raschke, 1978; Hedrich and Marten, 1993; Hedrich et al., 1994; Fernie and Martinoia, 2009; Araújo et al., 2011). Accordingly, malate is often discussed as one of the main organic osmoregulators in guard cells (Fernie and Martinoia, 2009). During stomatal opening, the accumulation of malate inside the guard cells occur based mainly on its influx via a specific transporter at the plasma membrane or as a product of the starch breakdown or anaplerotic $CO_2$ fixation (Lee et al., 2008; Daloso et al., 2015; Horrer et al., 2016). Malate acts as an osmoregulator and counter ion for $K^+$ in guard cells allowing the entrance of water and ultimately, stomatal opening. Moreover, it has also been suggested that malate can act as a signalling metabolite during stomatal opening, since cytosolic malate accumulation increases the currents through Aluminium-activated malate transporter (ALMT) members (De Angeli et al., 2013). On the other hand, during stomatal closure, previously accumulated malate can be metabolized, partially converted into starch, and released into the apoplastic space (Van Kirk and Raschke, 1978; Penfield et al., 2012; Lawson et al., 2014).

Over the last decade, three protein families were identified and functionally characterized to be involved in the transport of malate at the guard cell plasma membrane and at the tonoplast (Emmerlich et al., 2003; Lee et al., 2008; Meyer et al., 2010; Sasaki et al., 2010; Meyer et al., 2011). The transporter *At*ABCB14, a member of the ABC (*A*TP *B*inding *C*assette) family, is responsible for the transport of malate from the apoplast into guard cells (Lee et al., 2008). This transporter was described as a negative modulator of stomatal closure induced by high $CO_2$ concentrations, supporting the assumption that malate acts as a $CO_2$ response regulator (Hedrich et al., 1994). It has also been proposed that *At*ABCB14 is able to

transport auxin (Kaneda et al., 2011). Therefore, further studies aiming to determine the substrate specificity of this transporter will be required to confirm its real contribution to the stomatal movements and/or auxin-related processes. Additionally, a member of the ALMT family, *At*ALMT12/*At*QUAC1 (Quick activating Anion Channel 1), was identified and characterized as an ABA-dependent anion-selective channel responsible for the efflux of malate from guard cells to the apoplast during the stomatal closure in a voltage-dependent manner (Meyer et al., 2010; Sasaki et al., 2010; Mumm et al., 2013). It was further showed that the SnR kinase OST1 (Open Stomata 1), besides *At*SLAC1 (Slow anion channel 1), can also phosphorylate *At*QUAC1, providing the link between ABA signalling and malate transport (Imes et al., 2013). Furthermore, the functional lack of *At*QUAC1 resulted in an impaired stomatal closing kinetics in response to dark and high $CO_2$ levels and reduced ABA-induced stomatal closure coupled with changes in the organic acid accumulation as well as increases in both stomatal and mesophyll conductance (Meyer et al., 2010; Medeiros et al., 2016).

The vacuolar malate transport has also been characterized and the *t*onoplast *D*icarboxylate *T*ransporter (*At*tDT) was proposed to be the main transport system at the tonoplast being required for the proper accumulation of malate in Arabidopsis leaves (Emmerlich et al., 2003; Hurth et al., 2005), although its functional role in guard cells during stomatal movements remains unclear. Another ALMT member, *At*ALMT6, is involved in the malate transport being highly expressed at the vacuolar membrane of guard cells and regulated by cytosolic pH and malate concentrations (Meyer et al., 2011). These two cellular features modulate the tonoplast potential and thus determine the functionality of *At*ALMT6, as a malate influx or efflux channel. Intriguingly, despite *atalmt6* knockout plants displaying reduced malate current in isolated vacuoles when compared to WT, no differences in stomatal behaviour were observed, suggesting the possible redundancy in the malate transport at the tonoplast (Meyer et al., 2011).

Although less characterized, the organic acid metabolism inside the guard cells has also been reported to be involved in the regulation of stomatal function. During stomatal opening, the cytosolic phospho*enol*pyruvate carboxylase (PEPc) can catalyse the carboxylation of phospho*enol*pyruvate (PEP) yielding oxaloacetate (OAA), which is further reduced to malate via $NAD^+$-Malate dehydrogenase ($NAD^+$-MDH). Evidences supporting this pathway came from earlier studies with transgenic potato (*Solanum tuberosum*) plants in which PEPc activity was decreased and displayed a delay in the stomatal opening, whilst plants with increased PEPc activity exhibited faster stomatal opening (Gehlen et al., 1996). The operation of PEPc in tobacco (*Nicotiana tabacum*) guard cells during light-induced

stomatal opening was further supported by metabolic flux evaluation. The $^{13}C$ enrichment from $^{13}C$-$NaHCO_3$ into malate and fumarate increased to a much greater extent than that for succinate, suggesting that the label is being initially incorporated into OAA through PEPc, following the malate and fumarate production by $NAD^+$-MDH and fumarase, respectively (Daloso et al., 2015). During stomatal closing malate is potentially metabolized through NADP-Malic enzyme (NADP-ME), the TCA cycle, and gluconeogenesis (Santelia and Lawson, 2016). Indeed, NADP-ME was confirmed to be expressed in guard cells (Wheeler et al., 2005). Tobacco plants overexpressing NADP-ME from maize displayed decreased stomatal conductance and gained more fresh mass per unit of water consumed, but they were similar to the wild type in their growth (Laporte et al., 2002). Furthermore, loss of function of phosphoenolpyruvate carboxykinase 1 (*PCK1*), a key enzyme in the first steps of the gluconeogenesis that is responsible to convert OAA into PEP, resulted in a lower tolerance to drought, increased stomatal aperture, and conductance, as well as lower response to darkness in Arabidopsis plants (Penfield et al., 2012). These results suggest a role for NADP-ME and PCK1 in the mechanism by which stomata are closed and present a potential mechanism for genetically engineering plant with higher WUE.

Further evidences supporting the involvement of leaf organic acid metabolism on stomata movements were demonstrated. For instance, increased stomatal conductance and photosynthesis mediated by organic acid effect on guard cells of tomato (*Solanum lycopersicum* L.) plants with constitutively reduced expression of *SlSDH2-2*, which encodes the iron-sulphur subunit of succinate dehydrogenase (Araújo et al., 2011). Importantly, no effects were observed when the antisense construction for *SISDH2-2* was expressed under the control of the guard cell specific *MYB60* promoter (Araújo et al., 2011). By contrast, the constitutive inhibition of the mitochondrial fumarase in tomato plants decreased photosynthesis as a result of impaired stomatal function (Nunes-Nesi et al., 2007).

It has also been shown that the apoplastic malate concentrations rise on average from 1.0 to 3.1 mM in response to high $CO_2$ levels, which is able to activate R-type anion channels at the plasma membrane (Hedrich et al., 1994). These findings associated with those obtained for *At*ABCB14 and *At*QUAC1 provide strong evidence that the malate apoplastic concentration is an important player driving stomatal movements. When considered together, these studies, and the others discussed above, provide compelling evidence for a mechanism whereby organic acids, and particularly malate, can modulate stomatal function. Furthermore, they are in good agreement with the absence of guard cell autonomous control, but rather, further demonstrate that the mesophyll cells play a significant control over stomatal function.

*1.2. Sucrose: dual role in guard cells*

Due to the Suc osmotic proprieties, it has been reported since early 80´s as a key osmotic source in guard cells during the light-induced stomatal opening (Outlaw and Manchester, 1979). It was lately proposed that Suc has an important role as additional osmolyte, besides $K^+$, for stomatal opening (Talbott and Zeiger, 1993, 1996). These authors, then, proposed a model in which both $K^+$ and sucrose contribute to guard cell osmoregulation, but in two temporal phases throughout the day. Whereas $K^+$ is quickly increased during stomatal opening and together with its counter ions provide the osmotic control required in the early morning. Suc levels increase and replace $K^+$ later in the day (afternoon phase) (Talbott and Zeiger, 1998). Although these observations greatly fit with the proposed theory, the effect of Suc inducing the stomatal opening was not directly tested at that time. Furthermore, those finding were observed in epidermal peels from *Vicia faba* having not been reproduced in other species or growth conditions, therefore cannot be generalized (Daloso et al., 2016).

Starch breakdown, Calvin-Benson cycle, and transport from the apoplast are the three pathways commonly reported as the main sources of sucrose in guard cells. Although, evidences exist for all of them, it seems that Suc transport from the apoplastic space is more important than Suc catabolism and photosynthetic activity in guard cells (Santelia and Lawson (2016) and references therein). The Suc uptake from the surrounding apoplastic space occurs directly via sucrose-$H^+$ symporters or as glucose and fructose via hexoses-$H^+$ symporters, after Suc cleavage into hexoses mediated by cell wall invertases (Daloso et al., 2016). Transcriptome studies have also revealed that several genes encoding sucrose or hexoses transporters are highly expressed in guard cells in comparison to mesophyll cells. For instance, SUCROSE-PROTON SYMPORTER 1 (SUC1), SUC2, and SUC3 are the major Suc/$H^+$ cotransporters at the guard cell plasma membrane, whereas SUGAR TRANSPORT 1 (STP1) and STP2 are mainly related to the transport of monosaccharide/$H^+$ symport (Stadler et al., 2003; Leonhardt et al., 2004; Meyer et al., 2004; Wang et al., 2011; Bates et al., 2012; Bauer et al., 2013). Curiously, STP1 is mainly expressed during the dark, but it presents an expression peak at midday (Stadler et al., 2003), suggesting that the sugar transport is highly required at this time, in which guard cells accumulate high amount of sugars (Talbott and Zeiger, 1996).

The role of Suc as a link between mesophyll and guard cells, connecting the photosynthesis and transpiration has been recently reported (Kang et al., 2007; Kelly et al., 2013; Lugassi et al., 2015; Gago et al., 2016). The mechanism by which changes in Suc levels result in stomatal closure is not completely understood, but it is known as a transpiration-

linked and photosynthesis-dependent process (Kang et al., 2007). However, it was suggested as a phloem loader species exclusive mechanism, given that accumulation of metabolites in the apoplast of simplastic loader species occurs in a much lower rate, being not able to produce the osmotica required to quickly affect the stomatal movements (Kang et al., 2007). Later on, an alternative mechanism has been proposed in which hexokinase (HXK) appears as an important player linking the ABA signalling and mesophyll-derived Suc stomatal closure induction (Kelly et al., 2013). HXK, a sugar-phosphorylating enzyme involved in sugar-sensing, is able to mediate stomatal closure by coordinating photosynthesis and transpiration in both Arabidopsis and tomato. High exogenous concentration of sucrose (100 mM) can induce stomatal closure in a mechanism mediated by both ABA and HXK (Kelly et al., 2013). Furthermore, the expression of the Arabidopsis *HXK1* in citrus under the control of the guard cell-specific promoter *KST1* (inward rectifying $K^+$ channel) culminated with reduced stomatal conductance and transpiration without impairments on photosynthetic rates (Lugassi et al., 2015). These data support the contention of a photosynthesis mediated feedback inhibition for stomatal conductance/transpiration. Therefore, throughout the day when Suc is highly produced in the mesophyll and exceeds the phloem loading, it is carried out to the apoplastic space near the guard cell via transpiration stream and stimulate the stomatal closure in a HXK-dependent process, reducing water loss, when photosynthesis is highly activated (Kelly et al., 2013). This hypothesis is further supported by the recent multispecies meta-analysis which demonstrated an opposite correlation between Suc content in leaves and stomatal conductance (Gago et al., 2016).

An additional role for Suc as a glycolytic and respiratory substrate for mitochondrial energy demand and carbon skeleton production during the light- and $K^+$-induced stomatal opening has been recently proposed. This hypothesis arises from compelling studies showing that antisense inhibition of sucrose synthase 3 (SuSy 3) in potato culminated with lower stomatal conductance, whereas the overexpression of the *SUC2* gene from yeast, encoding the acid invertase specifically in guard cells, led to higher stomatal conductance (Antunes et al., 2012). Moreover, the guard cell-specific overexpression of SuSy3, led to increases in stomatal aperture and stomatal conductance, transpiration, photosynthesis, and growth (Daloso et al., 2016). Additionally, Suc degradation seems to occur during the light-induced stomatal opening in order to also provide carbon skeleton for organic acid production (Daloso et al., 2015). Indeed, [U-$^{13}$C]-$NaHCO_3^-$ isotope labelling experiment revealed enhanced $^{13}$C enrichment into malate after sucrose breakdown specifically when $K^+$ was present in the medium (Daloso et al., 2015), suggesting an increased demand for ATP and/or malate accumulation. These findings further support the idea that sucrose breakdown is a required

mechanism to stimulate mitochondrial metabolism during stomatal opening (Daloso et al., 2016). Although these results are in accordance with this hypothesis, whether Suc is degraded during light-induced stomatal opening is still a matter of debate and it has not been directly examined yet.

Taken together, the studies above reviewed suggest that guard cell Suc metabolism and transport has a key role on the regulation of stomata movements. Furthermore, Suc might have a dual role during the stomatal movements, since its accumulation in the apoplastic space can induce stomatal closure and its degradation within guard cells seems to be an important mechanism for both light- and $K^+$-induced stomatal opening and stomatal closure in a process mediated by HXK and ABA. It seems reasonable to assume that the role of Suc is far more complex than previously thought; therefore, more studies regarding its metabolism and transport within guard cells are required to fully elucidate the paradoxical role of Suc on the stomata function.

### *1.3. Layout and aims of the chapters*

This thesis is largely focused on the role of organic acid transport and sucrose metabolism during stomatal movements. That said, the main aims of this work were; *(i)* obtain a comprehensive picture of how and to which extent impairments in the organic acid transport might affect stomatal movements; *(ii)* provide experimental evidences for the role of sucrose as a substrate required during the light-induced stomatal opening. In order to reach these goals several different but complementary experimental approaches were taken and therefore this thesis is organized as a compilation of four independent stand-alone chapters. In each chapter an introduction and discussion as well as details of the methods used are included. At the end of the thesis, the chapter entitled “Concluding Remarks” synthesizes the main findings of this work and a brief discussion about the challenges and perspectives in understanding guard cells function is presented.

## Chapter 2. Utilizing systems biology to unravel stomatal function and the hierarchies underpinning its control

Although the guard cell has been used as a model for characterization of signalling pathways, several important questions about its functioning remain elusive. Current modelling approaches describe the stomatal conductance in terms of relatively few easy-to measure variables being unsuitable for in silico design of genetic manipulation strategies. In this chapter, the current studies using omics technologies in guard cells are reviewed and we argue that a system biology approach, combining modelling and high-throughput experiments, may

be used to elucidate the mechanisms underlying stomata control and to identify targets for modulation of stomatal responses to environment.

**Chapter 3. Enhanced photosynthesis and growth in *atquac1* knockout mutants are due to altered organic acid accumulation and increase in both stomatal and mesophyll conductance**

Despite a vast number of studies regarding the nature and kinetic of the transporters and channels in guard cells, little information concerning the metabolic changes caused by their impairment is currently available. Such information is of pivotal significance to understand stomatal movements, mainly considering that organic acids, especially the levels of malate in apoplastic/mesophyll cells, have been highlighted to play a key role within the leaf metabolism. In the chapter 3 a detailed physiological and metabolic characterization of mutant plants lacking *At*QUAC1 was performed. *At*QUAC1 is a R-type anion channel at the guard cell plasma membrane characterized so far being already described as involved in the regulation of the stomatal closure in Arabidopsis.

**Chapter 4. Impaired malate and fumarate accumulation due to the lack of *At*tDT strongly impacts mitochondrial metabolism, but does not affect stomatal behaviour**

The vacuolar malate transport has been characterized at molecular level and it is performed by at least one carrier protein and two channels in Arabidopsis. The absence of the *Arabidopsis thaliana* tonoplast Dicarboxylate Transporter (*At*tDT) in *attdt* knockout plants was associated with decreased malate and fumarate accumulation in the leaves. In this chapter we investigated in details how this impaired accumulation of organic acids in leaves affect the stomatal behaviour and photosynthetic capacity as well as its putative metabolic impacts in plants not only in whole rosettes but also in isolated guard cells.

**Chapter 5. Guard cell sucrose degradation promotes glycolysis and the TCA cycle during stomatal opening**

For decades sucrose has been thought to have an osmolytic role in stomatal opening process. However, the experimental evidence supporting this theory remained weak. Based on previous findings, it was hypothesized that sucrose is also used as a substrate instead of solely accumulating within guard cells as the most acceptable theory preconize. By using a combination of stomatal aperture assays coupled with isotope labelling kinetic experiment, we analysed the effects of exogenous sucrose addition on the stomatal aperture and further

investigate the carbon flux using $^{13}$C-sucrose as substrate during light-induced stomatal opening.

## Chapter 6. Concluding remarks

Our knowledge concerning guard cell function has significantly increased following the advantages of the electrophysiological studies as well as molecular physiology and omics approaches applied to single cells. In this chapter, I summarize the main findings in this work and briefly discuss the challenges and perspectives in enhancing our understanding of the physiology, metabolism, signalling, and modelling of this highly specialized cell type, with the practical biotechnological application for developing plants with higher WUE.

## LITERATURE CITED


**Antunes WC, Provart NJ, Williams TCR, Loureiro ME** (2012) Changes in stomatal function and water use efficiency in potato plants with altered sucrolytic activity. Plant Cell Environ **35:** 747-759

**Araújo WL, Fernie AR, Nunes-Nesi A** (2011) Control of stomatal aperture: a renaissance of the old guard. Plant Signal Behav **6:** 1305-1311

**Araújo WL, Nunes-Nesi A, Osorio S, Usadel B, Fuentes D, Nagy R, Balbo I, Lehmann M, Studart-Witkowski C, Tohge T, Martinoia E, Jordana X, DaMatta FM, Fernie AR** (2011) Antisense inhibition of the iron-sulphur subunit of succinate dehydrogenase enhances photosynthesis and growth in tomato via an organic acid-mediated effect on stomatal aperture. Plant Cell **23:** 600-627

**Assmann SM, Wang X-Q** (2001) From milliseconds to millions of years: guard cells and environmental responses. Curr Opin Plant Biol **4:** 421-428

**Bates GW, Rosenthal DM, Sun J, Chattopadhyay M, Peffer E, Yang J, Ort DR, Jones AM** (2012) A comparative study of the *Arabidopsis thaliana* guard-cell transcriptome and its modulation by sucrose. PLoS One **7:** e49641

**Bauer H, Ache P, Lautner S, Fromm J, Hartung W, Al-Rasheid KA, Sonnewald S, Sonnewald U, Kneitz S, Lachmann N, Mendel RR, Bittner F, Hetherington AM, Hedrich R** (2013) The stomatal response to reduced relative humidity requires guard cell-autonomous ABA synthesis. Curr Biol **23:** 53-57

**Bergmann DC, Sack FD** (2007) Stomatal Development. Annu Rev Plant Biol **58:** 163-181

**Berry JA, Beerling DJ, Franks PJ** (2010) Stomata: key players in the earth system, past and present. Curr Opin Plant Biol **13:** 232-239

**Blatt MR** (2000) Cellular signaling and volume control in stomatal movements in plants. Ann Rev Cell Dev Biol **16:** 221-241

**Casson SA, Hetherington AM** (2010) Environmental regulation of stomatal development. Curr Opin Plant Biol **13:** 90-95

**Daloso DM, Antunes WC, Pinheiro DP, Waquim JP, Araújo WL, Loureiro ME, Fernie AR, Williams TCR** (2015) Tobacco guard cells fix $CO_2$ by both Rubisco and PEPcase while sucrose acts as a substrate during light-induced stomatal opening. Plant Cell Environ **38:** 2353-2371

**Daloso DM, dos Anjos L, Fernie AR** (2016) Roles of sucrose in guard cell regulation. New Phytol **211:** 809-818

**Daloso DM, Williams TCR, Antunes WC, Pinheiro DP, Müller C, Loureiro ME, Fernie AR** (2016) Guard cell-specific upregulation of sucrose synthase 3 reveals that the role of sucrose in stomatal function is primarily energetic. New Phytol **209:** 1470-1483

**De Angeli A, Zhang J, Meyer S, Martinoia E** (2013) *At*ALMT9 is a malate-activated vacuolar chloride channel required for stomatal opening in Arabidopsis. Nat Commun **4:** 1804

**Dow GJ, Bergmann DC** (2014) Patterning and processes: how stomatal development defines physiological potential. Curr Opin Plant Biol **21:** 67-74

**Emmerlich V, Linka N, Reinhold T, Hurth MA, Traub M, Martinoia E, Neuhaus HE** (2003) The plant homolog to the human sodium/dicarboxylic cotransporter is the vacuolar malate carrier. Proc Natl Acad Sci USA **100:** 11122-11126

**Engineer CB, Hashimoto-Sugimoto M, Negi J, Israelsson-Nordström M, Azoulay-Shemer T, Rappel W-J, Iba K, Schroeder JI** (2016) $CO_2$ sensing and $CO_2$ regulation of stomatal conductance: advances and open questions. Trends Plant Sci **21:** 16-30

**Fernie AR, Martinoia E** (2009) Malate. Jack of all trades or master of a few? Phytochemistry **70:** 828-832

**Flexas J** (2016) Genetic improvement of leaf photosynthesis and intrinsic water use efficiency in C3 plants: Why so much little success? Plant Science **251:** 155-161

**Gago J, Daloso DdM, Figueroa CM, Flexas J, Fernie AR, Nikoloski Z** (2016) Relationships of leaf net photosynthesis, stomatal conductance, and mesophyll conductance to primary metabolism: a multispecies meta-analysis approach. Plant Physiol **171:** 265-279

**Gago J, Douthe C, Florez-Sarasa I, Escalona JM, Galmes J, Fernie AR, Flexas J, Medrano H** (2014) Opportunities for improving leaf water use efficiency under climate change conditions. Plant Sci **226:** 108-119

**Gehlen J, Panstruga R, Smets H, Merkelbach S, Kleines M, Porsch P, Fladung M, Becker I, Rademacher T, Häusler RE, Hirsch HJ** (1996) Effects of altered phosphoenolpyruvate carboxylase activities on transgenic C3 plant *Solanum tuberosum*. Plant Mol Biol **32:** 831-848

**Hedrich R, Marten I** (1993) Malate-induced feedback regulation of plasma membrane anion channels could provide a $CO_2$ sensor to guard-cells. EMBO J **12:** 897-901

**Hedrich R, Marten I, Lohse G, Dietrich P, Winter H, Lohaus G, Heldt HW** (1994) Malate-sensitive anion channels enable guard cells to sense changes in the ambient $CO_2$ concentration. Plant J **6:** 741-748

**Hetherington AM, Brownlee C** (2004) The generation of $Ca^{2+}$ signals in plants. Annu Rev Plant Biol **55:** 401-427

**Hills A, Chen Z-H, Amtmann A, Blatt MR, Lew VL** (2012) OnGuard, a computational platform for quantitative kinetic modeling of guard cell physiology. Plant Physiol **159:** 1026-1042

**Horrer D, Flütsch S, Pazmino D, Matthews Jack SA, Thalmann M, Nigro A, Leonhardt N, Lawson T, Santelia D** (2016) Blue light induces a distinct starch degradation pathway in guard cells for stomatal opening. Curr Biol **26:** 362-370

**Hurth MA, Suh SJ, Kretzschmar T, Geis T, Bregante M, Gambale F, Martinoia E, Neuhaus HE** (2005) Impaired pH homeostasis in Arabidopsis lacking the vacuolar dicarboxylate transporter and analysis of carboxylic acid transport across the tonoplast. Plant Physiol **137:** 901-910

**Imes D, Mumm P, Böhm J, Al-Rasheid KAS, Marten I, Geiger D, Hedrich R** (2013) Open stomata 1 (OST1) kinase controls R–type anion channel QUAC1 in Arabidopsis guard cells. The Plant Journal **74:** 372-382

**Israelsson M, Siegel RS, Young J, Hashimoto M, Iba K, Schroeder JI** (2006) Guard cell ABA and $CO_2$ signaling network updates and $Ca^{2+}$ sensor priming hypothesis. Curr Opin Plant Biol **9:** 654-663

**Kaneda M, Schuetz M, Lin BSP, Chanis C, Hamberger B, Western TL, Ehlting J, Samuels AL** (2011) ABC transporters coordinately expressed during lignification of Arabidopsis stems include a set of ABCBs associated with auxin transport. J Exp Bot **62:** 2063-2077

**Kang Y, Outlaw JWH, Fiore GB, Riddle KA** (2007) Guard cell apoplastic photosynthate accumulation corresponds to a phloem-loading mechanism. J Exp Bot **58:** 4061-4070

**Kang YUN, Outlaw WH, Andersen PC, Fiore GB** (2007) Guard-cell apoplastic sucrose concentration – a link between leaf photosynthesis and stomatal aperture size in the apoplastic phloem loader *Vicia faba* L. Plant Cell Environ **30:** 551-558

**Kelly G, Moshelion M, David-Schwartz R, Halperin O, Wallach R, Attia Z, Belausov E, Granot D** (2013) Hexokinase mediates stomatal closure. Plant J **75:** 977-988

**Kim T-H, Böhmer M, Hu H, Nishimura N, Schroeder JI** (2010) Guard cell signal transduction network: advances in understanding abscisic acid, $CO_2$, and $Ca^{2+}$ signaling. Annu Rev Plant Biol **61:** 561-591

**Kollist H, Nuhkat M, Roelfsema MRG** (2014) Closing gaps: linking elements that control stomatal movement. New Phytol **203:** 44-62

**Laporte MM, Shen B, Tarczynski MC** (2002) Engineering for drought avoidance: expression of maize NADP-malic enzyme in tobacco results in altered stomatal function. J Exp Bot **53:** 699-705

**Lawson T, Simkin AJ, Kelly G, Granot D** (2014) Mesophyll photosynthesis and guard cell metabolism impacts on stomatal behaviour. New Phytol **203:** 1064-1081

**Lee M, Choi Y, Burla B, Kim YY, Jeon B, Maeshima M, Yoo JY, Martinoia E, Lee Y** (2008) The ABC transporter *At*ABCB14 is a malate importer and modulates stomatal response to $CO_2$. Nat Cell Biol **10:** 1217-1223

**Leonhardt N, Kwak JM, Robert N, Waner D, Leonhardt G, Schroeder JI** (2004) Microarray expression analyses of Arabidopsis guard cells and isolation of a recessive abscisic acid hypersensitive protein phosphatase 2C mutant. Plant Cell **16:** 596-615

**Lugassi N, Kelly G, Fidel L, Yaniv Y, Attia Z, Levi A, Alchanatis V, Moshelion M, Raveh E, Carmi N, Granot D** (2015) Expression of Arabidopsis hexokinase in citrus guard cells controls stomatal aperture and reduces transpiration. Front Plant Sci **6**

**Medeiros DB, Martins SCV, Cavalcanti JHF, Daloso DM, Martinoia E, Nunes-Nesi A, DaMatta FM, Fernie AR, Araújo WL** (2016) Enhanced photosynthesis and growth in *atquac1* knockout mutants are due to altered organic acid accumulation and an increase in both stomatal and mesophyll conductance. Plant Physiol **170:** 86-101

**Meyer S, Lauterbach C, Niedermeier M, Barth I, Sjolund RD, Sauer N** (2004) Wounding enhances expression of AtSUC3, a sucrose transporter from Arabidopsis sieve elements and sink tissues. Plant Physiol **134:** 684-693

**Meyer S, Mumm P, Imes D, Endler A, Weder B, Al-Rasheid KAS, Geiger D, Marten I, Martinoia E, Hedrich R** (2010) *At*ALMT12 represents an R-type anion channel required for stomatal movement in Arabidopsis guard cells. Plant J **63:** 1054-1062

**Meyer S, Scholz-Starke J, De Angeli A, Kovermann P, Burla B, Gambale F, Martinoia E** (2011) Malate transport by the vacuolar *At*ALMT6 channel in guard cells is subject to multiple regulation. Plant J **67:** 247-257

**Mott KA** (2009) Opinion: Stomatal responses to light and $CO_2$ depend on the mesophyll. Plant Cell Environ **32:** 1479-1486

**Mumm P, Imes D, Martinoia E, Al-Rasheid KAS, Geiger D, Marten I, Hedrich R** (2013) C-Terminus-mediated voltage gating of Arabidopsis guard cell anion channel QUAC1. Mol Plant **6:** 1550-1563

**Nunes-Nesi A, Carrari F, Gibon Y, Sulpice R, Lytovchenko A, Fisahn J, Graham J, Ratcliffe RG, Sweetlove LJ, Fernie AR** (2007) Deficiency of mitochondrial fumarase activity in tomato plants impairs photosynthesis via an effect on stomatal function. Plant J **50:** 1093-1106

**Nunes-Nesi A, Nascimento VdL, de Oliveira Silva FM, Zsögön A, Araújo WL, Sulpice R** (2016) Natural genetic variation for morphological and molecular determinants of plant growth and yield. J Exp Bot **67:** 2989-3001

**Outlaw WH, Manchester J** (1979) Guard cell starch concentration quantitatively related to stomatal aperture. Plant Physiol **64:** 79-82

**Penfield S, Clements S, Bailey KJ, Gilday AD, Leegood RC, Gray JE, Graham IA** (2012) Expression and manipulation of *PHOSPHOENOLPYRUVATE CARBOXYKINASE 1* identifies a role for malate metabolism in stomatal closure. Plant J **69:** 679-688

**Roelfsema MRG, Hedrich R** (2005) In the light of stomatal opening: new insights into 'the Watergate'. New Phytol **167:** 665-691

**Santelia D, Lawson T** (2016) Rethinking guard cell metabolism. Plant Physiol **172:** 1371-1392

**Sasaki T, Mori IC, Furuichi T, Munemasa S, Toyooka K, Matsuoka K, Murata Y, Yamamoto Y** (2010) Closing plant stomata requires a homolog of an aluminum-activated malate transporter. Plant Cell Physiol **51:** 354-365

**Schroeder JI, Allen GJ, Hugouvieux V, Kwak JM, Waner D** (2001) Guard Cell Signal Transduction. Annu Rev Plant Physiol Plant Mol Biol **52:** 627-658

**Stadler R, Büttner M, Ache P, Hedrich R, Ivashikina N, Melzer M, Shearson SM, Smith SM, Sauer N** (2003) Diurnal and light-regulated expression of AtSTP1 in guard cells of Arabidopsis. Plant Physiol **133:** 528-537

**Talbott LD, Zeiger E** (1993) Sugar and organic acid accumulation in guard cells of *Vicia faba* in response to red and blue light. Plant Physiol **102:** 1163-1169

**Talbott LD, Zeiger E** (1996) Central roles for potassium and sucrose in guard-cell osmoregulation. Plant Physiol **111:** 1051-1057

**Talbott LD, Zeiger E** (1998) The role of sucrose in guard cell osmoregulation. J Exp Bot **49:** 329-337

**Van Kirk CA, Raschke K** (1978) Release of malate from epidermal strips during stomatal closure. Plant Physiol **61:** 474-475

**Vavasseur A, Raghavendra AS** (2005) Guard cell metabolism and $CO_2$ sensing. New Phytol **165:** 665-682

**Wang R-S, Pandey S, Li S, Gookin TE, Zhao Z, Albert R, Assmann SM** (2011) Common and unique elements of the ABA-regulated transcriptome of Arabidopsis guard cells. BMC Genomics **12:** 216

**Wheeler MCG, Tronconi MA, Drincovich MF, Andreo CS, Flügge U-I, Maurino VG** (2005) A comprehensive analysis of the NADP-Malic Enzyme gene family of Arabidopsis. Plant Physiol **139:** 39-51

# Chapter 2

## Utilizing systems biology to unravel stomatal function and the hierarchies underpinning its control

Plant, Cell & Environment

*Plant, Cell and Environment* (2015) **38**, 1457–1470 doi: 10.1111/pce.12517

## Opinion

# Utilizing systems biology to unravel stomatal function and the hierarchies underpinning its control

David B. Medeiros[1], Danilo M. Daloso[2], Alisdair R. Fernie[2], Zoran Nikoloski[3] & Wagner L. Araújo[1]

[1]*Max-Planck Partner Group, Departamento de Biologia Vegetal, Universidade Federal de Viçosa, Viçosa, Minas Gerais, Brazil,* [2]*Central Metabolism Group and* [3]*Systems Biology and Mathematical Modeling Group, Max Planck Institute of Molecular Plant Physiology, Potsdam-Golm, Germany*

## ABSTRACT

**Stomata control the concomitant exchange of $CO_2$ and transpiration in land plants. While a constant supply of $CO_2$ is need to maintain the rate of photosynthesis, the accompanying water losses must be tightly regulated to prevent dehydration and undesired metabolic changes. The factors affecting stomatal movement are directly coupled with the cellular networks of guard cells. Although the guard cell has been used as a model for characterization of signaling pathways, several important questions about its functioning remain elusive. Current modeling approaches describe the stomatal conductance in terms of relatively few easy-to-measure variables being unsuitable for *in silico* design of genetic manipulation strategies. Here, we argue that a system biology approach, combining modeling and high-throughput experiments, may be used to elucidate the mechanisms underlying stomata control and to determine targets for modulation of stomatal responses to environment. In support of our opinion, we review studies demonstrating how high-throughput approaches have provided a systems-view of guard cells. Finally, we emphasize the opportunities and challenges of genome-scale modeling and large-scale data integration for *in silico* manipulation of guard cell functions to improve crop yields, particularly under stress conditions which are of pertinence both to climate change and water use efficiency.**

## INTRODUCTION

Stomata are microscopic pores formed by pairs of specialized epidermal guard cells, which control the essential exchange of $CO_2$ with the environment concomitantly with transpiration in land plants. Although plants are in constant need of sufficient quantities of $CO_2$ to maintain their photosynthetic rates, the water losses associated with the $CO_2$ entry must also be strictly regulated to prevent dehydration and the subsequent unfavourable changes of metabolic state that this invokes. Furthermore, the influx of $CO_2$ and the absorption of minerals depend highly on the availability of water, which is usually a major limiting factor for the development and growth of terrestrial plants. For these reasons, most terrestrial plants are coated with a water-impermeable cuticle layer that prevents evaporation and water loss (Bessire *et al.* 2007; Schreiber 2010; Buschhaus & Jetter 2011). Accordingly, the majority of water lost to transpiration, and $CO_2$ absorption for that matter, occurs through stomatal pores rendering the stomata as the main control point, which regulates the flow of gases between plants and atmosphere (Schroeder *et al.* 2001).

Changes in guard cell metabolism can regulate the magnitude of the pore size in response to a range of environmental and endogenous plant stimulus (Kim *et al.* 2010). This regulation allows plants to occupy habitats with fluctuating environmental conditions. Therefore, it has been postulated that stomata must be important contributors to speciation and evolutionary adaptation (Hetherington & Woodward 2003). Moreover, stomatal behaviour and stomatal density are of fundamental importance not only for individual plant performance, but also for crop productivity and the terrestrial $CO_2$ and water cycles (Buckley & Mott 2013; Schroeder *et al.* 2013).

Stomatal pores open in response to an increase in guard cell volume driven by influx of water, which in turn is the result of a decrease in the water potential of the guard cell. Conversely, during stomatal closure, an efflux of osmolytes from guard cells is necessary with an associated increase in guard cell water potential, leading to efflux of water (Schroeder *et al.* 2001; Kim *et al.* 2010; Araújo *et al.* 2011a,c). Therefore, water potential is one of the key determinants of stomatal movements that is opening and closing.

In addition to the control of water loss, stomatal movements directly affect $CO_2$ assimilation in response to environmental cues by integrating a variety of stimuli, such as: light, vapour pressure deficit (VPD), abscisic acid (ABA) and $CO_2$ concentration (Blatt 2000; Hetherington & Woodward 2003; Shimazaki *et al.* 2007; Kim *et al.* 2010; Hubbard *et al.* 2012). Although guard cells have often been used as a model system in which to discover ABA receptors (Liu *et al.* 2007; Pandey *et al.* 2009; Park *et al.* 2009) and for the *in vitro* characterization of the ABA signalling pathway (Fujii *et al.* 2009), several important questions about guard cell functioning, particularly under suboptimal conditions, remain elusive.

For over a century, guard cells have been extensively studied, and considerable efforts have been made to better

*Correspondence: W. L. Araújo. Fax: +55 31 3899.2580; e-mail: wlaraujo@ufv.br*

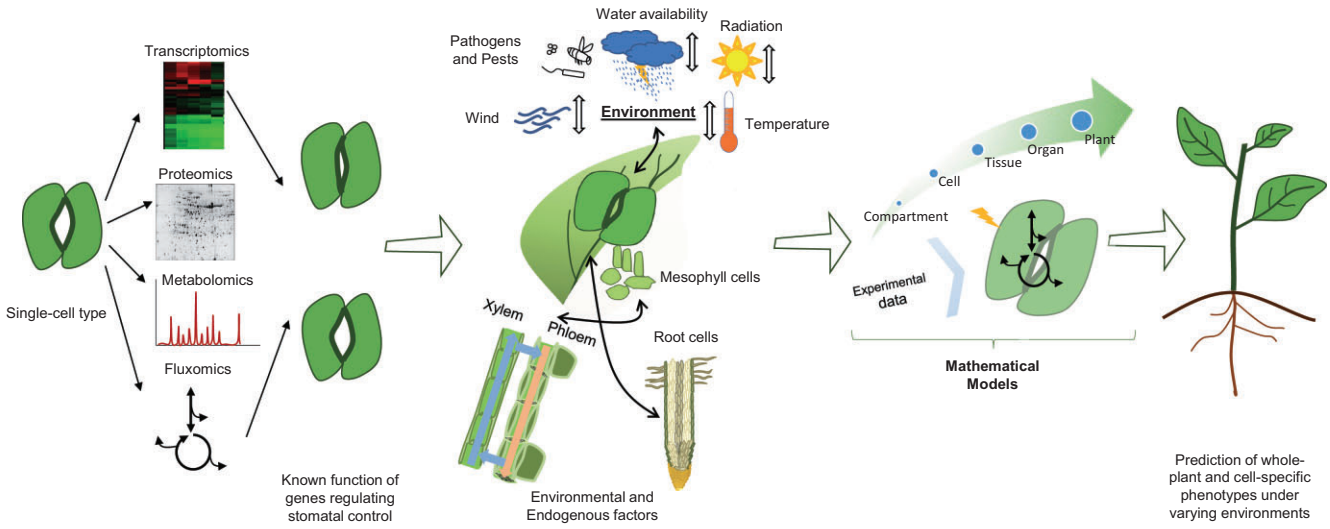


**Figure 1.** Schematic representation showing how systems analyses and modelling can help the knowledge of molecular hierarchy undergoing stomatal movements and in predictions about phenotypes. The system biology approaches (transcriptomics, proteomics, metabolomics, fluxomics and others) may aid the understanding of unknown questions still unclear about stomatal movements coupling with experimental data from interactions between guard cell – environmental and guard cell – endogenous signals from different cell types that, together with the feedback loops those interactions determine the integrated and coordinated plant behaviour. These data can be grouped in mathematical models to stomatal response and associated with reverse engineering will allow to provide biotechnological targets for generation of improved crop yields and to predict the phenotype under varying environments.

understand their structure, development and physiology (Bessey 1898; Bergmann & Sack 2007; Mott 2009; Berry *et al*. 2010; Casson & Hetherington 2010; Kim *et al*. 2010; Dow & Bergmann 2014). In addition, the relative ease of the isolation of the guard cells, which gate the stomatal pore, has facilitated experimental interrogation contributing to the increase in the understanding of these cells relative to other plant cell types (Hetherington & Brownlee 2004; Israelsson *et al*. 2006; Kim *et al*. 2010). These advances have rendered the guard cell as one of the best studied plant cell models for membrane transport, signalling and homeostasis (Blatt 2000; Roelfsema & Hedrich 2010; Hills *et al*. 2012).

Thorough understanding of stomatal behaviour and its regulation represents an important step towards obtaining plants with better water-use efficiency, which can be defined as the carbon fixed per unit of water (Lawson & Blatt 2014; Lawson *et al*. 2014; Way *et al*. 2014). Here, our first aim was to focus on high-throughput studies that have recently made considerable progress in elucidating the molecular and genetic bases underlying stomatal function and movement. However, the complexity of interactions involved in regulatory processes ranging from metabolite transport to the cell-autonomous metabolic and buffering activities of guard cells remains the main barrier to understand the regulatory networks governing stomatal movement (Blatt *et al*. 2013). In this context, we suggest that a systems biology approach offers itself as a comprehensive way to aid in elucidation of the mechanisms governing stomatal function and the molecular hierarchies underpinning the stomata control. Furthermore and given that systems biology approaches necessitate data-driven modelling to integrate datasets capturing various read-outs of the cell as well as to generate and validate (or refute) hypotheses, they can also ultimately be used to predict biotechnological targets for the manipulation of stomatal behaviour. To this end, our second aim was to outline the steps that are prerequisites for coupling reverse engineering of stomatal responses with *in silico* design and modelling in order to direct genetic manipulation for improved crop yield and water-use efficiency (Fig. 1). We additionally suggest an alternative approach to those commonly used to illuminate stomatal behaviour and in doing so hope to bridge the gap between ecophysiological and molecular views of this important cell-to-environment interaction.

## Why apply the systems biology approach to study stomatal function?

Over the last 20 years we have witnessed an increasing interest in the understanding of the molecular mechanisms by which guard cells sense and respond to stimuli such as ABA, plant water status, light, $CO_2$, temperature and humidity. As a consequence, guard cells have become an important model for studies of membrane transport and cell signalling (Assmann 2010). Advances in our understanding over this time period are mostly due to the identification and characterization of mutants deficient in stomatal closing and opening coupled with the currently challenging, but all the same feasible, isolation and screening of large populations of guard cells, employed in various high-throughput technologies (Table 1).

Several seminal studies and numerous reviews (Tallman 2004; Shimazaki *et al*. 2007; Kim *et al*. 2010; Meyer *et al*. 2010; Araújo *et al*. 2011a; Song *et al*. 2014), point out that stomatal

**Table 1.** Description of *Arabidopsis* mutants plants which have stomatal dysfunction and were identified and/or characterized by omics approaches

| Gene(s) AGI code | Mutant name | Functional description | Phenotype | Characterization | Technology* | References |
|---|---|---|---|---|---|---|
| AT1G72770 | *atp2C-HA-1* | Encodes the protein phosphatase 2C; regulates the activation of the Snf1-related kinase OST1 by ABA | ABA-hypersensitive regulation of stomatal closing a | Transcriptome | Microarray | Leonhardt *et al*. 2004 |
| AT4G34460.1 | *agb1* | Encodes the heterotrimeric G-protein $\beta$ subunit | ABA-hyposensitive | Transcriptome | Microarray | Pandey *et al*. 2010 |
| AT2G26300.1 | *gpa1* | Encodes the heterotrimeric G-protein $\alpha$ subunit | hyposensitive to ABA inhibition of stomatal opening | Transcriptome | Microarray | Pandey *et al*. 2010 |
| AT4G34460.1; AT2G26300.1 | *agb1 gpa1 (double mutant)* | Encodes the heterotrimeric G-protein $\alpha$ and $\beta$ subunits | ABA-hyposensitive | Transcriptme | Microarray | Pandey *et al*. 2010 |
| AT4G17770.1 | At4g17770 | Encodes an enzyme putatively involved in trehalose biosynthesis. | Stomatal conductance decreased without change stomatal density | Transcriptome | Microarray | Bates *et al*. 2012 |
| AT1G65370.1 | At1g65370 | Encodes a TRAF-like family protein | Stomatal conductance decreased without change stomatal density | Transcriptome | Microarray | Bates *et al*. 2012 |
| AT1G15440 | At1g15440 | Encodes a nucleolar protein that is a ribosome biogenesis co-factor. | Stomatal conductance decreased without change stomatal density | Transcriptome | Microarray | Bates *et al*. 2012 |
| AT1G16540.1 | *aba3-1* | Encodes molybdenum cofactor sulfurase. Involved in the conversion of ABA-aldehyde to ABA | Guard cell-autonomous ABA synthesis is sufficient for stomatal closure in response to low relative humidity | Transcriptome | Microarray | Bauer *et al*. 2013 |
| AT5G65590.1 | *scap1* | Encodes a plant-specific Dof-type transcription factor (TF). It regulates stomatal guard cell maturation and functions as a key TF regulating the final stages of guard cell differentiation | Impaired $CO_2$-induced stomatal closing and light-induced stomatal opening | Transcriptome | Microarray | Negi *et al*. 2013 |
| AT5G26000.1 | *tgg1* | Member of glycoside hydrolase family 1. Encodes one of two known functional myrosinase enzymes in *Arabidopsis*. The enzyme catalyses the hydrolysis of glucosinolates into compounds that are toxic to various microbes and herbivores. | Hyposensitive to ABA inhibition of guard cell inward $K^+$ channels and stomatal opening | Proteome | Identification from broad and narrow pH range 2D gels, and 2D liquid chromatography matrix-assisted laser desorption/ionization multidimensional protein identification | Zhao *et al*. 2008 |
| AT2G26300.1 | *gpa1-4* | Encodes the heterotrimeric G-protein $\alpha$ subunit | Hyposensitive to ABA inhibition of light-induced stomatal opening | Proteome | iTRAQ | Zhu *et al*. 2010 |
| AT4G33950.1; AT3G50500.2; AT5G66880.1 | *srk2dei (triple mutant)* | The three genes encode ABA-activated protein kinases, members of SNF1-related protein kinases (SnRK2) | ABA-insensitive showing severe wilting phenotype because of fully opened stomata | Proteome | Phosphoproteomic analyses; Nano-LC-MS/MS | Umezawa *et al*. 2013 |
| AT2G26300.1 | *gpa1* | Encodes the heterotrimeric G-protein $\alpha$ subunit | Hyposensitive to ABA inhibition of stomatal opening | Metabolome | LC-MS/MS with (MRM) | Jin *et al*. 2013 |

*Abbreviations for the technologies used.
iTRAQ, isobaric tags for relative and absolute quantitation; LC, liquid chromatography; MS, mass spectrometry; MRM, multiple reaction monitoring.

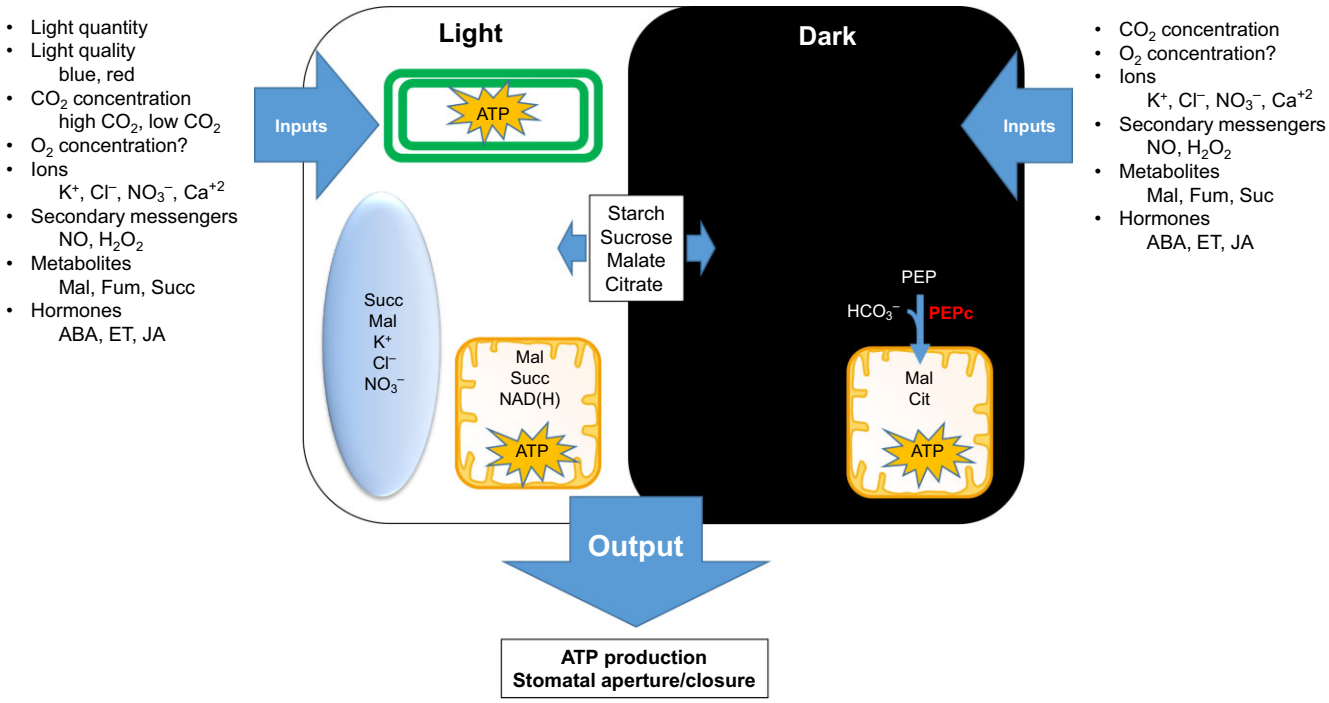


**Figure 2.** The main regulators of guard cell movements. Schematic representation of guard cell metabolism of C3 plants in both light and dark phases. For guard cell modelling it is important to consider the particularities of guard cell metabolism, which are represented in the figure by the number of possible inputs (environment signals, ions, secondary messengers, metabolites, hormones) and the high compartmentalization of the metabolism, which involves transport and accumulation of ions and metabolites in the apoplast and organelles (plastids, mitochondria and vacuole). It is also important to consider that guard cells have a metabolism similar to C4 plants and not C3 plants, represented in the figure through the activity of the enzyme phospho*enol*pyruvate carboxylase (PEPc) in the dark phase. Beyond ATP production, which is commonly used as output, guard cells have a specific output that has substantial physiological importance – stomatal aperture or closure. Abbreviations: ABA, abscisic acid; $Ca^{+2}$, calcium; $Cl^-$, chloride; Cit, Citrate; $CO_2$, Carbon dioxide; ET, ethylen, Fum, fumarate; $HCO_3^-$, Bicarbonate; $H_2O_2$, hydrogen peroxide; JA, jasmonic acid; $K^+$, potassium; Mal, malate; $NO_3^-$, nitrate; NO, nitric oxide; $O_2$, Oxygen; Succ, Succinate.

movement depends on many exogenous variables (Fig. 2) that affect the internal networks on multiple levels of cellular organization ranging from aspects of transcriptional regulatory networks, signalling and metabolism. For this reason, system perturbation by the application of a series of independent environmental cues (or their combinations), would make it increasingly difficult to distinguish between their primary and secondary effects. This complexity is further exacerbated in instances wherein these stress perturbations are not simply applied to wild-type tissues, but also to genetic variants such as mutants or transgenic lines. Moreover, the differential coverage of cellular components by high-throughput technologies currently renders data interpretation rather difficult (Fernie & Stitt 2012). It should be mentioned that these incoherencies are not only due to technical issues, but also related to the complexity and structure of metabolic networks (Araújo *et al*. 2012).

To this end, data-driven integrative modelling will likely prove highly useful for both *in silico* investigation of the effects of environmental changes and reverse engineering of the networks underlying guard cell functions. Moreover, using the outcome of the system-level simulations to plan validation experiments will be highly instructive and will likely result in several iterative cycles of experimentation and modelling. Such an approach may alleviate some of the problems encountered by guard cell experimentalists most acutely perhaps is reducing the number of experiments needed, which given that difficulties in obtaining the required number of guard cells often represents the bottleneck in the experimental studies of guard cells.

Finally, the ultimate goal of the systems biology approach is to understand the system with the aim of manipulating its function towards a desired outcome. Therefore, systems approach, carefully integrating high-throughput data with (possibly) large-scale models of metabolism and regulation/signalling can further contribute to identifying novel determinants on a molecular level as well as to plan intervention strategies (discussed in detail later in the section 'Opportunities and challenges in systems modelling of stomatal function').

## Application of systems biology approaches to stomata

The differential analysis of multiple cell types and organs is one approach to dissect regulatory signalling networks and metabolic pathways underlying complex molecular functions, and has been deemed crucial for the development of systems

biology (Ideker & Krogan 2012). Such comparative analyses require the use of high-throughput phenotyping technologies that permit the generation of large volumes of data. These data can, in turn, be used to either generate or test hypotheses with respect to the genes and their products (i.e. proteins) as well as to downstream metabolites, which exhibit differential behaviour across tissues or cells under different environmental conditions. A major bottleneck and challenge in plant cell-specific studies, however, is in obtaining different cell types in high enough quantity and quality for downstream analysis (Misra *et al*. 2014). Nevertheless, several elegant studies involving the parallel usage of different high-throughput technologies have employed guard cells. Most of these studies, mainly performed in *Arabidopsis*, focused on the identification of molecular components of the ABA signal cascade. We highlight these studies and the knowledge advances, which they provided in the first part of this paper and subsequently offer a perspective on the modelling of guard cell function. Finally, we will present what in our opinion are the major outstanding questions in understanding guard cell function.

## Transcriptomics studies

As a first step towards a deeper understanding of guard cell functioning, we provide a summary of publicly available transcriptomic data from guard cell studies. It is important to mention that most of studies available to date have been used to analyse the response to ABA and the ABA signalling pathway. Accordingly, most of the data available was generated in *Arabidopsis* mutant plants (Table 1). Given that the response of plants to environmental cues, particularly stresses, often involves the coordinated induction or repression of gene expression, transcriptomics studies provide investigation of one critical facet of the molecular response of guard cells.

Oligomer-based DNA microarray was used in earlier studies to profile gene expression in *Arabidopsis* guard cells, facilitating the identification of ~1300 genes, which were expressed in guard cells (Leonhardt *et al*. 2004). On comparison of guard cell expression profiles with those from mesophyll cells, 64 transcripts were identified to be preferentially expressed in guard cells. Importantly, the reliability of this approach was further confirmed by quantitative RT-PCR. Analysis of the expression profile of guard cells had additionally revealed the ABA-responsive genes that govern the behaviour of guard cell ABA-signalling components (Leonhardt *et al*. 2004).

In a more recent study, guard cell transcriptome data were used to identify novel modes of (heterotrimeric) G-proteins action (Pandey *et al*. 2010). G-proteins comprise three subunits, alpha (G$\alpha$), beta (G$\beta$) and gamma (G$\gamma$), and are important transmembrane components of signal transduction (Temple & Jones 2007; Kumar *et al*. 2014). Given that G-proteins can mediate a wide range of essential signalling pathways in eukaryotes this protein family might be involved in aspects of guard cell signalling (see discussion on 'Proteomics studies' later). By analysing microarray data from guard cells and excised leaves of G-protein subunit mutants of *Arabidopsis*, with and without ABA treatment, the classical mechanisms of G-protein signalling was confirmed and a novel route of G-protein signalling, in which G$\beta$ subunit regulates gene expression independently of G$\alpha$ subunit, was discovered. Notably, it was also observed that G-protein mode of transcriptional regulation differs between guard cells and leaves, supporting a system-specificity of G-protein signalling. These observations clearly improve resolution of the molecular network of ABA-responsive genes and could plausibly be used as new inputs in modelling approaches that predict stomatal movements in addition to those involving solute transport across membranes.

Another recent study involving ABA regulation of gene expression in guard cells have identified a unique *cis*-acting motif, GTCGG, associated with ABA-induction of gene expression specifically in guard cells (Wang *et al*. 2011). In addition, approximately 300 genes displaying ABA-specific regulation were uncovered in guard cells, including genes known to encode ion transporters associated with stomatal opening (e.g. the $H^+$-ATPase *OPEN STOMATA 2 – OST2*, the *POTASSIUM CHANNEL IN ARABIDOPSIS THALIANA 1 and 2 – KAT1* and *KAT2*, the *SUGAR TRANSPORTER 1 – STP1*, the endosomal $Na^+/H^+$ antiporter *CATION/H + EXCHANGER 20 – CHX20*, and the *NITRATE TRANSPORTER 1 – NRT1*). These genes were down-regulated upon ABA treatment, suggesting that this regulation may be an important aspect of mid- to long-term inhibition of stomatal opening by ABA as well as ensuring the maintenance of stomatal closure during stress situations such as drought. Moreover, these results provided evidence for cross-talk at the transcriptional level between ABA and another hormonal inhibitor of stomatal opening, namely, jasmonate (Wang *et al*. 2011).

Microarray analysis was additionally performed on guard cells from leaves of *Arabidopsis* treated with sucrose to test the hypothesis that photosynthesis-derived sugar acts as a signal in guard cells, which allows adjustment of their stomatal opening (Bates *et al*. 2012). This study revealed that the expression of 440 genes changed in response to sucrose in guard cells including genes involved in several important cellular functions such as photosynthesis and transport of sugars, water, amino acids and ions. Remarkably, investigation of T-DNA insertion lines for 50 genes highly responsive to sucrose revealed that 12 genes, which were not previously known to function in guard cells, are important in leaf conductance control, water-use efficiency and/or stomata development. Of these, three are of particular interest given that they showed similar effects in nearly all test of stomatal function without a change in stomatal density: a trehalose phosphate synthase *TPS5* (At4g17770), a TRAF domain-containing protein (At1g65370), and a WD repeat–containing protein (At1g15440) (Bates *et al*. 2012). Collectively, these results demonstrate the power of large-scale gene expression studies as an effective tool in revealing candidate genes with potential for practical application in field-related experiments.

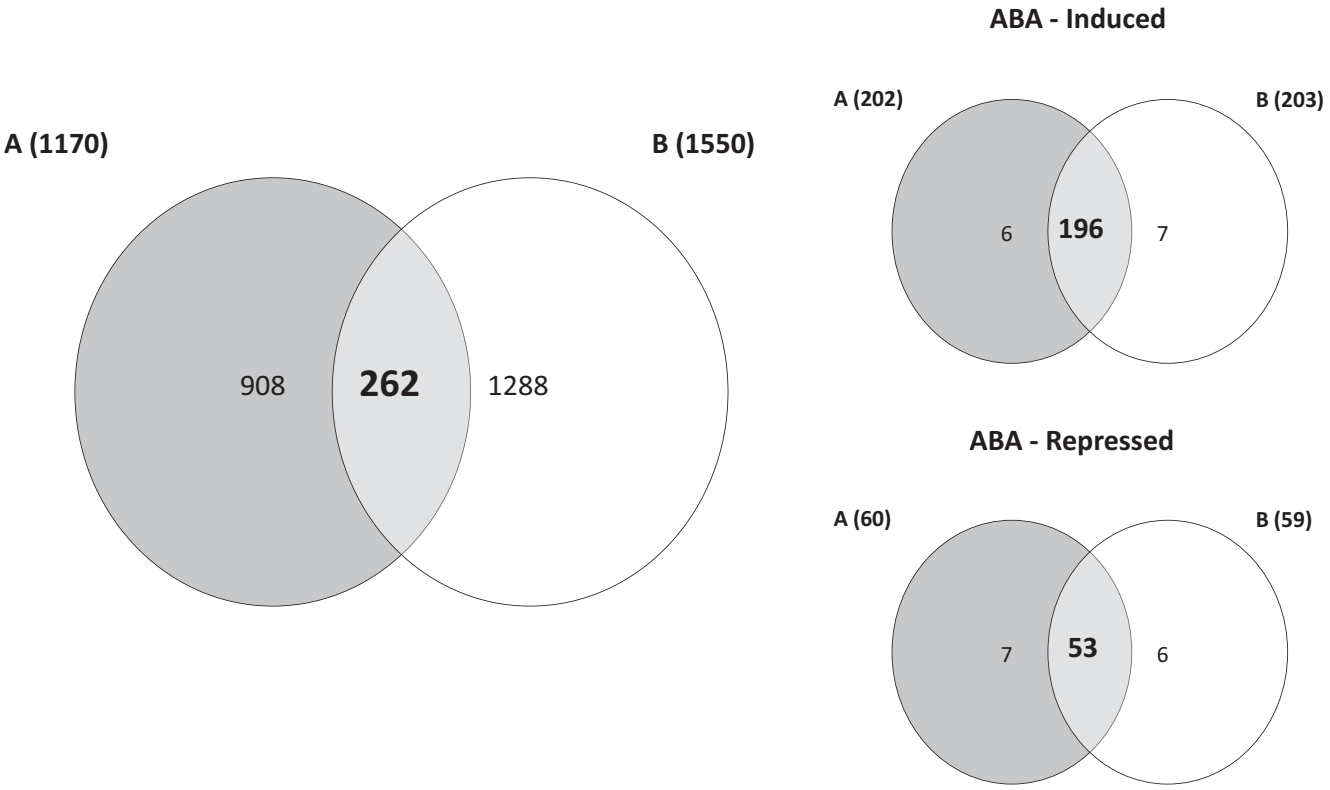


**Figure 3.** Venn diagram showing the transcriptome overlap of studies on ABA response in guard cells. (a) and (b) correspond to Wang *et al.* (2011) and Bauer *et al.* (2013), respectively. Notably, we found 262 genes that were responsive to ABA treatment in both studies. Additionally, we overlapped the genes that were ABA-induced (196) or repressed (53) from the list of the 262 genes previously found. The data used are available in the Supporting Information Table S1. The Venn diagram was constructed in the Pangloss Venn diagram generator (http://www.pangloss.com/seidel/Protocols/venn4.cgi).

In a similar approach, the expression profiles of *Arabidopsis* plants under dry air conditions, characterized by long-term stomatal closure, revealed 588 differentially regulated genes (Bauer *et al.* 2013). Given that transport is an essential activity of guard cells, it is not surprising that genes associated with this function were found to be highly expressed in guard cells (e.g. *KAT1*, *KAT2*, *GATED OUTWARDLY-RECTIFYING $K^+$ CHANNEL – GORK*, *SLOW ANION CHANNEL-ASSOCIATED 1 – SLAC1*, *SLAC1 HOMOLOGUE 3 – SLAH3*, and *QUICK-ACTIVATING ANION CHANNEL 1 – QUAC1*). It is worth mentioning that when treated with exogenous ABA, 1550 genes were sensitive to ABA of which 1080 were up-regulated and 470 were down-regulated (Bauer *et al.* 2013).

Most recently, Negi and collaborators isolated an *Arabidopsis* mutant, stomatal carpenter 1 (*scap1*) that develops irregularly shaped guard cells lacking normal stomatal function, and showing defects in $CO_2$-induced stomatal closing and light-induced stomatal opening from an M2 population of ethyl methanesulfonate (EMS)-mutagenized *Arabidopsis* plants (Negi *et al.* 2013). *SCAP1* was identified to encode a plant-specific DNA binding with one finger (Dof) transcription factor, and its role in guard cell gene expression was investigated by microarray experiments. These experiments identified 1540 genes that are expressed in guard cells, but not in mesophyll cells. The *scap1* mutation resulted in decreased expression of genes for several factors directly involved in stomatal opening and closure, namely, GORK (Hosy *et al.* 2003), PYL2, a regulatory component of ABA receptor 2 (Park *et al.* 2009) and MYB60, an essential transcriptional regulator for guard cell movements (Cominelli *et al.* 2005). Thus, SCAP1 regulates not only stomatal guard cell maturation, but also stomatal functions through its direct involvement in the final stages of guard cell differentiation.

By focusing on well-known ABA-responsive genes, we here utilize a Venn diagram to visualize the overlap of the findings from these most recent guard cell studies employing transcriptome analyses (Wang *et al.* 2011; Bauer *et al.* 2013). Notably, we found 262 genes that are responsive to ABA treatment in both experiments (Fig. 3 and Supporting Information Table S1). These genes could thus be strong candidates for being involved in the functional response to changes in ABA levels as well as representing potential targets for future experimental work to further dissect the ABA-response network.

Notably, transcriptomes as assessed by microarrays have produced an unprecedented amount of data regarding transcript identity and levels in plant systems and also in guard

cells network and cascades that have been elegantly elucidated. Additionally, although next-generation DNA sequencing technologies are driving increasingly rapid, affordable and high resolution analyses of plant transcriptomes through sequencing of their associated cDNA (complementary DNA) populations; an analytical platform commonly referred to as RNA-sequencing (RNA-seq) (Martin *et al*. 2013), not so much has been performed in guard cells thus far. Remarkably RNA-sequencing is currently well-established as a versatile platform with applications in an ever-growing number of fields of plant biology research, including naturally guard cell studies. Collectively, there is plenty of reason to believe that guard cell microarrays and transcriptome sequences can provide a valuable resource for plant breeding and research helping in the identification of novel insights into common plant responses to several environmental stress and offer candidate genes or markers that can be used to guide future efforts attempting to breed tolerant plants.

## Proteomics studies

Proteomics analyses complement transcriptomics-based studies and can provide better understanding of the interplay between cellular levels since proteins are generally functionally involved either in regulatory, signalling or metabolic processes. At the proteomic level, comparative analysis of purified guard cells and mesophyll cells from *Brassica napus* has first been performed using the isobaric tags for relative and absolute quantification (iTRAQ) technology alongside two-dimensional (2D) liquid chromatography mass spectrometry (Zhu *et al*. 2009). This strategy identified around 1450 non-redundant proteins in both guard cells and mesophyll cells. Interestingly, 427 of these proteins were quantified, and 74 of them were found to be enriched in guard cells. As would perhaps be anticipated, proteins involved in energy metabolism, transport, transcription, cell structure, and signalling were preferentially expressed in guard cells, providing further support to the idea that guard cells can, at least partially, function autonomously (Schroeder *et al*. 2001; Hashimoto *et al*. 2006; Young *et al*. 2006; Sirichandra *et al*. 2009).

In another study related to ABA signalling and stomatal movement, more than 1700 unique proteins from *Arabidopsis* guard cell protoplasts were identified using three complementary proteomic methods (Zhao *et al*. 2008). This extensive single-cell proteomics approach identified not only proteins whose encoding genes were not previously identified in transcriptome analyses of guard cells, but also signalling proteins, of which two were suggested to be related to guard cell function. For instance, THIOGLUCOSIDE GLUCOHYDROLASE1 (TGG1), a myrosinase, catalyses the production of toxic isothiocyanates from glucosinolates. This protein was more abundant in the guard cell proteome, and the *tgg1* mutants were hyposensitive to ABA inhibition of guard cell inward $K^+$ channels and stomatal opening. As such, this study revealed that the glucosinolate-myrosinase system, previously identified as a defense against biotic invaders, is also required for key ABA responses of guard cells of *Arabidopsis* (Zhao *et al*. 2008). That said it is important to note that glucosinolates are mainly present in the family Brassicaceae (Fahey *et al*. 2001), and as such this is very much a specialized rather than a general mechanism of guard cell regulation.

A further component of the *Arabidopsis* ABA-responsive network underpinning stomatal movement was also identified by using iTRAQ technology. In this study guard cell proteins whose abundance was affected by ABA supply and/or mutation in *G PROTEIN ALPHA SUBUNIT 1* (*GPA1*) in *Arabidopsis thaliana* were investigated. Accordingly, this elegant study has demonstrated that the G-protein $\alpha$ subunit, GPA1, is implicated in ABA-regulated guard cell movement, confirming thus a previous transcriptome analysis (Pandey *et al*. 2010). It is worthy to mention that the abundance of two proteins in Col-0 and six proteins in *gpa1-4*, a null mutant lacking the G$\alpha$ subunit, was affected by ABA treatment in guard cells, whereas 18 guard cell proteins were quantitatively affected by mutation in *GPA1*. Remarkably, these are proteins clearly involved in photosynthesis as they participate in the Calvin–Benson cycle, photosynthetic light reactions, ATP synthases and chloroplastic electron transfer. It is also worth mentioning that a further five proteins whose abundance increased in *gpa1-4* guard cells are members of the so-called 'response to stress' family including proteins involved in oxidative stress (Zhao *et al*. 2010). Altogether, the results of these studies indicated that GPA1 not only inhibits guard cell photosynthesis, but also promotes the availability of reactive oxygen species (ROS) in guard cells.

Analysis of ABA responsive proteins in *B. napus* guard cells has also been performed, with a total of 431 unique proteins being unequivocally identified, of which 66 increased and 38 decreased (Zhu *et al*. 2010). The proteins that were more highly abundant following ABA treatment included proteins involved in stress and defence while proteins with functions in spermidine synthesis, rhamnose biosynthesis, jasmonic acid biosynthesis, fatty acid beta-oxidation, purine metabolism, alkaloid biosynthesis and protein synthesis decreased. Surprisingly, some of the metabolic pathways that were suppressed are additionally important in plant stress and defence (Zhu *et al*. 2010). Furthermore, given that many of these proteins have not previously been reported as either being ABA responsive or being involved in stomatal movement, it suggests that further novel players involved in guard cell ABA signalling may yet remain to be identified.

At a more mechanistic level, a recent phosphoproteomic approach identified proteins that were phosphorylated following ABA treatment or under dehydration stress in *Arabidopsis* wild-type plants, but not in mutants lacking all three kinases of the SUCROSE NON FERMENTING 1 (SNF1)-RELATED PROTEIN KINASE 2s (SnRK2s) family (Umezawa *et al*. 2013), which are central components of ABA signalling pathways. The number of differentially phosphorylated peptides was greater in *srk2dei* plants treated with ABA than in the ones subjected to dehydration, suggesting that SnRK2 was mainly involved in ABA signal-

ling rather than dehydration. SnRK2 also promotes the ABA-induced activation of the Mitogen-activated protein kinases (MAPKs) AtMPK1 and AtMPK2, AREB1 (ABA-responsive element binding protein 1), and stimulate ABA-responsive gene expression. Furthermore, SnRK2-SUBSTRATE 1 (SNS1), a previously unknown protein, was phosphorylated *in vivo* following isolation and functional characterization of knockout mutants of SNS1 it was revealed that SNS1 is a negative regulator of ABA signalling at the post-germination stage in *Arabidopsis*.

As discussed earlier, proteomic approaches have recently expanded our view of the protein landscape required for and during stomatal movements and thus contributed significantly in advancing our mechanistic understanding of ABA signalling controlling guard cell movements. However, there are still large gaps in the knowledge concerning the changes of the proteome during adaptation to environmental stress conditions that lead to changes in stomatal aperture. With the application of proteomic methods, particularly 2D-gel and gel-free, LC/MS-based methods, insights into the composition and dynamic changes of the guard cell proteome could be obtained. It is reasonable to assume that a thorough understanding of guard cell response to abiotic stress at the molecular level is a prerequisite for its effective management. Notwithstanding, the molecular mechanism involved in guard cell movements is seemingly complex and requires information at the post-genomic level to understand it effectively. In this regard, the ever-growing field of proteomics is also being effectively employed for investigating guard cell responses in land plants. The development of proteomics techniques allowing increased proteome coverage and quantitative measurements of proteins will be particularly instrumental to characterize proteomes and their modulation during guard cell movements. Despite important advances, plant proteome analysis, including those of model plant species, remain constrained by limitations inherent to proteomics techniques and data interpretation. Here we have, accordingly, highlighted the prominent approaches and achievements of proteomics with model plant *Arabidopsis* and have not discussed the current limitations of plant proteomics, which has been expertly reviewed elsewhere (Lilley & Dupree 2007; Abril *et al*. 2011; Nakagami *et al*. 2012; Vanderschuren *et al*. 2013). We anticipate future directions that could advance the contribution of plant proteomics to crop improvement and additionally indicates that proteomic approaches could generate a huge amount of data, and therefore adequate advancements in computational and mathematical tools are a must to be achieved for effective analysis. It is important to note, however, that the integration of genomic-scale information to address complex genetics and physiological questions still remains challenging.

## Metabolomics studies

Last, but by no means not least, it is plausible that metabolomics of guard cells will ultimately become a highly powerful approach in dissecting the functioning of guard cells. Although no single analytical system is ever likely to cover the whole metabolome technological developments have considerably extended our ability to analyse complex biological systems, facilitating the simultaneous detection of different compound classes with diverse chemical properties (Osorio *et al*. 2012). Notably, the development of new technologies might ameliorate the problem of limited metabolite coverage. It is important to mention, however, that given the level of physical and chemical complexity of properties of metabolites coupled with other factors, such as the dynamic measurement range that is required, make the development of a single analytical platform that will provide a comprehensive analysis of the cellular metabolome a formidable challenge (Fernie *et al*. 2004; Misra *et al*. 2014), rendering metabolomics more complicated than other post-genomic analysis. To date, metabolomic analyses in guard cells are still incipient compared with transcriptomic and proteomic. Although the focus of metabolomics has largely been to elucidate the flow of mass in the substrate–product conversions, metabolomics may also be used as a tool for the elucidation of the information flow in cellular signalling networks, as we illustrate later.

Using liquid chromatography–multiple reaction monitoring mass spectrometry for targeted analysis of 85 signalling-related metabolites in *Arabidopsis* guard cell protoplasts over a time course of ABA treatment, it was possible to dissect signalling aspects of the guard cell in response to ABA (Jin *et al*. 2013). For this purpose, *Arabidopsis* wild-type plants (Col-0) and *gpa1* mutants, which have ABA-hyposensitive stomata (Zhao *et al*. 2010), were evaluated. The metabolomes of these plants revealed coordinated regulation of signalling metabolites in unrelated biochemical pathways. Interestingly, hormone metabolites were responsive to ABA, with generally greater responsiveness in Col-0 than in *gpa1*. Thus, for instance, indole-3-acetic acid (IAA) levels were decreased by ABA in wild-type guard cells, but not in *gpa1* guard cells. Additionally, the majority of hormones also displayed different ABA responses in guard cell metabolite profiles when compared with the one observed in mesophyll cell metabolomes, suggesting that ABA is most likely an upstream actor to regulate other hormones (Jin *et al*. 2013).

Indeed, it seems clear that hormones are good targets to investigate guard cell metabolomics and although great attention has been paid to ABA, there is a crosstalk between ABA and other hormones that can also affect stomatal movements. For instance, brassinosteroid and jasmonate can act concurrently with ABA promoting senescence and programmed cell death (Zhang *et al*. 2009; Hossain *et al*. 2011). On the other hand, other hormones such as cytokinin, auxin, salicylic acid and ethylene can act antagonistically to ABA in response to water deficit (Tanaka *et al*. 2005; Pinheiro & Chaves 2011; Ha *et al*. 2012; Chen *et al*. 2013; Meguro & Sato 2014).

The increased photosynthesis and whole-plant biomass observed in tomato plants where antisense inhibition of the iron–sulphur subunit of the succinate dehydrogenase (SDH) was performed seems to be related to an organic acid-mediated effect on stomatal aperture (Araújo *et al*. 2011c). These results are diametrically opposite to those obtained for

antisense inhibition of fumarase, where decreased photosynthesis and biomass were observed (Nunes-Nesi *et al*. 2007). Furthermore, measurement of apoplastic organic acid levels in SDH and fumarase antisense plants, revealed a negative correlation between the levels of fumarate and stomatal conductance, although the influence of fumarate appears to be weaker than that of malate (Araújo *et al*. 2011c). It is highly interesting that similar results were obtained by inhibiting two different complex II subunits, the iron–sulphur subunit in tomato (Araújo *et al*. 2011c) and the flavoprotein in *Arabidopsis* (Fuentes *et al*. 2011). Taken together, the results of these work provided compelling evidence to support that modulation of malate and fumarate concentration can strongly impact stomatal movements. Perhaps more importantly, these results also provide strong support of the theory that guard cells are not autonomously regulated (Mott 2009) and that the mesophyll harbours significant control over guard cell movements (Lee *et al*. 2008b; Fernie & Martinoia 2009; Mott 2009; Araújo *et al*. 2011b). Collectively, these results also indicate that mesophyll-derived signals (e.g. malate and fumarate), which play an important role in regulating stomatal movements (Hedrich *et al*. 1994; Araújo *et al*. 2011c), may be candidate signalling molecules. Importantly, further identification of mesophyll-derived signal molecules will provide essential information about $CO_2$-signalling mechanisms including guard cell receptors that sense $CO_2$ signals from the mesophyll. In summary, metabolite profiling has aided in the identification of novel interactions between the tricarboxylic acid (TCA) cycle and photosynthesis and stomatal function. Nevertheless, the metabolic and molecular regulatory hierarchy underlying this highly specialized cell type is as yet not fully understood and therefore further work is clearly required in order to establish the regulatory mechanisms involved in such responses.

Overall, while post-genomic technologies have already aided our understanding of guard cell metabolism at a systems level through additions to the 'parts list' of the metabolic network, they are poised to become more useful still through the discovery of new interactions and the provision of the quantitative data required for the construction of predictive models of metabolism. It should be mentioned that, alongside other studies, metabolic studies of this highly specialized cell type has demonstrate to be useful in increasing our understanding of the hormonal crosstalk and metabolic regulation of stomatal movement that is important for plant growth, development, yield and response to environmental factors. It is no doubt that the further development and combination of many analytical techniques (Fig. 1) will additionally allow a fuller description of the metabolic network in a guard cell context.

## Opportunities and challenges in systems modelling of stomatal function

Classical modelling approaches focus on expressing the stomatal conductance ($g_s$) as a function of other external and internal factors. The goal of this section is not to offer an overview of the existing modelling approaches; the reader is instructed to consult previous comprehensive reviews (Damour *et al*. 2010; Buckley & Mott 2013). These reviews have already categorized the existing models into three groups, largely based on the methodology used for their establishment, namely: purely data-based (e.g. developed by the boundary-line method; Jarvis 1976), mechanistic (e.g. based on the consideration of hydraulic properties and biophysical properties of guard cells) (Cowan 1972), and optimization-based (i.e. based on the idea that plants use the limiting resources in the most optimal way towards fulfilling a task) (Cowan & Farquhar 1977).

The above mentioned experimental evidence has clearly indicated that understanding of stomatal function has to directly consider the gradient in spatio-temporal scales, starting from modelling of single guard cell over fast changes in environmental determinants to theoretical investigations of the interactions between guard and mesophyll cells via various feedback loops and their coupling to data read-out to modelling of canopy over developmental and environmental gradients. The particular modelling question would determine the type of modelling strategy that has to be used; for instance, dynamic changes of well-characterized (sub)systems over short time intervals can be readily undertaken through kinetic modelling, whereas analysis of typical long-term or steady-state behaviour as well as integration of data from multiple cellular components is more readily tackled by means of large-scale stoichiometric models which often do not require kinetic parameterization (see following paragraphs for detailed discussion). The vast time scales of cellular processes that occur at different levels of cellular organization, ranging from metabolism (as fast) to protein synthesis and gene regulation (as slower) will also delineate the applicability of quasy-steady-state assumption as well as the lumping of various components as it is usually performed in modelling studies (Famili & Palsson 2003; Jamshidi & Palsson 2008).

The existing model categories and their combinations have clearly contributed to the predictive modelling and refinement of the relationship between $g_s$ and its determinants. They have, however, had limited success in illuminating how the changes in stomatal movement, and through it $g_s$, are affected by the interplay of the environment, the various cellular organizational levels (e.g. transcripts, proteins, and metabolites), and the coordination between different cell types (e.g. guard and mesophyll cells). Therefore, despite efforts made to link environmental and endogenous factors to stomatal movements in mathematical models, these modelling approaches have not been used to determine well-planned *in silico* genetic manipulation strategies to investigate means by which to alter conductance-dependent traits and do not integrate data from multiple environments with the purpose of more accurate parameterization. Furthermore, these modelling approaches need to be continuously improved and augmented by inspecting not only the fit of the model predictions under various environmental factors but also from genetic manipulation strategies altering conductance-dependent traits. In fact, our current view is that

to develop an integrated understanding of stomatal function, the modelling approaches must couple the several processes across all levels of stomatal movements. Accordingly, it seems reasonable to assume that a single model of stomatal function must encompass all of those surrounding processes, including naturally the interactions between guard cells and surrounding tissues and their coupling with the environment (Lawson & Blatt 2014). Finally, the importance of these models will become prominent due to their ultimate test from investigating and validating genetic manipulation strategies from seemingly unrelated aspects of cellular subsystems, from metabolism down to gene regulation.

These challenges could, in part, be addressed by kinetic stomatal models of smaller scale, for which the kinetic form of the reaction rates (e.g. Michaelis–Menten) together with its numerous parameters, may be more facile to obtain. The sole prominent example of this direction is the kinetic-based modelling approach proposed initially (Hills *et al*. 2012) and more thoroughly validated later (Chen *et al*. 2012; Wang *et al*. 2012; Blatt *et al*. 2013). This kinetic model is implemented within the OnGuard software package (Available at http://psrg.org.uk/guard-cell-modelling/), a computational platform incorporating properties of transporters at the plasma membrane and tonoplast, features of osmolite metabolism, as well as the characteristics such as the cytosolic pH and $Ca^{2+}$ buffering capacity (Lawson & Blatt 2014). We would like to point out that the current implementation includes data-driven parameterization of the model as well as investigation of the effects of parameter changes on the quantitative predictions. Thus, the existing *in silico* studies based on OnGuard have demonstrated the capacity of this framework to provide a multitude of quantitative predictions which can now readily be used for goodness-of-fit testing with data from independent experiments and for improved calibration of the model. While the currently implemented model has aided the quantitative understanding of stomata behaviour as a function of few metabolic reactions, related to proxies for osmolites, transport and signalling, its role in design of metabolic engineering strategies, because of the number of considered genes, enzymes and metabolites, remains to be experimentally demonstrated. Therefore, cell-specific manipulation of metabolic pathways and their effects on stomatal functions seem challenging to investigate in the framework of OnGuard.

Genome-scale metabolic modelling offers the opportunity to overcome the aforementioned problems of the existing modelling approaches. This is due to the fact that genome-scale metabolic models consider the entirety of the characterized biochemical reactions in a particular organism (Bordbar *et al*. 2014). Therefore, they readily facilitate a direct *in silico* inspection of the effects of environmental changes or reaction manipulations (e.g. knock-out mutants, silencing of expression or overexpression strategies) (Lewis *et al*. 2012) on particular composite traits such as biomass or reaction fluxes. Moreover, methodological advances have allowed direct integration of transcriptomics and proteomics datasets resulting in more physiologically relevant predictions of metabolic states of specific cell types under different conditions (Sweetlove & Ratcliffe 2011; Töpfer *et al*. 2013, 2014). Most importantly, recent studies have focused on using the data generated by these high-throughput technologies to arrive at context-specific metabolic networks, where a context stands either for a particular genotype, organ and cell type (e.g. guard cell), or for different environmental conditions (Estévez & Nikoloski 2014). Such models will have to be general enough to simulate different environments, which challenges the usage of condition-independent biomass reaction (Feist & Palsson 2010) (see critique in Töpfer *et al*. 2013 for plants) or different tasks such as ATP production (Fig. 2) usually assumed to be optimized for modelling using flux balance analysis (FBA) (Boyle *et al*. 2009; Raman & Chandra 2009), which is reasonable to apply for guard cell modelling given the importance of the ATP turnover in guard cells (Suetsugu *et al*. 2014; Wang *et al*. 2014a,b).

In parallel with modelling advances for C3 model plants, *Arabidopsis*, (de Oliveira Dal'Molin *et al*. 2010a; Arnold & Nikoloski 2013, 2014; and references therein), there have been developments and refinement of genome-scale metabolic models for C4 model plants (e.g. maize). The latter are more involved as they capture the interplay between two cell types, bundle sheath and mesophyll, via transport of different metabolites through the plasmodesmata (de Oliveira Dal'Molin *et al*. 2010b; Saha *et al*. 2011; Simons *et al*. 2014). Therefore, they can provide the impetus for modelling the communication between guard and mesophyll cells to simulate leaf growth. Such an approach would also provide the necessary comparison between C3 and C4 species with respect to the behaviour of such multicellular systems in terms of different properties, including efficiency of resource usage and patterns of (re)allocation upon different changes, giving this line of research an evolutionary perspective (Mallmann *et al*. 2014).

However, this approach also has numerous challenges because of the nature of the model and the type of reactions considered. First, as prominent constraint-based methods to analyse genome-scale models, FBA and its derivatives largely assume steady-state behaviour, although stomatal movement is a dynamic process. Therefore, it is necessary to develop novel methods to allow investigations of dynamical aspects of large-scale models, particularly as the existing solutions, such as dynamic FBA, can only be applied to models of small to moderate size because of the large computational demands of the employ formulation (Kleessen & Nikoloski 2012; Kleessen *et al*. 2012). Second, these genome-scale metabolic models mostly neglect regulatory and signalling cascade, which can modulate the behaviour of metabolism, although recent method developments have rendered the integration of transcriptional regulatory cascades possible in *Escherichia coli* and *Micobacterium tuberculosis* (Chandrasekaran & Price 2010, 2013) and signalling cascades in a small network for *Saccharomyces cerevisiae* (Lee *et al*. 2008a). Moreover, as the behaviour of signalling pathways usually depends on the concentration of the ligand (e.g. metabolite, which modulates the transduction of the signal to the other cellular levels), the genome-scale models will have

to move from flux-centric to concentration-centric in order to allow the association of flux distributions with the concentrations of the considered metabolites (Töpfer *et al*. 2015). Resolving these challenges in parallel with the development of large-scale models of guard cell metabolism will most likely pave the way for truly predictive modelling (and validation), which will certainly have far-reaching applications.

Finally, aside from the issues related to simulation of the dynamics process, one has to consider the effect of spatial scales. To this end, the existing models of $g_s$ for single leaves have been scaled up to the level of canopy, often performed following the big-leaf top-down approach (Baldocchi *et al*. 1991). To this end, there is the alternative of determining the canopy $g_s$ as the sum of the conductance of individual leaves (see Blonquist *et al*. 2009) or following the Penman–Monteith equation (Monteith 1981; Furon *et al*. 2007). The former could be used to combine multiple large-scale models of illuminated and shaded leaves, with the idea of expanding the applicability of the large-scale models on the level of canopy, a much desired extension of the applicability of constraint-based approaches.

## CONCLUDING REMARKS

Prompted by the discovery that genetic manipulation of guard cells is a promising strategy to improve plant growth, water-use efficiency and drought tolerance (Lebaudy *et al*. 2008; Antunes *et al*. 2012; De Angeli *et al*. 2013; Schroeder *et al*. 2013; Wang *et al*. 2014b), recent years have seen the accumulation of experimental evidence concerning different aspects of stomatal behaviour. This is largely due to elegant studies of molecular physiology of guard cells based on application of high-throughput technologies ranging from transcriptomics and proteomics to metabolomics. Our opinion is that the gathered large-scale datasets provide the basis for the creation of dynamic genome-scale metabolic models of guard cells. We posit that their coupling to models of other cell types will allow us to predict targets for genetic manipulation to improve crop yield, particularly under sub-optimal conditions.

Given the complexity of the interconnected networks governing stomatal movements under extremely variable internal and external conditions, we argue that a systems approach, which simultaneously uses different high-throughput technologies to gather data and then integrates them within large-scale models of regulation, signalling and metabolism is a viable strategy towards the rational design of intervention strategies. Such an approach is greatly facilitated by recent advances in context-specific models of plant metabolism and methods for integration of metabolomics data in flux-oriented approaches.

The grand challenge for this research field is to gain a fuller understanding as to how the regulation of stomatal movement occurs and how it may have evolved because of the interplay between genotypes and changing environments. Use of mathematical approaches to enhance our understanding of the interaction of the various molecular components of the cell (and their dynamic changes underlying this process) and how they are adjusted following environmental changes, can be evaluated in large-scale models in a relatively facile manner. While we are aware that achieving this goal is a vastly challenging task for any cell type we feel that the accessibility of guard cells and the relatively easy enrichment procedures involved in their isolation render them a valuable cell type not only for investigating this specific interaction between a plant cell and its environment as well as between different tightly coupled cell types, but also for looking at the specialization of plant cell function in general.

## ACKNOWLEDGMENTS

This work was supported by funding from the Max Planck Society (to A.R.F., Z.N., W.L.A.) and the National Council for Scientific and Technological Development (CNPq-Brazil, Grant 483525/2012-0 to W.L.A.). Scholarships granted by CNPq-Brazil and FAPEMIG to D.B.M. and D.M.D., and research fellowships granted by CNPq-Brazil to W.L.A. are also gratefully acknowledged.

**Conflicts of Interest:** The authors declare that the research was conducted in the absence of any commercial or financial relationships that could be construed as a potential conflict of interest.

## REFERENCES

Abril N., Gion J.-M., Kerner R., Müller-Starck G., Cerrillo R.M.N., Plomion C., . . . Jorrin-Novo J.V. (2011) Proteomics research on forest trees, the most recalcitrant and orphan plant species. *Phytochemistry* **72,** 1219–1242.

Antunes W.C., Provart N.J., Williams T.C.R. & Loureiro M.E. (2012) Changes in stomatal function and water use efficiency in potato plants with altered sucrolytic activity. *Plant, Cell & Environment* **35,** 747–759.

Araújo W.L., Fernie A.R. & Nunes-Nesi A. (2011a) Control of stomatal aperture: a renaissance of the old guard. *Plant Signaling & Behavior* **6,** 1305–1311.

Araújo W.L., Nunes-Nesi A. & Fernie A.R. (2011b) Fumarate: multiple functions of a simple metabolite. *Phytochemistry* **72,** 838–843.

Araújo W.L., Nunes-Nesi A., Osorio S., Usadel B., Fuentes D., Nagy R., . . . Fernie A.R. (2011c) Antisense inhibition of the iron–sulphur subunit of succinate dehydrogenase enhances photosynthesis and growth in tomato via an organic acid-mediated effect on stomatal aperture. *The Plant Cell* **23,** 600–627.

Araújo W.L., Nunes-Nesi A. & Williams T.C.R. (2012) Functional genomics tools applied to plant metabolism: a survey on plant respiration, its connections and the annotation of complex gene functions. *Frontiers in Plant Science* **3,** 210.

Arnold A. & Nikoloski Z. (2013) Comprehensive classification and perspective for modelling photorespiratory metabolism. *Plant Biology* **15,** 667–675.

Arnold A. & Nikoloski Z. (2014) Bottom-up metabolic reconstruction of *Arabidopsis* and its application to determining the metabolic costs of enzyme production. *Plant Physiology* **165,** 1380–1391.

Assmann S.M. (2010) Hope for humpty dumpty: systems biology of cellular signaling. *Plant Physiology* **152,** 470–479.

Baldocchi D.D., Luxmoore R.J. & Hatfield J.L. (1991) Discerning the forest from the trees: an essay on scaling canopy stomatal conductance. *Agricultural and Forest Meteorology* **54,** 197–226.

Bates G.W., Rosenthal D.M., Sun J., Chattopadhyay M., Peffer E., Yang J., . . . Jones A.M. (2012) A comparative study of the *Arabidopsis thaliana* guard-cell transcriptome and its modulation by sucrose. *PLoS ONE* **7,** e49641.

Bauer H., Ache P., Lautner S., Fromm J., Hartung W., Al-Rasheid Khaled A.S., . . . Hedrich R. (2013) The stomatal response to reduced relative humidity requires guard cell-autonomous ABA synthesis. *Current Biology* **23,** 53–57.

Bergmann D.C. & Sack F.D. (2007) Stomatal development. *Annual Review of Plant Biology* **58,** 163–181.

Berry J.A., Beerling D.J. & Franks P.J. (2010) Stomata: key players in the earth system, past and present. *Current Opinion in Plant Biology* **13,** 232–239.

Bessey C.E. (1898) Some considerations upon the functions of stomata. *Science* **7,** 13–16.

Bessire M., Chassot C., Jacquat A.-C., Humphry M., Borel S., Petétot J.M.-C., . . . Nawrath C. (2007) A permeable cuticle in *Arabidopsis* leads to a strong resistance to *Botrytis cinerea*. *The EMBO Journal* **26,** 2158–2168.

Blatt M.R. (2000) Cellular signaling and volume control in stomatal movements in plants. *Annual Review of Cell and Developmental Biology* **16,** 221–241.

Blatt M.R., Wang Y., Leonhardt N. & Hills A. (2013) Exploring emergent properties in cellular homeostasis using OnGuard to model $K^+$ and other ion transport in guard cells. *Journal of Plant Physiology* **171,** 770–778.

Blonquist J.M. Jr., Norman J.M. & Bugbee B. (2009) Automated measurement of canopy stomatal conductance based on infrared temperature. *Agricultural and Forest Meteorology* **149,** 1931–1945.

Bordbar A., Monk J.M., King Z.A. & Palsson B.O. (2014) Constraint-based models predict metabolic and associated cellular functions. *Nature Reviews Genetics* **15,** 107–120.

Boyle N.R., Shastri A.A. & Morgan J.A. (2009) Network stoichiometry. In *Plant Metabolic Networks* (ed. J. Schwender), pp. 211–243. Springer, New York, NY, USA.

Buckley T.N. & Mott K.A. (2013) Modelling stomatal conductance in response to environmental factors. *Plant, Cell & Environment* **36,** 1691–1699.

Buschhaus C. & Jetter R. (2011) Composition differences between epicuticular and intracuticular wax substructures: how do plants seal their epidermal surfaces? *Journal of Experimental Botany* **62,** 841–853.

Casson S.A. & Hetherington A.M. (2010) Environmental regulation of stomatal development. *Current Opinion in Plant Biology* **13,** 90–95.

Chandrasekaran S. & Price N.D. (2010) Probabilistic integrative modeling of genome-scale metabolic and regulatory networks in *Escherichia coli* and *Mycobacterium tuberculosis*. *Proceedings of the National Academy of Sciences of the United States of America* **107,** 17845–17850.

Chandrasekaran S. & Price N.D. (2013) Metabolic constraint-based refinement of transcriptional regulatory networks. *PLoS Computational Biology* **9,** e1003370.

Chen L.I.N., Dodd I.C., Davies W.J. & Wilkinson S. (2013) Ethylene limits abscisic acid- or soil drying-induced stomatal closure in aged wheat leaves. *Plant, Cell & Environment* **36,** 1850–1859.

Chen Z.-H., Hills A., Baetz U., Amtmann A., Lew V. & Blatt M.R. (2012) Systems dynamic modelling of the stomatal guard cell predicts emergent behaviours in transport, signalling and volume control. *Plant Physiology* **159,** 1235–1251.

Cominelli E., Galbiati M., Vavasseur A., Conti L., Sala T., Vuylsteke M., . . . Tonelli C. (2005) A guard-cell-specific MYB transcription factor regulates stomatal movements and plant drought tolerance. *Current Biology* **15,** 1196–1200.

Cowan I.R. (1972) Oscillations in stomatal conductance and plant functioning associated with stomatal conductance: observations and a model. *Planta* **106,** 185–219.

Cowan I.R. & Farquhar G.D. (1977) Stomatal function in relation to leaf metabolism and environment. *Symposia of the Society for Experimental Biology* **31,** 471–505.

de Oliveira Dal'Molin C.G., Quek L.-E., Palfreyman R.W., Brumbley S.M. & Nielsen L.K. (2010a) AraGEM, a genome-scale reconstruction of the primary metabolic network in *Arabidopsis*. *Plant Physiology* **152,** 579–589.

de Oliveira Dal'Molin C.G., Quek L.-E., Palfreyman R.W., Brumbley S.M. & Nielsen L.K. (2010b) C4GEM, a genome-scale metabolic model to study C4 plant metabolism. *Plant Physiology* **154,** 1871–1885.

Damour G., Simonneau T., Cochard H. & Urban L. (2010) An overview of models of stomatal conductance at the leaf level. *Plant, Cell & Environment* **33,** 1419–1438.

De Angeli A., Zhang J., Meyer S. & Martinoia E. (2013) *At*ALMT9 is a malate-activated vacuolar chloride channel required for stomatal opening in *Arabidopsis*. *Nature Communications* **4,** 1804.

Dow G.J. & Bergmann D.C. (2014) Patterning and processes: how stomatal development defines physiological potential. *Current Opinion in Plant Biology* **21,** 67–74.

Estévez S.R. & Nikoloski Z. (2014) Generalized framework for context-specific metabolic model extraction methods. *Frontiers in Plant Science* **5,** 491.

Fahey J.W., Zalcmann A.T. & Talalay P. (2001) The chemical diversity and distribution of glucosinolates and isothiocyanates among plants. *Phytochemistry* **56,** 5–51.

Famili I. & Palsson B.O. (2003) The convex basis of the left null space of the stoichiometric matrix leads to the definition of metabolically meaningful pools. *Biophysical Journal* **85,** 16–26.

Feist A.M. & Palsson B.O. (2010) The biomass objective function. *Current Opinion in Microbiology* **13,** 344–349.

Fernie A.R. & Martinoia E. (2009) Malate. Jack of all trades or master of a few? *Phytochemistry* **70,** 828–832.

Fernie A.R. & Stitt M. (2012) On the discordance of metabolomics with proteomics and transcriptomics: coping with increasing complexity in logic, chemistry, and network interactions scientific correspondence. *Plant Physiology* **158,** 1139–1145.

Fernie A.R., Trethewey R.N., Krotzky A.J. & Willmitzer L. (2004) Metabolite profiling: from diagnostics to systems biology. *Nature Reviews Molecular Cell Biology* **5,** 763–769.

Fuentes D., Meneses M., Nunes-Nesi A., Araújo W.L., Tapia R., Gómez I., . . . Jordana X. (2011) A deficiency in the flavoprotein of *Arabidopsis* mitochondrial complex II results in elevated photosynthesis and better growth in nitrogen-limiting conditions. *Plant Physiology* **157,** 1114–1127.

Fujii H., Chinnusamy V., Rodrigues A., Rubio S., Antoni R., Park S.-Y., . . . Zhu J.-K. (2009) *In vitro* reconstitution of an abscisic acid signalling pathway. *Nature* **462,** 660–664.

Furon A.C., Warland J.S. & Wagner-Riddle C. (2007) Analysis of scaling-up resistances from leaf to canopy using numerical simulations. *Agronomy Journal* **99,** 1483–1491.

Ha S., Vankova R., Yamaguchi-Shinozaki K., Shinozaki K. & Tran L.-S.P. (2012) Cytokinins: metabolism and function in plant adaptation to environmental stresses. *Trends in Plant Science* **17,** 172–179.

Hashimoto M., Negi J., Young J., Israelsson M., Schroeder J.I. & Iba K. (2006) *Arabidopsis* HT1 kinase controls stomatal movements in response to $CO_2$. *Nature Cell Biology* **8,** 391–397.

Hedrich R., Marten I., Lohse G., Dietrich P., Winter H., Lohaus G. & Heldt H.-W. (1994) Malate-sensitive anion channels enable guard cells to sense changes in the ambient $CO_2$ concentration. *The Plant Journal* **6,** 741–748.

Hetherington A.M. & Brownlee C. (2004) The generation of $Ca^{2+}$ signals in plants. *Annual Review of Plant Biology* **55,** 401–427.

Hetherington A.M. & Woodward F.I. (2003) The role of stomata in sensing and driving environmental change. *Nature* **424,** 901–908.

Hills A., Chen Z.-H., Amtmann A., Blatt M.R. & Lew V.L. (2012) OnGuard, a computational platform for quantitative kinetic modeling of guard cell physiology. *Plant Physiology* **159,** 1026–1042.

Hossain M.A., Munemasa S., Uraji M., Nakamura Y., Mori I.C. & Murata Y. (2011) Involvement of endogenous abscisic acid in methyl jasmonate-induced stomatal closure in *Arabidopsis*. *Plant Physiology* **156,** 430–438.

Hosy E., Vavasseur A., Mouline K., Dreyer I., Gaymard F., Porée F., . . . Sentenac H. (2003) The *Arabidopsis* outward $K^+$ channel GORK is involved in regulation of stomatal movements and plant transpiration. *Proceedings of the National Academy of Sciences of the United States of America* **100,** 5549–5554.

Hubbard K.E., Siegel R.S., Valerio G., Brandt B. & Schroeder J.I. (2012) Abscisic acid and $CO_2$ signalling via calcium sensitivity priming in guard cells, new CDPK mutant phenotypes and a method for improved resolution of stomatal stimulus–response analyses. *Annals of Botany* **109,** 5–17.

Ideker T. & Krogan N.J. (2012) Differential network biology. *Molecular Systems Biology* **8,** 565.

Israelsson M., Siegel R.S., Young J., Hashimoto M., Iba K. & Schroeder J.I. (2006) Guard cell ABA and $CO_2$ signaling network updates and $Ca^{2+}$ sensor priming hypothesis. *Current Opinion in Plant Biology* **9,** 654–663.

Jamshidi N. & Palsson B.Ø. (2008) Top-down analysis of temporal hierarchy in biochemical reaction networks. *PLoS Computational Biology* **4,** e1000177.

Jarvis P.G. (1976) The interpretation of the variations in leaf water potential and stomatal conductance found in canopies in the field. *Philosophical Transactions of the Royal Society of London. Series B* **273,** 503–610.

Jin X., Wang R.-S., Zhu M., Jeon B.W., Albert R., Chen S. & Assmann S.M. (2013) Abscisic acid-responsive guard cell metabolomes of *Arabidopsis* wild-type and *gpa1* G-protein mutants. *The Plant Cell* **25,** 4789–4811.

Kim T.-H., Böhmer M., Hu H., Nishimura N. & Schroeder J.I. (2010) Guard cell signal transduction network: advances in understanding abscisic acid, $CO_2$, and $Ca^{2+}$ signaling. *Annual Review of Plant Biology* **61,** 561–591.

Kleessen S. & Nikoloski Z. (2012) Dynamic regulatory on/off minimization for biological systems under internal temporal perturbations. *BMC Systems Biology* **6,** 16.

Kleessen S., Araújo W.L., Fernie A.R. & Nikoloski Z. (2012) Model-based confirmation of alternative substrates of mitochondrial electron transport chain. *The Journal of Biological Chemistry* **287,** 11122–11131.

Kumar R., Arya G.C. & Bisht N.C. (2014) Differential expression and interaction specificity of heterotrimeric G-protein family in *Brassica nigra* reveal their developmental and condition-specific roles. *Plant and Cell Physiology* **55,** 1954–1968.

Lawson T. & Blatt M.R. (2014) Stomatal size, speed, and responsiveness impact on photosynthesis and water use efficiency. *Plant Physiology* **164,** 1556–1570.

Lawson T., Simkin A.J., Kelly G. & Granot D. (2014) Mesophyll photosynthesis and guard cell metabolism impacts on stomatal behaviour. *The New Phytologist* **203,** 1064–1081.

Lebaudy A., Vavasseur A., Hosy E., Dreyer I., Leonhardt N., Thibaud J.-B., . . . Sentenac H. (2008) Plant adaptation to fluctuating environment and biomass production are strongly dependent on guard cell potassium channels. *Proceedings of the National Academy of Sciences of the United States of America* **105,** 5271–5276.

Lee J.M., Gianchandani E.P., Eddy J.A. & Papin J.A. (2008a) Dynamic analysis of integrated signaling, metabolic, and regulatory networks. *PLoS Computational Biology* **4,** e1000086.

Lee M., Choi Y., Burla B., Kim Y.-Y., Jeon B., Maeshima M., . . . Lee Y. (2008b) The ABC transporter *At*ABCB14 is a malate importer and modulates stomatal response to $CO_2$. *Nature Cell Biology* **10,** 1217–1223.

Leonhardt N., Kwak J.M., Robert N., Waner D., Leonhardt G. & Schroeder J.I. (2004) Microarray expression analyses of *Arabidopsis* guard cells and isolation of a recessive abscisic acid hypersensitive protein phosphatase 2C mutant. *The Plant Cell* **16,** 596–615.

Lewis N.E., Nagarajan H. & Palsson B.O. (2012) Constraining the metabolic genotype–phenotype relationship using a phylogeny of *in silico* methods. *Nature Reviews. Microbiology* **10,** 291–305.

Lilley K.S. & Dupree P. (2007) Plant organelle proteomics. *Current Opinion in Plant Biology* **10,** 594–599.

Liu X., Yue Y., Li B., Nie Y., Li W., Wu W.-H. & Ma L. (2007) A G protein-coupled receptor is a plasma membrane receptor for the plant hormone abscisic acid. *Science* **315,** 1712–1716.

Mallmann J., Heckmann D., Bräutigam A., Lercher M.J., Weber A.P., Westhoff P. & Gowik U. (2014) The role of photorespiration during the evolution of C4 photosynthesis in the genus. *Flaveria. eLife* **3,** e02478.

Martin L., Fei Z., Giovannoni J. & Rose J.K.C. (2013) Catalyzing plant science research with RNA-seq. *Frontiers in Plant Science* **4,** 66.

Meguro A. & Sato Y. (2014) Salicylic acid antagonizes abscisic acid inhibition of shoot growth and cell cycle progression in rice. *Scientific Reports* **4,** 4555.

Meyer S., De Angeli A., Fernie A.R. & Martinoia E. (2010) Intra- and extra-cellular excretion of carboxylates. *Trends in Plant Science* **15,** 40–47.

Misra B.B., Assmann S.M. & Chen S. (2014) Plant single-cell and single-cell-type metabolomics. *Trends in Plant Science* **19,** 637–646.

Monteith J.L. (1981) Evaporation and surface temperature. *Quarterly Journal of the Royal Meteorological Society* **107,** 1–27.

Mott K.A. (2009) Opinion: stomatal responses to light and $CO_2$ depend on the mesophyll. *Plant, Cell & Environment* **32,** 1479–1486.

Nakagami H., Sugiyama N., Ishihama Y. & Shirasu K. (2012) Shotguns in the front line: phosphoproteomics in plants. *Plant and Cell Physiology* **53,** 118–124.

Negi J., Moriwaki K., Konishi M., Yokoyama R., Nakano T., Kusumi K., . . . Iba K. (2013) A Dof transcription factor, SCAP1, is essential for the development of functional stomata in *Arabidopsis*. *Current Biology* **23,** 479–484.

Nunes-Nesi A., Carrari F., Gibon Y., Sulpice R., Lytovchenko A., Fisahn J., . . . Fernie A.R. (2007) Deficiency of mitochondrial fumarase activity in tomato plants impairs photosynthesis via an effect on stomatal function. *The Plant Journal* **50,** 1093–1106.

Osorio S., Do P.T. & Fernie A.R. (2012) Profiling primary metabolites of tomato fruit with gas chromatography/mass spectrometry. *Methods in Molecular Biology* **860,** 101–109.

Pandey S., Nelson D.C. & Assmann S.M. (2009) Two novel GPCR-type G Proteins are abscisic acid receptors in *Arabidopsis*. *Cell* **136,** 136–148.

Pandey S., Wang R.-S., Wilson L., Li S., Zhao Z., Gookin T.E., . . . Albert R. (2010) Boolean modeling of transcriptome data reveals novel modes of heterotrimeric G-protein action. *Molecular Systems Biology* **6,** 372.

Park S.-Y., Fung P., Nishimura N., Jensen D.R., Fujii H., Zhao Y., . . . Cutler S.R. (2009) Abscisic acid inhibits type 2C protein phosphatases via the PYR/PYL family of START proteins. *Science* **324,** 1068–1071.

Pinheiro C. & Chaves M.M. (2011) Photosynthesis and drought: can we make metabolic connections from available data? *Journal of Experimental Botany* **62,** 869–882.

Raman K. & Chandra N. (2009) Flux balance analysis of biological systems: applications and challenges. *Briefings in Bioinformatics* **10,** 435–449.

Roelfsema M.R.G. & Hedrich R. (2010) Making sense out of $Ca^{2+}$ signals: their role in regulating stomatal movements. *Plant, Cell & Environment* **33,** 305–321.

Saha R., Suthers P.F. & Maranas C.D. (2011) *Zea mays i*RS1563: a comprehensive genome-scale metabolic reconstruction of maize metabolism. *PLoS ONE* **6,** e21784.

Schreiber L. (2010) Transport barriers made of cutin, suberin and associated waxes. *Trends in Plant Science* **15,** 546–553.

Schroeder J.I., Allen G.J., Hugouvieux V., Kwak J.M. & Waner D. (2001) Guard cell signal transduction. *Annual Review of Plant Physiology and Plant Molecular Biology* **52,** 627–658.

Schroeder J.I., Delhaize E., Frommer W.B., Guerinot M.L., Harrison M.J., Herrera-Estrella L., . . . Sanders D. (2013) Using membrane transporters to improve crops for sustainable food production. *Nature* **497,** 60–66.

Shimazaki K., Doi M., Assmann S.M. & Kinoshita T. (2007) Light regulation of stomatal movement. *Annual Review of Plant Biology* **58,** 219–247.

Simons M., Saha R., Guillard L., Clément G., Armengaud P., Cañas R., . . . Hirel B. (2014) Nitrogen-use efficiency in maize (*Zea mays* L.): from 'omics' studies to metabolic modelling. *Journal of Experimental Botany* **65,** 5657–5671.

Sirichandra C., Wasilewska A., Vlad F., Valon C. & Leung J. (2009) The guard cell as a single-cell model towards understanding drought tolerance and abscisic acid action. *Journal of Experimental Botany* **60,** 1439–1463.

Song Y., Miao Y. & Song C.-P. (2014) Behind the scenes: the roles of reactive oxygen species in guard cells. *The New Phytologist* **201,** 1121–1140.

Suetsugu N., Takami T., Ebisu Y., Watanabe H., Iiboshi C., Doi M. & Shimazaki K. (2014) Guard cell chloroplasts are essential for blue light-dependent stomatal opening in *Arabidopsis*. *PLoS ONE* **9,** e108374.

Sweetlove L.J. & Ratcliffe R.G. (2011) Flux-balance modelling of plant metabolism. *Frontier in Plant Science* **2,** 38.

Tallman G. (2004) Are diurnal patterns of stomatal movement the result of alternating metabolism of endogenous guard cell ABA and accumulation of ABA delivered to the apoplast around guard cells by transpiration? *Journal of Experimental Botany* **55,** 1963–1976.

Tanaka Y., Sano T., Tamaoki M., Nakajima N., Kondo N. & Hasezawa S. (2005) Ethylene inhibits abscisic acid-induced stomatal closure in *Arabidopsis*. *Plant Physiology* **138,** 2337–2343.

Temple B.R.S. & Jones A.M. (2007) The plant heterotrimeric G-protein complex. *Annual Review of Plant Biology* **58,** 249–266.

Töpfer N., Caldana C., Grimbs S., Willmitzer L., Fernie A.R. & Nikoloski Z. (2013) Integration of genome-scale modeling and transcript profiling reveals metabolic pathways underlying light and temperature acclimation in *Arabidopsis*. *The Plant Cell* **25,** 1197–1211.

Töpfer N., Kleessen S. & Nikoloski Z. (2015) Integration of metabolite data into meabolic models. *Frontiers in Plant Science* **6,** 49.

Töpfer N., Scossa F., Fernie A. & Nikoloski Z. (2014) Variability of metabolite levels is linked to differential metabolic pathways in *Arabidopsis*'s responses to abiotic stresses. *PLoS Computational Biology* **10,** e1003656.

Umezawa T., Sugiyama N., Takahashi F., Anderson J.C., Ishihama Y., Peck S.C. & Shinozaki K. (2013) Genetics and phosphoproteomics reveal a protein phosphorylation network in the abscisic acid signaling pathway in *Arabidopsis thaliana*. *Science Signaling* **6,** rs8.

Vanderschuren H., Lentz E., Zainuddin I. & Gruissem W. (2013) Proteomics of model and crop plant species: status, current limitations and strategic advances for crop improvement. *Journal of Proteomics* **93,** 5–19.

Wang R.-S., Pandey S., Li S., Gookin T., Zhao Z., Albert R. & Assmann S. (2011) Common and unique elements of the ABA-regulated transcriptome of *Arabidopsis* guard cells. *BMC Genomics* **12,** 216.

Wang Y., Papanatsiou M., Eisenach C., Karnik R., Williams M., Hills A., . . . Blatt M.R. (2012) Systems dynamic modeling of a guard cell $Cl^-$ channel mutant uncovers an emergent homeostatic network regulating stomatal transpiration. *Plant Physiology* **160,** 1956–1967.

Wang Y., Hills A. & Blatt M. (2014a) Systems analysis of guard cell membrane transport for enhanced stomatal dynamics and water use efficiency. *Plant Physiology* **164,** 1593–1599.

Wang Y., Noguchi K., Ono N., Inoue S., Terashima I. & Kinoshita T. (2014b) Overexpression of plasma membrane $H^+$-ATPase in guard cells promotes light-induced stomatal opening and enhances plant growth. *Proceedings of the National Academy of Science of the United States of America* **111,** 533–538.

Way D.A., Katul G.G., Manzoni S. & Vico G. (2014) Increasing water use efficiency along the C3 to C4 evolutionary pathway: a stomatal optimization perspective. *Journal of Experimental Botany* **13,** 3683–3693.

Young J.J., Mehta S., Israelsson M., Godoski J., Grill E. & Schroeder J.I. (2006) $CO_2$ signaling in guard cells: calcium sensitivity response modulation, a $Ca^{2+}$-independent phase, and $CO_2$ insensitivity of the *gca2* mutant. *Proceedings of the National Academy of Science of the United States of America* **103,** 7506–7511.

Zhang S., Cai Z. & Wang X. (2009) The primary signaling outputs of brassinosteroids are regulated by abscisic acid signaling. *Proceedings of the National Academy of Science of the United States of America* **106,** 4543–4548.

Zhao Z., Zhang W., Stanley B.A. & Assmann S.M. (2008) Functional proteomics of *Arabidopsis thaliana* guard cells uncovers new stomatal signaling pathways. *The Plant Cell* **20,** 3210–3226.

Zhao Z., Stanley B.A., Zhang W. & Assmann S.M. (2010) ABA-regulated G protein signaling in *Arabidopsis* guard cells: a proteomic perspective. *Journal of Proteome Research* **9,** 1637–1647.

Zhu M., Dai S., McClung S., Yan X. & Chen S. (2009) Functional differentiation of *Brassica napus* guard cells and mesophyll cells revealed by comparative proteomics. *Molecular & Cellular Proteomics* **8,** 752–766.

Zhu M., Simons B., Zhu N., Oppenheimer D.G. & Chen S. (2010) Analysis of abscisic acid responsive proteins in *Brassica napus* guard cells by multiplexed isobaric tagging. *Journal of Proteomics* **73,** 790–805.

*Received 25 October 2014; received in revised form 20 January 2015; accepted for publication 27 January 2015*

## SUPPORTING INFORMATION

Additional Supporting Information may be found in the online version of this article at the publisher's web-site:

**Table S1.** Transcriptomic data from studies on ABA response in guard cells used for a Venn diagramm analysis.

## Supplemental Information*

**Table S1.** Transcriptomic data from studies on ABA response in guard cells used for a Venn diagramm analysis.

*Available online:
http://onlinelibrary.wiley.com/wol1/doi/10.1111/pce.12517/suppinfo

# Chapter 3

## Enhanced photosynthesis and growth in *atquac1* knockout mutants are due to altered organic acid accumulation and increase in both stomatal and mesophyll conductance

# Enhanced Photosynthesis and Growth in *atquac1* Knockout Mutants Are Due to Altered Organic Acid Accumulation and an Increase in Both Stomatal and Mesophyll Conductance[1]

**David B. Medeiros, Samuel C.V. Martins, João Henrique F. Cavalcanti, Danilo M. Daloso, Enrico Martinoia, Adriano Nunes-Nesi, Fábio M. DaMatta, Alisdair R. Fernie, and Wagner L. Araújo***

Departamento de Biologia Vegetal (D.B.M., S.C.V.M, J.H.F.C., A.N.-N., F.M.D., W.L.A.) and Max-Planck Partner Group at the Departamento de Biologia Vegetal (D.B.M., J.H.F.C., A.N.-N., W.L.A.), Universidade Federal de Viçosa, 36570-900, Viçosa, Minas Gerais, Brazil; Central Metabolism Group, Max Planck Institute of Molecular Plant Physiology, 14476 Potsdam-Golm, Germany (D.M.D., A.R.F.); and Institute of Plant Biology, University of Zurich, Zollikerstrasse 107, CH–8008 Zürich, Switzerland (E.M.)

**ORCID IDs: 0000-0001-9086-730X (D.B.M.); 0000-0002-1136-6564 (J.H.F.C.).**

Stomata control the exchange of $CO_2$ and water vapor in land plants. Thus, whereas a constant supply of $CO_2$ is required to maintain adequate rates of photosynthesis, the accompanying water losses must be tightly regulated to prevent dehydration and undesired metabolic changes. Accordingly, the uptake or release of ions and metabolites from guard cells is necessary to achieve normal stomatal function. The *AtQUAC1*, an R-type anion channel responsible for the release of malate from guard cells, is essential for efficient stomatal closure. Here, we demonstrate that mutant plants lacking AtQUAC1 accumulated higher levels of malate and fumarate. These mutant plants not only display slower stomatal closure in response to increased $CO_2$ concentration and dark but are also characterized by improved mesophyll conductance. These responses were accompanied by increases in both photosynthesis and respiration rates, without affecting the activity of photosynthetic and respiratory enzymes and the expression of other transporter genes in guard cells, which ultimately led to improved growth. Collectively, our results highlight that the transport of organic acids plays a key role in plant cell metabolism and demonstrate that AtQUAC1 reduce diffusive limitations to photosynthesis, which, at least partially, explain the observed increments in growth under well-watered conditions.

Stomata are functionally specialized microscopic pores that control the essential exchange of $CO_2$ and $H_2O$ with the environment in land plants. Stomata are found on the surfaces of the majority of the aerial parts of plants, rendering them as the main control point regulating the flow of gases between plants and their surrounding atmosphere. Accordingly, the majority of water loss from plants occurs through stomatal pores, allowing plant transpiration and $CO_2$ absorption for the photosynthetic process (Bergmann and Sack, 2007; Kim et al., 2010). The maintenance of an adequate water balance through stomatal control is crucial to plants because cell expansion and growth require tissues to remain turgid (Sablowski and Carnier Dornelas, 2014), and minor reductions in cell water volume and turgor pressure will therefore compromise both processes (Thompson, 2005). As a result, the high sensitivity of plant tissues to turgor has prompted the use of reverse genetic studies in attempt to engineer plants with improved performance (Cowan and Troughton, 1971; Xiong et al., 2009; Borland et al., 2014; Franks et al., 2015).

In most land plants, not only redox signals invoked by shifts in light quality (Busch, 2014) but also the transport of inorganic ions (e.g. $K^+$, $Cl^-$, and $NO^-_3$) as well as metabolites such as the phytohormone abscisic acid (ABA), Suc, and malate, are important players controlling stomatal movements (Hetherington, 2001; Roelfsema and Hedrich, 2005; Pandey et al., 2007; Blatt et al., 2014; Kollist et al., 2014). In this context, although organic acids in plants is known to support numerous

[1] This work was supported by funding from the Max Planck Society (to W.L.A.), the National Council for Scientific and Technological Development (CNPq-Brazil, grant no. 483525/2012-0 to W.L.A.), and the FAPEMIG (Foundation for Research Assistance of the Minas Gerais State, Brazil, grant nos. APQ-01106-13 and APQ-01357-14 to W.L.A.). Scholarships granted by FAPEMIG to D.B.M., CNPq to D.M.D. and S.C.V.M., and Coordination for the Improvement of Higher Level Personnel (CAPES) to J.H.F.C. Fellowships granted by CNPq-Brazil to A.N.N and W.L.A. are gratefully acknowledged.

* Address correspondence to wlaraujo@ufv.br.

The author responsible for distribution of materials integral to the findings presented in this article in accordance with the policy described in the Instructions for Authors (www.plantphysiol.org) is: Wagner L. Araújo (wlaraujo@ufv.br).

D.B.M., A.R.F., and W.L.A. designed the research; D.B.M., S.C.V.M., and J.H.F.C. performed the research; D.M.D., E.M., A.N.N., and F.M.D. contributed new reagents/analytic tools; D.B.M., S.C.V.M., F.M.D., A.R.F., and W.L.A. analyzed the data; and D.B.M., A.R.F., and W.L.A. wrote the article with input from all the others.

www.plantphysiol.org/cgi/doi/10.1104/pp.15.01053

 

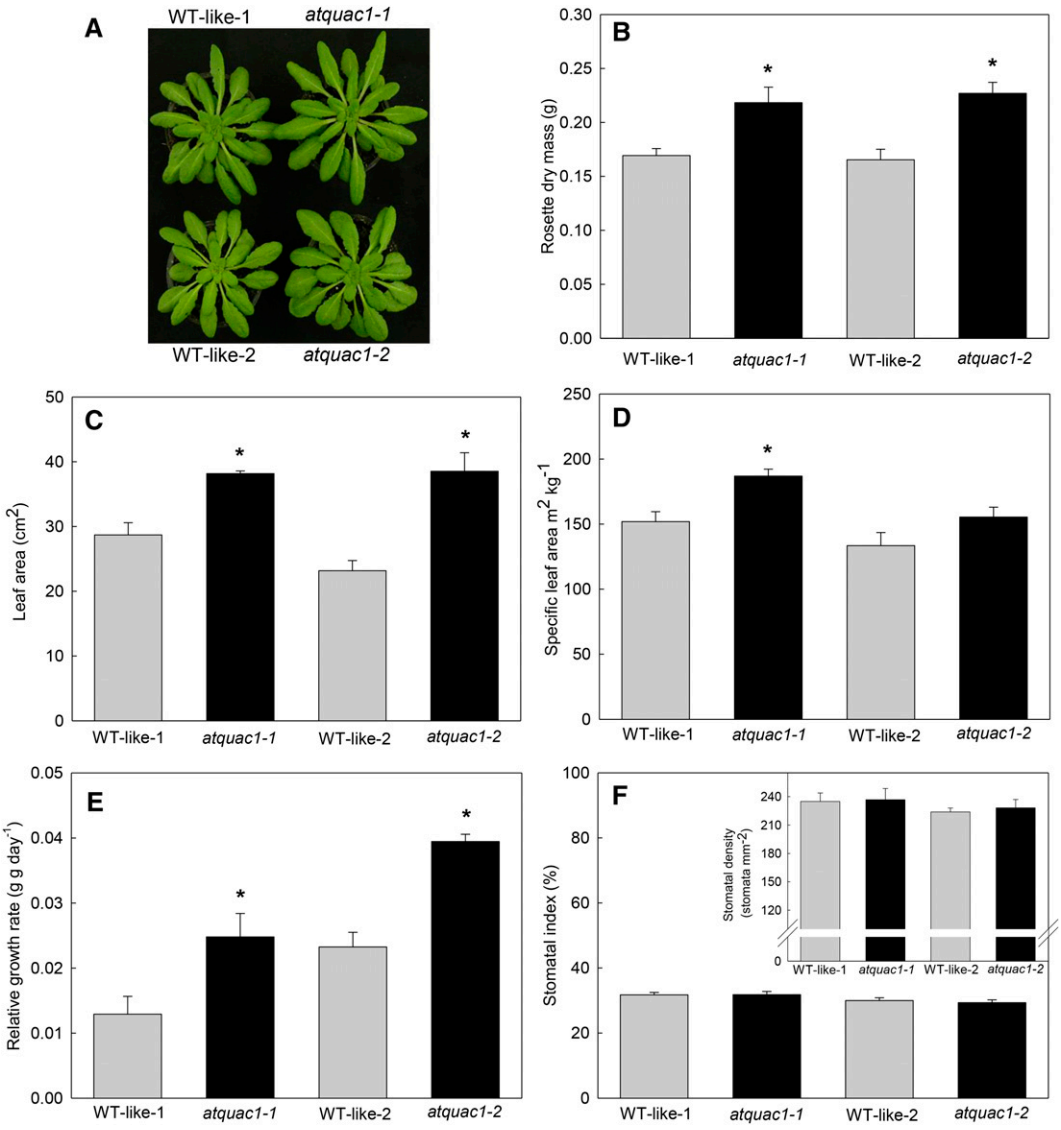


**Figure 1.** Phenotype, growth, and morphological parameters in WT-like and *atquac1* mutant plants under normal growth conditions. A, Representative images of 5-week-old Arabidopsis plants observed in at least four independent assays. Plants with reduced expression of *AtQUAC1* were compared with plants that genotyped as wild-type (WT-like) during homozygous screening by PCR (for details, see Meyer et al., 2010). In all analyses performed, *atquac1-1* and *atquac1-2* mutant lines were directly compared with the corresponding WT lines (WT-like-1 and WT-like-2, respectively). B, RDM. C, LA. D, SLA. E, RGR. F, Stomatal index and stomatal density. Values are presented as means ± SE ($n = 8$) obtained in two independent assays (four in each assay); values in bold in *atquac1* plants were determined by Student's *t* test to be significantly different ($P < 0.05$) from their corresponding WT-like.

and diverse functions both within and beyond cellular metabolism, only recently have we obtained genetic evidence to support that modulation of guard cell malate and fumarate concentration can greatly influence stomatal movements (Nunes-Nesi et al., 2007; Araújo et al., 2011b; Penfield et al., 2012; Medeiros et al., 2015). Notably malate, in particular, has been considered as a key metabolite and one of the most important organic metabolites involved in guard cell movements (Hedrich and Marten, 1993; Fernie and Martinoia, 2009; Meyer et al., 2010). During stomatal aperture, the flux of malate into guard cells coupled with hexoses generated on starch breakdown lead to decreases in the water potential, and consequently, water uptake by the guard cells ultimately opens the stomata pore (Roelfsema and Hedrich, 2005; Vavasseur and Raghavendra, 2005; Lee et al., 2008). On the other hand, during stomatal closure, malate is believed to be converted into starch, which has no osmotic activity (Penfield et al., 2012) or, alternatively, is released from the guard cells to the surrounding apoplastic space (Lee et al., 2008; Negi et al., 2008; Vahisalu et al., 2008; Meyer et al., 2010).

The role of organic acids on the stomatal movements has been largely demonstrated by studies related to

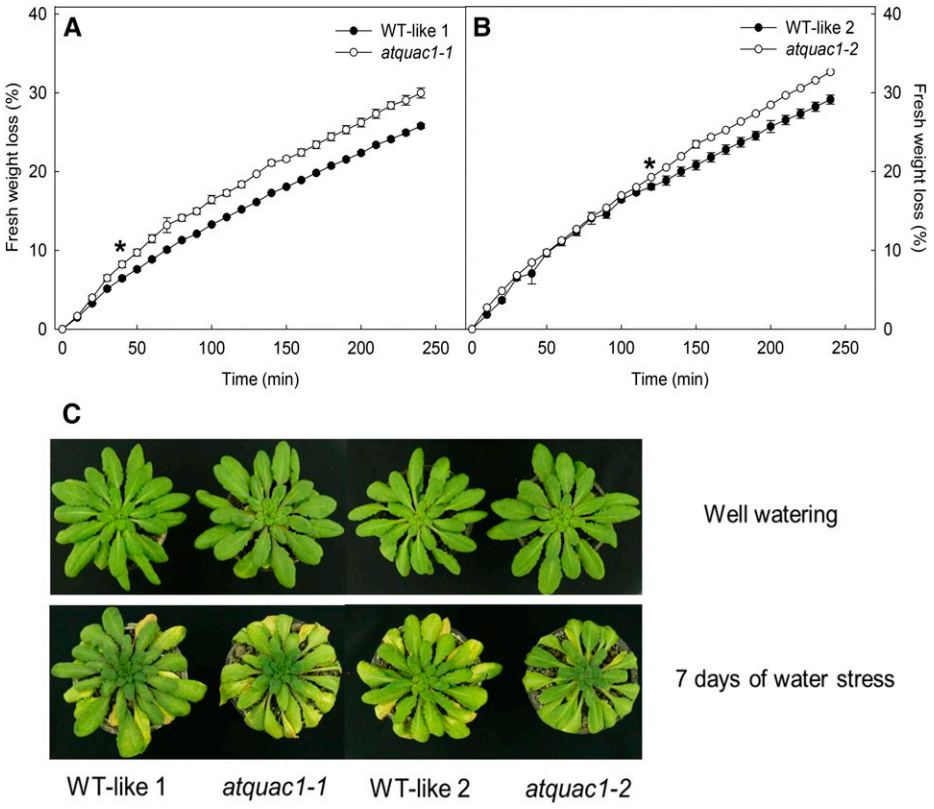


**Figure 2.** *atquac1* mutant plants lost water faster than WT-like plants. A and B, Fresh weight loss from detached whole rosettes in WT-like-1 and *atquac1-1* (A) and WT-like-2 and *atquac1-2* (B), respectively. Data show percentage of initial fresh weight loss from detached rosettes incubated under the same plant growth conditions. Values are presented as means ± SE ($n$ = 8) obtained in two independent assays. Asterisk indicates that from this point and above, the values from mutant lines were determined by Student's $t$ test to be significantly different ($P < 0.05$) from its corresponding WT-like. C, Phenotype of 5-week-old, short-day-grown Arabidopsis mutants and wild-type plants (WT) 7 d after water limitation. *atquac1* plants are more sensitive to drought; 7 d after stopping watering (bottom panel), WT-like plants are still turgid while the corresponding *atquac1* plants are mostly dehydrated.

malate transport (Lee et al., 2008; Meyer et al., 2010; Sasaki et al., 2010). In the last decade, two protein families were identified and functionally characterized to be directly involved with organic acid transport at the guard cell plasma membrane and to be required for stomatal functioning (Lee et al., 2008; Meyer et al., 2010; Sasaki et al., 2010). In summary, AtABCB14, a member of the ABC (ATP binding cassette) family, which is involved in malate transport from apoplast to guard cells, was described as a negative modulator of stomatal closure induced by high $CO_2$ concentration; notably, exogenous application of malate minimizes this response (Lee et al., 2008). In addition, members of a small gene family, which encode the anion channels SLAC1 (slow anion channel 1) and four SLAC1-homologs (SLAHs) in Arabidopsis (*Arabidopsis thaliana*), have been described to be involved in stomatal movements. SLAC1 is a well-documented S-type anion channel that preferentially transports chloride and nitrate as opposed to malate (Vahisalu et al., 2008, 2010; Geiger et al., 2010; Du et al., 2011; Brandt et al., 2012; Kusumi et al., 2012). Lack of SLAC1 in Arabidopsis and rice (*Oryza sativa*) culminated in a failure in stomatal closure in response to high $CO_2$ levels, low relative humidity, and dark conditions (Negi et al., 2008; Vahisalu et al., 2008; Kusumi et al., 2012). Although mutations in AtSLAC1 impair S-type anion channel functions as a whole, the R-type anion channel remained functional (Vahisalu et al., 2008). Indeed, a member of the aluminum-activated malate transporter (ALMT) family, AtALMT12, an R-type anion channel, has been demonstrated to be involved in malate transport, particularly at the plasma membrane of guard cells (Meyer et al., 2010; Sasaki et al., 2010). Although AtALMT12 is a member of ALMT family, it is not activated by aluminum, and therefore Meyer et al. (2010) proposed to rename it as AtQUAC1 (quick-activating anion channel 1; Imes et al., 2013; Mumm et al., 2013). Hereafter, we will follow this nomenclature. Deficiency of a functional AtQUAC1 has been documented to lead to changes in stomatal closure in response to high levels of $CO_2$, dark, and ABA (Meyer et al., 2010). Taken together, these studies have clearly demonstrated that both S- and R-type anion channels are key modulators of stomatal movements in response to several environmental factors.

Despite a vast number of studies involving the above-mentioned anion channels, little information concerning the metabolic changes caused by their impairment is currently available. Such information is important to understand stomatal movements, mainly considering that organic acids, especially the levels of malate in apoplastic/mesophyll cells, have been highlighted as of key importance in leaf metabolism (Fernie and Martinoia, 2009; Araújo et al., 2011a, 2011b; Lawson et al., 2014; Medeiros et al., 2015). Here, we demonstrate that a disruption in the expression of *AtQUAC1*, which leads to impaired stomatal closure (Meyer et al., 2010), was accompanied by increases in mesophyll conductance ($g_m$), which is defined as the conductance for the transfer of $CO_2$ from the intercellular airspaces ($C_i$) to the sites of carboxylation in the chloroplastic stroma ($C_c$). By further

**Table I.** *Gas exchange and chlorophyll a fluorescence parameters in WT-like and atquac1 plants*

Values are presented as means ± SE ($n$ = 10) obtained using the ninth leaf totally expanded from 10 different plants per genotype in two independent assays (five plants in each assay). Values in bold in *atquac1* plants were determined by Student's $t$ test to be significantly different ($P < 0.05$) from its corresponding WT-like.

| Parameters[a] | WT-Like-1 | *atquac1-1* | WT-Like-2 | *atquac1-2* |
|---|---|---|---|---|
| $A_N$ ($\mu$mol $CO_2$ $m^{-2}$ $s^{-1}$) | 6.23 ± 0.49 | **8.74 ± 0.20** | 6.53 ± 0.30 | **7.65 ± 0.35** |
| $g_s$ (mol $H_2O$ $m^{-2}$ $s^{-1}$) | 0.15 ± 0.03 | **0.22 ± 0.01** | 0.15 ± 0.01 | **0.20 ± 0.02** |
| *WUEi* ($A_N/g_s$) | 41.0 ± 5.5 | 40.7 ± 1.2 | 41.1 ± 3.0 | 40.3 ± 3.3 |
| $R_d$ ($\mu$mol $CO_2$ $m^{-2}$ $s^{-1}$) | 0.85 ± 0.10 | **1.29 ± 0.17** | 0.66 ± 0.14 | **1.28 ± 0.13** |
| $F_v/F_m$ | 0.79 ± 0.01 | 0.78 ± 0.02 | 0.77 ± 0.03 | 0.78 ± 0.01 |
| $F_v'/F_m'$ | 0.57 ± 0.007 | 0.58 ± 0.007 | 0.56 ± 0.006 | 0.57 ± 0.005 |
| $J_{flu}$ ($\mu$mol $m^{-2}$ $s^{-1}$) | 70.8 ± 2.12 | **79.8 ± 1.8** | 71.0 ± 4.4 | 75.7 ± 2.6 |

[a]$A_N$, Net photosynthesis rate; $g_s$, stomatal conductance; *WUEi*, intrinsic water use efficiency; $F_v/F_m$, maximum PSII photochemical efficiency; $F_v'/F_m'$, actual PSII photochemical efficiency; $J_{flu}$, electron transport rate estimated by chlorophyll fluorescence parameters.

characterization of *atquac1* knockout plants, we demonstrated that reduced diffusive limitations resulted in higher photosynthetic rates and altered respiration that, in turn, led to enhanced biomass accumulation. Overall, the results obtained are discussed both in terms of the importance of organic acid transport in plant cell metabolism and with regard to the contribution that it plays in the regulation of both stomatal function and growth.

## RESULTS

### *atquac1* Plants Exhibited Slightly Elevated Leaf Growth

Given that stomata are the main gate to control $CO_2$ influx into leaves, we investigated whether mutations in *AtQUAC1* affected growth parameters in the two independent *atquac1* T-DNA lines (*atquac1-1* and *atquac1-2*) described in detail by Meyer et al. (2010). We first confirmed the absence of *AtQUAC1* transcripts in leaves of the mutants by reverse transcription PCR (Supplemental Fig. S1). The mutant lines, which had no visible aberrant phenotypes during the vegetative growth phase (Fig. 1A), displayed enhanced rosette dry mass (Fig. 1B) and relative growth rate (RGR; Fig. 1E), coupled with increased total leaf area (LA; Fig. 1C) and specific leaf area (SLA; Fig. 1D). Although we observed clear differences between the two mutant lines in their RGR, when compared to their respective WT-like (for genotyped as wild type) plants, we noticed that the enhancement observed in RGR was proportionally similar between *atquac1* T-DNA lines. We additionally observed that stomatal density and stomatal index (Fig. 1F) were unaltered in both mutant lines.

### Closing Kinetics, Water Loss, and Sensitivity to Drought Are Affected in *atquac1* plants

The absence of AtQUAC1 has been previously demonstrated to impact stomatal closure in response to both $CO_2$, dark, and ABA (Meyer et al., 2010). To further assess the impact of the lack of a functional AtQUAC1 on stomatal conductance ($g_s$) and water loss in Arabidopsis plants, we next adopted three complementary approaches. First, we confirmed the duration of stomatal responses following dark-to-light and light-to-dark transitions as well as normal-to-high and high-to-normal $CO_2$ concentrations (Supplemental Fig. S2). Our results confirmed the deficient stomatal regulation in mutant plants, which showed slower stomatal closing kinetics in response to both light-to-dark transitions (Supplemental Fig. S2, A and B) and normal-to-high $CO_2$ concentrations (Supplemental Fig. S2, C and D). In contrast, the light-stimulated opening kinetics was less affected, albeit we also observed a relative tendency of faster opening and higher $g_s$, even in response to high $CO_2$ levels. Given that *atquac1* plants have slower stomatal closing, despite similar stomatal density (Fig. 1F), we next performed a time scale water loss experiment from excised rosettes by analyzing fresh weight loss. Consistent with slower stomatal closure, water loss was similar in both WT-like and *atquac1* plants during the beginning of the experiment. However, after 240 min, water loss from *atquac1* plants resulted in 32% fresh weight loss against 28% in WT-like plants (Fig. 2, A and B). These data suggest that *atquac1* plants most likely exhibit higher sensitivity to stress conditions. However, given that fresh weight loss in the detached rosette might not reflect the situation *in planta*, we next decided to analyze the response of those plants following water restriction in plants growing on soil. Indeed, after suspension of irrigation, *atquac1* plants showed earlier symptoms of chlorosis and leaf wilting, i.e. 4 to 5 d after withholding watering against 6 to 7 d in both WT-like plants (Fig. 2C). Thus, absence of *AtQUAC1* in Arabidopsis plants is likely to increase its sensitivity to drought episodes.

### AtQUAC1 Deficiency Results in Increased $g_m$ and Enhanced Photosynthesis Rate

Considering that most of plant biomass is derived from photosynthesis, we fully characterized the

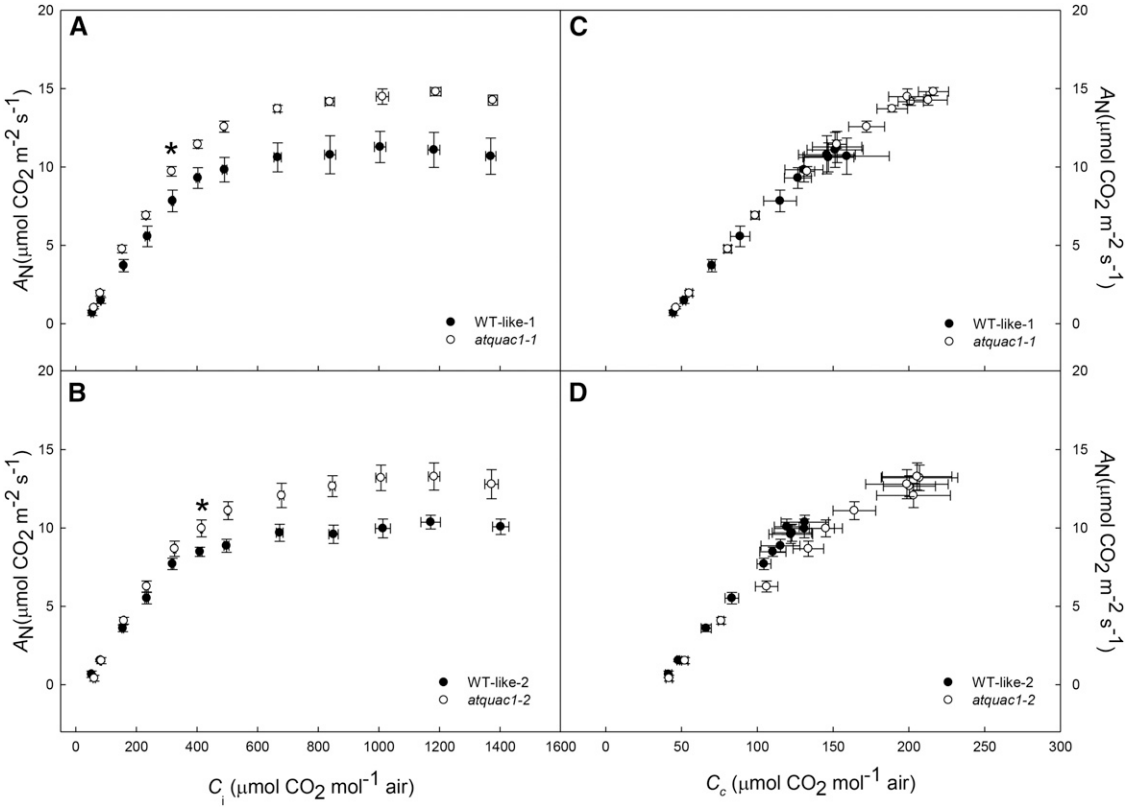


**Figure 3.** Net photosynthesis ($A_N$) curves in response to substomatal ($C_i$) or chloroplastic ($C_c$) $CO_2$ concentrations in WT-like and *atquac1* plants. A to D, $A_N/C_i$ curves (A and B) and $A_N/C_c$ curves (C and D) to WT-like-1/*atquac1-1* and WT-like-2/*atquac1-2*, respectively. Asterisk indicates that from this point and above, the $A_N$ in *atquac1* plants were statistically higher than WT-like ones by Student's *t* test ($P < 0.05$). Values are presented as means ± SE ($n = 10$) obtained using the ninth leaf totally expanded from ten different plants per genotype in two independent assays (five plants in each assay).

photosynthetic performance by analyzing diffusional, photochemical, and biochemical constraints to photosynthesis. Compared with their respective WT control, mutant plants displayed higher net photosynthetic rates ($A_N$) and $g_s$ whereas no differences in intrinsic water use efficiency (*WUEi*) were observed (Table I). Dark respiration ($R_d$) was higher (approximately 40%) in *atquac1* plants than in their respective WT-like counterparts (Table I). The differences in $A_N$ were unlikely to have been related to photochemical constraints given that both the maximum quantum efficiency of photosystem II (PSII; $F_v/F_m$) and capture efficiency of excitation energy ($F_v'/F_m'$) remained invariant. Additionally, the electron transport rate ($J_{flu}$) was marginally increased only in *atquac1-1* (Table I).

By further analyzing gas exchange under photosynthetically active photon flux density (PPFD) that ranged from 0 to 1000 $\mu$mol $m^{-2}$ $s^{-1}$, we observed that mutant plants exhibited unaltered $A_N$ irrespective of the irradiance. Indeed, the saturation irradiance ($I_s$) and the light-saturated $A_N$ ($A_{PPFD}$) were increased only in *atquac1-2* plants with no changes both in the compensation irradiance ($I_c$) and light use efficiency (Supplemental Table S1; Supplemental Fig. S3). Additionally, the response of $A_N$ to the internal $CO_2$ concentration ($A_N/C_i$ curves; Fig. 3, A and B) was obtained, which were further converted into responses of $A_N$ to chloroplastidic $CO_2$ concentration ($A_N/C_c$ curves; Fig. 3, C and D). Interestingly, under ambient $CO_2$ concentration (400 $\mu$mol $mol^{-1}$), $C_i$ estimations were similar between *atquac1* and WT-like plants, whereas $C_c$ was increased in *atquac1* plants (Table II). $g_m$, estimated using a combination of gas exchange and chlorophyll *a* fluorescence parameters via two independent methods, was significantly higher (29%) in *atquac1* plants in comparison to their respective WT-like (Table II). In addition, the maximum carboxylation velocity ($V_{cmax}$) and maximum capacity for electron transport rate ($J_{max}$) were higher in both mutant lines only when estimated on a $C_i$ basis, whereas on a $C_c$ basis $J_{max}$ was increased only in *atquac1-1* line (Table II). Moreover, the similarities in the $J_{max}$:$V_{cmax}$ ratios suggest that although differences in $A_N$ were observed an adequate functional balance between carboxylation and electron transport rates probably occurred.

The overall photosynthetic limitations were next partitioned into their functional components: stomatal

**Table II.** *Photosynthetic characterization of WT-like and atquac1 plants*

Values are presented as means ± SE ($n$ = 10) obtained using the ninth leaf totally expanded from 10 different plants per genotype in two independent assays (five plants in each assay). Values in bold in *atquac1* plants were determined by Student's $t$ test to be significantly different ($P < 0.05$) from their corresponding WT-like.

| Parameters[a] | WT-Like-1 | *atquac1-1* | WT-Like-2 | *atquac1-2* |
|---|---|---|---|---|
| $C_i$ ($\mu$mol $CO_2$ $mol^{-1}$) | 317.4 ± 7.9 | 319.4 ± 2.4 | 315.7 ± 7.4 | 324.5 ± 6.2 |
| $C_c$ ($\mu$mol $CO_2$ $mol^{-1}$) | 100.1 ± 7.3 | **133.1 ± 3.76** | 104.4 ± 5.0 | **133.7 ± 11.0** |
| $g_{m\_Harley}$ (mol $CO_2$ $m^{-2}$ $s^{-1}$ $bar^{-1}$) | 0.029 ± 0.005 | **0.043 ± 0.002** | 0.030 ± 0.003 | **0.042 ± 0.004** |
| $g_{m\_Ethier}$ (mol $CO_2$ $m^{-2}$ $s^{-1}$ $bar^{-1}$) | 0.035 ± 0.005 | **0.049 ± 0.002** | 0.031 ± 0.003 | **0.043 ± 0.004** |
| $V_{cmax-Ci}$ ($\mu$mol $m^{-2}$ $s^{-1}$) | 26.8 ± 2.3 | **35.9 ± 0.9** | 26.4 ± 1.8 | **32.2 ± 1.2** |
| $V_{cmax-Cc}$ ($\mu$mol $m^{-2}$ $s^{-1}$) | 81.6 ± 1.9 | 84.8 ± 1.4 | 81.5 ± 7.1 | 82.8 ± 6.0 |
| $J_{max\_Ci}$ ($\mu$mol $m^{-2}$ $s^{-1}$) | 53.3 ± 4.1 | **81.2 ± 0.7** | 55.6 ± 2.9 | **74.8 ± 4.1** |
| $J_{max\_Cc}$ ($\mu$mol $m^{-2}$ $s^{-1}$) | 103.5 ± 3.3 | **117.1 ± 1.2** | 106.8 ± 7.1 | 106.7 ± 5.1 |
| $J_{max\_Ci}$: $V_{cmax-Ci}$ | 2.2 ± 0.10 | 2.3 ± 0.06 | 2.1 ± 0.10 | **2.3 ± 0.09** |
| $J_{max\_Cc}$: $V_{cmax-Cc}$ | 1.2 ± 0.05 | 1.4 ± 0.02 | 1.3 ± 0.03 | **1.3 ± 0.05** |
| Stomatal limitation | 0.197 ± 0.023 | 0.197 ± 0.007 | 0.197 ± 0.020 | 0.182 ± 0.020 |
| Mesophyll limitation | 0.646 ± 0.026 | **0.561 ± 0.013** | 0.642 ± 0.034 | **0.529 ± 0.033** |
| Biochemical limitation | 0.157 ± 0.030 | **0.242 ± 0.011** | 0.160 ± 0.019 | **0.289 ± 0.039** |

[a] $C_i$, Substomatal $CO_2$ concentration; $C_c$, chloroplastic $CO_2$ concentration; $g_m$, mesophyll conductance to $CO_2$ estimated according to the Harley or Ethier method; $V_{cmax-Ci\ or\ Cc}$, maximum carboxylation capacity based on $C_i$ or $C_c$; $J_{max\_Ci\ or\ Cc}$, maximum capacity for electron transport rate based on $C_i$ or $C_c$.

($l_s$), mesophyll ($l_m$), and biochemical ($l_b$; Table II). The photosynthetic rates were mainly constrained by $l_m$ (64% and 54% in WT-like and *atquac1* plants, respectively), whereas $l_s$ accounted for, on average, 19% in both WT-like and *atquac1* plants, and $l_b$ contributed with 16% and 26% in WT-like and *atquac1* plants, respectively. These analyses demonstrated that *atquac1* plants exhibits lower $l_m$ compared to the WT-like plants in close agreement with the higher $g_m$ observed (Table II).

### Mutations in *AtQUAC1* Affect Mainly Carbon Metabolism without Strong Effects in Activity of Related Enzymes

To explore the consequences of changes in photosynthetic capacity among the genotypes, we further conducted a detailed metabolic analysis in leaves of the mutants and WT-like plants. Evaluation of compounds related to nitrogen metabolism revealed that there were no changes in the levels of nitrate, chlorophylls, total amino acids, and soluble proteins in a consistent manner with the altered expression of *AtQUAC1* (Supplemental Figs. S4 and S5). During the light period, mutant lines accumulated more Glc (Fig. 4, A and B), Suc (Fig. 4, E and F), and starch (Fig. 4, G and H), reaching higher values at the end of this period. Notably, the mutant lines were able to fully degrade these metabolites by the end of the dark period, reaching similar values to those observed in WT-like plants (Fig. 4), corroborating the increased $R_d$ observed in *atquac1* plants (Table I). Suc was the main storage sugar in all genotypes reaching, on average, 3 and 15 times higher contents than those of Glc and Fru, respectively. It is important to note that the higher concentrations of starch and sugars observed in *atquac1* plants were accompanied by higher $A_N$.

Diel changes in the levels of organic acids (malate and fumarate) were similar to those observed for sugars and starch, with higher values being consistently observed in mutant plants. Remarkably, *atquac1* plants showed increases in both malate and fumarate content mainly at the middle of the light period (Fig. 5; Supplemental Fig. S3).

We next decided to extend this study to major primary pathways of plant photosynthetic metabolism by using an established gas chromatography-mass spectrometry (GC-MS) protocol (Lisec et al., 2006). This analysis revealed, however, that among the 40 successfully annotated compounds related to primary metabolism, only a relatively small number of changes were evident (Fig. 5). By analyzing 13 individual amino acids, we observed increases only in Gln, Pro, Gly, and Ala, which were moreover only significantly different in *atquac1-1* plants (Fig. 5). When considering the levels of the organic acids, we also observed that only the levels of maleic acid, malate, fumarate, succinate (only in *atquac1-1*), and glycerate (only in *atquac1-2*) increased in mutant lines. Other changes of note in the metabolite profiles were the significant increases in glycerol and myoinositol (in both lines, Fig. 5).

We next investigated whether the metabolic perturbation observed could also affect the activity of important enzymes related to photosynthetic and respiratory metabolism (Table III). Although changes in both photosynthesis and respiration were observed in *atquac1* plants, there were no changes in either Rubisco or NADP-dependent malate dehydrogenase (NADP-MDH). Moreover, increases in transketolase activity were observed in both *atquac1* lines, whereas glyceraldehyde 3-phosphate dehydrogenase (GAPDH)

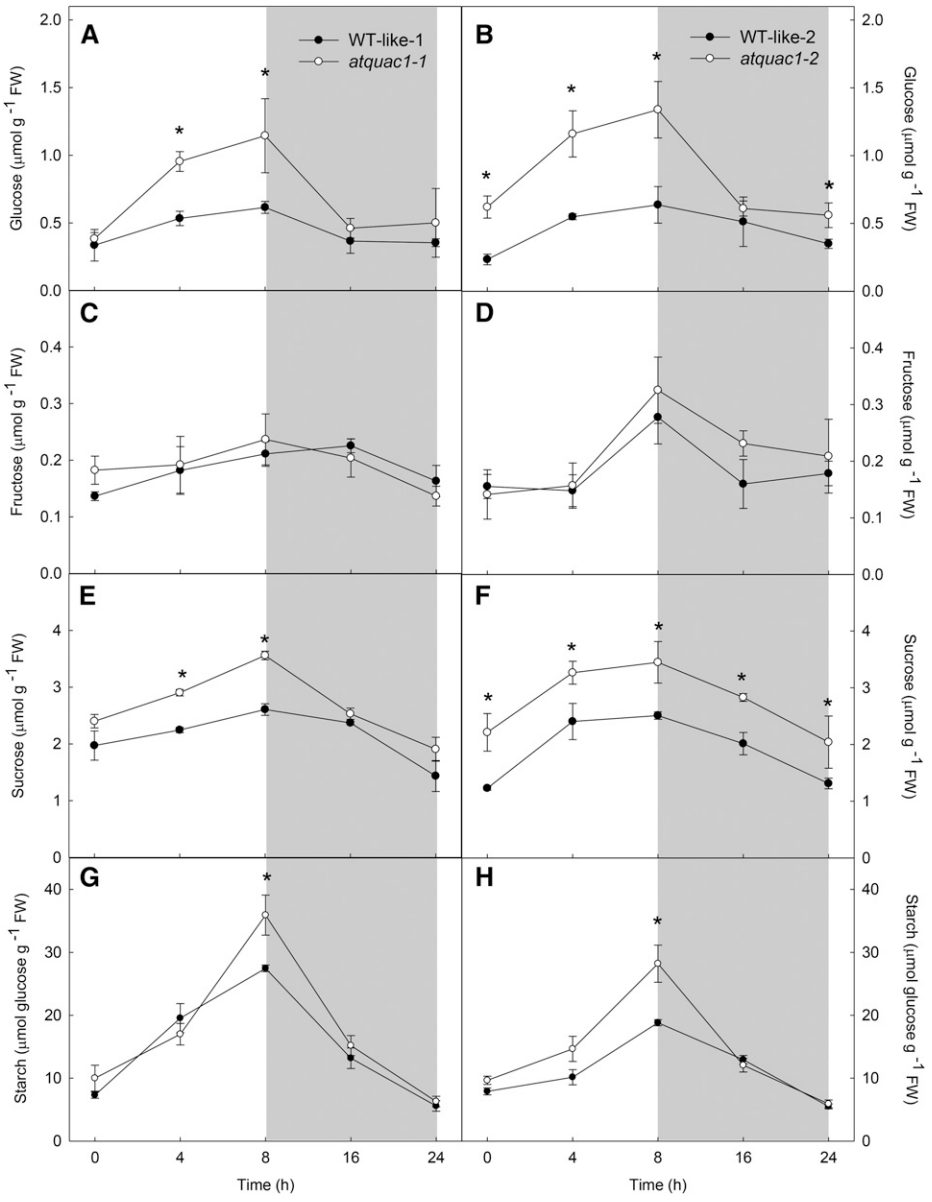


**Figure 4.** Leaf metabolite levels in WT-like and *atquac1* plants. A and B, Glc; C and D, Fru; E and F, Suc; G and H, starch to WT-like-1 and *atquac1-1* as well as WT-like-2 and *atquac1-2*, respectively. Values are presented as means ± SE ($n$ = 5) from whole rosettes harvested in different times along the cycle of light/dark. Asterisks indicate the time where the values from mutant lines were determined by Student's $t$ test to be significantly different ($P < 0.05$) from their corresponding WT-like.

activity was increased only in *atquac1-1* plants. Regarding enzymes related to respiratory metabolism, no significant changes were observed for the activities of Suc synthase (Susy), phosphoglycerate kinase (PGK), or NAD-dependent malate dehydrogenase (NAD-MDH).

### *AtQUAC1* Repression Does Not Strongly Affect the Expression of Other Genes Related to Ion Transport in Guard Cells

We next analyzed whether *AtQUAC1* repression affected the expression of genes currently known to or putatively related to organic and inorganic ion transport, as well as genes involved in guard cell movements. We felt such experiments were important given that the loss of function of *AtSLAC1* was associated with downregulation of several guard-cell-expressed transporters (Laanemets et al., 2013). To extend this molecular characterization, we attempted to look at the expression levels of several ion channels and transporter in guard cells from isolated epidermal fragments, including *ALMT6*, *ALMT9*, *AtABCB14*, *AtSLAC1*, *AHA1*, *AHA5*, *KAT1*, *KAT2*, *AKT1*, *AKT2*, *AtKC1*, *TPC1*, and *GORK* (for further details, see "Materials and Methods" and Supplemental Table S2). Quantitative real-time PCR (qRT-PCR) analysis of the transcript levels of these genes revealed, in sharp contrast to the situation observed in the case of *atslac1* plants (Laanemets et al., 2013), that the vast majority of evaluated genes in *atquac1* plants were unaltered

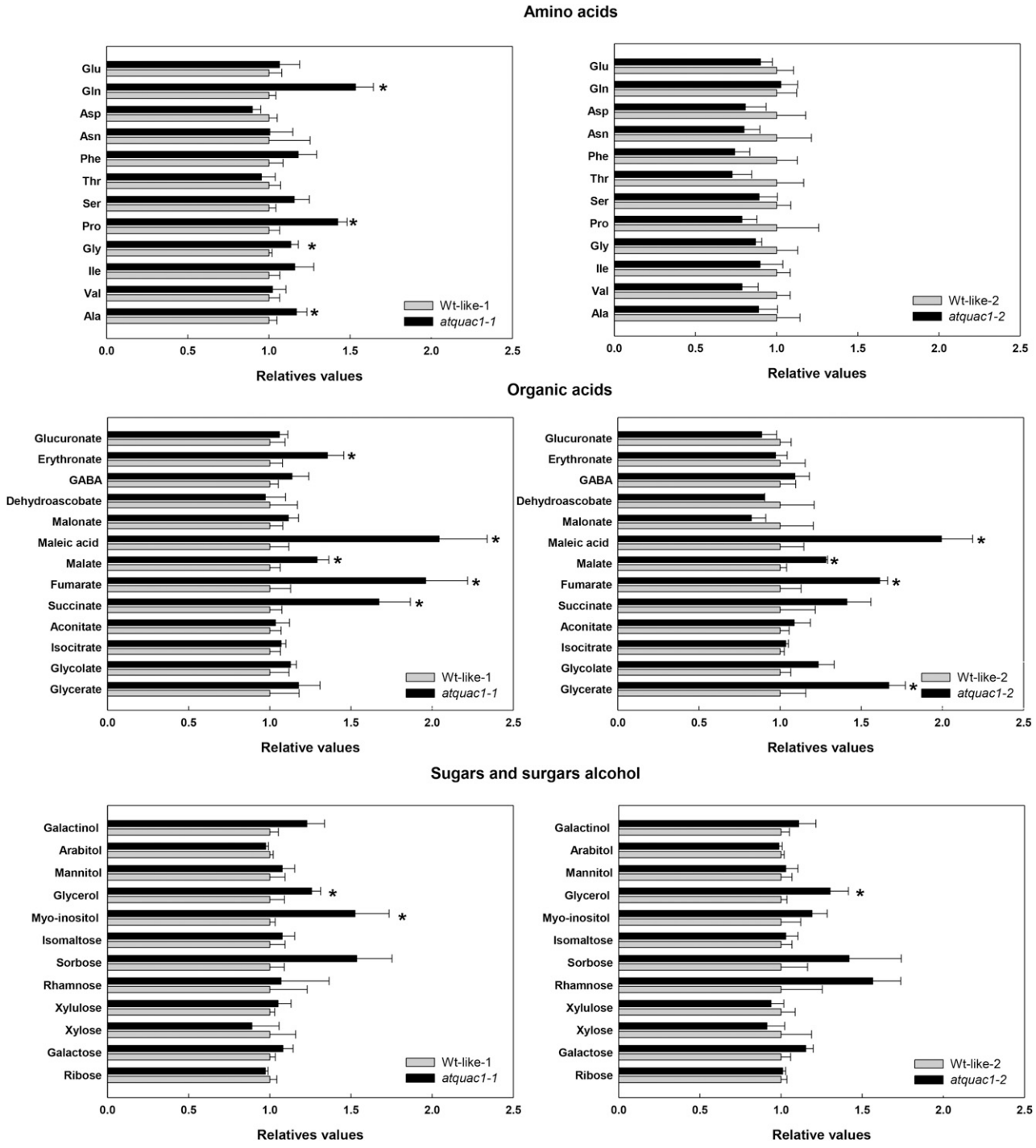


**Figure 5.** Relative metabolite content in leaves of WT-like and *atquac1* plants. Amino acids, organic acids, and sugars and sugar-alcohols were determined by GC-MS as described in "Materials and Methods." The full data sets from these metabolic profiling studies are additionally available in Supplemental Table S3. Data are normalized with respect to the mean response calculated for the corresponding WT-like (to allow statistical assessment, individual plants from this set were normalized in the same way). WT-like-1 or -2, Gray bars; *atquac1-1* or *-2*, black bars. Values are presented as means ± SE ($n = 5$). Asterisks indicate that the values from mutant lines were determined by Student's *t* test to be significantly different ($P < 0.05$) from their corresponding WT-like.

(Fig. 6). Thus, although *KAT1* and *KAT2* were reduced in *atquac1-2* plants only and the *AHA5* transcript level was increased in *atquac1-1* plants only, our results indicate that the stomatal effects observed here were not likely to be mediated by an alteration in the general efficiency of transport of the guard cells.

**Table III.** *Enzyme activities in WT-like and atquac1 plants*

Activities were determined in whole rosettes (5-week-old) harvested at middle of the photoperiod. Values are presented as means ± SE ($n = 5$); values in bold type in *atquac1* plants were determined by Student's *t* test to be significantly different ($P < 0.05$) from their corresponding WT-like. FW, Fresh weight.

| Enzymes | WT-Like-1 | *atquac1-1* | WT-Like-2 | *atquac1-2* |
|---|---|---|---|---|
| | *nmol min$^{-1}$ g$^{-1}$ FW* | | | |
| Rubisco initial | 946.4 ± 69.2 | 1078.0 ± 105.2 | 909.3 ± 77.8 | 896.8 ± 112.6 |
| Rubisco total | 1450.9 ± 71.3 | 1629.5 ± 24.7 | 1229.7 ± 93.3 | 1396.4 ± 66.7 |
| Rubisco activation state[a] | 66.7 ± 1.9 | 66.5 ± 7.4 | 68.0 ± 3.1 | 68.9 ± 2.7 |
| Transketolase | 303.8 ± 13.9 | **404.9 ± 8.9** | 299.4 ± 15.4 | **347.9 ± 12.3** |
| NADP-GAPDH | 37.3 ± 1.7 | **74.0 ± 1.8** | 46.4 ± 3.8 | 44.7 ± 0.7 |
| NADP-MDH initial | 39.0 ± 1.7 | 40.6 ± 2.4 | 33.0 ± 1.6 | 32.3 ± 2.3 |
| NADP-MDH total | 63.8 ± 4.5 | 65.9 ± 4.2 | 62.9 ± 2.4 | 61.4 ± 3.9 |
| NADP-MDH activation state[a] | 62.1 ± 3.9 | 58.8 ± 5.8 | 51.9 ± 2.9 | 48.7 ± 4.7 |
| Susy | 512.7 ± 15.9 | 548.4 ± 22.9 | 458.1 ± 19.4 | 444.9 ± 3.4 |
| PGK[b] | 12.5 ± 0.4 | 13.8 ± 0.6 | 11.6 ± 0.6 | 12.6 ± 0.5 |
| NAD-MDH[b] | 24.7 ± 0.7 | 27.0 ± 0.9 | 25.5 ± 0.8 | 27.0 ± 0.6 |

[a]Activation state expressed in percentage (%). [b]Values expressed in $\mu$mol min$^{-1}$ g$^{-1}$ fresh weight.

## DISCUSSION

Ion transport from guard cells to their surroundings has been proven essential to stomatal movements. Indeed, it is well known that the efflux of malate from guard cells can regulate the activity of anion channels on guard cell membrane (Hedrich and Marten, 1993; Hedrich et al., 1994; Raschke, 2003; Lee et al., 2008; Negi et al., 2008; Kim et al., 2010), suggesting that the organic acid accumulation on the apoplast space might influence stomatal movements. Indeed, the role of the organic acids (e.g. malate and fumarate) on the regulation of stomata movements was recently confirmed (Nunes-Nesi et al., 2007; Meyer et al., 2010; Araújo et al., 2011b; Medeiros et al., 2015). However, the metabolic hierarchy regulating those highly specialized cell types, as yet, remains elusive. Here, by using a combination of physiological and biochemical approaches, we provide evidence that the genetic manipulation of organic acid transport has significant potential to biotechnological applications (Martinoia et al., 2012; Schroeder et al., 2013; Medeiros et al., 2015). Both the data we provide and the recent molecular characterization of Arabidopsis plants deficient in the expression of *AtQUAC1* (Meyer et al., 2010; Sasaki et al., 2010) and data concerning the regulation of AtQUAC1 (Imes et al., 2013; Mumm et al., 2013) add further support to the importance of this anion channel regulating stomatal movements. Importantly, we showed that other aspects of photosynthetic and respiratory metabolism, the GC-MS-based metabolite profile (Fig. 5; Supplemental Table S3), and the transcript levels of some key channels and transporters involved in guard cell ion transport (Fig. 6) all displayed relatively few and mild changes. Such observations likely indicate that AtQUAC1 plays little part in terms of total cellular homeostasis. It is important to note here that impairments in the AtSLAC1 activity also reduced stomatal opening kinetics that were associated not only with the repression of an organic acid transporter (reduction in *AtABCB14* expression), but mainly due the dramatic reductions of inward $K^+$ channel currents (Laanemets et al., 2013). In this study, the authors also identified a compensatory feedback control in *atslac1* plants involving the elevation of cytosolic $Ca^{2+}$ concentrations, which downregulated the inward $K^+$ channel activity. By contrast, stomatal opening kinetics were not significantly altered in *atquac1* plants (Supplemental Fig. S2). Furthermore, as changes in the activities of key enzymes of photosynthetic and respiratory metabolism were not observed (Table III) and $V_{cmax}$ on a $C_c$ basis (Table II) was similar between WT-like and *atquac1* plants, we contend that diffusive rather than biochemical limitations had a major role explaining the changes in photosynthetic rates. These results, coupled with those obtained by Meyer et al. (2010) and Sasaki et al. (2010), provide strong evidence that AtQUAC1 is essential for an efficient stomatal closure yet does not strongly affect the central primary metabolism.

### Functional Absence of AtQUAC1 Alters Stomatal Movements and Mesophyll Conductance

Given the increased photosynthetic rates and subsequent increases in LA and RGR (Figs. 1 and 3; Table I), we next investigated the mechanisms underlying this positive growth response. Since the changes described above took place independently of changes in the stomatal density and photosynthetic pigment levels (Fig. 1F; Supplemental Fig. S4), it is reasonable to assume that molecular and metabolic mechanisms occurred enabling a reprogramming in response to impaired stomatal closure in *atquac1* plants under our experimental conditions. The results presented here provide further evidence that the functional lack of AtQUAC1 leads to slower stomatal closure in response to dark and high $CO_2$ concentrations (Supplemental Fig. S2). Additional compelling evidence supporting the role of AtQUAC1 on the regulation of stomatal function was

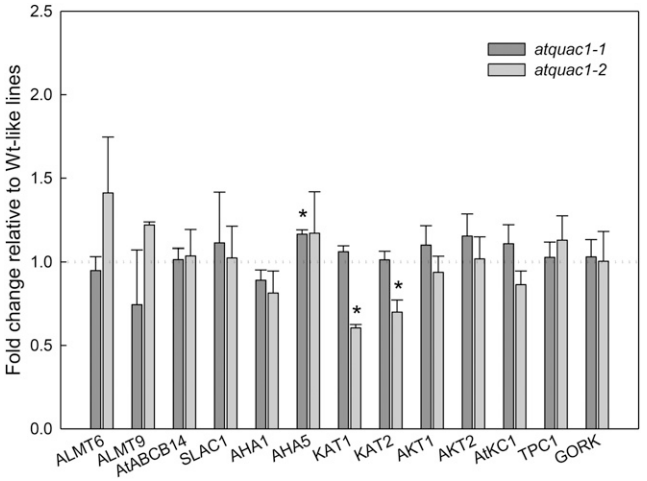


**Figure 6.** Relative transcript responses of genes involved in organic and inorganic ion transport in guard cell. Transcript abundance of Arabidopsis plasma membrane $H^+$-ATPases *AHA1* and *AHA5*, transporter *AtABCB14*, and ion channels *ALMT6*, *ALMT9*, *SLAC1*, *KAT1*, *KAT2*, *AKT1*, *AKT2*, *TPC1*, *AtKC1*, and *GORK* was determined. RNA was isolated from epidermal fragments. Data are normalized with respect to the mean response calculated for the corresponding WT-like. *atquac1-1*, Black bars; *atquac1-2*, gray bars. Values are presented as means ± SE ($n = 4$); asterisks indicate values that were determined by Student's *t* test to be significantly different ($P < 0.05$) from their corresponding WT-like.

further obtained from assays of fresh weight water loss and drought stress (Fig. 2). Collectively, these analyses showed that the mutant lines lost water faster than their respective WT-like, characterizing a water-spending phenotype and likely more sensitive to drought events (Fig. 2C). Thus, these data clearly document the importance of AtQUAC1 and, by extension, organic acid transport in guard cell function.

Plant photosynthetic capacity was considered for a long time to be limited only by the rate of $CO_2$ diffusion through the stomata and by the capability of the photosynthetic machinery to convert the light energy into biochemical one (Flexas et al., 2012). However, it is now recognized that the pathway to $CO_2$ diffusion from stomata to the Rubisco carboxylation sites in the chloroplasts can become an important limiting factor to the photosynthetic process due to the several resistances in the gas and liquid phases during this way. Thus, $g_m$, previously considered large enough to have any impact on photosynthesis (Farquhar et al., 1980), has recently turned out to be a key point in explaining limitations during this process (Bernacchi et al., 2002; Flexas et al., 2007, 2012, 2013; Warren, 2008b; Bown et al., 2009; Niinemets et al., 2009; Jin et al., 2011; Scafaro et al., 2011; Martins et al., 2013). Noteworthy, $g_s$ and $g_m$ are very often coregulated (Flexas et al., 2012), which can reflect either a strong coordination between $A_N$ and $g_s$ or a compensatory mechanism, where $g_m$ tends to compensate changes in $g_s$ particularly under suboptimal conditions (e.g. drought). In such cases, where $g_s$ seems to be more affected than $g_m$, this coregulation has the purpose of optimizing $A_N$ (Warren, 2008a; Duan et al., 2009; Vrábl et al., 2009; Galmés et al., 2011; Flexas et al., 2012; Galmés et al., 2013). Accordingly, photosynthetic limitations were estimated and revealed that the mesophyll fraction had a greater contribution to the lower $A_N$ observed in WT-like compared to *atquac1* plants (Table II). Collectively, the results presented here demonstrate that the higher capacity of $CO_2$ fixation in *atquac1* plants was associated with a higher $C_c$ due to increased $g_m$ in *atquac1* mutant plants that can, at least partially, explain the increased growth presented by those plants (Fig. 1). The observed effects on $g_s$, which were followed by increases in $g_m$ (Tables I and II) without changes in the stomatal density (Fig. 1F), indicate that the diffusional component was the main player controlling $A_N$. Detailed biochemical and physiological analyses delimited this response as a consequence of perturbation of stomatal function; however, the exact mechanisms underlying this phenomenon are not immediately evident. Although several studies have attempted to explain both stomata physiology and variations in $g_m$ (Kollist et al., 2014; Lawson et al., 2014), which may rely on anatomical properties (Peguero-Pina et al., 2012), our understanding of this subject remains far from complete. Accordingly, a parameter commonly used to characterize the physical limitation inside the leaves is the leaf dry mass per unit area (LMA) that increase as a function of increases in cell wall thickness, potentially decreasing the velocity of $CO_2$ diffusion (Flexas et al., 2008; Niinemets et al., 2009; Flexas et al., 2012). The LMA is considered a key trait in plant growth and performance, allowing plants to cope with different environmental conditions most likely because the amount of light absorbed by a leaf and the diffusion pathway of $CO_2$ through the leaf depend partially on its thickness (Vile et al., 2005; Poorter et al., 2009, Villar et al., 2013). The inverse of LMA is the ratio of leaf area to leaf mass or SLA; thus, a reduction in LMA is translated into increments in SLA and, in turn, increases in $g_m$. Indeed, the values of SLA found here are in agreement with this hypothesis once we observed higher values of both SLA and $g_m$ in *atquac1* plants (Fig. 1D; Table II). In this vein, although we have not observed changes in stomatal density but increased SLA, studies related to the leaf anatomy of these mutants might help to explain whether the increases in $g_m$ are governed by anatomic traits or by further investments of nitrogen to mesophyll proteins involved in increasing $g_m$, such as carbonic anhydrases, aquaporins, Rubisco, and others (Buckley and Warren, 2014). Accordingly, it is not without precedence to suggest that changes in $g_m$ will eventually correlate with changes in sugars, which are cell wall precursors, and, to a lower extent, to organic acids, as observed here. In this sense, it seems plausible that an interaction between these compounds may exist and, thus, directly or indirectly be associated with enhancement of $g_m$, and by extension $A_N$. It will be important to establish the functional significance of this observation in future studies.

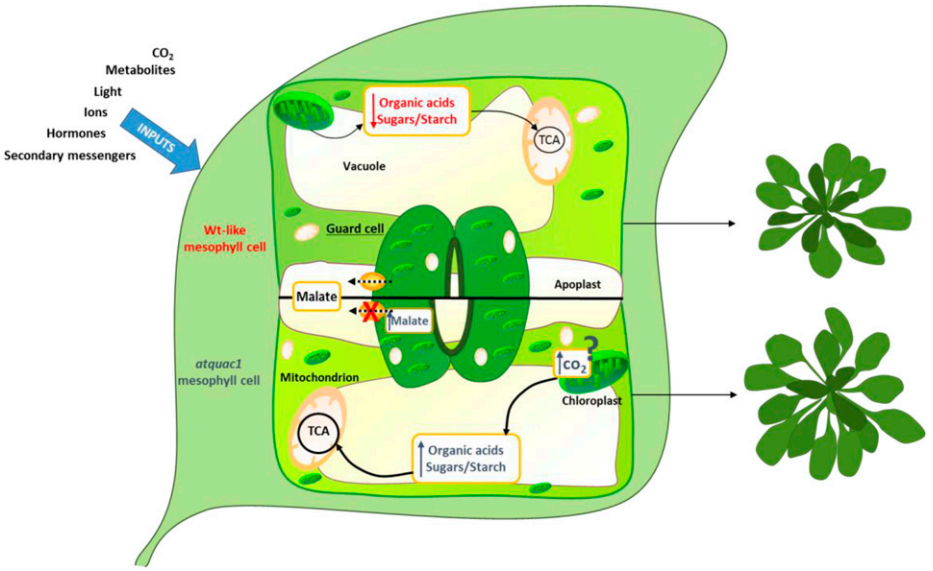


**Figure 7.** Hypothetical model connecting the malate accumulation and stomatal movements. The functional lack of *AtQUAC1* is most likely associated with an accumulation of malate inside guard cells, which consequently maintains stomatal pore aperture for a longer time. Although photosynthetic rates are increased through a mechanism not yet fully understood, this is likely related to the maintenance of a high chloroplastic $CO_2$ concentration given that mesophyll conductance is also increased. Moreover, carbon balance and metabolism are changed through increased levels of sugars, starch, organic acids, and dark respiration rates. Altogether, increased respiration, carbohydrate pool, and photosynthesis can partially explain the observed growth enhancement in *atquac1* plants.

### Carbon Metabolism Is Changed as Consequence of the Higher Photosynthetic Rates in *atquac1* Plants

The organic acid levels in the apoplast exhibited a negative correlation between the malate and fumarate content and $g_s$, with a greater contribution of malate (Nunes-Nesi et al., 2007; Araújo et al., 2011b). This information, coupled to the results obtained with the malate transporter AtABCB14 (Lee et al., 2008), provides strong evidence that the apoplastic content of malate and fumarate can modulate the functioning of guard cells and, in turn, affect the stomatal movements with effects on leaf metabolism. The results presented here demonstrate that impaired organic acid transport, which culminates with alteration in $g_s$ and $g_m$, promote minor changes in primary metabolism, mainly in carbon metabolism, under normal growth conditions. This fact notwithstanding, the increases in the hexose contents in *atquac1* plants were observed not to be primarily due to increases in Suc or starch breakdown since these metabolites accumulated over the course of the light period (Fig. 4). In good agreement with the higher $A_N$ observed in *atquac1* plants (Table I), higher levels of sugars were also observed, which were properly remobilized during the dark period supporting higher $R_d$ (Table I) and, in turn, leading to the enhanced growth observed in those plants (Fig. 1). However, it is important to mention that caution should be taken when analyzing such results obtained under well-controlled under situations. This is particularly true given that the growth benefit observed here (Fig. 1A), which was obtained under well-watered conditions, is not maintained under drought situations (Fig. 2C) most likely associated with a higher $g_s$ and $g_m$ observed in *atquac1* mutant plants. In contrast to the situations observed here, reductions in another stomatal channel protein (SLAC1) in rice were associated with increments in both $A_N$ and $g_s$ without any growth benefit under well-watered conditions (Kusumi et al., 2012) but culminated in lower productivity and yield of rice plants under field conditions. Taken together, these data indicate that an increased sensitivity to water limitations episodes associated with higher $g_s$ and $g_m$ can exceed the enhanced $CO_2$ assimilation under less favorably environments. Accordingly, our understanding of plant responses to water limitation is still fragmentary, most likely due to the complex responses involving adaptive changes and /or deleterious effects. Under field conditions, the responses can be synergistically or antagonistically modified by the interaction with other plants and/or superimposition of other stresses and therefore caution should be taken when interpreting the results described here and as such further investigation should be performed within the context of understanding the stomata responses to water stress.

Regarding to the nitrogen metabolism, it has been demonstrated an inverse relationship between amino acid contents and growth, given that even under nitrogen starvation (which leads to reduced growth), the amino acid levels have been shown to increase without changes in Rubisco activation, total protein, and chlorophyll contents (Tschoep et al., 2009). Interestingly, increases

in both $A_N$ and growth in *atquac1* plants were neither followed by changes in chlorophyll, amino acid, or total soluble protein content (Supplemental Figs. S4 and S5), nor by changes in Rubisco activation state (Table III), highlighting that the increases in $A_N$ were indeed associated with lower diffusional limitations (Table II). Furthermore, similar values of $J_{max}$:$V_{cmax}$ ratio (Table II) and unchanging activities of some enzymes related to photosynthetic metabolism (e.g. Rubisco) are consistent with a photosynthetic functional balance since plants are able to adjust Rubisco content/activation and other photosynthetic machinery components to maintain the balance among the enzymatic reactions (e.g. Rubisco) and light harvesting (e.g. chlorophylls; Stitt and Schulze, 1994). Collectively, our results suggest that inefficient regulation of the stomatal closure via repression of *AtQUAC1* culminates in higher growth and photosynthetic rates through increased $g_m$ and $g_s$, albeit promoting minor changes on carbon metabolism. This hypothesis is illustrated in Figure 7 and would hence explain why the accumulation of organic acids, in special malate within the guard cells, will culminate with a longer stomatal aperture in *atquac1* plants. This model further suggests that increased $A_N$ is likely related to the maintenance of a high chloroplastic $CO_2$ concentration, ultimately leading to growth enhancement. It should be borne in mind that the changes observed in several sugars, as well as in dark respiration in *atquac1* plants can, at least partially, explain the higher growth rates. The exact mechanism by which changes in organic acid transport induced simultaneous changes in both $g_s$ and $g_m$ remains as yet unclear; however, it seems reasonable to anticipate this might be related to an as-yet-unknown signaling compound associated with higher photosynthetic rates.

## MATERIALS AND METHODS

### Plant Material and Growth Conditions

All Arabidopsis (*Arabidopsis thaliana*) plants used here were of the Colombia ecotype (Col-0) background. Seeds were surface-sterilized and imbibed for 2 d at 4°C in the dark on agar plates containing half-strength Murashige and Skoog media (Murashige and Skoog, 1962). Seeds were subsequently germinated and grown in a growth chamber under short-day conditions (8 h/16 h of light/dark) with 150 $\mu$mol $m^{-2}$ $s^{-1}$ white light, 22°C/20°C throughout the day/night cycle, and 60% relative humidity. The T-DNA mutant lines *atquac1-1* (SM_3_38592) and *atquac1-2* (SM_3_1713) were obtained from the John Innes Centre JIC collection (Tissier et al., 1999) and were previously described (Meyer et al., 2010). Plants with reduced expression of *AtQUAC1* were compared with plants that genotyped as wild-type (WT-like) during homozygous screening by PCR (for details, see Meyer et al., 2010). In all analyses performed, *atquac1-1* and *atquac1-2* mutant lines were directly compared with the corresponding WT lines (WT-like-1 and WT-like-2, respectively). The abundance of transcripts was confirmed by semiquantitative PCR using specific primers pairs designed to span the T-DNA insertion site of the two mutant loci (for details, see Supplemental Fig. S1).

### Growth Analysis

Whole rosettes from 5-week-old plants were harvested and the RDW, LA, SLA, RGR were evaluated. LA was measured by digital image method using a scanner (Hewlett-Packard Scanjet G2410) and the images were after processed using the Rosette Tracker software (De Vylder et al., 2012). SLA and RGR, which is the net dry weight increase per unit dry weight per day (g $g^{-1}$ $day^{-1}$), were calculated using the classical approach described by Hunt et al. (2002) with the following equations:

$$\mathrm{SLA}\left(\mathrm{m^2\ kg^{-1}}\right) = \frac{\mathrm{LA}}{\mathrm{LDW}^*}$$

*LDW = Leaves dry weight

$$\mathrm{RGR}\left(\mathrm{g\ g^{-1}\ day^{-1}}\right) = \frac{ln\mathrm{RDW}_2 - ln\mathrm{RDW}_1}{t_2 - t_1}$$

$RDW_1$ was measured 20 d after germination when the rosettes are expected to be with 20% of its final size (Boyes et al., 2001).

### Stomatal Density and Stomatal Index

After 2 h of illumination in the night-day cycle described above, leaf impressions were taken from the abaxial surface of the ninth leaf totally expanded with dental resin imprints (Berger and Altmann, 2000). Nail polish copies were made using a colorless glaze (Von Groll et al., 2002), and the images were taken with a digital camera (Axiocam MRc) attached to a microscope (Zeiss, model AX10). The measurements were performed on the images using the Cell$^P$ software (Soft Imaging System). Stomatal density and stomatal index (the ratio of stomata to stomata plus other epidermal cells) were determined in at least 10 fields of 0.04 $mm^2$ per leaf from eight different plants.

### Gas Exchange and Chlorophyll Fluorescence Measurements

Gas exchange parameters were determined simultaneously with chlorophyll *a* fluorescence measurements using an open-flow infrared gas exchange analyzer system (LI-6400XT; LI-COR) equipped with an integrated fluorescence chamber (LI-6400-40; LI-COR). Instantaneous gas exchanges were measured after 1 h illumination during the light period under 700 $\mu$mol $m^{-2}$ $s^{-1}$ at the leaf level (light saturation) of PPFD, determined by *A*/PPFD curves (net photosynthesis ($A_N$) in response to PPFD curves; Supplemental Fig. S3; Supplemental Table S1). The reference $CO_2$ concentration was set at 400 $\mu$mol $CO_2$ $mol^{-1}$ air. All measurements were performed using the 2 $cm^2$ leaf chamber at 25°C, and the leaf-to-air vapor pressure deficit was kept at 1.2 to 2.0 kPa, while the amount of blue light was set to 10% PPFD to optimize stomatal aperture.

The initial fluorescence ($F_0$) was measured by illuminating dark-adapted leaves (1 h) with weak modulated measuring beams (0.03 $\mu$mol $m^{-2}$ $s^{-1}$). A saturating white light pulse (8000 $\mu$mol $m^{-2}$ $s^{-1}$) was applied for 0.8 s to obtain the maximum fluorescence ($F_m$), from which the variable-to-maximum chlorophyll fluorescence ratio was then calculated: $F_v/F_m=[(F_m - F_0)/F_m)]$. In light-adapted leaves, the steady-state fluorescence yield ($F_s$) was measured with the application of a saturating white light pulse (8000 $\mu$mol $m^{-2}$ $s^{-1}$) to achieve the light-adapted maximum fluorescence ($F_m'$). A far-red illumination (2 $\mu$mol $m^{-2}$ $s^{-1}$) was applied after turn off the actinic light to measure the light-adapted initial fluorescence ($F_0'$). The capture efficiency of excitation energy by open PSII reaction centers ($F_v'/F_m'$) was estimated following Logan et al. (2007) and the actual PSII photochemical efficiency ($\phi_{PSII}$) was estimated as $\phi_{PSII} = (F_m' - F_s)/F_m'$ (Genty et al., 1989).

As the $\phi_{PSII}$ represents the number of electrons transferred per photon absorbed in the PSII, the electron transport rate ($J_{flu}$) was calculated as $J_{flu} = \phi_{PSII} \cdot \alpha \cdot \beta \cdot PPFD$, where $\alpha$ is leaf absorptance and $\beta$ reflects the partitioning of absorbed quanta between PSII and PSI, and the product $\alpha\beta$ was adopted as described in the literature for Arabidopsis as equal to 0.451 (Flexas et al., 2007).

Dark respiration ($R_d$) was measured using the same gas exchange system as described above after at least 1 h during the dark period and it was divided by two ($R_d/2$) to estimate the mitochondrial respiration rate in the light ($R_L$; Niinemets et al., 2005, 2006; Niinemets et al., 2009).

*A*/PPFD curves were initiated at ambient $CO_2$ concentration ($C_a$) of 400 $\mu$mol $mol^{-1}$ and PPFD of 600 $\mu$mol $m^{-2}$ $s^{-1}$. Then, the PPFD was increased to 1000 $\mu$mol $m^{-2}$ $s^{-1}$ and after decreased until 0 $\mu$mol $m^{-2}$ $s^{-1}$ (11 different PPFD steps). Simultaneously chlorophyll *a* fluorescence parameters were obtained (Yin et al., 2009). The responses of $A_N$ to $C_i$ ($A/C_i$ curves) were performed at 700 $\mu$mol $m^{-2}$ $s^{-1}$ at 25°C under ambient $O_2$. Briefly, the measurements started at ambient $CO_2$ concentration ($C_a$) of 400 $\mu$mol $mol^{-1}$ and once the steady state was reached, $C_a$ was decreased stepwise to 50 $\mu$mol $mol^{-1}$. Upon completion of the measurements at low $C_a$, $C_a$ was returned to 400 $\mu$mol $mol^{-1}$ to restore the

original $A_N$. Next, $C_a$ was increased stepwise to1600 $\mu$mol mol$^{-1}$ in a total of 13 different $C_a$ values (Long and Bernacchi, 2003). Corrections for the leakage of $CO_2$ into and water vapor out of the leaf chamber of the LI-6400 were applied to all gas exchange data as described by Rodeghiero et al. (2007). $A/C_i$ and $A_N$/PPFD curves were obtained using the ninth leaf totally expanded from ten different plants per genotype in two independent assays (five plants in each assay).

## Estimation of Mesophyll Conductance ($g_m$), Maximum Rate of Carboxylation ($V_{cmax}$), Maximum Rate of Carboxylation Limited by Electron Transport ($J_{max}$), and Photosynthetic Limitations

The concentration of $CO_2$ in the carboxylation sites ($C_c$) was calculated following Harley et al. (1992) as:

$$C_c = \left(\Gamma^*\left(J_{flu} + 8(A_N + R_L)\right)\right) \Big/ \left(J_{flu} - 4(A_N + R_L)\right)$$

where the conservative value of $\Gamma^*$ for Arabidopsis was taken from Walker et al. (2013). Then, $g_m$ was estimated as the slope of the $A_N$ versus $C_i - C_c$ relationship as:

$$g_m = A_N/(C_i - C_c)$$

Thus, estimated $g_m$ is an averaged value over the points used in the relationship ($C_i < 300$ $\mu$mol mol$^{-1}$).

Given that current methods for estimating $g_m$ include several assumptions as well as technical limitations and sources of error that need to be considered to obtain reliable values (Pons et al., 2009), $g_m$ was estimated by the Ethier and Livingston (2004) method, which fits $A_N/C_i$ curves with a nonrectangular hyperbola version Farquhar-von Caemmerer-Berry FvCB model, based on the hypothesis that $g_m$ reduces the curvature of the Rubisco-limited portion of an $A_N/C_i$ curve.

From $A_N/C_i$ and $A_N/C_c$ curves, the maximum carboxylation velocity ($V_{cmax}$) and the maximum capacity for electron transport rate ($J_{max}$) were calculated by fitting the mechanistic model of $CO_2$ assimilation (Farquhar et al., 1980) using the $C_i$ or $C_c$-based temperature dependence of kinetic parameters of Rubisco ($K_c$ and $K_o$; Walker et al., 2013). Then $V_{cmax}$, $J_{max}$, and $g_m$ were normalized to 25°C using the temperature response equations from (Sharkey et al., 2007).

The photosynthetic limitations estimated based on the approach described by Grassi and Magnani (2005). This method uses the values of $A_N$, $g_s$, $g_m$, $V_{cmax}$, $\Gamma^*$, $C_c$, and $K_m = K_c\ (1 + O/K_o)$ and permits the partitioning into the functional components of photosynthetic constraints related to stomatal ($l_s$), mesophyll ($l_m$), and biochemical ($l_b$) limitations:

$$l_s = \frac{\left(\frac{g_{tot}}{g_s} \times \frac{\partial A_N}{\partial C_c}\right)}{\left(g_{tot} + \frac{\partial A_N}{\partial C_c}\right)}$$

$$l_m = \frac{\left(\frac{g_{tot}}{g_m} \times \frac{\partial A_N}{\partial C_c}\right)}{\left(g_{tot} + \frac{\partial A_N}{\partial C_c}\right)}$$

$$l_b = \frac{g_{tot}}{\left(g_{tot} + \frac{\partial A_N}{\partial C_c}\right)}$$

$g_{tot}$ is the total conductance to $CO_2$ from ambient air to chloroplasts ($g_{tot}$=1/[(1/$g_s$) + (1/$g_m$)]). The fraction $\partial A_N/\partial C_c$ was calculated as:

$$\frac{\partial A_N}{\partial C_c} = \frac{\left[V_{cmax}(\Gamma^* + K_m)\right]}{(C_c + K_m)}$$

## Stomatal Opening and Closing Kinetics Measurements

The $g_s$ values were recorded at intervals of 1 min using the same gas-exchange system described above. The $g_s$ responses to dark/light/dark transitions were measured in plants adapted to dark, at least for 2 h. The light in the chamber was kept turned off, and then turned on and then off for 10/60/60 min. The $CO_2$ concentration in the chamber was 400 $\mu$mol mol$^{-1}$ air. For responses to $CO_2$ concentration, transitions leaves were exposed to 400/800/400 $\mu$mol $CO_2$ mol$^{-1}$ air for 10/60/40 min under PPFD of 150 $\mu$mol m$^{-2}$ s$^{-1}$.

## Water Loss Measurements

For water loss measurements, the weight of detached rosettes, incubated abaxial side up under the same growth conditions described above, were determined over 4 h at the indicated time points. Water loss was calculated as a percentage of the initial fresh weight (Araújo et al., 2011b).

## Determination of Metabolite Levels

Whole rosettes were harvested in different times along of the light/dark cycle (0, 4, 8, 16, and 24 h). Rosettes were flash-frozen in liquid nitrogen and stored at −80°C until further analyses. Metabolite extraction was performed by rapid grinding in liquid nitrogen and immediate addition of the appropriate extraction buffer. The levels of starch, Suc, Fru, and Glc in the leaf tissues were determined exactly as described previously (Fernie et al., 2001). Malate and fumarate were determined exactly as detailed by Nunes-Nesi et al. (2007). Proteins and amino acids were determined as described previously (Gibon et al., 2004b). The levels of others metabolites were quantified by GC-MS as described by Roessner et al. (2001), whereas photosynthetic pigments were determined exactly as described before (Porra et al., 1989).

## Analyses of Enzymatic Activities

The enzymatic extract was prepared as previously described (Gibon et al., 2004a). Rubisco, PGK, transketolase, NADP-GAPDH, NAD-MDH, NADP-MDH, and Susy activities were determined as described by Sulpice et al. (2007), Burrell et al. (1994), Gibon et al. (2004a), Leegood and Walker (1980), Jenner et al. (2001), Scheibe and Stitt (1988), and Zrenner et al. (1995), respectively.

## Isolation of Guard-Cell-Enriched Epidermal Fragments

The isolation of guard-cell-enriched epidermal fragments was performed as described previously (Pandey et al., 2002) with minor adaptations. Fully expanded leaves from four rosettes per sample were blended for 1 min and then for 30 s to 1 min (twice for 30 s) using a warring blender (Phillips, RI 2044) with an internal filter to clarify the epidermal fragments of mesophyll and fibrous cells. Subsequently, epidermal fragments were collected on a nylon membrane (200 $\mu$m mesh) and washed to avoid apoplast contamination before being frozen in liquid nitrogen. This protocol resulted in a guard cell purity of approximately 98% as assessed by Antunes et al. (2012).

## qRT-PCR

qRT-PCR analysis was performed with total RNA isolated from epidermal fragments using the TRizol reagent (Ambion, Life Technology) following the manufacturer's manual. The integrity of the RNA was checked on 1% (w/v) agarose gels, and the concentration was measured before and after DNase I digestion using a spectrophotometer. Digestion with DNase I (Amplication Grade DNase I, Invitrogen) was performed according to the manufacturer's instructions. Subsequently, total RNA was reverse-transcribed into cDNA using Universal RiboClone cDNA Synthesis System (Promega) according to the respective manufacturer's protocols. For analysis of gene expression, the Power SYBR Green PCR Master Mix was used with the MicroAmp Optical 96-well Reaction Plate (both from Applied Biosystems) and MicroAmp Optical Adhesive Film (Applied Biosystems). The obtained cycle number at threshold was adjusted, and the estimation of the amplification efficiency was calculated using the Real-Time PCR Miner tool (Zhao and Fernald, 2005). The relative expression levels were normalized using the constitutively expressed genes *F-BOX* and *TIP41-LIKE* (Czechowski et al., 2005) and calculated using the ΔΔCT method. The primers used for qRT-PCR were designed using the QuantPrime software (Arvidsson et al., 2008) or taken from those described by Laanemets et al. (2013). Detailed primer information is described in Supplemental Table S2. The following genes were analyzed: *ALUMINUM ACTIVATED MALATE TRANSPORTER6* and *-9*, *ALMT6* and *ALMT9*; *ARABIDOPSIS THALIANA ATP-BINDING CASSETTE B14*, *AtABCB14* (Lee et al., 2008); *SLAC1*; *H$^+$-ATPASE1* and *-5*, *AHA1* and *AHA5* (Ueno et al., 2005); *POTASSIUM CHANNEL IN ARABIDOPSIS THALIANA1*, *KAT1* (Nakamura et al., 1995) and *KAT2*

(Pilot et al., 2001); *K+ TRANSPORTER1* and *-2*, *AKT1* and *AKT2* (Cao et al., 1995); *ARABIDOPSIS THALIANA K+ RECTIFYING CHANNEL1*, *AtKC1* (Reintanz et al., 2002); the $K^+$ outflow channel *GATED OUTWARDLY-RECTIFYING $K^+$ CHANNEL*, *GORK* (Ache et al., 2000); and *TWO-PORE CHANNEL1*, *TPC1* (Peiter et al., 2005).

## Experimental Design and Statistical Analysis

The data were obtained from the experiments using a completely randomized design using all four genotypes (two WT-like genotypes × two T-DNA mutant lines *atquac1*). Data are expressed as the mean ± SE. Data were submitted to ANOVA and tested for significant ($P < 0.05$) differences using Student's *t* tests. All the statistical analyses were performed using the algorithm embedded into Excel (Microsoft).

## Supplemental Data

The following supplemental materials are available.

**Supplemental Figure S1.** *AtQUAC1* gene structure and semiquantitative RT-PCR.

**Supplemental Figure S2.** Stomatal aperture and closure kinetics in response to light and $CO_2$.

**Supplemental Figure S3.** Net photosynthesis curves in response to PPFD.

**Supplemental Figure S4.** Total chlorophyll content and chlorophyll *a*/*b* ratio.

**Supplemental Figure S5.** Nitrate, free amino acids, and soluble protein content.

**Supplemental Figure S6.** Organic acid content.

**Supplemental Table S1.** Photosynthetic parameters obtained from light-response curves.

**Supplemental Table S2.** Primers utilized for qRT-PCR.

**Supplemental Table S3.** Relative metabolite levels determined by GC-MS.

Received July 7, 2015; accepted November 5, 2015; published November 5, 2015.

## LITERATURE CITED

**Ache P, Becker D, Ivashikina N, Dietrich P, Roelfsema MRG, Hedrich R** (2000) GORK, a delayed outward rectifier expressed in guard cells of Arabidopsis thaliana, is a $K(^+)$-selective, $K(^+)$-sensing ion channel. FEBS Lett **486:** 93–98

**Antunes WC, Provart NJ, Williams TCR, Loureiro ME** (2012) Changes in stomatal function and water use efficiency in potato plants with altered sucrolytic activity. Plant Cell Environ **35:** 747–759

**Araújo WL, Nunes-Nesi A, Fernie AR** (2011a) Fumarate: multiple functions of a simple metabolite. Phytochemistry **72:** 838–843

**Araújo WL, Nunes-Nesi A, Osorio S, Usadel B, Fuentes D, Nagy R, Balbo I, Lehmann M, Studart-Witkowski C, Tohge T, et al** (2011b) Antisense inhibition of the iron-sulphur subunit of succinate dehydrogenase enhances photosynthesis and growth in tomato via an organic acid-mediated effect on stomatal aperture. Plant Cell **23:** 600–627

**Arvidsson S, Kwasniewski M, Riaño-Pachón DM, Mueller-Roeber B** (2008) QuantPrime–a flexible tool for reliable high-throughput primer design for quantitative PCR. BMC Bioinformatics **9:** 465

**Berger D, Altmann T** (2000) A subtilisin-like serine protease involved in the regulation of stomatal density and distribution in Arabidopsis thaliana. Genes Dev **14:** 1119–1131

**Bergmann DC, Sack FD** (2007) Stomatal development. Annu Rev Plant Biol **58:** 163–181

**Bernacchi CJ, Portis AR, Nakano H, von Caemmerer S, Long SP** (2002) Temperature response of mesophyll conductance. Implications for the determination of Rubisco enzyme kinetics and for limitations to photosynthesis in vivo. Plant Physiol **130:** 1992–1998

**Blatt MR, Wang Y, Leonhardt N, Hills A** (2014) Exploring emergent properties in cellular homeostasis using OnGuard to model $K^+$ and other ion transport in guard cells. J Plant Physiol **171:** 770–778

**Borland AM, Hartwell J, Weston DJ, Schlauch KA, Tschaplinski TJ, Tuskan GA, Yang X, Cushman JC** (2014) Engineering crassulacean acid metabolism to improve water-use efficiency. Trends Plant Sci **19:** 327–338

**Bown HE, Watt MS, Mason EG, Clinton PW, Whitehead D** (2009) The influence of nitrogen and phosphorus supply and genotype on mesophyll conductance limitations to photosynthesis in Pinus radiata. Tree Physiol **29:** 1143–1151

**Boyes DC, Zayed AM, Ascenzi R, McCaskill AJ, Hoffman NE, Davis KR, Görlach J** (2001) Growth stage-based phenotypic analysis of Arabidopsis: a model for high throughput functional genomics in plants. Plant Cell **13:** 1499–1510

**Brandt B, Brodsky DE, Xue S, Negi J, Iba K, Kangasjärvi J, Ghassemian M, Stephan AB, Hu H, Schroeder JI** (2012) Reconstitution of abscisic acid activation of SLAC1 anion channel by CPK6 and OST1 kinases and branched ABI1 PP2C phosphatase action. Proc Natl Acad Sci USA **109:** 10593–10598

**Buckley TN, Warren CR** (2014) The role of mesophyll conductance in the economics of nitrogen and water use in photosynthesis. Photosynth Res **119:** 77–88

**Burrell M, Mooney P, Blundy M, Carter D, Wilson F, Green J, Blundy K, Rees T** (1994) Genetic manipulation of 6-phosphofructokinase in potato tubers. Planta **194:** 95–101

**Busch FA** (2014) Opinion: the red-light response of stomatal movement is sensed by the redox state of the photosynthetic electron transport chain. Photosynth Res **119:** 131–140

**Cao Y, Ward JM, Kelly WB, Ichida AM, Gaber RF, Anderson JA, Uozumi N, Schroeder JI, Crawford NM** (1995) Multiple genes, tissue specificity, and expression-dependent modulation contribute to the functional diversity of potassium channels in Arabidopsis thaliana. Plant Physiol **109:** 1093–1106

**Cowan IR, Troughton JH** (1971) The relative role of stomata in transpiration and assimilation. Planta **97:** 325–336

**Czechowski T, Stitt M, Altmann T, Udvardi MK, Scheible W-R** (2005) Genome-wide identification and testing of superior reference genes for transcript normalization in Arabidopsis. Plant Physiol **139:** 5–17

**De Vylder J, Vandenbussche F, Hu Y, Philips W, Van Der Straeten D** (2012) Rosette tracker: an open source image analysis tool for automatic quantification of genotype effects. Plant Physiol **160:** 1149–1159

**Du QS, Fan XW, Wang CH, Huang RB** (2011) A possible $CO_2$ conducting and concentrating mechanism in plant stomata SLAC1 channel. PLoS One **6:** e24264

**Duan B, Li Y, Zhang X, Korpelainen H, Li C** (2009) Water deficit affects mesophyll limitation of leaves more strongly in sun than in shade in two contrasting Picea asperata populations. Tree Physiol **29:** 1551–1561

**Ethier GJ, Livingston NJ** (2004) On the need to incorporate sensitivity to $CO^2$ transfer conductance into the Farquhar–von Caemmerer–Berry leaf photosynthesis model. Plant Cell Environ **27:** 137–153

**Farquhar GD, von Caemmerer S, Berry JA** (1980) A biochemical model of photosynthetic $CO_2$ assimilation in leaves of C 3 species. Planta **149:** 78–90

**Fernie AR, Martinoia E** (2009) Malate. Jack of all trades or master of a few? Phytochemistry **70:** 828–832

**Fernie AR, Roscher A, Ratcliffe RG, Kruger NJ** (2001) Fructose 2,6-bisphosphate activates pyrophosphate: fructose-6-phosphate 1-phosphotransferase and increases triose phosphate to hexose phosphate cycling in heterotrophic cells. Planta **212:** 250–263

**Flexas J, Barbour MM, Brendel O, Cabrera HM, Carriquí M, Díaz-Espejo A, Douthe C, Dreyer E, Ferrio JP, Gago J, et al** (2012) Mesophyll diffusion conductance to $CO_2$: an unappreciated central player in photosynthesis. Plant Sci **193-194:** 70–84

**Flexas J, Niinemets U, Gallé A, Barbour MM, Centritto M, Diaz-Espejo A, Douthe C, Galmés J, Ribas-Carbo M, Rodriguez PL, et al** (2013) Diffusional conductances to $CO_2$ as a target for increasing photosynthesis and photosynthetic water-use efficiency. Photosynth Res **117:** 45–59

**Flexas J, Ortuño MF, Ribas-Carbo M, Diaz-Espejo A, Flórez-Sarasa ID, Medrano H** (2007) Mesophyll conductance to $CO_2$ in Arabidopsis thaliana. New Phytol **175:** 501–511

**Flexas J, Ribas-Carbó M, Diaz-Espejo A, Galmés J, Medrano H** (2008) Mesophyll conductance to $CO_2$: current knowledge and future prospects. Plant Cell Environ **31:** 602–621

**Franks PJW, W Doheny-Adams T, Britton-Harper ZJ, Gray JE** (2015) Increasing water-use efficiency directly through genetic manipulation of stomatal density. New Phytol **207:** 188–195

**Galmés J, Conesa MÀ, Ochogavía JM, Perdomo JA, Francis DM, Ribas-Carbó M, Savé R, Flexas J, Medrano H, Cifre J** (2011) Physiological and morphological adaptations in relation to water use efficiency in Mediterranean accessions of Solanum lycopersicum. Plant Cell Environ **34:** 245–260

**Galmés J, Ochogavía JM, Gago J, Roldán EJ, Cifre J, Conesa MÀ** (2013) Leaf responses to drought stress in Mediterranean accessions of Solanum lycopersicum: anatomical adaptations in relation to gas exchange parameters. Plant Cell Environ **36:** 920–935

**Geiger D, Scherzer S, Mumm P, Marten I, Ache P, Matschi S, Liese A, Wellmann C, Al-Rasheid KAS, Grill E, et al** (2010) Guard cell anion channel SLAC1 is regulated by CDPK protein kinases with distinct $Ca^{2+}$ affinities. Proc Natl Acad Sci USA **107:** 8023–8028

**Genty B, Briantais JM, Baker NR** (1989) The relationship between the quantum yield of photosynthetic electron transport and quenching of chlorophyll fluorescence. Biochim Biophys Acta **990:** 87–92

**Gibon Y, Blaesing OE, Hannemann J, Carillo P, Höhne M, Hendriks JH, Palacios N, Cross J, Selbig J, Stitt M** (2004a) A Robot-based platform to measure multiple enzyme activities in Arabidopsis using a set of cycling assays: comparison of changes of enzyme activities and transcript levels during diurnal cycles and in prolonged darkness. Plant Cell **16:** 3304–3325

**Gibon Y, Bläsing OE, Palacios-Rojas N, Pankovic D, Hendriks JH, Fisahn J, Höhne M, Günther M, Stitt M** (2004b) Adjustment of diurnal starch turnover to short days: depletion of sugar during the night leads to a temporary inhibition of carbohydrate utilization, accumulation of sugars and post-translational activation of ADP-glucose pyrophosphorylase in the following light period. Plant J **39:** 847–862

**Grassi G, Magnani F** (2005) Stomatal, mesophyll conductance and biochemical limitations to photosynthesis as affected by drought and leaf ontogeny in ash and oak trees. Plant Cell Environ **28:** 834–849

**Harley PC, Loreto F, Di Marco G, Sharkey TD** (1992) Theoretical considerations when estimating the mesophyll conductance to $CO_2$ flux by analysis of the response of photosynthesis to $CO_2$. Plant Physiol **98:** 1429–1436

**Hedrich R, Marten I** (1993) Malate-induced feedback regulation of plasma membrane anion channels could provide a $CO_2$ sensor to guard cells. EMBO J **12:** 897–901

**Hedrich R, Marten I, Lohse G, Dietrich P, Winter H, Lohaus G, Heldt HW** (1994) Malate-sensitive anion channels enable guard-cells to sense changes in the ambient $CO_2$ concentration. Plant J **6:** 741–748

**Hetherington AM** (2001) Guard cell signaling. Cell **107:** 711–714

**Hunt R, Causton DR, Shipley B, Askew AP** (2002) A modern tool for classical plant growth analysis. Ann Bot (Lond) **90:** 485–488

**Imes D, Mumm P, Böhm J, Al-Rasheid KAS, Marten I, Geiger D, Hedrich R** (2013) Open stomata 1 (OST1) kinase controls R-type anion channel QUAC1 in Arabidopsis guard cells. Plant J **74:** 372–382

**Jenner HL, Winning BM, Millar AH, Tomlinson KL, Leaver CJ, Hill SA** (2001) NAD malic enzyme and the control of carbohydrate metabolism in potato tubers. Plant Physiol **126:** 1139–1149

**Jin SH, Huang JQ, Li XQ, Zheng BS, Wu JS, Wang ZJ, Liu GH, Chen M** (2011) Effects of potassium supply on limitations of photosynthesis by mesophyll diffusion conductance in Carya cathayensis. Tree Physiol **31:** 1142–1151

**Kim T-H, Böhmer M, Hu H, Nishimura N, Schroeder JI** (2010) Guard cell signal transduction network: advances in understanding abscisic acid, $CO_2$, and $Ca^{2+}$ signaling. Annu Rev Plant Biol **61:** 561–591

**Kollist H, Nuhkat M, Roelfsema MRG** (2014) Closing gaps: linking elements that control stomatal movement. New Phytol **203:** 44–62

**Kusumi K, Hirotsuka S, Kumamaru T, Iba K** (2012) Increased leaf photosynthesis caused by elevated stomatal conductance in a rice mutant deficient in SLAC1, a guard cell anion channel protein. J Exp Bot **63:** 5635–5644

**Laanemets K, Wang Y-F, Lindgren O, Wu J, Nishimura N, Lee S, Caddell D, Merilo E, Brosche M, Kilk K, et al** (2013) Mutations in the SLAC1 anion channel slow stomatal opening and severely reduce $K^+$ uptake channel activity via enhanced cytosolic [$Ca^{2+}$] and increased $Ca^{2+}$ sensitivity of $K^+$ uptake channels. New Phytol **197:** 88–98

**Lawson T, Simkin AJ, Kelly G, Granot D** (2014) Mesophyll photosynthesis and guard cell metabolism impacts on stomatal behaviour. New Phytol **203:** 1064–1081

**Lee M, Choi Y, Burla B, Kim YY, Jeon B, Maeshima M, Yoo JY, Martinoia E, Lee Y** (2008) The ABC transporter AtABCB14 is a malate importer and modulates stomatal response to $CO_2$. Nat Cell Biol **10:** 1217–1223

**Leegood RC, Walker DA** (1980) Autocatalysis and light activation of enzymes in relation to photosynthetic induction in wheat chloroplasts. Arch Biochem Biophys **200:** 575–582

**Lisec J, Schauer N, Kopka J, Willmitzer L, Fernie AR** (2006) Gas chromatography mass spectrometry-based metabolite profiling in plants. Nat Protoc **1:** 387–396

**Logan BA, Adams WW, Demmig-Adams B** (2007) Avoiding common pitfalls of chlorophyll fluorescence analysis under field conditions. Funct Plant Biol **34:** 853–859

**Long SP, Bernacchi CJ** (2003) Gas exchange measurements, what can they tell us about the underlying limitations to photosynthesis? Procedures and sources of error. J Exp Bot **54:** 2393–2401

**Martinoia E, Meyer S, De Angeli A, Nagy R** (2012) Vacuolar transporters in their physiological context. Annu Rev Plant Biol **63:** 183–213

**Martins SCV, Galmés J, Molins A, DaMatta FM** (2013) Improving the estimation of mesophyll conductance to $CO_2$: on the role of electron transport rate correction and respiration. J Exp Bot **64:** 1–14

**Medeiros DB, Daloso DM, Fernie AR, Nikoloski Z, Araújo WL** (2015) Utilizing systems biology to unravel stomatal function and the hierarchies underpinning its control. Plant Cell Environ **38:** 1457–1470

**Meyer S, Mumm P, Imes D, Endler A, Weder B, Al-Rasheid KAS, Geiger D, Marten I, Martinoia E, Hedrich R** (2010) AtALMT12 represents an R-type anion channel required for stomatal movement in Arabidopsis guard cells. Plant J **63:** 1054–1062

**Mumm P, Imes D, Martinoia E, Al-Rasheid KAS, Geiger D, Marten I, Hedrich R** (2013) C-terminus-mediated voltage gating of Arabidopsis guard cell anion channel QUAC1. Mol Plant **6:** 1550–1563

**Murashige T, Skoog F** (1962) A revised medium for a rapid growth and bioassays with tobacco tissues cultures. Physiol Plant **15:** 473–497

**Nakamura RL, McKendree WL Jr, Hirsch RE, Sedbrook JC, Gaber RF, Sussman MR** (1995) Expression of an Arabidopsis potassium channel gene in guard cells. Plant Physiol **109:** 371–374

**Negi J, Matsuda O, Nagasawa T, Oba Y, Takahashi H, Kawai-Yamada M, Uchimiya H, Hashimoto M, Iba K** (2008) $CO_2$ regulator SLAC1 and its homologues are essential for anion homeostasis in plant cells. Nature **452:** 483–486

**Niinemets Ü, Cescatti A, Rodeghiero M, Tosens T** (2005) Leaf internal diffusion conductance limits photosynthesis more strongly in older leaves of Mediterranean evergreen broad-leaved species. Plant Cell Environ **28:** 1552–1566

**Niinemets U, Cescatti A, Rodeghiero M, Tosens T** (2006) Complex adjustments of photosynthetic potentials and internal diffusion conductance to current and previous light availabilities and leaf age in Mediterranean evergreen species Quercus ilex. Plant Cell Environ **29:** 1159–1178

**Niinemets U, Díaz-Espejo A, Flexas J, Galmés J, Warren CR** (2009) Role of mesophyll diffusion conductance in constraining potential photosynthetic productivity in the field. J Exp Bot **60:** 2249–2270

**Nunes-Nesi A, Carrari F, Gibon Y, Sulpice R, Lytovchenko A, Fisahn J, Graham J, Ratcliffe RG, Sweetlove LJ, Fernie AR** (2007) Deficiency of mitochondrial fumarase activity in tomato plants impairs photosynthesis via an effect on stomatal function. Plant J **50:** 1093–1106

**Pandey S, Wang X-Q, Coursol SA, Assmann SM** (2002) Preparation and applications of Arabidopsis thaliana guard cell protoplasts. New Phytol **153:** 517–526

**Pandey S, Zhang W, Assmann SM** (2007) Roles of ion channels and transporters in guard cell signal transduction. FEBS Lett **581:** 2325–2336

**Peguero-Pina JJ, Flexas J, Galmés J, Niinemets U, Sancho-Knapik D, Barredo G, Villarroya D, Gil-Pelegrín E** (2012) Leaf anatomical properties in relation to differences in mesophyll conductance to $CO(_2)$ and photosynthesis in two related Mediterranean Abies species. Plant Cell Environ **35:** 2121–2129

**Peiter E, Maathuis FJM, Mills LN, Knight H, Pelloux J, Hetherington AM, Sanders D** (2005) The vacuolar $Ca^{2+}$-activated channel TPC1 regulates germination and stomatal movement. Nature **434:** 404–408

**Penfield S, Clements S, Bailey KJ, Gilday AD, Leegood RC, Gray JE, Graham IA** (2012) Expression and manipulation of phosphoenolpyruvate carboxykinase 1 identifies a role for malate metabolism in stomatal closure. Plant J **69:** 679–688

**Pilot G, Lacombe B, Gaymard F, Cherel I, Boucherez J, Thibaud JB, Sentenac H** (2001) Guard cell inward $K^+$ channel activity in arabidopsis involves expression of the twin channel subunits KAT1 and KAT2. J Biol Chem **276:** 3215–3221

**Pons TL, Flexas J, von Caemmerer S, Evans JR, Genty B, Ribas-Carbó M, Brugnoli E** (2009) Estimating mesophyll conductance to $CO_2$: methodology, potential errors and recommendations. J Exp Bot **60:** 2217–2234

**Poorter H, Niinemets U, Poorter L, Wright IJ, Villar R** (2009) Causes and consequences of variation in leaf mass per area (LMA): a meta-analysis. New Phytol **182:** 565–588

**Porra RJ, Thompson WA, Kriedemann PE** (1989) Determination of accurate extinction coefficients and simultaneous equations for assaying chlorophylls a and b extracted with four different solvents: verification

of the concentration of chlorophyll standards by atomic absorption spectroscopy. BBA - Bioenergetics **975:** 384–394

**Raschke K** (2003) Alternation of the slow with the quick anion conductance in whole guard cells effected by external malate. Planta **217:** 651–657

**Reintanz B, Szyroki A, Ivashikina N, Ache P, Godde M, Becker D, Palme K, Hedrich R** (2002) AtKC1, a silent Arabidopsis potassium channel $\alpha$ -subunit modulates root hair $K^+$ influx. Proc Natl Acad Sci USA **99:** 4079–4084

**Rodeghiero M, Niinemets U, Cescatti A** (2007) Major diffusion leaks of clamp-on leaf cuvettes still unaccounted: how erroneous are the estimates of Farquhar et al. model parameters? Plant Cell Environ **30:** 1006–1022

**Roelfsema MRG, Hedrich R** (2005) In the light of stomatal opening: new insights into 'the Watergate'. New Phytol **167:** 665–691

**Roessner U, Luedemann A, Brust D, Fiehn O, Linke T, Willmitzer L, Fernie A** (2001) Metabolic profiling allows comprehensive phenotyping of genetically or environmentally modified plant systems. Plant Cell **13:** 11–29

**Sablowski R, Carnier Dornelas M** (2014) Interplay between cell growth and cell cycle in plants. J Exp Bot **65:** 2703–2714

**Sasaki T, Mori IC, Furuichi T, Munemasa S, Toyooka K, Matsuoka K, Murata Y, Yamamoto Y** (2010) Closing plant stomata requires a homolog of an aluminum-activated malate transporter. Plant Cell Physiol **51:** 354–365

**Scafaro AP, Von Caemmerer S, Evans JR, Atwell BJ** (2011) Temperature response of mesophyll conductance in cultivated and wild Oryza species with contrasting mesophyll cell wall thickness. Plant Cell Environ **34:** 1999–2008

**Scheibe R, Stitt M** (1988) Comparison of NADP-malate dehydrogenase activation, QA reduction and $O_2$ evolution in spinach leaves. Plant Physiol Biochem **26:** 473–481

**Schroeder JI, Delhaize E, Frommer WB, Guerinot ML, Harrison MJ, Herrera-Estrella L, Horie T, Kochian LV, Munns R, Nishizawa NK, et al** (2013) Using membrane transporters to improve crops for sustainable food production. Nature **497:** 60–66

**Sharkey TD, Bernacchi CJ, Farquhar GD, Singsaas EL** (2007) Fitting photosynthetic carbon dioxide response curves for C(3) leaves. Plant Cell Environ **30:** 1035–1040

**Stitt M, Schulze D** (1994) Does Rubisco control the rate of photosynthesis and plant growth? An exercise in molecular ecophysiology. Plant Cell Environ **17:** 465–487

**Sulpice R, Tschoep H, VON Korff M, Büssis D, Usadel B, Höhne M, Witucka-Wall H, Altmann T, Stitt M, Gibon Y** (2007) Description and applications of a rapid and sensitive non-radioactive microplate-based assay for maximum and initial activity of D-ribulose-1,5-bisphosphate carboxylase/oxygenase. Plant Cell Environ **30:** 1163–1175

**Thompson DS** (2005) How do cell walls regulate plant growth? J Exp Bot **56:** 2275–2285

**Tissier AF, Marillonnet S, Klimyuk V, Patel K, Torres MA, Murphy G, Jones JD** (1999) Multiple independent defective suppressor-mutator transposon insertions in Arabidopsis: a tool for functional genomics. Plant Cell **11:** 1841–1852

**Tschoep H, Gibon Y, Carillo P, Armengaud P, Szecowka M, Nunes-Nesi A, Fernie AR, Koehl K, Stitt M** (2009) Adjustment of growth and central metabolism to a mild but sustained nitrogen-limitation in Arabidopsis. Plant Cell Environ **32:** 300–318

**Ueno K, Kinoshita T, Inoue S, Emi T, Shimazaki K** (2005) Biochemical characterization of plasma membrane $H^+$-ATPase activation in guard cell protoplasts of Arabidopsis thaliana in response to blue light. Plant Cell Physiol **46:** 955–963

**Vahisalu T, Kollist H, Wang Y-F, Nishimura N, Chan W-Y, Valerio G, Lamminmäki A, Brosché M, Moldau H, Desikan R, et al** (2008) SLAC1 is required for plant guard cell S-type anion channel function in stomatal signalling. Nature **452:** 487–491

**Vahisalu T, Puzõrjova I, Brosché M, Valk E, Lepiku M, Moldau H, Pechter P, Wang Y-S, Lindgren O, Salojärvi J, et al** (2010) Ozone-triggered rapid stomatal response involves the production of reactive oxygen species, and is controlled by SLAC1 and OST1. Plant J **62:** 442–453

**Vavasseur A, Raghavendra AS** (2005) Guard cell metabolism and $CO_2$ sensing. New Phytol **165:** 665–682

**Vile D, Garnier E, Shipley B, Laurent G, Navas M-L, Roumet C, Lavorel S, Díaz S, Hodgson JG, Lloret F, et al** (2005) Specific leaf area and dry matter content estimate thickness in laminar leaves. Ann Bot (Lond) **96:** 1129–1136

**Villar R, Ruiz-Robleto J, Ubera JL, Poorter H** (2013) Exploring variation in leaf mass per area (LMA) from leaf to cell: an anatomical analysis of 26 woody species. Am J Bot **100:** 1969–1980

**Von Groll U, Berger D, Altmann T** (2002) The subtilisin-like serine protease SDD1 mediates cell-to-cell signaling during Arabidopsis stomatal development. Plant Cell **14:** 1527–1539

**Vrábl D, Vasková M, Hronková M, Flexas J, Šantrůček J** (2009) Mesophyll conductance to $CO(_2)$ transport estimated by two independent methods: effect of variable $CO(_2)$ concentration and abscisic acid. J Exp Bot **60:** 2315–2323

**Walker B, Ariza LS, Kaines S, Badger MR, Cousins AB** (2013) Temperature response of in vivo Rubisco kinetics and mesophyll conductance in Arabidopsis thaliana: comparisons to Nicotiana tabacum. Plant Cell Environ **36:** 2108–2119

**Warren CR** (2008a) Soil water deficits decrease the internal conductance to $CO_2$ transfer but atmospheric water deficits do not. J Exp Bot **59:** 327–334

**Warren CR** (2008b) Stand aside stomata, another actor deserves centre stage: the forgotten role of the internal conductance to $CO_2$ transfer. J Exp Bot **59:** 1475–1487

**Xiong TC, Hann CM, Chambers JP, Surget M, Ng CK-Y** (2009) An inducible, modular system for spatio-temporal control of gene expression in stomatal guard cells. J Exp Bot **60:** 4129–4136

**Yin X, Struik PC, Romero P, Harbinson J, Evers JB, VAN DER Putten PEL, Vos J** (2009) Using combined measurements of gas exchange and chlorophyll fluorescence to estimate parameters of a biochemical C photosynthesis model: a critical appraisal and a new integrated approach applied to leaves in a wheat (Triticum aestivum) canopy. Plant Cell Environ **32:** 448–464

**Zhao S, Fernald RD** (2005) Comprehensive algorithm for quantitative real-time polymerase chain reaction. J Comput Biol **12:** 1047–1064

**Zrenner R, Salanoubat M, Willmitzer L, Sonnewald U** (1995) Evidence of the crucial role of sucrose synthase for sink strength using transgenic potato plants (Solanum tuberosum L.). Plant J **7:** 97–107

**Supplemental information**

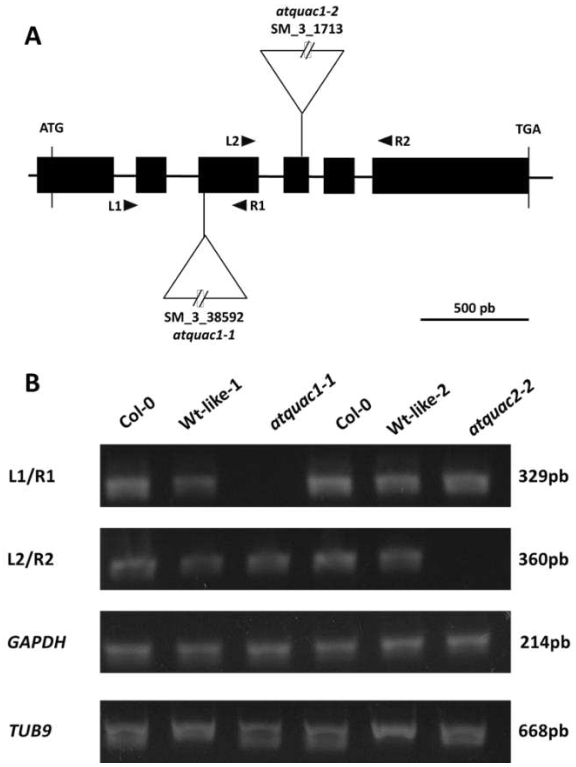


**Supplemental Figure S1: (A)** *AtQUAC1* gene structure. Arrows indicate the position of annealing of the primers used to genotyping as well as to semi quantitative RT-PCR. Black boxes indicate exons. Bar correspond to 500 pb. T-DNA insertion were identified in the third and fourth exons to *atquac1-1* and *atquac1-2* respectively. **(B)** Semi quantitative RT-PCR from total RNA extracted from Col-0, WT-like-1, WT-like-2, as well as *atquac1-1* and *atquac1-2* leaves. The primers used are indicated in the figure left. Gene expression by RT-PCR showed absence transcript in both mutant lines. *atquac1-1:* L1, 5´-GTTGTGCAAAGGGCTTAATAGAG-3´/R1 5´-CAAGAAGGCTCATGAAAAGACAG-3´; *atquac1-2*, L2 5´-ACAAGACCACCGTTGGTAAACTC-3´/R2 5´-CTCCGGCTAATCTTACACAAGG-3´). Gliceraldeide-3-phosphate-dehydrogenase (GAPDH) – AT1G16300: forward 5´-TGGTTGATCTCGTTGTGCAGGTCTC-3´ and reverse 5´-GTCAGCCAAGTCAACAACTCTCTG-3´, and β-tubuline (TUB9) – AT4G20890: forward 5´-GATATCTGTTTCCGTACCTTGAAGC-3´ and reverse 5´-CCGACTGTAGCATCTTGATATTGC-3´, were used as control. The standard PCR program was: (i) *AtQUAC1*: 30 cycles of 30 s at 94°C, 30 s at 54°C, and 30 s at 72°C with a 2 min extension of the first cycle at 94°C and a 3 min final extension at 72°C; (ii) *GAPDH:* 30 cycles of 30 s at 94°C, 30 s at 59°C, and 45 s at 72°C with a 2 min extension

of the first cycle at 94°C and a 3 min final extension at 72°C; and (iii) *TUB9:* 30 cycles of 30 s at 94°C, 30 s at 56°C, and 45 s at 72°C with a 2 min extension of the first cycle at 94°C and a 3 min final extension at 72°C. PCR products were analyzed by gel electrophoresis in a 1% (w/v) agarose gels.

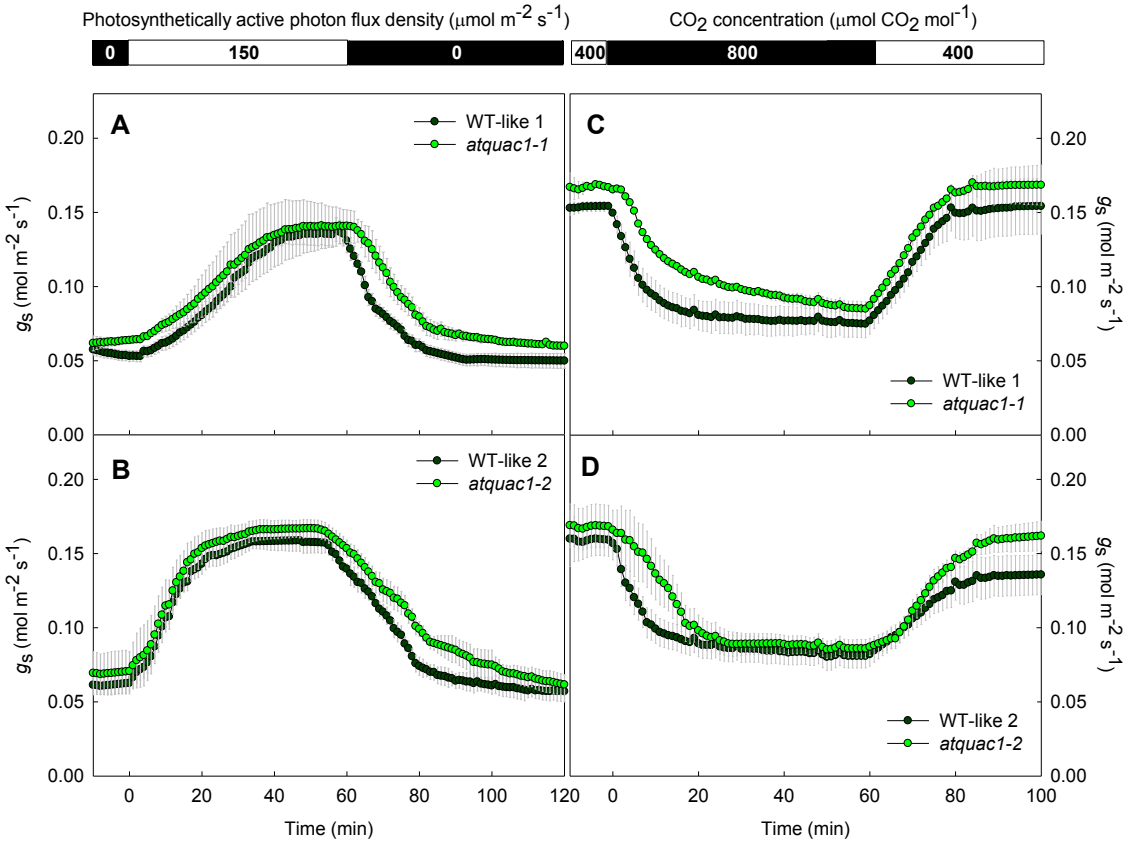


**Supplemental Figure S2:** Stomatal aperture and closure kinetics in response to light and $CO_2$ concentrations in WT-like and *atquac1* plants. Stomatal conductance ($g_s$) was evaluated in *atquac1-1* and *atquac1-2* and their corresponding WT-like in response to changes in light intensity (**A** and **B**, respectively) and $CO_2$ levels (**C** e **D**, respectively). Data presented are mean ± SE obtained using the 9$^{th}$ leaf totally expanded from ten different plants per genotype in two independent assays (five plants in each assay).

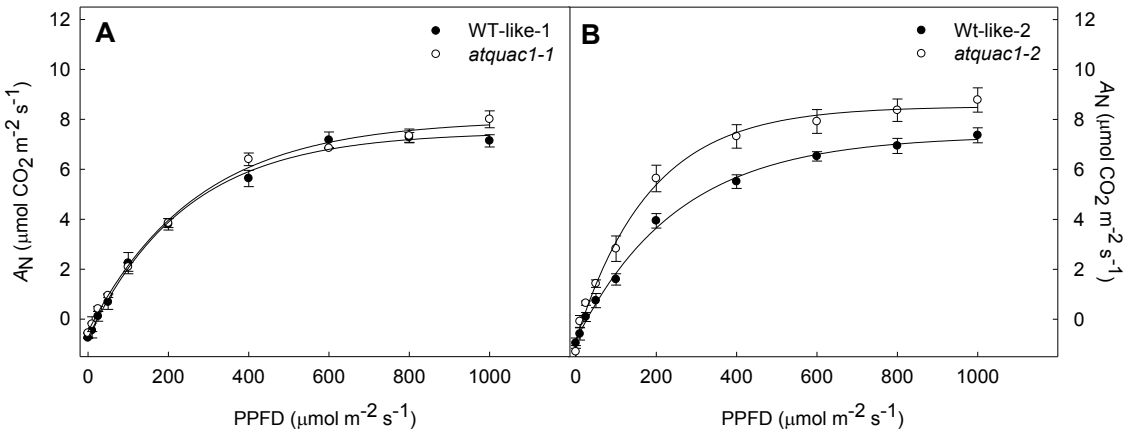


**Supplemental Figure S3:** Net photosynthesis ($A_N$) curves in response to changes in photosynthetically active photon flux density (PPFD). **(A)** $A_N$/ PPFD curves in WT-like-1 and *atquac1-1*. **(B)** $A_N$/ PPFD curves in WT-like-2 and *atquac1-2*. Data presented are mean ± SE obtained using the 9$^{th}$ leaf totally expanded from ten different plants per genotype in two independent assays (five plants in each assay).

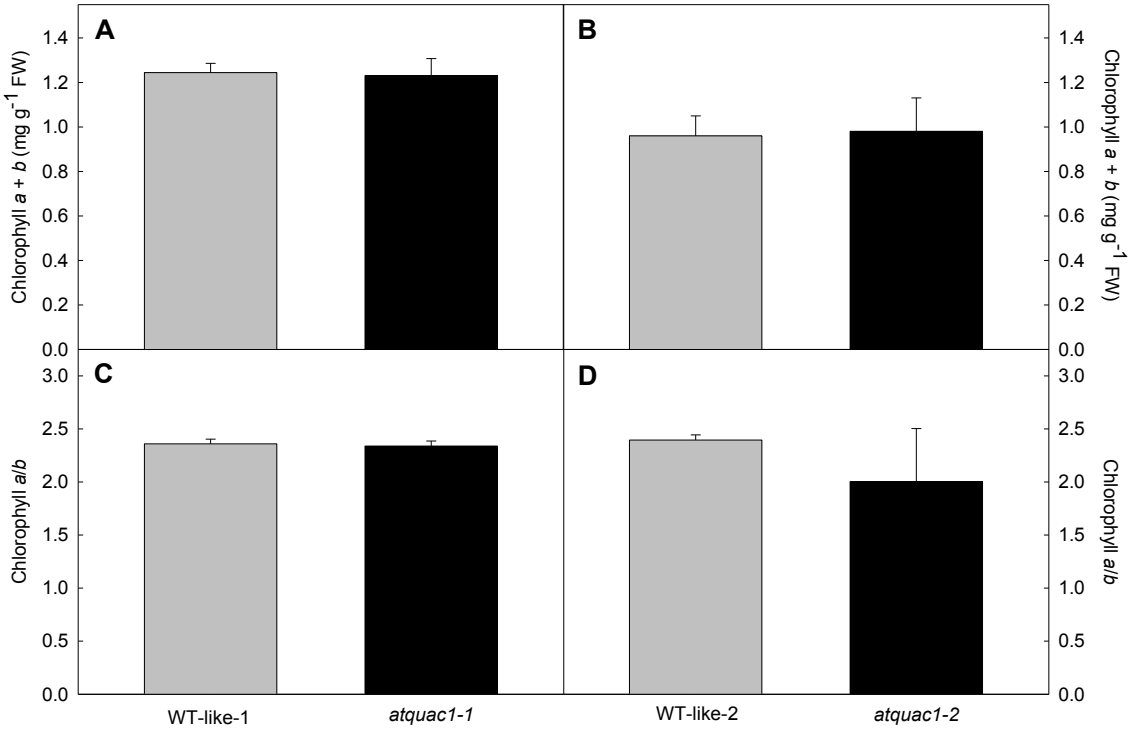


**Supplemental Figure S4:** Total chlorophyll content (*a* + *b*) as well as the *a*/*b* ratio in WT-like and *atquac1* plants. **(A)** and **(C)** to WT-like-1/*atquac1-1*; **(B)** and **(D)** to WT-like-2/*atquac1-2*, respectively. Data presented are mean ± SE (n = 5) from rosettes harvested at middle of the photoperiod.

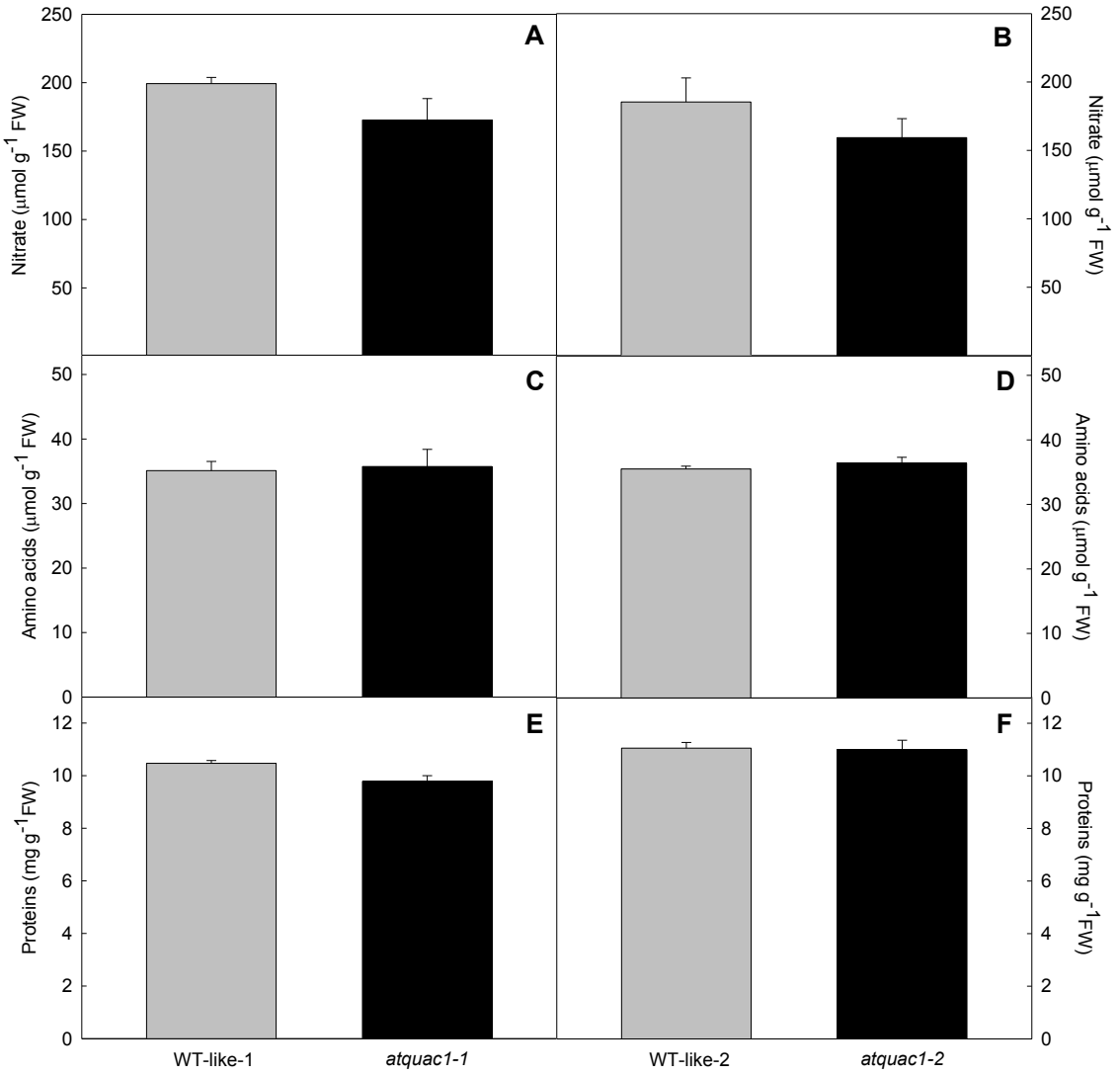


**Supplemental Figure S5:** Nitrate, free amino acids and soluble proteins content in WT-like and *atquac1* plants. **(A)** and **(B)** nitrate content; **(C)** and **(D)** free amino acids content; **(E)** and **(F)** soluble proteins in WT-like-1/*atquac1-1* and WT-like-2/*atquac1-2*, respectively. Data presented are mean ± SE (n = 5) from rosettes harvested at middle of the photoperiod.

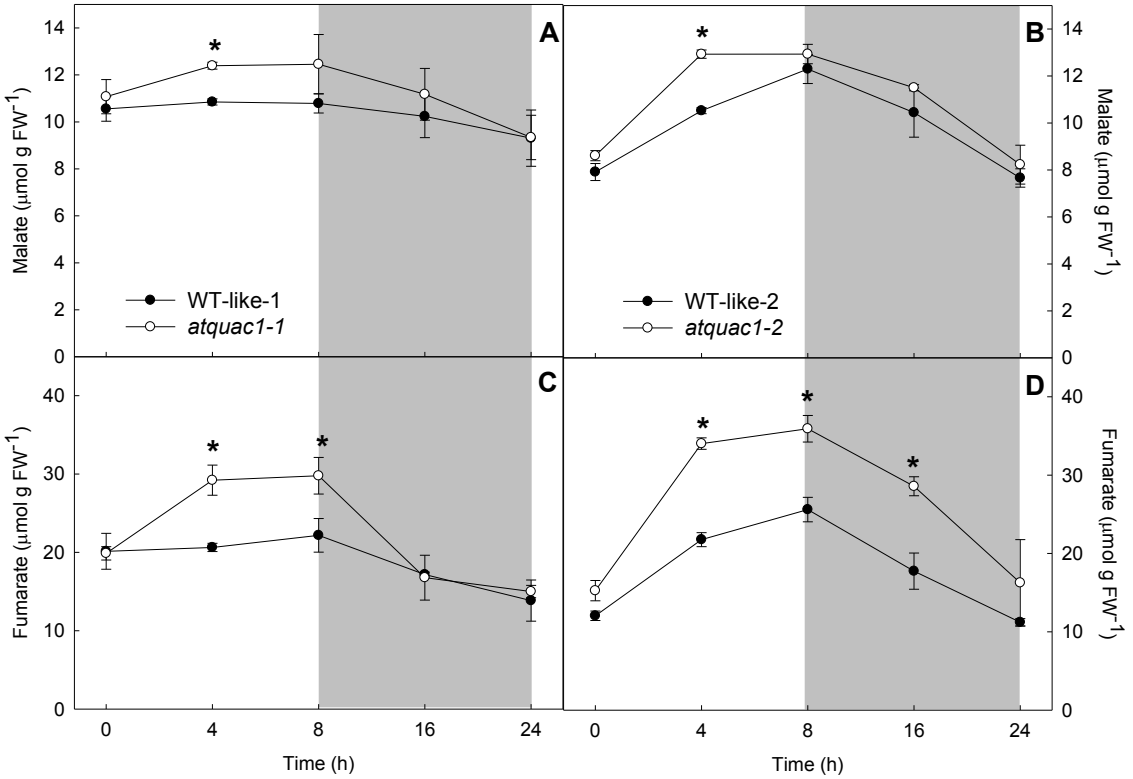


**Supplemental Figure S6:** Organic acids content in WT-like and *atquac1* plants. **(A)** and **(B)** malate; **(C)** and **(D)** fumarate to WT-like-1/*atquac1-1* and to WT-like-2/*atquac1-2*, respectively. Values are presented as means ± SE (n = 5) from whole rosettes harvested in different times along of the cycle of light/dark. Asterisk indicates the time where the values from mutants lines were determined by the Student's *t* test to be significantly different ($P < 0.05$) from its corresponding WT-like.

**Supplemental Table S1:** Photosynthetic parameters from light-response curves in WT-like and *atquac1* plants. Data presented are mean ± SE obtained using the 9th leaf totally expanded from ten different plants per genotype in two independent assays (five plants in each assay). Values set in bold in *atquac1* plants were determined by the Student's *t* test to be significantly different ($P < 0.05$) from their corresponding WT-like.

| Parameters* | WT-like-1 | *atquac1 - 1* | WT-like-2 | *atquac1 - 2* |
|---|---|---|---|---|
| $A_{PPFD}$ (μmol $CO_2$ $m^{-2}$ $s^{-1}$) | 6.8 ± 0.4 | 6.9 ± 0.1 | 6.5 ± 0.2 | **7.9 ± 0.5** |
| $I_c$ (μmol $m^{-2}$ $s^{-1}$) | 20.7 ± 0.3 | 22.2 ± 1.4 | 26.0 ± 1.6 | 24.9 ± 0.6 |
| $I_s$ (μmol $m^{-2}$ $s^{-1}$) | 698.2 ± 6.8 | 704.3 ± 37.8 | 540.0 ± 53.2 | **772.3 ± 16.1** |
| 1/ϕ (μmol photons $mol^{-1}$ $CO_2$) | 25.9 ± 0.8 | 27.5 ± 3.6 | 29.6 ± 1.2 | 25.4 ± 1.4 |

*$A_{PPFD}$: Net $CO_2$ assimilation rate saturated by light; $I_c$: light compensation point; $I_s$: light saturation point; 1/ϕ: Light use efficiency.

**Supplemental Table S2.** Primers utilized to qRT-PCR.

| Gene | Locus | Efficiency | Sequence 5'-3' |
|---|---|---|---|
| *F-BOX* | At5g15710 | 0.88 | Forward 5'-TTTCGGCTGAGAGGTTCGAGT-3' |
| *(Control)* | | | Reverse 5'-GATTCCAAGACGTAAAGCAGATCAA-3' |
| *TIP41-like* | At4g34270 | 0.86 | Forward 5'-GTGAAAACTGTTGGAGAGAAGCAA-3' |
| *(Control)* | | | Reverse 5'- TCAACTGGATACCCTTTCGCA-3' |
| *ALMT6* | At2g17470 | 0.82 | Forward 5'-AGCCTCCACATGGACCTTACAG-3' |
| | | | Reverse 5'-GATACAGGCAGCTCCAGAGAAACG-3' |
| *ALMT9* | At3g18440 | 0.86 | Forward 5'-TCTCTCAGAAATCCAGGCACCAG-3' |
| | | | Reverse 5'-ACGCCCACTCTCTGAAGTTCTTG-3' |
| *AtABCB14* | At1g28010 | 0.83 | Forward 5'-AGCTTTCTACAGACCCGAATGCC-3' |
| | | | Reverse 5'-TGCATCCAACAAGCAACTCCAATC-3' |
| *SLAC1* | At1g12480 | 0.81 | Forward 5'-ATGGCCAATTCGACGGATGTT-3' |
| | | | Reverse 5'-ACCACGCCACTGAGAACTTAAATC-3' |
| *AHA1* | At2g18960 | 0.82 | Forward 5'-CTGGGAGGCTACCAAGCCA-3' |
| | | | Reverse 5'-CTCACACCGAACTTGTCCGA-3' |
| *AHA5* | At2g24520 | 0.83 | Forward 5'-5'-GGCTGTTGCAAGACAGGAA-3' |
| | | | Reverse 5'-CGGAGGATCAAAAAGAGGTAAA-3' |
| *KAT1* | At5g46240 | 0.82 | Forward 5'-AGCATGGGATGGGAAGAGTGGAG-3' |
| | | | Reverse 5'-AGAGCAGTGTCGGAAGTCGGAT-3' |
| *KAT2* | At4g18290 | 0.85 | Forward 5'- 5'-TAGCTCGCTGTTTGCAAGG-3' |
| | | | Reverse 5'-CAAACAGTGTCACCGAAATGA-3' |
| *AKT1* | At2g26650 | 0.84 | Forward 5'-ACA TCCTTG TGAACGGAACC-3' |
| | | | Reverse 5'-CCTCTCTCACAATGCTTTCTGTT-3' |
| *AKT2* | At4g22200 | 0.83 | Forward 5'-5'-GCTGCTTTCGACTTCTATCAGT-3' |
| | | | Reverse 5'-ATCAGTCCATGTCTTTCCTTGGT-3' |
| *AtKC1* | At4g32650 | 0.81 | Forward 5'-CTCAAGACATGAAAATGGACAGAT-3' |
| | | | Reverse 5'-GAATCACCATTGTTTTTGTTATCTTG-3' |
| *TPC1* | At4g03560 | 0.78 | Forward 5'-CGCTTGATATCGAAGAAAGCTC-3' |
| | | | Reverse 5'-TCTCCAACACATATATCCAACCA-3' |
| *GORK* | At5g37500 | 0.85 | Forward 5'-GCATCAATCCGCGCCAAGATT-3' |
| | | | Reverse 5'-GTGGAGCAGCCTTTGAAGAGA-3' |

**Supplemental Table S3.** Relative metabolite content in WT-like and *atquac1* plants (5-week-old). Data are normalized with respect to the mean response calculated for the corresponding WT-like (to allow statistical assessment, individual plants from this set were normalized in the same way). Data are presented as means ± SE (n=5). Values set in bold in *atquac1* plants were determined by the Student's *t* test to be significantly different ($P < 0.05$) from their corresponding WT-like.

| **Amino acids** | **WT-like-1** | ***atquac1-1*** | **WT-like-2** | ***atquac1-2*** |
|---|---|---|---|---|
| Alanine | 1.00 ± 0.05 | **1.17 ± 0.06** | 1.00 ± 0.14 | 0.89 ± 0,11 |
| Valine | 1.00 ± 0.07 | 1.02 ± 008 | 1.00 ± 0.08 | 0.79 ± 0,10 |
| Isoleucine | 1.00 ± 0.07 | 1.15 ± 0.11 | 1.00 ± 0.08 | 0.90 ± 0,14 |
| Glycine | 1.00 ± 0.02 | **1.13 ± 0.04** | 1.00 ± 0.13 | 0.86 ± 0,04 |
| Proline | 1.00 ± 0.06 | **1.42 ± 0.05** | 1.00 ± 0.26 | 0.79 ± 0,09 |
| Serine | 1.00 ± 0.04 | 1.15 ± 0.09 | 1.00 ± 0.09 | 0.89 ± 0,11 |
| Threonine | 1.00 ± 0.07 | 0.95 ± 0.08 | 1.00 ± 0.17 | 0.72 ± 0,12 |
| Phenylalanine | 1.00 ± 0.09 | 1.18 ± 0.11 | 1.00 ± 0.13 | 0.74 ± 0,09 |
| Asparagine | 1.00 ± 0.25 | 1.00 ± 0.14 | 1.00 ± 0.21 | 0.80 ± 0,10 |
| Aspartate | 1.00 ± 0.05 | 0.90 ± 0.05 | 1.00 ± 0.18 | 0.81 ± 0,12 |
| Glutamine | 1.00 ± 0.04 | **1.53 ± 0.11** | 1.00 ± 0.12 | 1.03 ± 0,10 |
| Glutamate | 1.00 ± 0.08 | 1.06 ± 0.12 | 1.00 ± 0.10 | 0.90 ± 0,07 |
| **Organic acids** | | | | |
| Glycerate | 1.00 ± 0.18 | 1.18 ± 0.13 | 1.00 ± 0.15 | **1.67 ± 0.10** |
| Glycolate | 1.00 ± 0.12 | 1.13 ± 0.04 | 1.00 ± 0.06 | 1.23 ± 0.10 |
| Isocitrate | 1.00 ± 0.06 | 1.07 ± 0.03 | 1.00 ± 0.02 | 1.03 ± 0.01 |
| Aconitate | 1.00 ± 0.07 | 1.03 ± 0.09 | 1.00 ± 0.05 | 1.09 ± 0.10 |
| Succinate | 1.00 ± 0.07 | **1.67 ± 0.19** | 1.00 ± 0.21 | 1.41 ± 0.15 |
| Fumarate | 1.00 ± 0.13 | **1.96 ± 0.26** | 1.00 ± 0.13 | **1.61 ± 0.05** |
| Malate | 1.00 ± 0.06 | **1.29 ± 0.07** | 1.00 ± 0.04 | **1.28 ± 0.01** |
| Maleic acid | 1.00 ± 0.12 | **2.04 ± 0.29** | 1.00 ± 0.14 | **1.99 ± 0.19** |

| | | | | |
|---|---|---|---|---|
| Malonate | 1.00 ± 0.08 | 1.11 ± 0.06 | 1.00 ± 0.20 | 0.82 ± 0.09 |
| Dehydroascorbate | 1.00 ± 0.17 | 0.97 ± 0.12 | 1.00 ± 0.21 | 0.90 ± 0.01 |
| GABA | 1.00 ± 0.05 | 1.14 ± 0.10 | 1.00 ± 0.10 | 1.09 ± 0.09 |
| Erythronate | 1.00 ± 0.08 | **1.35 ± 0.10** | 1.00 ± 0.15 | 0.97 ± 0.07 |
| Glucuronate | 1.00 ± 0.09 | 1.06 ± 0.05 | 1.00 ± 0.07 | 0.89 ± 0.09 |
| **Sugars** | | | | |
| Ribose | 1.00 ± 0.04 | 0.97 ± 0,02 | 1.00 ± 0.04 | 1.01 ± 0.02 |
| Galactose | 1.00 ± 0.03 | 1.08 ± 0,06 | 1.00 ± 0.06 | 1.15 ± 0.05 |
| Xylose | 1.00 ± 0.16 | 0.89 ± 0,17 | 1.00 ± 0.19 | 0.91 ± 0.11 |
| Xylulose | 1.00 ± 0.03 | 1.05 ± 0,08 | 1.00 ± 0.09 | 0.94 ± 0.08 |
| Rhamnose | 1.00 ± 0.23 | 1.07 ± 0,29 | 1.00 ± 0.25 | 1.56 ± 0.17 |
| Sorbose | 1.00 ± 0.09 | 1.08 ± 0,08 | 1.00 ± 0.07 | 1.03 ± 0.07 |
| **Sugars alcohols** | | | | |
| Myo-inositol | 1.00 ± 0.03 | **1.52 ± 0.21** | 1.00 ± 0.12 | 1.19 ± 0.09 |
| Glycerol | 1.00 ± 0.09 | **1.26 ± 0.05** | 1.00 ± 0.04 | **1.30 ± 0.11** |
| Mannitol | 1.00 ± 0.09 | 1.08 ± 0.08 | 1.00 ± 0.07 | 1.03 ± 0.07 |
| Arabitol | 1.00 ± 0.02 | 0.97 ± 0.02 | 1.00 ± 0.02 | 0.99 ± 0.02 |
| Galactinol | 1.00 ± 0.05 | 1.23 ± 0.10 | 1.00 ± 0.05 | 1.11 ± 0.11 |
| **Other metabolites** | | | | |
| Spermidine | 1.00 ± 0.08 | 1.00 ± 0.05 | 1.00 ± 0.14 | 0.91 ± 0,08 |
| Phosphoric acid | 1.00 ± 0.10 | 1.07 ± 0.12 | 1.00 ± 0.08 | 1.00 ± 0,07 |

# Chapter 4

## Impaired malate and fumarate accumulation due to the mutation of the tonoplast dicarboxylate transporter has little effects on stomatal behaviour[1]

[1]*Accepted for publication in Plant Physiology*

**Title:** Impaired malate and fumarate accumulation due to the mutation of the tonoplast dicarboxylate transporter has little effects on stomatal behaviour

**Authors:** David B. Medeiros[1,2,3], Kallyne A. Barros[1,2], Jessica Aline S. Barros[1,2], Rebeca P. Omena-Garcia[1,2], Stéphanie Arrivault[3], Lílian M.V.P. Sanglard[2], Kelly C. Detmann[2], Willian Batista Silva[1,2], Danilo M. Daloso[3§], Fábio M. DaMatta[2], Adriano Nunes-Nesi[1,2], Alisdair R. Fernie[3], Wagner L. Araújo[1,2]*

[1]*Max-Planck Partner Group at the Departamento de Biologia Vegetal, Universidade Federal de Viçosa, 36570-900, Viçosa, Minas Gerais, Brazil*

[2]*Departamento de Biologia Vegetal, Universidade Federal de Viçosa, 36570-900, Viçosa, Minas Gerais, Brazil*

[3]*Max Planck Institute of Molecular Plant Physiology, 14476 Potsdam-Golm, Germany*

*Corresponding author: wlaraujo@ufv.br

**One-sentence summary:** Manipulation of tonoplastic organic acid transport by inhibition of the tDT impacts mitochondrion metabolism, whilst the overall stomatal and photosynthetic performance is not affected.

**Key words:** organic acids; growth; primary metabolism; respiration, stomata

**Footnotes:**

[§]Present address: *Departamento de Bioquímica e Biologia Molecular, Universidade Federal do Ceará, Fortaleza, Ceará, Brasil.*

**Author contributions:**

DBM, ARF, and WLA designed the research; DBM performed most of the research with the support of KAB, JASB, RPOG, SA, LMVPS, and KCD; WBS, DMD, ANN, and FMD contributed new reagents/analytic tools; ANN, FMD, and SA analysed the data, discussed the results and complemented the writing; DBM, ARF, and WLA analysed the data and wrote the article which was later approved by all the others.

**Funding information**

This work was supported by funding from the Max Planck Society, the CNPq (National Council for Scientific and Technological Development, Brazil, Grant 483525/2012-0), and the FAPEMIG (Foundation for Research Assistance of the Minas Gerais State, Brazil, Grant APQ-

01078-15 and APQ-01357-14) to WLA. Scholarship granted by FAPEMIG to DBM. (BDS-00020-16), CNPq to KAB and JASB, as well as research fellowships granted by CNPq-Brazil to ANN and WLA are also gratefully acknowledged.

## Abstract

Malate is a central metabolite involved in a multiplicity of plant metabolic pathways, being associated with mitochondrial metabolism and playing significant roles in stomatal movements. Vacuolar malate transport has been characterized at the molecular level and is performed by at least one carrier protein and two channels in Arabidopsis vacuoles. The absence of the *Arabidopsis thaliana* tonoplast Dicarboxylate Transporter (tDT) in *tdt* knockout mutant was previously associated with an impaired accumulation of malate and fumarate in leaves. Here, we investigated the consequences of this lower accumulation on stomatal behaviour and photosynthetic capacity as well as its putative metabolic impacts. Neither the stomatal conductance ($g_s$) nor the kinetic responses to dark, light or high $CO_2$ were highly affected in *tdt* plants. In addition, we did not observe any impact on stomatal aperture following incubation with either abscisic acid (ABA), malate or citrate. Further, an effect on photosynthetic capacity was not observed in the mutant lines. However, leaf mitochondrial metabolism was affected in the *tdt* plants. Levels of the intermediates of the tricarboxylic acid cycle were altered and increases in both light and dark respiration were observed. We conclude that manipulation of the tonoplastic organic acid transporter impacted mitochondrial metabolism, while the overall stomatal and photosynthetic capacity were unaffected.

## Introduction

Malate is a central metabolite in all plant species fulfilling a multiplicity of functions as both an intermediate of the tricarboxylic acid (TCA) cycle (Fernie et al., 2004) and carbon skeletons exported from the mitochondrion supporting amino acid biosynthesis (Tronconi et al., 2008). Malate is also involved in several processes including cellular pH regulation (Hurth et al., 2005), partial control over nutrient uptake (Weisskopf et al., 2006), aluminium tolerance (Delhaize et al., 2007), pathogen response (Bolwell et al., 2002), and stomatal movements (Hedrich et al., 1994). Moreover, it has been demonstrated to be a transcriptional regulator in metabolite signalling (Finkemeier et al., 2013), an important carbon storage molecule in C3 plants (Zell et al., 2010), and a key component of photosynthesis in C4 and CAM plants (Maier et al., 2011).

The vacuolar malate transport, which has been characterized at the molecular level, is thought to be essential to maintain normal cellular function (Emmerlich et al., 2003). First, the

gene encoding the vacuolar malate transporter, a plant homolog to the human sodium ion/dicarboxylate cotransporter, the tDT (tonoplast Dicarboxylate Transporter), was identified in *Arabidopsis*. The *tDT* knockout mutants are deficient in vacuolar malate transport activity, exhibited substantially reduced levels of malate and fumarate in the leaves and isolated vacuoles from these mutants were highly impaired in the import of [$^{14}$C]-malate yet respired exogenously applied [$^{14}$C]-malate faster than WT plants (Emmerlich et al., 2003). However, in contrast to its homolog in animal cells, the plant protein resides at the tonoplast and transport of malate by the tDT is not sodium-dependent (Emmerlich et al., 2003). In addition, Hurth et al. (2005) demonstrated that tDT is critical for the regulation of pH homeostasis under altered pH conditions. These authors further suggested that Arabidopsis vacuoles contain at least two types of carrier proteins and a channel for transport of dicarboxylates and citrate, thus providing the metabolic flexibility needed by plants to respond to different environmental circumstances. A member of the Aluminium-malate transporter family (ALMT), the ALMT9, was the first channel characterized to mediate malate and fumarate currents directed into the vacuole of mesophyll cells in Arabidopsis (Kovermann et al., 2007). However, it was later demonstrated to mediate malate-induced chloride currents that are also important for stomatal opening (De Angeli et al., 2013). A second member of the ALMT family, ALMT6, mediates $Ca^{2+}$- and pH-dependent malate currents into guard cell vacuoles (Meyer et al., 2011). Despite *ALMT6* expression is much higher in guard cells than in the mesophyll suggesting an important role of this channel in stomatal movements, no obvious stomatal or growth phenotype was observed under optimal growth conditions (Meyer et al., 2011).

Accumulation of malate either in guard cell cytosol and vacuoles or in the apoplastic space can impact stomatal movements and also regulate the activity of anion channels at guard cell plasma or vacuolar membrane (Hedrich and Marten, 1993; Hedrich et al., 1994; Raschke, 2003; Lee et al., 2008; Negi et al., 2008; Kim et al., 2010; De Angeli et al., 2013). Indeed, the role of organic acids (e.g. malate and fumarate) in the regulation of guard cell movements occurs not only by providing the osmotic control but also by playing a critical role in meeting the energetic demand of the guard cells (Santelia and Lawson, 2016). This fact apart, our knowledge about the metabolic hierarchy regulating guard cells movements in response to changes in organic acids remains fragmentary. Interestingly, further evidence supporting the involvement of organic acid metabolism in leaves by linking mitochondrial metabolism and stomatal function have been demonstrated (Nunes-Nesi et al., 2007; Araújo et al., 2011). Tomato (*Solanum lycopersicum* L.) plants with constitutively reduced expression of *SlSDH2-2* which encodes the iron-sulphur subunit of succinate dehydrogenase presented increased stomatal conductance and photosynthesis mediated by organic acids effects on the stomata

(Araújo et al., 2011). Importantly, no effects were observed when the antisense construction for *SISDH2-2* was expressed under the control of the guard cell specific *MYB60* promoter (Araújo et al., 2011). By contrast, the constitutive inhibition of the mitochondrial fumarase in tomato plants decreased photosynthesis as a result of impaired stomatal function (Nunes-Nesi et al., 2007).

In an attempt to investigate whether the lower levels of malate and fumarate observed in the *tdt* knockout plants has a greater impact on stomatal movement or mitochondrial metabolism in Arabidopsis, we here combined a range of physiological and biochemical approaches. Our results provide evidence that manipulation of organic acid tonoplastic transport by suppressing tDT greatly impact mitochondrial metabolism, but has only minor effects on stomatal and photosynthetic capacity. When considered in the context of current knowledge concerning the compartmentation of these metabolites (Gerhardt et al., 1987; Winter et al., 1993; Hedrich et al., 1994; Martinoia and Rentsch, 1994; Winter et al., 1994; Lohaus et al., 2001), this observation suggests that following the mobilisation of the vacuolar malate pool to the cytosol it is preferentially exported to the apoplast and used to support mitochondrial respiration.

## Results

### *attdt* plants exhibit a small reduction in vegetative growth under short-day conditions

Plants lacking a functional tDT display lower levels of malate and fumarate in leaves and isolated vacuoles (Emmerlich et al., 2003; Hurth et al., 2005). Given that these organic acids serve as important carbon storage molecules also in Arabidopsis plants (Zell et al., 2010), we investigated whether loss-of-function of *tDT* affects growth in two independent *tdt* T-DNA insertion lines (*tdt*-1 and *tdt*-2). We initially confirmed the absence of *tDT* transcripts in leaves of the mutants by reverse transcription PCR (Supplemental Fig. S1). Interestingly, no changes in growth were observed under neutral day conditions (12h/12h), with no differences in the rosette fresh weight between WT and *tdt* mutant plants (Supplemental Fig. S2A). However, under short-day conditions (8h/16h) the mutant lines displayed a slightly reduction in their growth being characterized by lower rosette fresh weight (Supplemental Fig. S2B). To investigate further this apparent growth phenotype we evaluated in detail the growth pattern and the metabolism of the genotypes only under short-day conditions. We observed that *tdt* plants presented reductions in the rosette and leaf dry mass (RDM and LDM), total leaf area (LA), rosette area (RA), but no significant differences in specific leaf area (SLA; Table I). We additionally evaluated the stomatal density and stomatal index with both being unaltered in the mutant lines under short-day conditions (Table I).

**Table I:** Growth and morphology parameters in WT and *tdt* mutant plants. Data presented are mean ± SE ($n$ = 6) obtained in two independent assays; values set in bold in *tdt* plants were determined by the Student's $t$ test to be significantly different ($P < 0.05$) from WT.

| Parameters* | WT | *tdt-1* | *tdt-2* |
|---|---|---|---|
| LA ($cm^2$) | 53.8 ± 2.9 | **44.1 ± 2.2** | **42.4 ± 2.3** |
| LDM (mg) | 95.9 ± 4.2 | **77.1 ± 5.7** | **72.2 ± 4.2** |
| RA ($cm^2$) | 43.4 ± 1.5 | **38.9 ± 1.3** | **34.9 ± 1.7** |
| RDM (mg) | 122.2 ± 4.1 | **93.6 ± 6.4** | **88.1 ± 5.5** |
| SLA ($m^2\ kg^{-1}$) | 60.1 ± 1.3 | 57.9 ± 1.8 | 56.3 ± 0.9 |
| SD (stomata $mm^{-2}$) | 270.9 ± 10.8 | 288.8 ± 3.4 | 273.8 ± 1.4 |
| SI (%) | 32.9 ± 1.3 | 31.4 ± 0.5 | 29.4 ± 0.9 |

*LA: total leaf area; LDM: leaves dry mass; RA: rosette area; RDM: Rosette dry mass; SLA: specific leaf area; SD: stomata density; SI: Stomatal Index.

**Lack of tDT has little effect on stomatal response to different stimuli**

Altered organic acid accumulation impacts stomatal behaviour coupling mesophyll mitochondrial activity to stomata and, subsequently, to plant growth (Nunes-Nesi et al., 2007; Araújo et al., 2011; Medeiros et al., 2016). To further assess the impact caused by an altered accumulation of malate and fumarate due to the lack of a functional tDT on stomatal conductance ($g_s$) in Arabidopsis, we adopted the following complementary approaches. First, we evaluated the stomatal kinetics during dark-to-light and light-to-dark transitions as well as following changes from normal-to-high and high-to-normal $CO_2$ concentrations. Secondly, we evaluated the response of intact leaves following incubation with ABA, malate, fumarate, and citrate individually by isolating epidermal fragments and analysing stomatal aperture. Surprisingly, the impaired accumulation of malate and fumarate in *tdt* leaves did not compromise the stomatal response to dark, light or high $CO_2$ levels (Fig. 1A-C). Although no statistical differences were observed ($P$<0.05) in response to light, dark, and $CO_2$ concentration, we estimated the half-times of the stomatal kinetic curves by fitting the time-course of $g_s$ to an exponential model (Martins et al., 2016). Accordingly, the half-times (expressed in min ± SE) for stomatal kinetics curves were also not significantly altered. However, it is noteworthy that the half-time for light-induced stomatal opening in *tdt-2* plants was lower (8.5 ± 0.7), whereas the values for WT and *tdt-1* plants were 13.2 ± 2.3 and 12.5 ± 1.5, respectively. For dark-induced stomatal closure, the half-times were only slightly reduced in *tdt-1* (4.5 ± 0.6) and *tdt-2* (4.5 ± 0.5) when compared to WT (5.2 ± 1.0). The half-times following high $CO_2$-induced

stomatal closure were also only slightly changed in *tdt-1* (5.0 ± 0.9) and *tdt-2* (4.2 ± 0.5) lines compared to WT plants (3.2 ± 0.5). During the recovery, back to ambient $CO_2$ concentration ($C_a$) of 400 µmol $mol^{-1}$, while *tdt-1* plants appeared to be slightly faster in stomatal opening (8.5 ± 1.6), *tdt-2* and WT presented half-times values of 12.8 ± 2.3 and 13.6 ± 3.9, respectively. Additionally, no effect on the stomatal aperture following the incubation with ABA, malate or citrate was observed (Fig. 1D).

Given that malate can affect *tDT* transcript accumulation (Emmerlich et al., 2003), first, we decided to evaluate whether *tDT* is expressed in guard cells by comparing its expression level in both guard cell-enriched epidermal fragments and isolated mesophyll cell protoplast; second, we measured the transcript levels of currently known genes related to organic and inorganic ion transport as well as genes involved in guard cell movements. For this purpose, we investigated by quantitative real-time PCR (qRT-PCR) the transcript levels of ion channels and transporters in guard cells-enriched epidermal fragments including *ALMT6*, *ALMT9*, *QUAC1*, *ABCB14*, *SLAC1*, *AHA1*, *AHA2*, *AHA5*, *KAT1*, *KAT2*, *AKT1*, *TPC1*, and *GORK* (for a complete description see Materials and Methods and Supplemental Table S1). Regarding the *tDT* expression pattern, our results confirmed previous transcriptome data (Bates et al., 2012), which showed higher expression levels in mesophyll cells than in guard cells (Supplemental Fig. S3 and Supplemental Fig. S4A). Furthermore, the transcript levels of the vast majority of the evaluated genes were only marginally altered in *tdt* plants (Supplemental Fig.S5).

To provide further information that could explain the lack of stomatal phenotype in *tdt* plants, we next quantified the content of organic acids in the apoplastic fluid. To this end, we collected the apoplastic fluid at the middle of the light period from completely water infiltrated leaves by centrifugation and quantified the absolute levels of fumarate, malate, and citrate in the apoplastic fraction by gas-chromatography coupled to mass-spectrometry technique (GC-MS). The unchanged fumarate, malate, and citrate levels in the apoplastic fluid (Fig. 2), probably best explains the lack of effect on stomatal function, since the apoplastic solute concentration is of pivotal significance in driving stomatal movements.

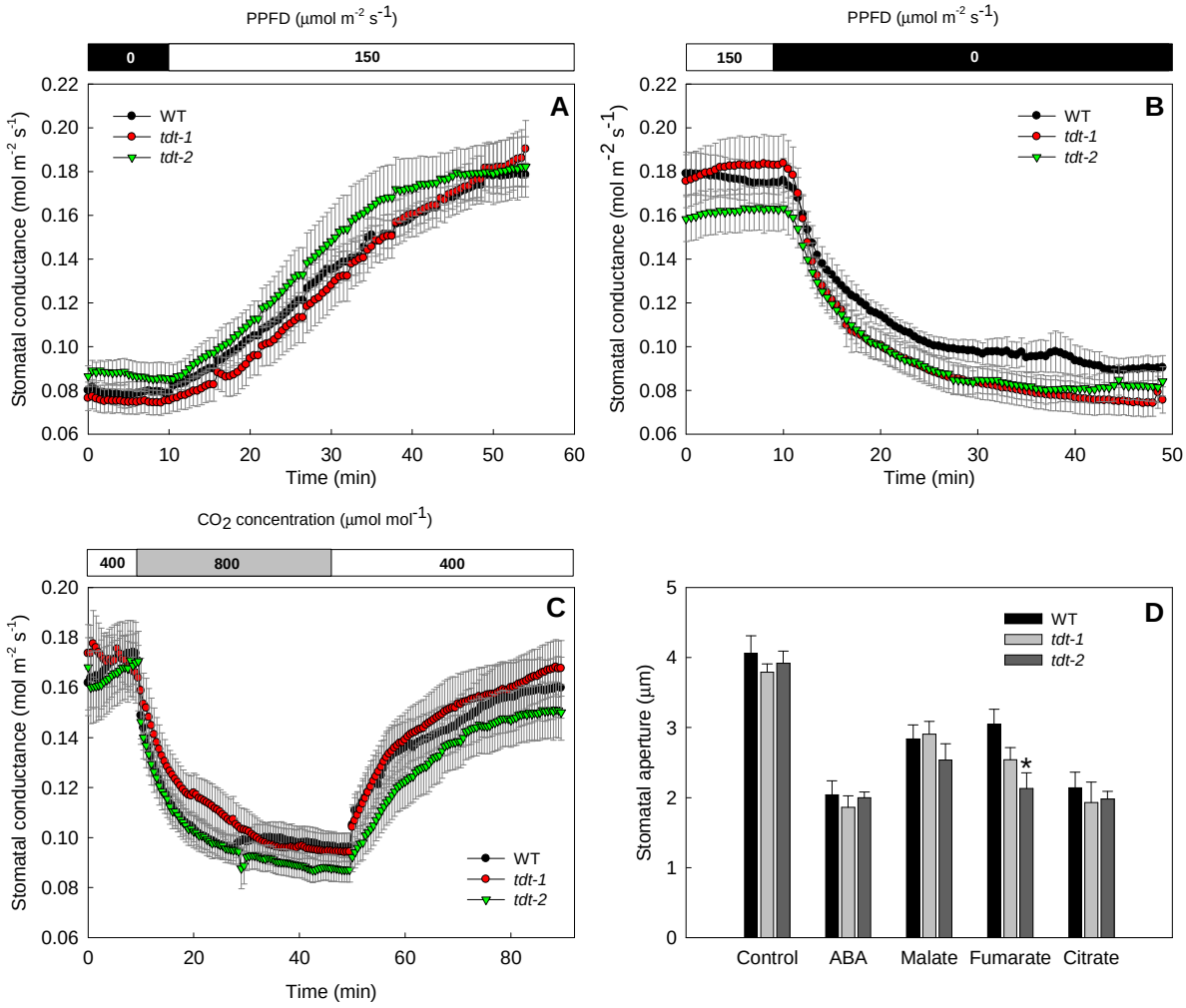


**Figure 1.** Stomatal responses of *tdt* plant following different stimuli. Stomatal opening and closing kinetics in response to light and $CO_2$ concentrations. Stomatal conductance ($g_s$) was evaluated in *tdt-1* and *tdt-2* and WT in response to light **(A)**, dark **(B)** and $CO_2$ levels **(C)**. Data presented are mean ± SE ($n$ = 10). **D**, Stomatal aperture after incubation with abscisic acid (ABA), malate, fumarate, and citrate. The 5$^{th}$ leaf totally expanded of 4-week-old plants were floated on stomatal opening buffer containing 10 mM KCl, 50 µM $CaCl_2$ and 5 mM MES-Tris (pH 6.15) for 2 h in the light (150 µmol $m^{-2}$ $s^{-1}$) to pre-open stomata. After, ABA, malate, fumarate, and citrate or ethanol (solvent control) were added to the opening buffer. After more 2 h of incubation the stomatal aperture was then examined in the isolated epidermal fragments. Six leaves from different plants were evaluated and the apertures of at least 20 stomata per leaf were measured totalizing at least 120 stomata per genotype. Data are mean ± SE ($n$ = 6) obtained in two independent experiments with comparable results. Asterisk indicates values that were determined by the Student's $t$ test to be significantly different ($P$ < 0.05) from WT.

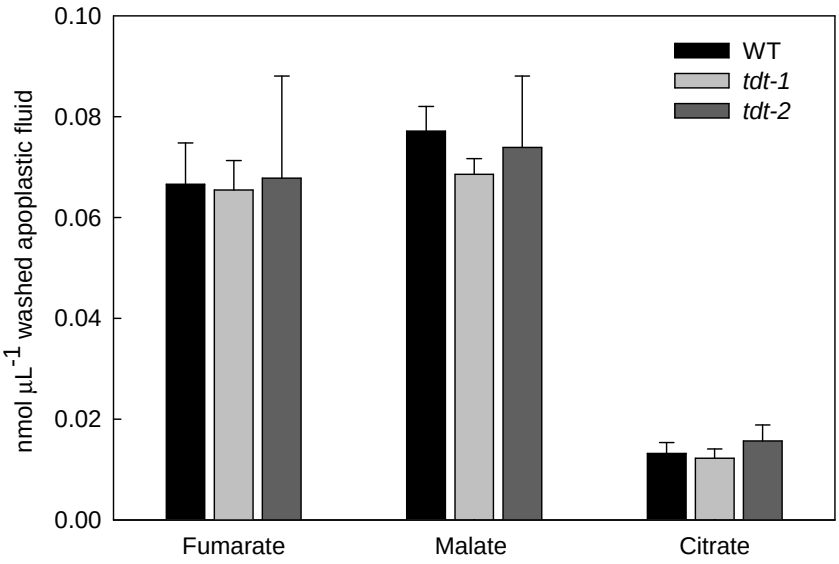


**Figure 2.** Apoplastic concentrations of organic acids in *tdt* plants. The apoplastic concentrations of fumarate, malate, and malate were determined as described in Material and Methods section. Values are presented as means ± SE of six individual determinations per genotype. All measurements were performed in 5-week-old plants.

**Photosynthetic capacity is not altered in *tdt* mutant plants**

We decided to perform a full characterization of the photosynthetic capacity of *tdt* plants. In close agreement with the stomatal kinetics, no differences were observed in instantaneous gas exchange parameters under either growth irradiance (Table II) or saturation irradiance (Supplemental Table S2). By further analysing $A_N$ under photosynthetically active photon flux density (PPFD) that ranged from 0 to 1200 µmol $m^{-2}$ $s^{-1}$, we observed that mutant plants exhibited unaltered $A_N$ irrespective of the irradiance (Supplemental Table S3). The light-saturated $A_N$ ($A_{PPFD}$), light saturation ($I_s$) and compensation ($I_c$) points, and light use efficiency remained similar among the genotypes (Supplemental Table S3). Additionally, the response of $A_N$ to the internal $CO_2$ concentration ($A_N/C_i$ curves; Supplemental Fig. S6A) was obtained and then were further converted into responses of $A_N$ to chloroplastidic $CO_2$ concentration ($A_N/C_c$ curves; Supplemental Fig. S6B). Under ambient $CO_2$ concentration (400 µmol $mol^{-1}$), $C_i$ and $C_c$ estimations in *tdt* lines were similar to those of the WT (Supplemental Table S4). $g_m$, estimated by a combination of gas exchange and chlorophyll *a* fluorescence parameters using two independent methods, remained unaltered in *tdt* plants (Supplemental Table S4). Accordingly, the maximum carboxylation velocity ($V_{cmax}$) and maximum capacity for electron transport rate ($J_{max}$) was also similar between WT and mutant lines both as a function of $C_i$ and $C_c$ (Supplemental Table S4).

**Table II.** Gas exchange and chlorophyll *a* fluorescence parameters in WT and *tdt* mutant plants measured under growth irradiance (150 µmol $m^{-2}$ $s^{-1}$). Data presented are mean ± SE ($n$ = 10) obtained in two independent assays (five plants in each assay).

| Parameters* | WT | *tdt-1* | *tdt-2* |
|---|---|---|---|
| $A_N$ (µmol $CO_2$ $m^{-2}$ $s^{-1}$) | 5.4 ± 0.2 | 5.9 ± 0.1 | 5.6 ± 0.2 |
| $g_s$ (mol $H_2O$ $m^{-2}$ $s^{-1}$) | 0.19 ± 0.01 | 0.18 ± 0.01 | 0.20 ± 0.01 |
| $E$ (mmol $H_2O$ $m^{-2}$ $s^{-1}$) | 1.9 ± 0.2 | 1.7 ± 0.1 | 1.9 ± 0.2 |
| $F_v/F_m$ | 0.78 ± 0.02 | 0.76 ± 0.01 | 0.75 ± 0.01 |

*$A_N$: Net photosynthesis; $E$: transpiration, $g_s$: stomatal conductance; $F_v/F_m$: PSII maximum photochemical efficiency

**Mutations in *tDT* affect starch, organic acid, and amino acids profiles in both leaves and guard cells**

Given that tDT was previously shown to be important for the maintenance of cellular homeostasis, specifically under situations of altered cellular pH (Hurth et al., 2005), we decided to explore the metabolic changes in *tdt* plants by conducting a detailed metabolic analysis in leaves and in enriched-guard cell epidermal fragments of the mutants and WT plants. There were no significant changes in the levels of chlorophylls (Supplemental Fig. S7). Similarly, during the light/dark cycle changes were not observed in the leaf levels of glucose, fructose, and sucrose between mutant and WT plants (Supplemental Fig. S8). However, starch metabolism in the leaves was strongly affected in *tdt* plants during the diurnal cycle (Fig. 3A). Notably, the average starch synthesis and degradation rates were estimated as the difference between starch at the end of the day and the end of the night, divided by the length of the light period or the night, respectively. Starch synthesis rate were 53% (1.43 µmol glc $g^{-1}$ FW $h^{-1}$) and 46% (1.64 µmol glc $g^{-1}$ FW $h^{-1}$) lower in *tdt-1* and *tdt-2* plants, by comparison to the WT (3.04 µmol glc $g^{-1}$ FW $h^{-1}$), respectively. For starch degradation rates the values were on average 59% (0.64 µmol glc $g^{-1}$ FW $h^{-1}$) and 48% (0.82 µmol glc $g^{-1}$ FW $h^{-1}$) lower in *tdt-1* and *tdt-2* plants than in WT ones (1.58 µmol glc $g^{-1}$ FW $h^{-1}$), respectively. It should be remembered that lower levels of starch observed in *tdt* plants were not accompanied by any change $A_N$.

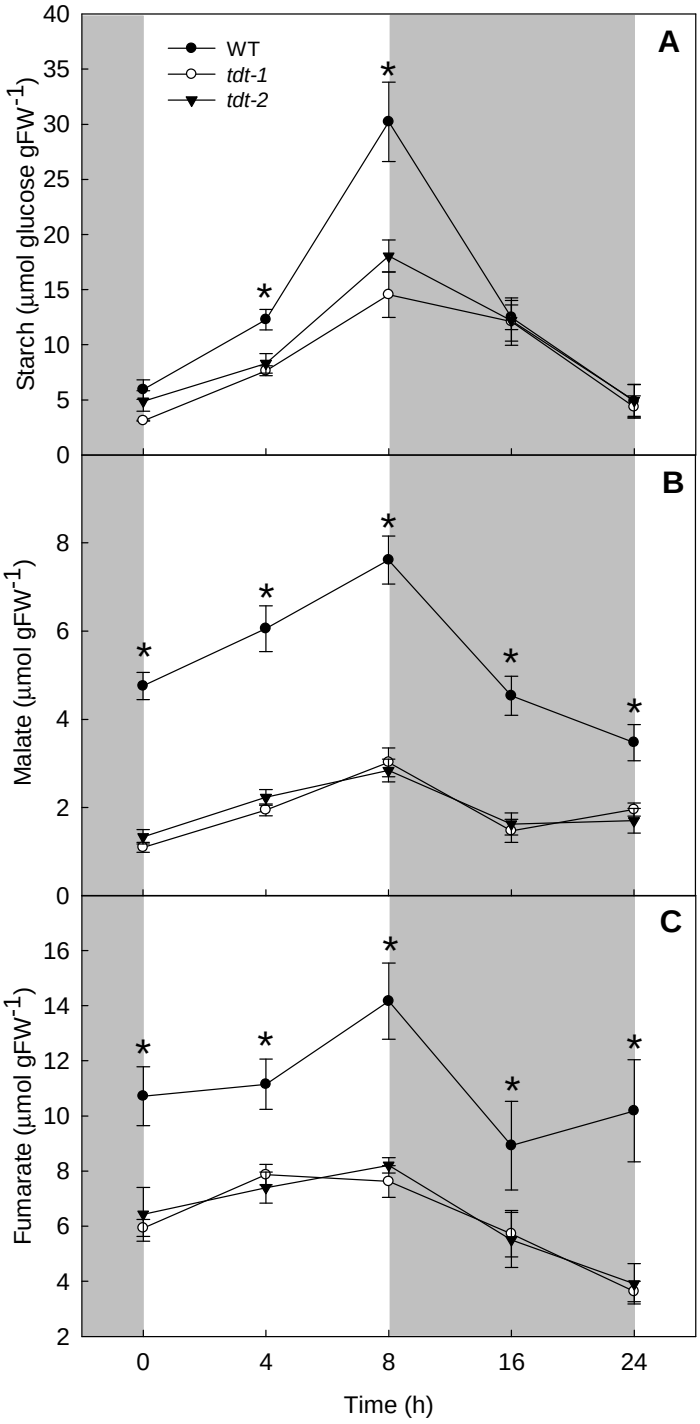


**Figure 3.** Starch and organic acid content in WT and *tdt* plants. **A** starch; **B** malate; and **C** fumarate content in whole rosettes harvested in different time points along of the light/dark cycle. Values are presented as mean ± SE ($n$ = 6) and asterisk indicates the time where the values from mutant lines were determined by the Student's $t$ test to be significantly different ($P$ < 0.05) from WT.

Impaired accumulation of malate and fumarate was previously observed in *tdt* mutants leaves (Emmerlich et al., 2003; Hurth et al., 2005). We additionally evaluated the malate and fumarate accumulation/usage pattern (Fig. 3). Further, by combining non-aqueous fractionation (NAF) and quantification by enzymatic assays and GC-MS we were able to estimate their subcellular distribution as well as of other organic acids (Supplemental Table S6). Regarding the malate and fumarate accumulation during the diurnal cycle it showed a very similar pattern to that observed for starch, with values observed in *tdt* plants being consistently lower than in WT during the entire diurnal cycle. Remarkably, *tdt* plants showed decreases in both malate (Fig. 3B) and fumarate (Fig. 3C) on average of 62% and 44% at the end of the light period. Interestingly, malate was the only organic acid showing differences in its subcellular distribution. Whereas citrate, isocitrate, and fumarate were predominantly found in the vacuoles, malate was significantly reduced in the vacuoles, however increases in malate were observed in the cytosol of the mutant lines (Supplemental Table S6).

We next decided to perform a detailed analysis of the primary metabolism in leaves and in enriched-guard cells epidermal fragments by using the established GC-MS approach (Lisec et al., 2006). This analysis revealed that, among the 48 successfully annotated compounds, considerable changes in amino acids, and in both TCA cycle and photorespiratory intermediaries were observed (Fig. 4; Supplemental Table S5). By analysing individual amino acids, we observed significant increases in leaves for both lines in asparagine (Asn), aspartate (Asp), and lysine (Lys) levels as well as the branched chain amino acids (BCAAs) leucine (Leu), isoleucine (Ile), and the aromatic amino acid tyrosine (Tyr) was also increased in the *attdt* plants. Notably, glycolate and glycine (Gly), intermediates of the photorespiratory pathway, were significantly decreased in leaves, whereas glutamine (Gln) levels increased in mutant plants in both leaves and guard cells. The levels of some organic acids found in the first half of the TCA cycle citrate (only in leaves) and isocitrate (in both leaves and guard cells) were strongly increased while succinate, fumarate, and malate were reduced in mutant lines only in leaves. Other changes of note observed in the metabolite profile were the significant increases in *myo*-inositol and reduction in maltose levels in leaves in both lines. Intriguingly, significant increases were observed in the levels of glucose, fructose, and trehalose in guard cells.

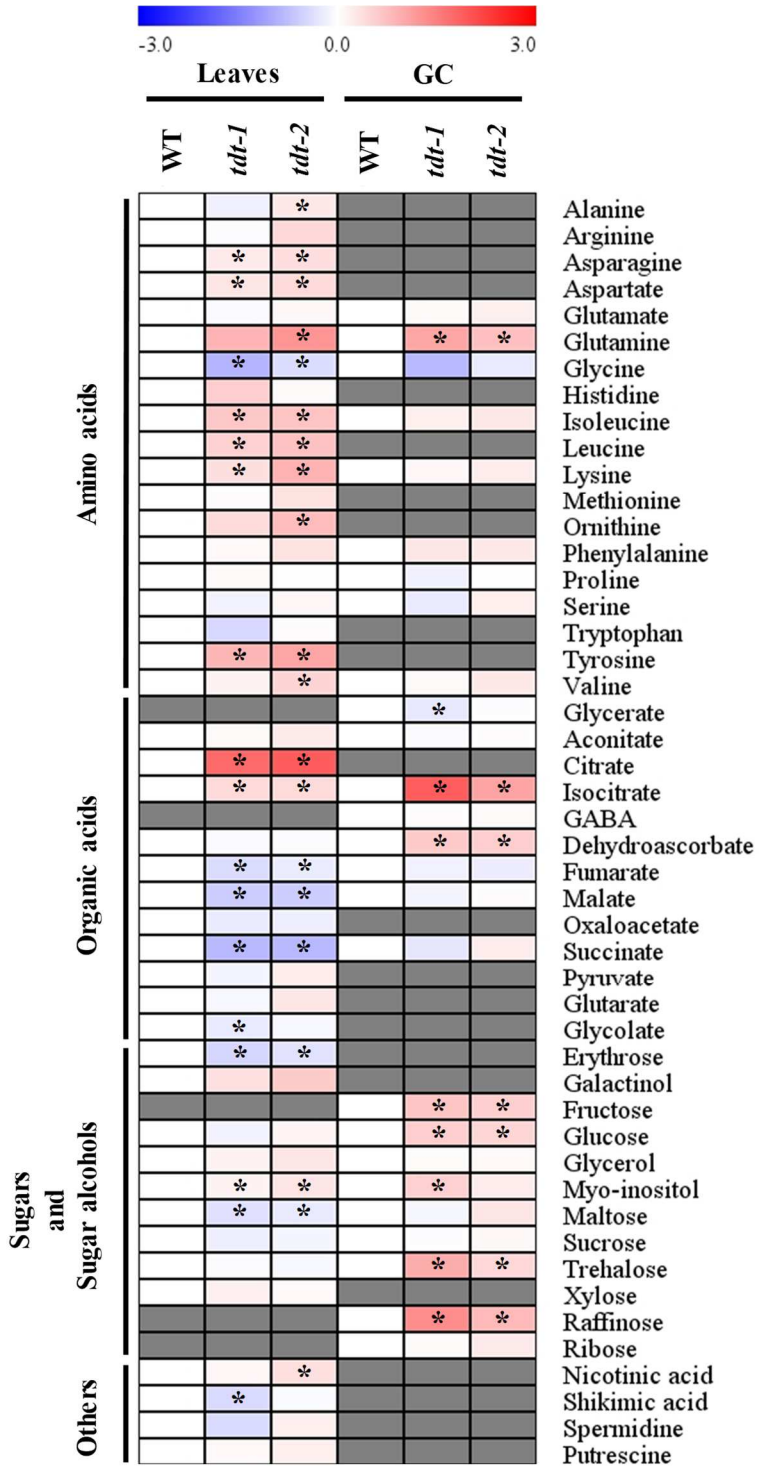


**Figure 4.** Heat map representing the changes in relative metabolite content in leaves and guard cell-enriched epidermal fragments from WT and *tdt* plants. The full data sets from these metabolic profiling studies are additionally available in Supplemental Table S5. The colour code of the heat map is given at the log(2) following the scale above the diagram. Data are normalized with respect to the mean response calculated for WT (to allow statistical assessment, individual plants from this set were normalized in the same way). Values are presented as means ± SE ($n$ = 5). Asterisks indicate that the values from mutant lines were determined by Student's $t$ test to be significantly different ($P < 0.05$) from WT. In grey, the metabolites which were not detected or could not be annotated.

We next evaluated whether the metabolic perturbations observed were accompanied by changes in the activity of important enzymes in leaves, which are associated with glycolysis and carbohydrate metabolism (Table III). Interestingly, the maximum activity of phosphoglycerate kinase (PGK), pyruvate kinase (PK), and aldolase (significantly only for *tdt-2*) were higher in *tdt* than in WT plants. There were no changes in the activity of hexokinase (HK), phosphofructokinase (PFK), enolase or triose phosphate isomerase (TPI). Similarly, transaldolase and glucose-6-phosphate dehydrogenase (G6PDH), both related to the pentose phosphate pathway, and sucrose synthase were unaltered in *tdt* plants. However, the activity of acid invertase was decreased in the mutant lines.

**Table III.** Enzyme activity analyses in WT and *tdt* plants. Activities were determined in whole 5-weeks-old rosettes harvested at the middle of the light period. Values are presented as means ± SE ($n$ = 5); values in bold type in *tdt* plants were determined by Student's $t$ test to be significantly different ($P < 0.05$) from WT. FW, Fresh weight

| Enzymes* | WT | *tdt-1* | *tdt-2* |
|---|---|---|---|
| Hexokinase[a] | 13.3 ± 0.5 | 13.6 ± 0.7 | 14.7 ± 1.2 |
| PGK[a] | 10.5 ± 1.2 | **14.5 ± 0.6** | **18.4 ± 0.5** |
| Pyruvate kinase[b] | 105.6 ± 8.0 | **162.2 ± 17.5** | **175.2 ± 9.6** |
| Phosphofructokinase[a] | 1.6 ± 0.1 | 1.6 ± 0.1 | 1.8 ± 0.2 |
| Enolase[a] | 8.3 ± 0.5 | 7.6 ± 0.3 | 8.2 ± 0.2 |
| TPI[a] | 157.7 ± 8.1 | 144.0 ± 3.1 | 157.5 ± 4.4 |
| Aldolase[b] | 541.8 ± 39.1 | 676.4 ± 50.1 | **837.2 ± 62.1** |
| Transaldolase[a] | 2.0 ± 0.2 | 2.2 ± 0.1 | 1.6 ± 0.1 |
| G6PDH[b] | 221.9 ± 16.2 | 239.8 ± 10.2 | 269.7 ± 14.3 |
| Sucrose synthase[b] | 245.8 ± 16.8 | 234.0 ± 5.2 | 245.5 ± 19.0 |
| Acid invertase[a] | 46.0 ± 1.4 | **32.2 ± 2.4** | **34.9 ± 1.5** |

[a]Values expressed in μmol $min^{-1}$ $g^{-1}$ FW. [b]Values expressed in nmol $min^{-1}$ $g^{-1}$ FW
*Abbreviations: PGK: Phosphoglycerate kinase; TPI: Triose phosphate isomerase; G6PDH: Glucose-6- phosphate dehydrogenase.

### *tdt* knockout plants present altered flux through the TCA cycle

We decided to directly assess the respiration rate by performing two complementary approaches. First, we directly evaluated the rate of light respiration in the mutant lines by measuring the $^{14}CO_2$ evolution following incubation of leaf discs with positional-labeled $^{14}C$-glucose ($^{14}C$-Glc) molecules to assess the relative rate of flux through the TCA cycle. For this, we incubated leaf discs under light supplied with either [1-$^{14}C$]-Glc or [3,4-$^{14}C$]-Glc over a period of 6 h. During that period, we collected the $^{14}CO_2$ evolved at hourly intervals. $CO_2$ can

be released from the C1 position by the action of enzymes that are not associated with mitochondrial respiration, but $CO_2$ released from the C3,4 positions of glucose cannot (Nunes-Nesi et al., 2007). Therefore, the ratio of $CO_2$ evolution from C3,4 to C1 positions provides a reliable indication of the relative rate of the TCA cycle versus other carbohydrate oxidation processes. By comparing the $^{14}CO_2$ release from mutant lines to WT plants we observed that significant increases occurred only for *tdt-2* line after 5 h of incubation following incubation with [1-$^{14}$C]-Glc (Fig. 5A), whereas when supplied with [3,4-$^{14}$C]-Glc the $^{14}CO_2$ release was significantly increased in both mutant lines from 4 h onwards (Fig. 5B). In addition, the C3,4/C1 ratio was higher in mutant lines than in WT plants after 6 h incubation (Fig. 5C), revealing that a higher proportion of carbohydrate oxidation was performed by the TCA cycle in illuminated leaves. Furthermore, the higher dark respiration ($R_d$), measured by using an infra-red gas analyser system, revealed higher rates of $CO_2$ evolution in the leaves of *tdt* plants than in the WT (Fig. 5D).

## Discussion

### Functional absence of tDT does not alter stomatal movements and photosynthetic capacity

To evaluate the reasons underlying the growth impairment observed in *tdt* plants under short-day conditions (Supplemental Fig. S1 and Table I), we decided to investigate whether the impaired organic acid accumulation affected stomatal function and thereby photosynthetic capacity in these plants. We were somewhat surprised to find that the growth phenotype was independent of changes in stomatal density, stomatal index, and photosynthetic capacity (Table I; Table II; Supplemental Fig. S6; Supplemental Table S2; S3; S4). Collectively, these results indicate that guard cell function is not highly affected in *tdt* plants (Fig. 1), and the stomata were most likely able to reprogram their metabolism to overcome the impaired vacuolar malate storage observed previously (Emmerlich et al., 2003) and confirmed here during the entire diurnal cycle and in the non-aqueous fractionation experiments (Fig. 3 and Supplemental Table S6). Notably, although tDT is essential for mediating correct compartmentation of the dicarboxylates, *tdt* plants still exhibit residual malate importing activity (Emmerlich et al., 2003; Hurth et al., 2005). It has been suggested that tDT is the major transporter responsible for malate and fumarate through the tonoplast in mesophyll cells (Hurth et al., 2005); however, members of the ALMT family are also implicated in this function as malate channels in plants. For instance, ALMT6 which is more expressed in guard cells than in the mesophyll ones (Supplemental Fig. S3) was shown to mediate $Ca^{2+}$- and pH-dependent malate currents into guard cell vacuoles, suggesting that it could be the main vacuolar transport system for organic acids in guard cells (Meyer et al., 2011). Because this channel does not exhibit sufficient activity

to accumulate dicarboxylates at concentrations required for normal metabolic functioning it may not be able to fully compensate the absence of tDT in mesophyll cells (Hurth et al., 2005). Furthermore, ALMT9 was first observed to mediate malate and fumarate currents directed into the vacuole, it was later shown to mediate malate-induced chloride current, which is also important for stomatal opening (Kovermann et al., 2007; De Angeli et al., 2013). Notably, our gene expression analyses did not reveal any significant difference at the mRNA levels of ALMT6 and ALMT9 between WT and *tdt* plants (Supplemental Fig. S5).

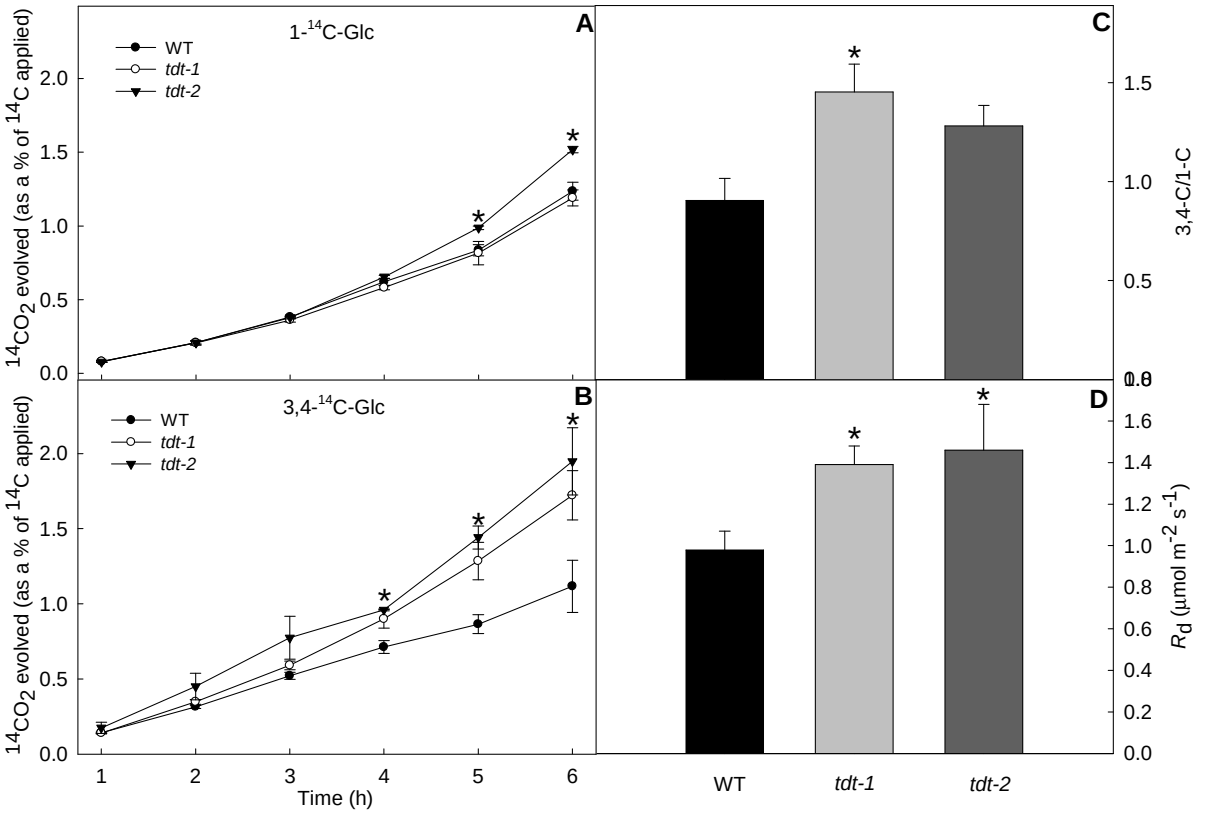


**Figure 5.** Respiration parameters in leaf disks from WT and *tdt* plants. $^{14}CO_2$ evolution from isolated leaf discs was determined under light conditions. The leaf discs were taken from 5-week-old plants and incubated in 10 mm MES–KOH solution, pH 6.5, 0.3 mM Glucose (Glc), 0.1 mM $CaSO_4$ supplemented with 0.62 kBq $mL^{-1}$ of **(A)** [1-$^{14}$C]-Glc; or **(B)** [3,4-$^{14}$C]-Glc at an irradiance of 100 µmol $m^{-2}$ $s^{-1}$. The $^{14}CO_2$ released was captured (at hourly intervals) in a KOH trap and the amount of radiolabel released was subsequently quantified by liquid scintillation counting. **C**, Ratio of carbon dioxide evolution from C3,4 to C1 positions of Glc in leaves of *tdt* plants. Values are presented as means ± SE ($n$ = 3) **D**, Dark respiration measurements performed on 5-week-old plants. Values presented are mean ± SE ($n$ = 10) obtained in two independent assays (five plants in each assay). An asterisk indicates values that were determined by the Student's $t$ test to be significantly different ($P < 0.05$) from the WT plants.

We previously demonstrated that there is a negative correlation between the apoplastic levels of malate and fumarate and both stomatal aperture and gas exchange in tomato antisense lines for genes encoding fumarase and succinate dehydrogenase enzymes (Araújo et al., 2011). Consistent with the lack of change in stomatal function, in the current study we did not observe any change in apoplastic levels of fumarate, malate, and citrate (Fig. 2). In keeping with this, it is highly tempting to suggest that although malate and fumarate cannot be properly accumulated in the vacuoles due the lack of a functional tDT transporter, the majority of these compounds produced need to be further redistributed within the cell. This would support the proper stomatal function by the maintenance of apoplastic concentrations of organic acids even with decreased total amounts in the leaves (Fig. 3). Moreover, it also indicates that these compounds are highly metabolized by the TCA cycle (Fig. 5), as previously suggested (Emmerlich et al., 2003). Thus, it seems that mitochondrial metabolism, especially of those pathways associated with malate, has great potential to improve photosynthesis, and growth ultimately, most likely through a better control of stomatal movements (Nunes-Nesi et al., 2011). That said it remains to be elucidated whether the functional redundancy in the vacuolar organic acid transport in guard cells is responsible for lack of stomatal phenotype in *tdt* plants.

**Lower growth in *tdt* plants was not related to impairments in the photosynthetic capacity**

A detailed photosynthetic characterization revealed that the lower vegetative growth in *tdt* plants was not due to an impaired photosynthetic capacity. This analysis was necessary despite the lack of change in stomatal behaviour since the rate of $CO_2$ diffusion through the stomata is not the only constraint to the photosynthetic performance in plants and the pathway to $CO_2$ diffusion from stomata to the Rubisco carboxylation sites in the chloroplasts can become an important limiting factor to the photosynthetic process as well as the Rubisco carboxylic capacity (Gerhardt et al., 1987; Martins et al., 2013). Our results demonstrated an invariable instantaneous net $CO_2$ assimilation in *tdt* plants both under growth irradiance and light saturation (Table II and Supplemental Table S2). This was also observed when we estimated the photosynthetic capacity from response curves of $A_N$ to $C_i$ or $C_c$ as well as to PPFD (Supplemental Fig. S6 and Supplemental Table S3 and S4). Arabidopsis plants with highly reduced levels of malate and fumarate due to the overexpression of a maize (*Zea mays*) plastidic NADP-malic enzyme (MEm) exhibited smaller rosettes with decreased biomass accumulation and thinner leaves when compared to WT plants. This was almost certainly the consequence of a reduced photosynthetic performance under short-day conditions in these plants (Zell et al., 2010), suggesting that the long dark period and extremely low levels of malate and fumarate are not sufficient to support the sugar depletion after the usage of carbohydrate stored during

the night. Interestingly, these findings were not observed when these plants were grown under long-day conditions (Fahnenstich et al., 2007). Indeed, the rates of starch and organic acid usage during the night correlate with one another and with the relative growth rate, indicating that although these two carbon sources are independently regulated their utilization is highly coordinated (Fahnenstich et al., 2007; Gibon et al., 2009; Zell et al., 2010; Sulpice et al., 2014; Figueroa et al., 2016; Lauxmann et al., 2016). Although many of the molecular details concerning the connection between starch and organic acid metabolism in governing plant growth are being revealed (Figueroa et al., 2016), deeper elucidation of how plants and in particular crop species adjust their metabolism to support growth will be important and strategic research avenues to be pursued in the near future.

We showed here that *tdt* plants were impaired in their growth under short-day conditions, which can be explained, at least partially, by the reduced malate and fumarate content in the leaves of these plants across the entire diurnal cycle (Fig. 3B and Fig. 3C). Moreover, starch accumulation in *tdt* mutant lines in our growth conditions was negatively affected, with reduced values at the end of the light period (Fig. 3A). It is, therefore, reasonable to assume that *tdt* plants display a carbon-starvation phenotype when grown under SD conditions, given that no visible growth phenotype was observed when we grew these mutant plants under 12h/12h light/dark photoperiod (Supplemental Fig. S2).

**Respiratory metabolism is changed as consequence of the *tDT* repression**

The impaired malate exchange observed in *tdt* plants has been previously proposed to be able to provoke unknown regulatory reactions at the expense of cytosolic energy equivalents (Emmerlich et al., 2003; Hurth et al., 2005). This assumption was further reinforced by the demonstration that radiolabelled malate fed into mutant leaf discs entered the TCA cycle much faster than in WT tissues (Emmerlich et al., 2003). Furthermore, the observation that *tdt* leaf discs exhibited both an increased respiratory activity and increased respiratory quotient (Hurth et al., 2005) demonstrated the accelerated usage of cytosolic carboxylic acids as an energy source in plants lacking a functional tDT transporter. Here, we provide compelling evidence that the absence of tDT strongly affects the mitochondrial metabolism in vivo. By using complementary approaches, we further confirmed that the slower growth in *tdt* plants was accompanied by enhanced dark and light respiration (Fig. 5), providing more evidence for the connection between the TCA cycle functioning and growth (Nunes-Nesi et al., 2007; Araújo et al., 2011). Tomato plants exhibiting either an antisense inhibition of fumarase (Nunes-Nesi et al., 2007) or the iron-sulfur subunit of succinate dehydrogenase (Araújo et al., 2011) displayed an impaired mitochondrial metabolism. In these transgenic plants, the flux through the TCA

cycle was clearly reduced; however, whereas deficiency in fumarase led to lower $CO_2$ assimilation and reduction in growth (Nunes-Nesi et al., 2007), the succinate dehydrogenase antisense lines showed higher transpiration and $g_s$, followed by elevated $CO_2$ assimilation and growth (Araújo et al., 2011). These differences were both ascribed to the apoplastic levels of malate and fumarate as mentioned above, which were elevated in the fumarase antisense lines and reduced in the succinate dehydrogenase antisense lines (Araújo et al., 2011). That respiratory metabolism was affected in these lines is by no means surprising given that they are directly effected in the TCA cycle. That the *tdt* lines are also affected is highly interesting since it suggests that the TCA cycle is, to a considerable extent, fuelled directly by malate supply, which is accumulated in the cytosol in these plants (Supplemental Table S6). Moreover, it is in keeping with previous suggestions of a non-cyclic flux mode of the TCA cycle in leaves under light conditions (Sweetlove et al., 2010; António et al., 2016). This scenario is further supported by the steady-state levels of the intermediates of the TCA cycle in leaves observed here (Fig. 4 and Supplemental Table S5) and are in good agreement with the high dependence on the metabolic and physiological cell demands associated with organic acid metabolism (Sweetlove et al., 2010).

It is important to highlight that the levels of succinate, fumarate, and malate were decreased in leaves, but not in guard cells of mutant lines (Fig. 4). This observation suggests a different functional importance of the tDT transporter in mesophyll and guard cells, which is in agreement with the differential expression pattern of *tDT*, being more expressed in mesophyll cells than in guard cells (Bates et al. (2012) and Supplemental Fig. S4). Moreover, the high expression of the ALMT6 at the guard cell tonoplast seems to compensate the lack of tDT, at least regarding the proper storage of malate and fumarate in those cells (Fig. 4). Curiously, since we observed a strong accumulation of citrate in leaves and isocitrate in both leaves and guard cells and this accumulation is addressed occurring within the vacuole (Supplemental Table S6), it is tempting to speculate that tDT might also be somehow involved with the compartmentalization of these organic acids. Although we were not able to ascertain in the current study which organic acids are effectively transported by the tDT it will be interesting to further investigate whether the mitochondrial metabolism in guard cell is also affected when tDT is repressed in future studies.

Collectively, our results suggest that impaired accumulation of malate and fumarate as a consequence of non-functional tDT affects the cellular homeostasis in mesophyll cells by changing mitochondrial metabolism, without negative impacts to the stomatal and photosynthetic behaviours. When the relative concentrations of the apoplastic and subcellular malate pools are considered (Gerhardt et al., 1987; Winter et al., 1993; Hedrich et al., 1994;

Martinoia and Rentsch, 1994; Winter et al., 1994; Lohaus et al., 2001), it is tempting to speculate that the impact on mitochondrial metabolism is most likely due to increased consumption of carboxylates within the cell, since it cannot be properly stored into the vacuole. Additionally, transporting the increased cytosolic malate pools for the maintenance of apoplastic levels could be a mechanism by which *tdt* plants maintain the stomatal function. This observation is thus consistent with our previous studies both suggesting that apoplastic malate levels play a crucial role in stomatal function.

## Material and methods

### Plant material and growth conditions

All *Arabidopsis thaliana* plants used here were of the Wassilewskija ecotype (Ws) background. WT and *tdt* plants were grown in a growth chamber under short-day (8 h/16 h of light/dark) or neutral-day (12 h/12 h of light/dark), irradiance of 150 μmol $m^2$ $s^{-1}$, 22ºC/20ºC during the light/dark cycle, and 60% relative humidity. The T-DNA mutant lines *tdt-1* and *tdt-2* were identified by screening a library of T-DNA lines from Arabidopsis Knockout Facility, University of Wisconsin Biotechnology Center (Emmerlich et al., 2003). The abundance of transcripts was confirmed by semi-quantitative PCR, using specific primers pair for *tDT* gene - At5g47560: forward 5´-ACACTACAACATCCATCGCC-3´ and reverse 5´-ATGCATCCACATGCTTACGT-3´. *GLYCERALDEHYDE-3-PHOSPHATE-DEHYDROGENASE* (*GAPDH*) – At1g16300 expression was also evaluated as a control using the following primers pair: forward 5´-TGGTTGATCTCGTTGTGCAGGTCTC-3´ and reverse 5´-GTCAGCCAAGTCAACAACTCTCTG-3´.

### Growth analysis

Whole rosettes from 5-week-old plants were harvested and the rosette fresh and dry weight (RDW), total leaf area (LA), specific leaf area (SLA) were measured. LA was measured by digital image method using a scanner (Hewlett Packard Scanjet G2410, Palo Alto, CA, USA) and the images were processed using the ImageJ software (Schindelin et al., 2015). SLA were calculated as described in Hunt et al. (2002).

### Stomatal analysis

After 2 h of illumination in the light/dark cycle, leaf impressions were taken from the abaxial surface of the 5$^{th}$ leaf totally expanded with dental resin imprints (Berger and Altmann, 2000). Nail polish copies were made using a colorless glaze (Von Groll et al., 2002) and the

images were taken with a digital camera (Axiocam MRc) attached to a microscope (Zeiss, model AX10, Jena, Germany). The measurements were performed on the images using the AxionVision software (Carls Zeiss, Germany). Stomatal density and stomatal index (the ratio of stomata to stomata plus other epidermal cells) were determined in at least 10 fields of 0.09 $mm^2$ per leaf from eight different plants. For stomatal aperture assay the $5^{th}$ leaf totally expanded of 5-week-old plants were floated on stomatal opening buffer containing 10 mM KCl, 50 μM $CaCl_2$ and 5 mM MES-Tris (pH 6.15) for 2 h under light (150 μmol $m^{-2}$ $s^{-1}$) to pre-open stomata. After, ABA, malate, fumarate, and citrate or ethanol (solvent control) were added to the opening buffer to final concentration of 10 μM, 10 mM, 10 mM, 10 mM or 0.1 % (v/v), respectively. After 2 h of incubation the stomatal aperture was evaluated. The leaves were gently dried and the adaxial epidermis was carefully fixed to an autoclave tape. The abaxial surface of the leaves were then peeled off by fixing an adhesive film (tesafilm® crystal clear, Tesa, Hamburg, Germany) and the images were immediately taken (Azoulay-Shemer et al., 2015). Six leaves from different plants were evaluated and the aperture of at least 20 stomata per leaf was measured giving a total of at least 120 stomata per genotype.

**Stomatal opening and closing kinetics measurements**

The $g_s$ values were recorded at intervals of 1 min using an open-flow infrared gas exchange analyser system (LI-6400XT; LI-COR Inc., Lincoln, NE) equipped with an integrated fluorescence chamber (LI-6400-40; LI-COR Inc.). The $g_s$ responses to dark/light and light/dark transitions were measured in plants acclimated to dark or light, for at least 2 h. The light in the chamber was kept turned off, and then turned on for 10/40 min and turned on/turned off 10/40 min. The $CO_2$ concentration in the chamber was kept at 400 μmol $mol^{-1}$ air. For responses to $CO_2$ concentration transitions leaves were exposed to 400/800/400 μmol $CO_2$ $mol^{-1}$ air for 10/40/40 min under PPFD of 150 μmol $m^{-2}$ $s^{-1}$ (Medeiros et al., 2016). The half-times, expressed in min, for the stomatal kinetics curves were calculated as ln(2)/k. The rate constant, k, was fitted by non-linear fitting using the Microsoft Excel's Solver add-in as described previously (Martins et al., 2016).

**Guard cell-enriched epidermal fragments and mesophyll cell protoplast isolation**

The isolation of guard cell-enriched epidermal fragments was performed as described previously (Pandey et al., 2002). Briefly, fully expanded leaves from five rosettes per sample were blended for 1 min plus 1 min (twice for 30 s) using a warring blender (Phillips, RI 2044) with an internal filter to clarify the epidermal fragments of mesophyll and fibrous cells.

Subsequently, epidermal fragments were collected on a nylon membrane (200 µm mesh) and washed to avoid apoplast contamination before being frozen in liquid nitrogen. This protocol resulted in a guard cell purity of approximately 98% (Antunes et al., 2012). For mesophyll cell protoplasts isolation, approximately 20 fully expanded leaves per replicate were harvested at the middle of the light period. The protoplasts were isolated using the TAPE-sandwich method as described by Wu et al. (2009).

**qRT-PCR**

qRT-PCR analysis was performed with total RNA isolated from mature leaves using the TRizol® reagent (Ambion, Life Technology) following the manufacturer's manual. For guard cell-enriched fragments and mesophyll cell protoplast the total RNA was isolated using the NucleoSpin® RNA Plant kit (MACHEREY-NAGEL GmbH & Co. KG). The integrity of the RNA was checked on 1% (w/v) agarose gels, and the concentration was measured using the system QIAxpert (QIAGEN). Digestion with DNase I (Amplication Grade DNase I, Invitrogen) was performed according to the manufacturer's instructions. Subsequently, total RNA was reverse transcribed into cDNA using Universal RiboClone® cDNA Synthesis System (Promega, Madison, WI, USA) according to the respective manufacturer's protocols. For analysis of gene expression, the Fast SYBR® Green PCR Master Mix was used with the MicroAmp™ Optical 96-well Reaction Plate and MicroAmp™ Optical Adhesive Film (Applied Biosystems, Foster City, CA, USA). The relative expression levels were normalised using the constitutively expressed genes *F-BOX* and *TIP41-LIKE* (Czechowski et al., 2005), and calculated using the ΔCT method. The primers used for qRT-PCR were designed using the QuantPrime software (Messinger et al., 2006) or taken from those described by De Angeli et al. (2013). Detailed primers information is described in the Supplemental Table S1. The following genes were analysed: *ALUMINIUM ACTIVATED MALATE TRANSPORTER 6* and *9*, *ALMT6* and *ALMT9*; *QUICK ANION CHANNEL 1*, *QUAC1* (Medeiros et al., 2016); *ARABIDOPSIS THALIANA ATP-BINDING CASSETTE B14 AtABCB14* (Lee et al., 2008); *SLAC1*; $H^+$*-ATPASE 1* and *5*, *AHA1*, *AHA2*, and *AHA5* (Ueno et al., 2005); *POTASSIUM CHANNEL IN ARABIDOPSIS THALIANA 1*, *KAT1* (Nakamura et al., 1995) and *KAT2* (Pilot et al., 2001); $K^+$ *TRANSPORTER 1*, *AKT1* (Cao et al., 1995); the $K^+$ outflow channel *GATED OUTWARDLY-RECTIFYING* $K^+$ *CHANNEL,* GORK (Ache et al., 2000), and *TWO-PORE CHANNEL 1*, *TPC1* (Peiter et al., 2005).

**Collection of apoplastic fluid and organic acids quantification**

The leaf apoplastic fluid was collected as previously described with few modifications (Madsen et al., 2016). Briefly, six completely expanded leaves were cut with a razor blade and immediately submerged in deionized water to remove any surface contaminants at the middle of the light period. After, the leaves were submerged in the washing solution (deionized water). Then, applied vacuum to infiltrate the leaves (ca. -70 kPa) and released slowly (this procedure was repeated three times (1 min each) to give 100% of infiltration). After vacuum infiltration, leaf surfaces were completely and gently dried. Leaves were placed in a parafilm sheet, which was folded in such way that the leaves were stacked between layers of parafilm. Finally, this leaf-parafilm "sandwich" was mounted as described (Madsen et al., 2016) and after centrifugation in swinging buckets at 300 *g* for 10 min at 4 ºC the volume of apoplastic washing fluid was measured with a pipette. The apoplastic washing solutions were dried in lyophilizer. By using standards for citrate, malate, and fumarate we were able to quantify the absolute amount of these organic acids in the apoplastic fraction using an established GC-MS approach (Lisec et al., 2006),

**Gas exchange and chlorophyll fluorescence measurements**

Gas exchange parameters were determined simultaneously with chlorophyll *a* (Chl *a*) fluorescence measurements using the same gas exchange system described above. Instantaneous gas exchanges were measured after 1 h illumination during the light period under 150 µmol $m^{-2}$ $s^{-1}$ (light of growth) or 1000 µmol $m^{-2}$ $s^{-1}$ (light saturation) of photosynthetically active photon flux density (PPFD) at the leaf level. The reference $CO_2$ concentration was set at 400 µmol $CO_2$ $mol^{-1}$ air. All measurements were performed using the 2 $cm^2$ leaf chamber at 25 °C, while the amount of blue light was set to 10% PPFD to optimize stomatal aperture.

All the Chl *a* fluorescence parameters were measured exactly as described in Medeiros et al. (2016). As the actual PSII photochemical efficiency ($\phi_{PSII}$), estimated by chl *a* fluorescence parameters, represents the number of electrons transferred per photon absorbed in the PSII, the electron transport rate ($J_{flu}$) was calculated as $J_{flu} = \phi_{PSII} \cdot \alpha \cdot \beta \cdot PPFD$, where $\alpha$ is leaf absorptance and $\beta$ reflects the partitioning of absorbed quanta between PSII and PSI, and the product $\alpha\beta$ was adopted as be in the literature to Arabidopsis 0.451 (Flexas et al., 2007).

Dark respiration ($R_d$) was measured using the same gas exchange system as described above after at least 1 h during the dark period and it was divided by two ($R_d/2$) to estimate the mitochondrial respiration rate in the light ($R_L$) (Niinemets et al., 2005, 2006; Niinemets et al., 2009).

Photosynthetic light-response curves (*A*/PPFD) were initiated at ambient $CO_2$ concentration ($C_a$) of 400 µmol $mol^{-1}$ and PPFD of 1000 µmol $m^{-2}$ $s^{-1}$. Then, the PPFD was increased to 1200 µmol $m^{-2}$ $s^{-1}$ and after decreased stepwise to 0 µmol $m^{-2}$ $s^{-1}$ (13 different PPFD steps). Simultaneously, Chl *a* fluorescence parameters were obtained (Yin et al., 2009). The responses of $A_N$ to $C_i$ ($A_N$ /$C_i$ curves) were performed at saturated light of 1000 µmol $m^{-2}$ $s^{-1}$ at 25°C under ambient $O_2$. Briefly, the measurements started at ambient $CO_2$ concentration ($C_a$) of 400 µmol $mol^{-1}$ and when the steady state was reached, $C_a$ was decreased stepwise to 50 µmol $mol^{-1}$. Upon completion of the measurements at low $C_a$, $C_a$ was returned to 400 µmol $mol^{-1}$ to restore the original $A_N$. Next, $C_a$ was increased stepwise to 1600 µmol $mol^{-1}$ in a total of 13 different $C_a$ values (Long and Bernacchi, 2003).

**Estimation of mesophyll conductance ($g_m$), maximum rate of carboxylation ($V_{cmax}$), maximum rate of carboxylation limited by electron transport ($J_{max}$) and photosynthetic limitations**

The concentration of $CO_2$ at the carboxylation sites ($C_c$) was calculated following Harley et al. (1992) as :

$$C_c = (\Gamma^* (J_{flu} + 8(A_N + R_L)))/(J_{flu} - 4(A_N + R_L))$$

where the conservative value of $\Gamma^*$ for Arabidopsis was taken from Mott et al. (2008). Then, $g_m$ was estimated as the slope of the $A_N$ vs $C_i - C_c$ relationship as:

$$g_m = A_N/(C_i - C_c)$$

Thus, estimated $g_m$ is an averaged value over the points used in the relationship ($C_i$ < 300 µmol $mol^{-1}$).

$g_m$ was also estimated by a second method (Ethier and Livingston, 2004), which fits $A_N/C_i$ curves with a non-rectangular hyperbola version Farquhar–von Caemmerer–Berry (FvCB) model, based on the hypothesis that $g_m$ reduces the curvature of the Rubisco-limited portion of an $A_N/C_i$ curve.

From $A_N/C_i$ and $A_N/C_c$ curves, the maximum carboxylation velocity ($V_{cmax}$) and the maximum capacity for electron transport rate ($J_{max}$) were calculated by fitting the mechanistic model of $CO_2$ assimilation (Farquhar et al., 1980), using the $C_i$ or $C_c$-based temperature dependence of kinetic parameters of Rubisco ($K_c$ and $K_o$) (Mott et al., 2008). Then $V_{cmax}$, $J_{max}$ and $g_m$ were normalized to 25ºC using the temperature-response equations from Sharkey et al. (2007).

**Determination of metabolite levels**

Whole rosettes were harvested in different times along of the light/dark cycle (0; 4; 8; 16; 24 h). Rosettes were flash frozen in liquid nitrogen and stored at -80 ºC until further analyses. The levels of starch, sucrose, fructose, and glucose in the leaf tissues were determined as described previously (Fernie et al., 2001). Malate and fumarate were determined as detailed by Nunes-Nesi et al. (2007). The photosynthetic pigments were determined as described (Porra et al., 1989). The metabolite profiling was carried out in samples harvested at the middle of the day for both leaves (Lisec et al., 2006) and guard cell-enriched epidermal fragments as described previously (Daloso et al., 2015), with some modifications. Specifically, after isolation the guard cell-enriched epidermal fragments were snap frozen in liquid nitrogen and lyophilized for one week Approximately 30 mg of lyophilized guard cell-enriched epidermal fragments were disrupted by shaking together with metal balls. The extraction was performed using 1 mL of methanol and shaking (1000 rpm) at 70 ºC for 15 min, 60 µL of Ribitol (0.2 mg $mL^{-1}$) was added as an internal standard. The followed extraction and derivatization procedure was performed exactly as described (Daloso et al., 2015). Peaks were manually annotated, and ion intensity was determined by the aid of TagFinder software (Luedemann et al., 2012), using a reference library from the Golm Metabolome Database (Kopka et al., 2005) and following the recommended reporting format (Fernie et al., 2011).

**Non-aqueous fractionation (NAF)**

Five-week-old rosettes grown under short-day were harvested (pool of five per replicate) in the middle of the light period, flash frozen, and ground to a fine powder at -70 °C using a cryogenic grinding robot (Stitt et al., 2007), and stored at -80 °C until further use. Approximately 4 g of powder were freeze-dried (-80 °C) for one week. NAF was performed as described (Arrivault et al., 2014; Krueger et al., 2014), and the gradient were divided into 8 fractions. After the last centrifugation at 3,200 g (4 °C) for 10 min, the supernatant was discarded to remove the solvent from the fractions. The pellet was resuspended in 7 mL of heptane and divided into 6 aliquots of equal volumes. Finally, the suspension was dried in a vacuum concentrator avoiding heating; aliquots were stored at -80 °C until further use. Prior to analysis, the dried pellets were homogenized with the appropriate extraction buffer by addition of one steel ball bearing and shaking at 25 Hz for 1 min in a ball mill (Retsch MM300, Retsch GmbH, Haan, Germany). Enzyme and metabolite markers (adenosine diphosphate glucose pyrophosphorylase and RubisCO activities for the chloroplast, phospho*enol*pyruvate carboxylase and uridine diphosphate

glucose pyrophosphorylase activities for the cytosol and acid invertase activity and nitrate amounts for the vacuole) were determined as described in Arrivault et al. (2014). Malate and fumarate were quantified via coupled enzymatic assays (Cross et al., 2006). Citrate was quantified via enzymatic assay adapted from (Tompkins and Toffaletti, 1982) in samples obtained with chloroform/methanol/water extraction (Arrivault et al., 2009). Aliquots of extracts (10 µl) or standards (10µl of 0, 125, 250, 500 µM, and 1 mM) were dispensed directly into a microplate, followed by 100 µl 50 mM buffer (Tricine/KOH, pH 8) containing 0.1 mM $ZnSO_4$, 0.5 mM NADH, 1.5 units malate dehydrogenase, 2.3 units lactate dehydrogenase. Absorbance was monitored at 340 nm until OD stabilized, 0.014 units citrate lyase added and absorbance monitored until stable. The other metabolites were measured using the GC-MS method also detailed above. Determination of subcellular distribution was performed using the BestFit software (Klie et al., 2011).

**Enzyme activity measurements**

The enzymatic extract was prepared as previously described (Gibon et al., 2004). Then, the maximum activities of PGK, PK, PFK, Aldolase, G6PH and Acid invertase were determined as described by Gibon et al. (2004); hexokinase, enolase, and TPI following Fernie et al. (2001); SuSy as in Zrenner et al. (1995); and transaldolase according to Debnam and Emes (1999).

**TCA cycle flux on the basis of $^{14}CO_2$ evolution**

Estimations of the TCA cycle flux on the basis of $^{14}CO_2$ evolution were performed following incubation of isolated leaf discs in 10 mM MES-KOH, pH 6.5, containing 0.3 mM Glc and supplied with 0.62 kBq $mL^{-1}$ of [1-$^{14}$C]- and [3,4-$^{14}$C]-Glc under 150 µmol photons $m^{-2}$ $s^{-1}$. The evolved $^{14}CO_2$ was trapped in KOH 10% (w/v) and quantified by liquid scintillation counter (Beckman LS 6500; Beckman Instruments, Fullerton, CA, USA). The results were interpreted following Rees and Beevers (1960).

**Experimental design and statistical analysis**

The data were obtained from the experiments using a completely randomized design using three genotypes, with the exception of the stomatal opening and closing kinetics, which were performed in randomized block design. All data are expressed as the mean ± standard error (SE). Data were tested for significant ($P < 0.05$) differences using Student's *t* tests. All the statistical analyses were performed using the algorithm embedded into Microsoft Excel® (Microsoft, Seattle).

**Supplemental Data**

**Supplemental Fig. S1:** Gene expression by semi quantitative RT-PCR.

**Supplemental Fig. S2:** Growth phenotype of WT and *tdt* plants.

**Supplemental Fig. S3:** Transcriptome data in leaves and guard cell manually dissected from Arabidopsis leaves.

**Supplemental Fig. S4:** Relative transcript levels of *tDT*.

**Supplemental Fig. S5:** Relative transcript levels of genes involved in organic and inorganic ion transport in guard cell.

**Supplemental Fig. S6:** Net photosynthesis ($A_N$) curves in response to substomatal ($C_i$) or chloroplastic ($C_c$) $CO_2$ concentrations in WT and *tdt* plants.

**Supplemental Fig. S7:** Total chlorophyll content ($a + b$) as well as the $a/b$ ratio in WT and *tdt* plants.

**Supplemental Fig. S8:** Sugar content in WT and *tdt* plants.

**Table S1:** Primers utilized for the quantitative real time - PCR.

**Table S2:** Gas exchange and chlorophyll *a* fluorescence parameters in WT and *tdt* plants.

**Table S3:** Photosynthetic parameters from light-response curves in WT and *tdt* plants.

**Table S4:** Photosynthetic characterization of *tdt* mutant plants.

**Table S5:** Relative metabolite content for WT and *tdt* plants in leaves and guard cell-enriched epidermal fragments.

**Table S6:** Organic acids subcellular distribution.

**Acknowledgements**

The authors acknowledge Dr. Laíse Rosado, Ina Krahnert, and Manuela Guenther (all from the Max Planck Institute of Molecular Plant Physiology-MPIMP) for the helpful technical support. We are also grateful to Acácio Salvador for the excellent photographic work. Discussions with Prof. Mark Stitt and Dr. Saleh Alseekh (both from the MPIMP) regarding the NAF assays and GC-MS analysis, respectively, were highly valuable in the development of this work. We also thank Prof. Samuel V.C. Martins (Universidade Federal de Viçosa, Brazil) for useful discussions concerning gas exchange analyses.

**LITERATURE CITED**

**Ache P, Becker D, Ivashikina N, Dietrich P, Roelfsema MRG, Hedrich R** (2000) GORK, a delayed outward rectifier expressed in guard cells of *Arabidopsis thaliana*, is a $K^+$-selective, $K^+$-sensing ion channel. FEBS Letters **486:** 93-98

**António C, Päpke C, Rocha M, Diab H, Limami AM, Obata T, Fernie AR, van Dongen JT** (2016) Regulation of primary metabolism in response to low oxygen availability as revealed by carbon and nitrogen isotope redistribution. Plant Physiol **170:** 43-56

**Antunes WC, Provart NJ, Williams TCR, Loureiro ME** (2012) Changes in stomatal function and water use efficiency in potato plants with altered sucrolytic activity. Plant Cell Environ **35:** 747-759

**Araújo WL, Nunes-Nesi A, Osorio S, Usadel B, Fuentes D, Nagy R, Balbo I, Lehmann M, Studart-Witkowski C, Tohge T, Martinoia E, Jordana X, DaMatta FM, Fernie AR** (2011) Antisense inhibition of the iron-sulphur subunit of succinate dehydrogenase enhances photosynthesis and growth in tomato via an organic acid-mediated effect on stomatal aperture. Plant Cell **23:** 600-627

**Arrivault S, Guenther M, Florian A, Encke B, Feil R, Vosloh D, Lunn JE, Sulpice R, Fernie AR, Stitt M, Schulze WX** (2014) Dissecting the subcellular compartmentation of proteins and metabolites in Arabidopsis leaves using non-aqueous fractionation. Mol Cell Proteomics **13:** 2246-2259

**Arrivault S, Guenther M, Ivakov A, Feil R, Vosloh D, Van Dongen JT, Sulpice R, Stitt M** (2009) Use of reverse-phase liquid chromatography, linked to tandem mass spectrometry, to profile the Calvin cycle and other metabolic intermediates in Arabidopsis rosettes at different carbon dioxide concentrations. Plant J **59:** 826-839

**Azoulay-Shemer T, Palomares A, Bagheri A, Israelsson-Nordstrom M, Engineer CB, Bargmann BOR, Stephan AB, Schroeder JI** (2015) Guard cell photosynthesis is critical for stomatal turgor production, yet does not directly mediate $CO_2$- and ABA-induced stomatal closing. Plant Journal **83:** 567-581

**Bates GW, Rosenthal DM, Sun J, Chattopadhyay M, Peffer E, Yang J, Ort DR, Jones AM** (2012) A comparative study of the *Arabidopsis thaliana* guard-cell transcriptome and its modulation by sucrose. PLoS One **7:** e49641

**Berger D, Altmann T** (2000) A subtilisin-like serine protease involved in the regulation of stomatal density and distribution in *Arabidopsis thaliana*. Genes Dev **14:** 1119-1131

**Bolwell GP, Bindschedler LV, Blee KA, Butt VS, Davies DR, Gardner SL, Gerrish C, Minibayeva F** (2002) The apoplastic oxidative burst in response to biotic stress in plants: a three-component system. J Exp Bot **53:** 1367-1376

**Cao Y, Ward JM, Kelly WB, Ichida AM, Gaber RF, Anderson JA, Uozumi N, Schroeder JI, Crawford NM** (1995) Multiple genes, tissue specificity, and expression-dependent modulation contribute to the functional diversity of potassium channels in *Arabidopsis thaliana*. Plant Physiol **109:** 1093-1106

**Cross JM, von Korff M, Altmann T, Bartzetko L, Sulpice R, Gibon Y, Palacios N, Stitt M** (2006) Variation of enzyme activities and metabolite levels in 24 Arabidopsis accessions growing in carbon-limited conditions. Plant Physiol **142:** 1574-1588

**Czechowski T, Stitt M, Altmann T, Udvardi MK, Scheible W-R** (2005) Genome-wide identification and testing of superior reference genes for transcript normalization in Arabidopsis. Plant Physiol **139:** 5-17

**Daloso DM, Antunes WC, Pinheiro DP, Waquim JP, Araújo WL, Loureiro ME, Fernie AR, Williams TCR** (2015) Tobacco guard cells fix $CO_2$ by both Rubisco and PEPcase while sucrose acts as a substrate during light-induced stomatal opening. Plant Cell Environ **38:** 2353-2371

**De Angeli A, Zhang J, Meyer S, Martinoia E** (2013) *At*ALMT9 is a malate-activated vacuolar chloride channel required for stomatal opening in Arabidopsis. Nat Commun **4:** 1804

**Debnam PM, Emes MJ** (1999) Subcellular distribution of enzymes of the oxidative pentose phosphate pathway in root and leaf tissues. J Exp Bot **50:** 1653-1661

**Delhaize E, Gruber BD, Ryan PR** (2007) The roles of organic anion permeases in aluminium resistance and mineral nutrition. FEBS Letters **581:** 2255-2262

**Emmerlich V, Linka N, Reinhold T, Hurth MA, Traub M, Martinoia E, Neuhaus HE** (2003) The plant homolog to the human sodium/dicarboxylic cotransporter is the vacuolar malate carrier. Proc Natl Acad Sci USA **100:** 11122-11126

**Ethier GJ, Livingston NJ** (2004) On the need to incorporate sensitivity to $CO_2$ transfer conductance into the Farquhar–von Caemmerer–Berry leaf photosynthesis model. Plant Cell Environ **27:** 137-153

**Fahnenstich H, Saigo M, Niessen M, Zanor MI, Andreo CS, Fernie AR, Drincovich MF, Flügge U-I, Maurino VG** (2007) Alteration of organic acid metabolism in Arabidopsis overexpressing the maize C4 NADP-Malic Enzyme causes accelerated senescence during extended darkness. Plant Physiol **145:** 640-652

**Farquhar GD, von Caemmerer S, Berry JA** (1980) A biochemical model of photosynthetic $CO_2$ assimilation in leaves of C3 species. Planta **149:** 78-90

**Fernie AR, Aharoni A, Willmitzer L, Stitt M, Tohge T, Kopka J, Carroll AJ, Saito K, Fraser PD, DeLuca V** (2011) Recommendations for reporting metabolite data. The Plant Cell **23:** 2477-2482

**Fernie AR, Carrari F, Sweetlove LJ** (2004) Respiratory metabolism: glycolysis, the TCA cycle and mitochondrial electron transport. Curr Opin Plant Biol **7:** 254-261

**Fernie AR, Roscher A, Ratcliffe RG, Kruger NJ** (2001) Fructose 2,6-bisphosphate activates pyrophosphate: fructose-6-phosphate 1-phosphotransferase and increases triose phosphate to hexose phosphate cycling in heterotrophic cells. Planta **212:** 250-263

**Figueroa CM, Feil R, Ishihara H, Watanabe M, Kölling K, Krause U, Höhne M, Encke B, Plaxton WC, Zeeman SC, Li Z, Schulze WX, Hoefgen R, Stitt M, Lunn JE** (2016) Trehalose 6–phosphate coordinates organic and amino acid metabolism with carbon availability. Plant J **85:** 410-423

**Finkemeier I, König A-C, Heard W, Nunes-Nesi A, Pham PA, Leister D, Fernie AR, Sweetlove LJ** (2013) Transcriptomic analysis of the role of carboxylic acids in metabolite signaling in Arabidopsis leaves. Plant Physiol **162:** 239-253

**Flexas J, Ortuno MF, Ribas-Carbo M, Diaz-Espejo A, Florez-Sarasa ID, Medrano H** (2007) Mesophyll conductance to $CO_2$ in *Arabidopsis thaliana*. New Phytol **175:** 501-511

**Gerhardt R, Stitt M, Heldt HW** (1987) Subcellular metabolite levels in spinach leaves: regulation of sucrose synthesis during diurnal alterations in photosynthetic partitioning. Plant Physiol **83:** 399-407

**Gibon Y, Blaesing OE, Hannemann J, Carillo P, Hohne M, Hendriks JH, Palacios N, Cross J, Selbig J, Stitt M** (2004) A Robot-based platform to measure multiple enzyme activities in Arabidopsis using a set of cycling assays: comparison of changes of enzyme activities and transcript levels during diurnal cycles and in prolonged darkness. Plant Cell **16:** 3304-3325

**Gibon Y, Pyl E-T, Sulpice R, Lunn JE, Höhne M, Günther M, Stitt M** (2009) Adjustment of growth, starch turnover, protein content and central metabolism to a decrease of the carbon supply when Arabidopsis is grown in very short photoperiods. Plant Cell Environ **32:** 859-874

**Harley PC, Loreto F, Di Marco G, Sharkey TD** (1992) Theoretical considerations when estimating the mesophyll conductance to $CO_2$ flux by analysis of the response of photosynthesis to $CO_2$. Plant Physiol **98:** 1429-1436

**Hedrich R, Marten I** (1993) Malate-induced feedback regulation of plasma membrane anion channels could provide a $CO_2$ sensor to guard-cells. EMBO J **12:** 897-901

**Hedrich R, Marten I, Lohse G, Dietrich P, Winter H, Lohaus G, Heldt HW** (1994) Malate-sensitive anion channels enable guard cells to sense changes in the ambient $CO_2$ concentration. Plant J **6:** 741-748

**Hunt R, Causton DR, Shipley B, Askew AP** (2002) A modern tool for classical plant growth analysis. Ann Bot **90:** 485-488

**Hurth MA, Suh SJ, Kretzschmar T, Geis T, Bregante M, Gambale F, Martinoia E, Neuhaus HE** (2005) Impaired pH homeostasis in Arabidopsis lacking the vacuolar dicarboxylate transporter and analysis of carboxylic acid transport across the tonoplast. Plant Physiol **137:** 901-910

**Kim T-H, Böhmer M, Hu H, Nishimura N, Schroeder JI** (2010) Guard cell signal transduction network: advances in understanding abscisic acid, $CO_2$, and $Ca^{2+}$ signaling. Annu Rev Plant Biol **61:** 561-591

**Klie S, Krueger S, Krall L, Giavalisco P, Flügge U-I, Willmitzer L, Steinhauser D** (2011) Analysis of the compartmentalized metabolome – A validation of the non-aqueous fractionation technique. Front Plant Sci **2:** 55

**Kopka J, Schauer N, Krueger S, Birkemeyer C, Usadel B, Bergmüller E, Dörmann P, Weckwerth W, Gibon Y, Stitt M, Willmitzer L, Fernie AR, Steinhauser D** (2005) GMD@CSB.DB: the Golm Metabolome Database. Bioinformatics **21:** 1635-1638

**Kovermann P, Meyer S, Hörtensteiner S, Picco C, Scholz-Starke J, Ravera S, Lee Y, Martinoia E** (2007) The Arabidopsis vacuolar malate channel is a member of the ALMT family. Plant J **52:** 1169-1180

**Krueger S, Steinhauser D, Lisec J, Giavalisco P** (2014) Analysis of subcellular metabolite distributions within *Arabidopsis thaliana* leaf tissue: A primer for subcellular metabolomics. Methods Mol. Biol. **1062:** 575-596

**Lauxmann MA, Annunziata MG, Brunoud G, Wahl V, Koczut A, Burgos A, Olas JJ, Maximova E, Abel C, Schlereth A, Soja AM, Bläsing OE, Lunn JE, Vernoux T, Stitt M** (2016) Reproductive failure in *Arabidopsis thaliana* under transient carbohydrate limitation: flowers and very young siliques are jettisoned and the meristem is maintained to allow successful resumption of reproductive growth. Plant Cell Environ **39:** 745-767

**Lee M, Choi Y, Burla B, Kim YY, Jeon B, Maeshima M, Yoo JY, Martinoia E, Lee Y** (2008) The ABC transporter *At*ABCB14 is a malate importer and modulates stomatal response to $CO_2$. Nat Cell Biol **10:** 1217-1223

**Lisec J, Schauer N, Kopka J, Willmitzer L, Fernie AR** (2006) Gas chromatography mass spectrometry-based metabolite profiling in plants. Nature Protocols **1:** 387-396

**Lohaus G, Pennewiss K, Sattelmacher B, Hussmann M, Hermann Muehling K** (2001) Is the infiltration-centrifugation technique appropriate for the isolation of apoplastic fluid? A critical evaluation with different plant species. Physiol Plant **111:** 457-465

**Long SP, Bernacchi CJ** (2003) Gas exchange measurements, what can they tell us about the underlying limitations to photosynthesis? Procedures and sources of error. J Exp Bot **54:** 2393-2401

**Luedemann A, von Malotky L, Erban A, Kopka J** (2012) TagFinder: Preprocessing Software for the Fingerprinting and the Profiling of Gas Chromatography–Mass Spectrometry Based Metabolome Analyses. *In* NW Hardy, RD Hall, eds, Plant Metabolomics: Methods and Protocols. Humana Press, Totowa, NJ, pp 255-286

**Madsen SR, Nour-Eldin HH, Halkier BA** (2016) Collection of apoplastic fluids from *Arabidopsis thaliana* Leaves. *In* GA Fett-Neto, ed, Biotechnology of plant secondary metabolism: Methods and Protocols. Springer New York, New York, NY, pp 35-42

**Maier A, Zell MB, Maurino VG** (2011) Malate decarboxylases: evolution and roles of NAD(P)-ME isoforms in species performing C4 and C3 photosynthesis. J Exp Bot **62:** 3061-3069

**Martinoia E, Rentsch D** (1994) Malate compartmentation - responses to a complex metabolism. Annu Rev Plant Physiol Plant Mol Biol **45:** 447-467

**Martins SCV, Galmés J, Molins A, DaMatta FM** (2013) Improving the estimation of mesophyll conductance to $CO_2$: on the role of electron transport rate correction and respiration. J Exp Bot **64:** 1-14

**Martins SCV, McAdam SA, Deans RM, DaMatta FM, Brodribb TJ** (2016) Stomatal dynamics are limited by leaf hydraulics in ferns and conifers: results from simultaneous measurements of liquid and vapour fluxes in leaves. Plant Cell Environ **39:** 694-705

**Medeiros DB, Martins SCV, Cavalcanti JHF, Daloso DM, Martinoia E, Nunes-Nesi A, DaMatta FM, Fernie AR, Araújo WL** (2016) Enhanced photosynthesis and growth in *atquac1* knockout mutants are due to altered organic acid accumulation and an increase in both stomatal and mesophyll conductance. Plant Physiol **170:** 86-101

**Messinger SM, Buckley TN, Mott KA** (2006) Evidence for involvement of photosynthetic processes in the stomatal response to $CO_2$. Plant Physiol **140:** 771-778

**Meyer S, Scholz-Starke J, De Angeli A, Kovermann P, Burla B, Gambale F, Martinoia E** (2011) Malate transport by the vacuolar *At*ALMT6 channel in guard cells is subject to multiple regulation. Plant J **67:** 247-257

**Mott KA, Sibbernsen ED, Shope JC** (2008) The role of the mesophyll in stomatal responses to light and $CO_2$. Plant Cell Environ **31:** 1299-1306

**Nakamura RL, McKendree Jr WL, Hirsch RE, Sedbrook JC, Gaber RF, Sussman MR** (1995) Expression of an Arabidopsis potassium channel gene in guard cells. Plant Physiol **109:** 371-374

**Negi J, Matsuda O, Nagasawa T, Oba Y, Takahashi H, Kawai-Yamada M, Uchimiya H, Hashimoto M, Iba K** (2008) $CO_2$ regulator SLAC1 and its homologues are essential for anion homeostasis in plant cells. Nature **452:** 483-486

**Niinemets Ü, Cescatti A, Rodeghiero M, Tosens T** (2005) Leaf internal diffusion conductance limits photosynthesis more strongly in older leaves of Mediterranean evergreen broad-leaved species. Plant Cell Environ **28:** 1552-1566

**Niinemets Ü, Cescatti A, Rodeghiero M, Tosens T** (2006) Complex adjustments of photosynthetic potentials and internal diffusion conductance to current and previous light availabilities and leaf age in Mediterranean evergreen species *Quercus ilex*. Plant Cell Environ **29:** 1159-1178

**Niinemets Ü, Díaz-Espejo A, Flexas J, Galmés J, Warren CR** (2009) Role of mesophyll diffusion conductance in constraining potential photosynthetic productivity in the field. Journal of Experimental Botany **60:** 2249-2270

**Nunes-Nesi A, Araújo WL, Fernie AR** (2011) Targeting mitochondrial metabolism and machinery as a means to enhance photosynthesis. Plant Physiol **155:** 101-107

**Nunes-Nesi A, Carrari F, Gibon Y, Sulpice R, Lytovchenko A, Fisahn J, Graham J, Ratcliffe RG, Sweetlove LJ, Fernie AR** (2007) Deficiency of mitochondrial fumarase activity in tomato plants impairs photosynthesis via an effect on stomatal function. Plant J **50:** 1093-1106

**Pandey S, Wang X-Q, Coursol SA, Assmann SM** (2002) Preparation and applications of *Arabidopsis thaliana* guard cell protoplasts. New Phytol **153:** 517-526

**Peiter E, Maathuis FJM, Mills LN, Knight H, Pelloux J, Hetherington AM, Sanders D** (2005) The vacuolar $Ca^{2+}$-activated channel TPC1 regulates germination and stomatal movement. Nature **434:** 404-408

**Pilot G, Lacombe Bt, Gaymard F, Chérel I, Boucherez J, Thibaud J-B, Sentenac H** (2001) Guard cell inward $K^+$ channel activity in Arabidopsis involves expression of the twin channel subunits KAT1 and KAT2. J Biol Chem **276:** 3215-3221

**Porra RJ, Thompson WA, Kriedemann PE** (1989) Determination of accurate extinction coefficients and simultaneous equations for assaying chlorophylls a and b extracted with four different solvents: verification of the concentration of chlorophyll standards by atomic absorption spectroscopy. BBA - Bioenergetics **975:** 384-394

**Raschke K** (2003) Alternation of the slow with the quick anion conductance in whole guard cells effected by external malate. Planta **217:** 651-657

**Rees TA, Beevers H** (1960) Pathways of glucose dissimilation in carrot slices. Plant Physiol **35:** 830-838

**Santelia D, Lawson T** (2016) Rethinking guard cell metabolism. Plant Physiol **172:** 1371-1392

**Schindelin J, Rueden CT, Hiner MC, Eliceiri KW** (2015) The ImageJ ecosystem: An open platform for biomedical image analysis. Molecular Reproduction and Development **82:** 518-529

**Sharkey TD, Bernacchi CJ, Farquhar GD, Singsaas EL** (2007) Fitting photosynthetic carbon dioxide response curves for C3 leaves. Plant Cell Environ **30:** 1035-1040

**Stitt M, Sulpice R, Gibon Y, Whitwell A, Skilbeck R, Parker S, Ellison R** (2007) Cryogenic grinder system. Germany patent number **08146.0025U1**. *In*,

**Sulpice R, Flis A, Ivakov AA, Apelt F, Krohn N, Encke B, Abel C, Feil R, Lunn JE, Stitt M** (2014) Arabidopsis coordinates the diurnal regulation of carbon allocation and growth across a wide range of photoperiods. Molecular Plant **7:** 137-155

**Sweetlove LJ, Beard KFM, Nunes-Nesi A, Fernie AR, Ratcliffe RG** (2010) Not just a circle: flux modes in the plant TCA cycle. Trends Plant Sci **15:** 462-470

**Tompkins D, Toffaletti J** (1982) Enzymic determination of citrate in serum and urine, with use of the Worthington "ultrafree" device. Clin Chem **28:** 192-195

**Tronconi MA, Fahnenstich H, Gerrard Weehler MC, Andreo CS, Flügge U-I, Drincovich MF, Maurino VG** (2008) Arabidopsis NAD-Malic enzyme functions as a homodimer and heterodimer and has a major impact on nocturnal metabolism. Plant Physiol **146:** 1540-1552

**Ueno K, Kinoshita T, Inoue S-i, Emi T, Shimazaki K-i** (2005) Biochemical characterization of plasma membrane $H^+$-ATPase ativation in guard cell protoplasts of *Arabidopsis thaliana* in response to blue light. Plant Cell Physiol **46:** 955-963

**Von Groll U, Berger D, Altmann T** (2002) The subtilisin-like serine protease SDD1 mediates cell-to-cell signaling during Arabidopsis stomatal development. The Plant Cell **14:** 1527-1539

**Weisskopf L, Abou-Mansour E, Fromin N, Tomasi N, Santelia D, Edelkott I, Neumann G, Aragno M, Tabacchi R, Martinoia E** (2006) White lupin has developed a complex strategy to limit microbial degradation of secreted citrate required for phosphate acquisition. Plant Cell Environ **29:** 919-927

**Winter H, Robinson DG, Heldt HW** (1993) Subcellular volumes and metabolite concentrations in barley leaves. Planta **191:** 180-190

**Winter H, Robinson DG, Heldt HW** (1994) Subcellular volumes and metabolite concentrations in spinach leaves. Planta **193:** 530-535

**Wu F-H, Shen S-C, Lee L-Y, Lee S-H, Chan M-T, Lin C-S** (2009) Tape-Arabidopsis Sandwich - a simpler Arabidopsis protoplast isolation method. Plant Methods **5:** 16

**Yin X, Struik PC, Romero P, Harbinson J, Evers JB, Van Der Putten PEL, Vos JAN** (2009) Using combined measurements of gas exchange and chlorophyll fluorescence to estimate parameters of a biochemical C3 photosynthesis model: a critical appraisal and a new integrated approach applied to leaves in a wheat (*Triticum aestivum*) canopy. Plant Cell Environ **32:** 448-464

**Zell MB, Fahnenstich H, Maier A, Saigo M, Voznesenskaya EV, Edwards GE, Andreo C, Schleifenbaum F, Zell C, Drincovich MF, Maurino VG** (2010) Analysis of Arabidopsis with highly reduced levels of malate and fumarate sheds light on the role of these organic acids as storage carbon molecules. Plant Physiol **152:** 1251-1262

**Zrenner R, Salanoubat M, Willmitzer L, Sonnewald U** (1995) Evidence of the crucial role of sucrose synthase for sink strength using transgenic potato plants (*Solanum tuberosum* L.). Plant J **7:** 97-107

**SUPPLEMENTAL DATA**

**FIGURES**

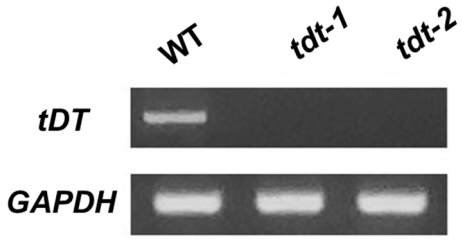


**Supplemental Fig. S1:** Gene expression by semi quantitative RT-PCR showed absence of transcripts in both mutant lines.

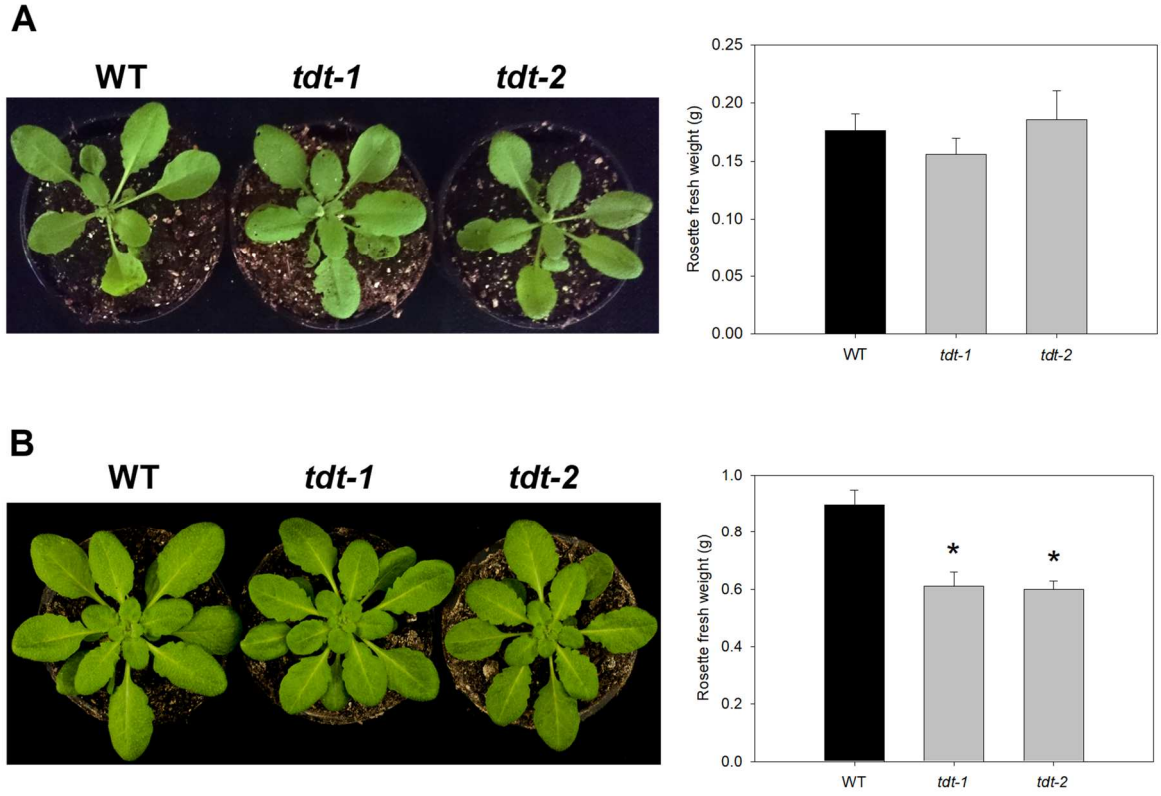


**Supplemental Fig. S2:** Growth phenotype of WT and *tdt*. **A**, Representative images and Rosette fresh weight of 4-week-old Arabidopsis plants grown under neutral-day conditions 12h/12h (light/dark). **B**, Representative images and Rosette fresh weight of 4-week-old Arabidopsis plants grown under short-day 8 h/16 h (light/dark). In both conditions (neutral and short days), plants were grown in a growth chamber with irradiance of 150 µmol $m^2$ $s^{-1}$, temperature was set as 22ºC/20ºC during the day/night cycle, and 60% relative humidity. Rosette fresh weight are presented as means ± SE ($n$ = 6).

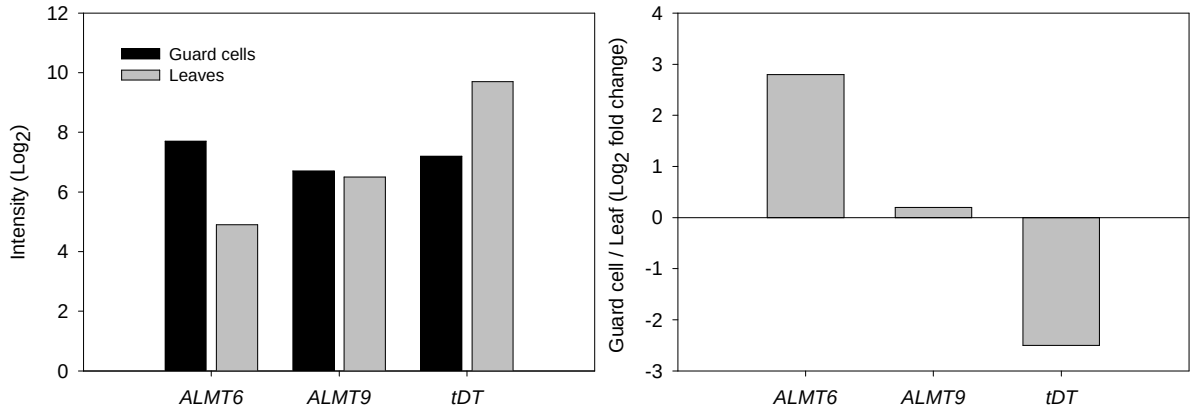


**Supplemental Fig. S3:** Transcriptome data obtained by Bates et al. (2012) in leaves and guard cell manually dissected from Arabidopsis leaves. The signal intensities are presented as log2 normalized values. The complete data set from this study is available online: http://journals.plos.org/plosone/article?id=10.1371/journal.pone.0049641.

Reference: **Bates GW, Rosenthal DM, Sun J, Chattopadhyay M, Peffer E, Yang J, Ort DR, Jones AM** (2012) A comparative study of the *Arabidopsis thaliana* guard-cell transcriptome and its modulation by sucrose. PLoS One 7: e49641

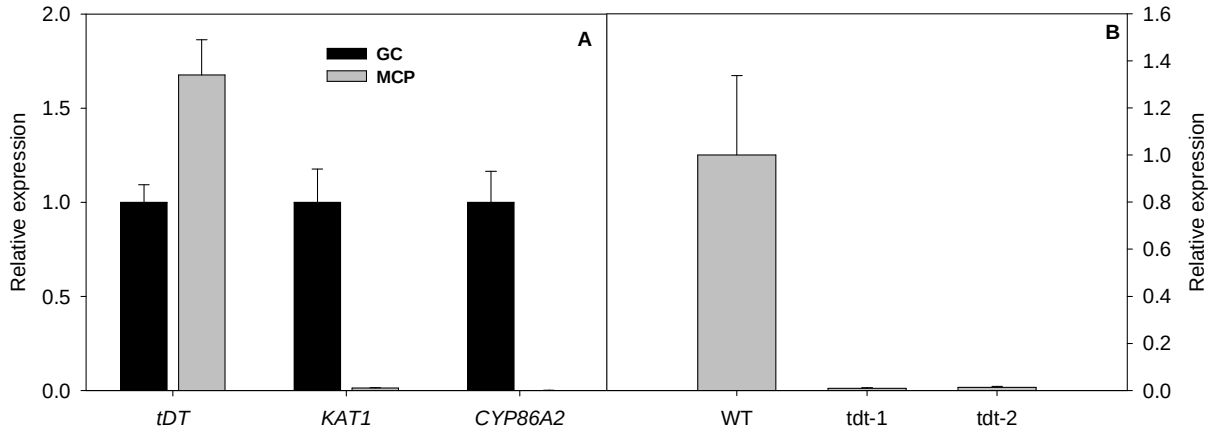


**Supplemental Fig. S4:** Relative transcript levels of *tDT*. **A**, RNA was isolated from WT (Wassilewskija ecotype) guard cell-enriched epidermal fragments (GC) and mesophyll cell protoplasts (MCP). The genes *POTASSIUM CHANNEL IN ARABIDOPSIS THALIANA 1* (*KAT1*) and *CYTOCHROME P450, FAMILY 86, SUBFAMILY A, POLYPEPTIDE 2* (*CYP86A2*) were used as guard cell specific gene markers. **B,** Relative *AttDT* expression in WT and *tdt* mutant lines. RNA was isolated from WT and *tdt* guard cell-enriched epidermal fragments (GC). Values are presented as means ± SE (*n = 3*).

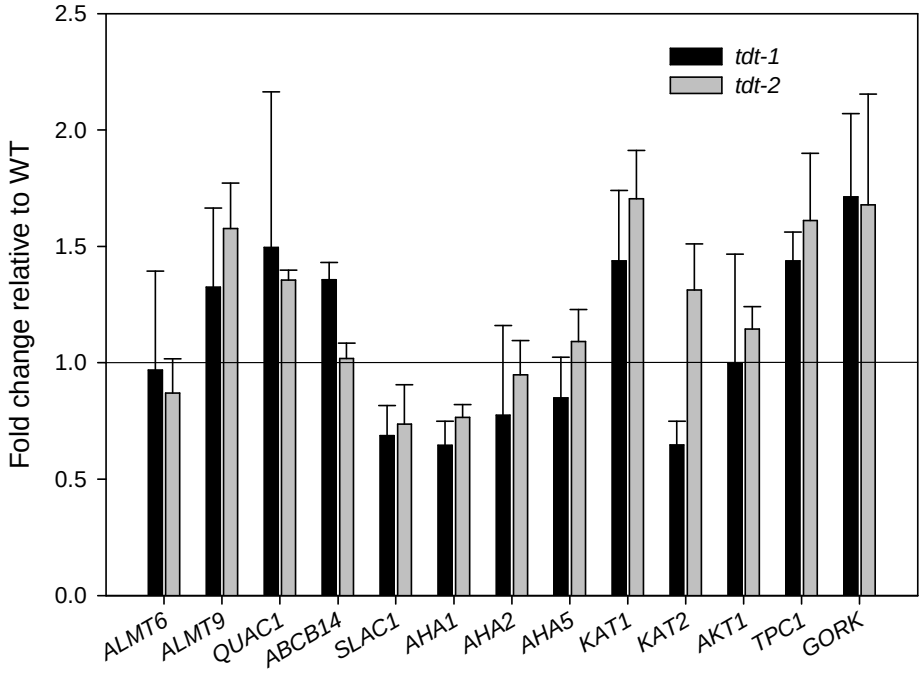


**Supplemental Fig. S5:** Relative transcript levels of genes involved in organic and inorganic ion transport in guard cell. Transcript abundance of *Arabidopsis thaliana* plasma membrane $H^+$-ATPases *AHA1, AHA2,* and *AHA5*, transporter *ABCB14*, and ion channels *ALMT6, ALMT9, QUAC1, SLAC1, KAT1, KAT2, AKT1, TPC1,* and *GORK* was determined. RNA was isolated from guard-cell enriched epidermal fragments. Values are presented as means ± SE (*n*=4). *tdt-1*: black bars and *tdt-2*: gray bars.

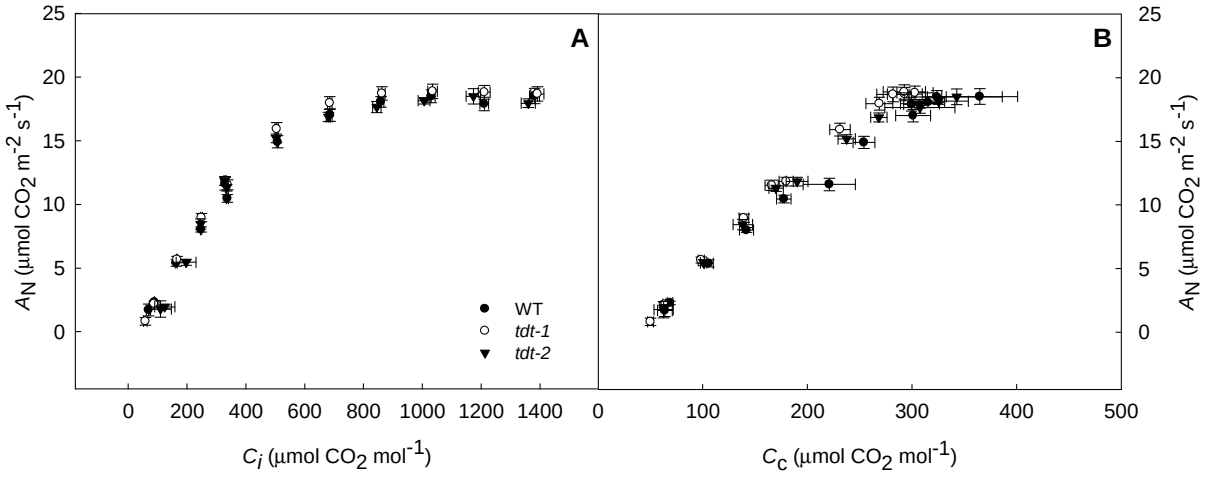


**Supplemental Fig. S6:** Net photosynthesis ($A_N$) curves in response to substomatal ($C_i$) or chloroplastic ($C_c$) $CO_2$ concentrations in WT and *tdt* plants. **A**, $A_N/C_i$ curves. **B**, $A_N/C_c$ curves. Data presented are mean ± SE ($n$ = 10) obtained in two independent assays (five plants in each assay).

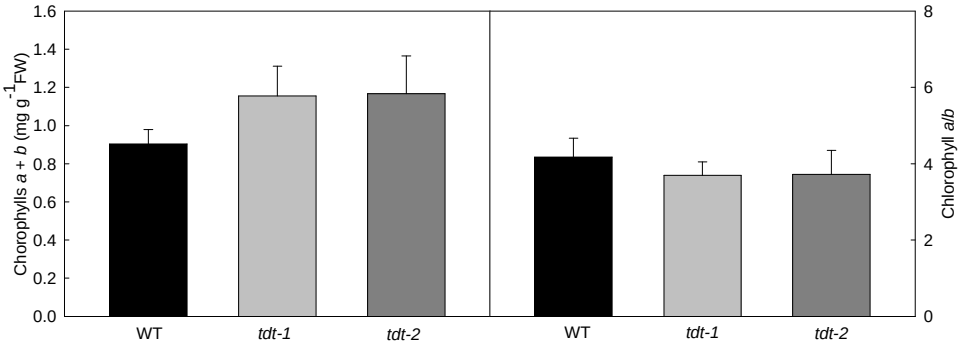


**Supplemental Fig. S7:** Total chlorophyll content (*a* + *b*) as well as the *a*/*b* ratio in WT and *tdt* plants. Data presented are mean ± SE (*n* = 5) from rosettes harvested at middle of the photoperiod.

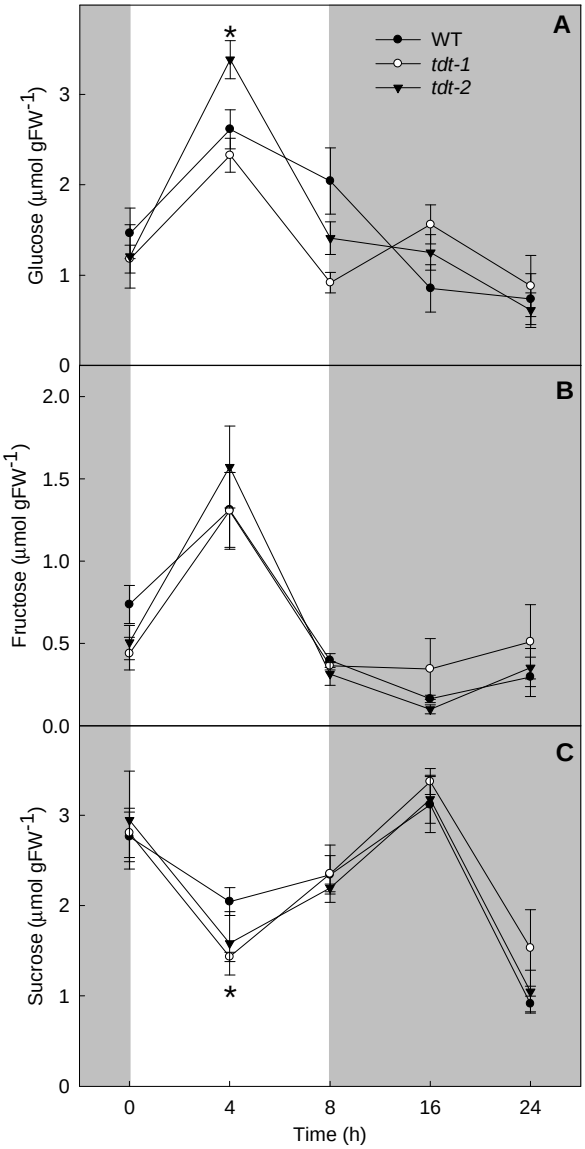


**Supplemental Fig. S8:** Sugar content in WT and *tdt* plants. A, Glucose; B, Fructose; C, Sucrose content in rosettes harvested in different times along of the light/dark cycle, values are presented as means ± SE (*n* = 6) from whole and asterisk indicates the time where the values from mutant lines were determined by the Student's *t* test to be significantly different ($P < 0.05$) from WT.

**TABLES**

**Supplemental Table S1.** Primers utilized for the quantitative real time - PCR.

| Gene | Locus | Sequence 5'-3' |
|---|---|---|
| *F-BOX (Control)* | At5g15710 | Forward 5'-TTTCGGCTGAGAGGTTCGAGT-3'<br>Reverse 5'-GATTCCAAGACGTAAAGCAGATCAA-3' |
| *TIP41-like (Control)* | AT4G34270 | Forward 5'-GTGAAAACTGTTGGAGAGAAGCAA-3'<br>Reverse 5'- TCAACTGGATACCCTTTCGCA-3' |
| *ALMT6* | At2g17470 | Forward 5'-AGCCTCCACATGGACCTTACAG-3'<br>Reverse 5'-GATACAGGCAGCTCCAGAGAAACG-3' |
| *ALMT9* | At3g18440 | Forward 5'-TCTCTCAGAAATCCAGGCACCAG-3'<br>Reverse 5'-ACGCCCACTCTCTGAAGTTCTTG-3' |
| *ABCB14* | At1g28010 | Forward 5'-AGCTTTCTACAGACCCGAATGCC-3'<br>Reverse 5'-TGCATCCAACAAGCAACTCCAATC-3' |
| *QUAC1* | At4g17970 | Forward 5'-CGGCAAAGTCCTTCGAGCTATC-3'<br>Forward 5'-CATTGGAGCGGCTGCTACTTATAT-3' |
| *SLAC1* | At1g12480 | Forward 5'-ATGGCCAATTCGACGGATGTT-3'<br>Reverse 5'-ACCACGCCACTGAGAACTTAAATC-3' |
| *AHA1* | At2g18960 | Forward 5'-CTGGGAGGCTACCAAGCCA-3'<br>Reverse 5'-CTCACACCGAACTTGTCCGA-3' |
| *AHA2* | At4g30190 | Forward 5'-CCGGAGTCTTCCCAGGTT-3'<br>Reverse 5'-TTTAGAGCAGGGGCATCATT-3' |
| *AHA5* | At2g24520 | Forward 5'-5'-GGCTGTTGCAAGACAGGAA-3'<br>Reverse 5'-CGGAGGATCAAAAAGAGGTAAA-3' |
| *KAT1* | At5g46240 | Forward 5'-AGCATGGGATGGGAAGAGTGGAG-3'<br>Reverse 5'-AGAGCAGTGTCGGAAGTCGGAT-3' |
| *KAT2* | At4g18290 | Forward 5'- 5'-TAGCTCGCTGTTTGCAAGG-3'<br>Reverse 5'-CAAACAGTGTCACCGAAATGA-3' |
| *AKT1* | At2g26650 | Forward 5'-ACA TCCTTG TGAACGGAACC-3'<br>Reverse 5'-CCTCTCTCACAATGCTTTCTGTT-3' |
| *AtKC1* | At4g32650 | Forward 5'-CTCAAGACATGAAAATGGACAGAT-3'<br>Reverse 5'-GAATCACCATTGTTTTTGTTATCTTG-3' |
| *TPC1* | At4g03560 | Forward 5'-CGCTTGATATCGAAGAAAGCTC-3'<br>Reverse 5'-TCTCCAACACATATATCCAACCA-3' |
| *GORK* | At5g37500 | Forward 5'-GCATCAATCCGCGCCAAGATT-3'<br>Reverse 5'-GTGGAGCAGCCTTTGAAGAGA-3' |
| *AttDT* | AT5G47560 | Forward 5'-GCCGGCTTGCCCTTAACATAAC-3'<br>Reverse 5'-GCAGATGCCAAGCAGAAGTAGC-3' |
| *CYP86A2* | AT4G00360 | Forward 5'-TGAATTCACCACCAGGACGT-3'<br>Reverse 5'-AACCGGCTCGTAATTGTTCTG-3' |

**Supplemental Table S2:** Gas exchange and chlorophyll *a* fluorescence parameters in WT and *tdt* plants under 1000 µmol $CO_2$ $m^{-2}$ $s^{-1}$. Data presented are mean ± SE ($n$ = 10) obtained in two independent assays (five plants in each assay). Data were tested for significance by the Student's $t$ ($P < 0.05$).

| Parameters* | WT | *tdt-1* | *tdt-2* |
|---|---|---|---|
| $A_N$ (µmol $CO_2$ $m^{-2}$ $s^{-1}$) | 10.6 ± 0.2 | 11.4 ± 0.3 | 11.3 ± 0.2 |
| $g_s$ (mol $H_2O$ $m^{-2}$ $s^{-1}$) | 0.38 ± 0.02 | 0.39 ± 0.02 | 0.41 ± 0.03 |
| $E$ (mmol $H_2O$ $m^{-2}$ $s^{-1}$) | 4.2 ± 0.3 | 4.0 ± 0.2 | 4. 4 ± 0.1 |
| $F_v/F_m$ | 0.78 ± 0.02 | 0.76 ± 0.01 | 0.75 ± 0.01 |

*$A_N$: Net photosynthesis; $E$: transpiration, $g_s$: stomatal conductance; '$F_v/F_m$: PSII maximum photochemical efficiency; $F_v'/F_m'$: PSII real photochemical efficiency; $J_{flu}$: electron transport rate estimated by fluorescence parameters.

**Supplemental Table S3:** Photosynthetic parameters from light-response curves in WT and *tdt* plants. Data presented are mean ± SE ($n$ = 8). Data were tested for significance by the Student's $t$ ($P < 0.05$).

| Parameters* | WT | *tdt-1* | *tdt-2* |
|---|---|---|---|
| $A_{PPFD}$ (µmol $CO_2$ $m^{-2}$ $s^{-1}$) | 8.3 ± 0.4 | 9.7 ± 0.8 | 9.4 ± 0.3 |
| $I_c$ (µmol $m^{-2}$ $s^{-1}$) | 12.2 ± 1.0 | 13.7 ± 1.1 | 14.9 ± 1.8 |
| $I_s$ (µmol $m^{-2}$ $s^{-1}$) | 420.0 ± 48.1 | 465.0 ± 52.3 | 406.0 ± 42.8 |
| 1/ϕ (µmol photons $mol^{-1}$ $CO_2$) | 12.6 ± 0.8 | 12.3 ± 1.0 | 12.8 ± 0.8 |

*$A_{PPFD}$: Net $CO_2$ assimilation rate saturated by light; $I_c$: light compensation point; $I_s$: light saturation point; 1/ϕ: Light use efficiency.

**Supplemental Table S4:** Photosynthetic characterization of *tdt* mutant plants. Data presented are mean ± SE ($n$ = 10) obtained using the ninth leaf totally expanded from 10 different plants per genotype in two independent assays (five plants in each assay).

| Parameters* | WT | *tdt-1* | *tdt-2* |
|---|---|---|---|
| $C_i$ (µmol $CO_2$ $mol^{-1}$) | 338.2 ± 2.6 | 337.9 ± 2.3 | 341.4 ± 4.8 |
| $C_c$ (µmol $CO_2$ $mol^{-1}$) | 172.4 ± 4.8 | 166.0 ± 6.7 | 171.3 ± 8.9 |
| $g_{m\_Harley}$ (mol $CO_2$ $m^{-2}$ $s^{-1}$ $bar^{-1}$) | 0.064 ± 0.003 | 0.070 ± 0.004 | 0.073 ± 0.007 |
| $g_{m\_Ethier}$ (mol $CO_2$ $m^{-2}$ $s^{-1}$ $bar^{-1}$) | 0.066 ± 0.007 | 0.061 ± 0.005 | 0.069 ± 0.008 |
| $V_{cmax\_Ci}$ (µmol $m^{-2}$ $s^{-1}$) | 37.6 ± 1.2 | 40.6 ± 1.1 | 38.8 ± 1.3 |
| $V_{cmax\_Cc}$ (µmol $m^{-2}$ $s^{-1}$) | 65.0 ± 1.6 | 69.5 ± 3.3 | 65.3 ± 2.4 |
| $J_{max\_Ci}$ (µmol $m^{-2}$ $s^{-1}$) | 81.8 ± 3.0 | 90.1 ± 2.4 | 83.9 ± 2.7 |
| $J_{max\_Cc}$ (µmol $m^{-2}$ $s^{-1}$) | 106.8 ± 2.8 | 119.1 ± 2.5 | 105.4 ± 2.9 |

*$C_i$: sub-stomatal $CO_2$ concentration; $C_c$: chloroplastic $CO_2$ concentration; $g_m$: mesophyll conductance to $CO_2$ estimated by Harley or Ethier method; $V_{cmax\_Ci\ ou\ Cc}$: maximum carboxylation capacity based in $C_i$ or $C_c$; $J_{max\_Ci\ ou\ Cc}$: maximum capacity for electron transport rate based in $C_i$ or $C_c$.

**Supplemental Table S5.** Relative metabolite content for WT and *tdt* plants in leaves and guard cell-enriched epidermal fragments (5-week-old plants). Data are normalized with respect to the mean relative amount calculated for WT (to allow statistical assessment, individual plants from this set were normalized in the same way). Data are presented as means ± SE ($n$ = 5). Values set in bold in *tdt* plants were determined by the Student's $t$ test to be significantly different ($P < 0.05$) from WT.

| | Leaves | | | Guard cells | | |
|---|---|---|---|---|---|---|
| **Amino acids** | **WT** | ***tdt-1*** | ***tdt-2*** | **WT** | ***tdt-1*** | ***tdt-2*** |
| Alanine | 1.00 ± 0.02 | 0.89 ± 0.05 | **1.21 ± 0.06** | - | - | - |
| β-Alanine | 1.00 ± 0.03 | **1.18 ± 0.06** | **1.37 ± 0.04** | - | - | - |
| Arginine | 1.00 ± 0.19 | 0.99 ± 0.08 | 1.38 ± 0.16 | - | - | - |
| Asparagine | 1.00 ± 0.05 | **1.19 ± 0.04** | **1.31 ± 0.05** | - | - | - |
| Aspartate | 1.00 ± 0.07 | **1.24 ± 0.03** | **1.36 ± 0.06** | - | - | - |
| Glutamate | 1.00 ± 0.08 | 0.97 ± 0.01 | 1.07 ± 0.05 | 1.00 ± 0.22 | 1.05 ± 0.06 | 1.14 ± 0.08 |
| Glutamine | 1.00 ± 0.29 | 1.85 ± 0.35 | **2.39 ± 0.32** | 1.00 ± 0.17 | **2.05 ± 0.07** | **1.68 ± 0.12** |
| Glycine | 1.00 ± 0.05 | **0.55 ± 0.04** | **0.76 ± 0.05** | 1.00 ± 0.21 | 0.57 ± 0.01 | 0.84 ± 0.11 |
| Histidine | 1.00 ± 0.08 | 1.50 ± 0.20 | 1.06 ± 0.10 | - | - | - |
| Homoserine | 1.00 ± 0.01 | 1.02 ± 0.05 | 1.14 ± 0.06 | - | - | - |
| Isoleucine | 1.00 ± 0.11 | **1.58 ± 0.17** | **1.63 ± 0.13** | 1.00 ± 0.10 | 1.15 ± 0.12 | 1.22 ± 0.09 |
| Leucine | 1.00 ± 0.10 | **1.46 ± 0.11** | **1.65 ± 0.17** | - | - | - |
| Lysine | 1.00 ± 0.07 | **1.30 ± 0.09** | **1.88 ± 0.20** | 1.00 ± 0.12 | 1.07 ± 0.11 | 1.17 ± 0.08 |
| Methionine | 1.00 ± 0.08 | 1.02 ± 0.20 | 1.27 ± 0.14 | - | - | - |
| Ornithine | 1.00 ± 0.17 | 1.35 ± 0.09 | **1.74 ± 0.09** | - | - | - |
| Phenylalanine | 1.00 ± 0.11 | 1.06 ± 0.07 | 1.29 ± 0.09 | 1.00 ± 0.09 | 1.23 ± 0.11 | 1.21 ± 0.11 |
| Proline | 1.00 ± 0.10 | 1.04 ± 0.02 | 1.00 ± 0.12 | 1.00 ± 0.07 | 0.89 ± 0.04 | 1.01 ± 0.11 |
| Serine | 1.00 ± 0.16 | 1.15 ± 0.09 | 0.89 ± 0,11 | 1.00 ± 0.15 | 0.85 ± 0.02 | 1.15 ± 0.10 |
| Tryptophan | 1.00 ± 0.32 | 0.72 ± 0.13 | 1.03 ± 0.11 | - | - | - |
| Tyrosine | 1.00 ± 0.13 | **1.80 ± 0.07** | **2.09 ± 0.17** | - | - | - |
| Valine | 1.00 ± 0.01 | 1.12 ± 0.07 | **1.41 ± 0.09** | 1.00 ± 0.10 | 1.05 ± 0.04 | 1.21 ± 0.11 |
| **Organic acids** | | | | | | |
| Glycerate | - | - | - | 1.00 ± 0.03 | **0.83 ± 0.02** | 0.99 ± 0.04 |
| Aconitate | 1.00 ± 0.16 | 1.06 ± 0.04 | 1.19 ± 0.11 | 1.00 ± 0.04 | 0.97 ± 0.02 | 1.03 ± 0.05 |
| Citrate | 1.00 ± 0.08 | **3.41 ± 0.51** | **3.76 ± 0.60** | - | - | - |
| Isocitrate | 1.00 ± 0.08 | **1.36 ± 0.10** | **1.35 ± 0.06** | 1.00 ± 0.10 | **3.72 ± 0.65** | **2.11 ± 0.08** |
| GABA | - | - | - | 1.00 ± 0.08 | 1.03 ± 0.10 | 1.05 ± 0.09 |
| Dehydroascorbate | 1.00 ± 0.03 | 0.96 ± 0.03 | 0.98 ± 0.11 | 1.00 ± 0.09 | **1.55 ± 0.19** | **1.50 ± 0.10** |
| Fumarate | 1.00 ± 0.03 | **0.75 ± 0.05** | **0.86 ± 0.03** | 1.00 ± 0.34 | 0.89 ± 0.12 | 0.87 ± 0.14 |
| Malate | 1.00 ± 0.03 | **0.66 ± 0.02** | **0.67 ± 0.03** | 1.00 ± 0.16 | 0.92 ± 0.08 | 1.03 ± 0.04 |
| Oxalacetate | 1.00 ± 0.11 | 0.85 ± 0.25 | 0.87 ± 0.08 | - | - | - |
| Succinate | 1.00 ± 0.12 | **0.57 ± 0.04** | **0.57 ± 0.03** | 1.00 ± 0.09 | 0.82 ± 0.05 | 1.18 ± 0.07 |
| Pyruvate | 1.00 ± 0.10 | 0.93 ± 0.09 | 1.17 ± 0.05 | - | - | - |
| Glutarate | 1.00 ± 0.12 | 0.94 ± 0.07 | 1.23 ± 0.14 | - | - | - |
| Glycolate | 1.00 ± 0.05 | **0.84 ± 0.03** | 0.94 ± 0.03 | - | - | - |
| **Sugars and sugars alcohols** | | | | | | |
| Erythrose | 1.00 ± 0.20 | 0.72 ± 0.11 | 0.79 ± 0.10 | - | - | - |
| Galactinol | 1.00 ± 0.08 | **1.29 ± 0.08** | **1.54 ± 0.06** | - | - | - |
| Fructose | - | - | - | 1.00 ± 0.05 | **1.62 ± 0.14** | **1.49 ± 0.02** |
| Glucose | 1.00 ± 0.07 | 0.91 ± 0.09 | 1.10 ± 0.07 | 1.00 ± 0.05 | **1.51 ± 0.12** | **1.40 ± 0.04** |
| Glycerol | 1.00 ± 0.04 | 1.11 ± 0.04 | **1.25 ± 0.04** | 1.00 ± 0.05 | 1.04 ± 0.06 | 1.06 ± 0.08 |
| Myo-inositol | 1.00 ± 0.02 | **1.11 ± 0.03** | **1.24 ± 0.06** | 1.00 ± 0.04 | **1.48 ± 0.13** | 1.18 ± 0.14 |
| Maltose | 1.00 ± 0.01 | **0.78 ± 0.05** | **0.85 ± 0.02** | 1.00 ± 0.10 | 0.93 ± 0.09 | 1.24 ± 0.13 |
| Sucrose | 1.00 ± 0.05 | 0.87 ± 0.05 | 0.92 ± 0.09 | 1.00 ± 0.03 | 0.99 ± 0.02 | 1.07 ± 0.05 |
| Trehalose | 1.00 ± 0.13 | 0.98 ± 0.06 | 0.95 ± 0.34 | 1.00 ± 0.07 | **1.97 ± 0.32** | **1.38 ± 0.09** |
| Xylose | 1.00 ± 0.07 | 1.13 ± 0.06 | 1.06 ± 0.11 | - | - | - |
| Raffinose | - | - | - | 1.00 ± 0.17 | **2.53 ± 0.29** | **1.77 ± 0.03** |
| Ribose | - | - | - | 1.00 ± 0.03 | 1.05 ± 0.01 | 1.19 ± 0.09 |
| **Other metabolites** | | | | | | |
| Nicotinic acid | 1.00 ± 0.08 | 1.08 ± 0.04 | **1.29 ± 0.06** | - | - | - |
| Shikimic acid | 1.00 ± 0.03 | **0.73 ± 0.03** | 0.97 ± 0.04 | - | - | - |
| Spermidine | 1.00 ± 0.16 | 0.75 ± 0.11 | 1.15 ± 0.10 | - | - | - |
| Putrescine | 1.00 ± 0.09 | 1.07 ± 0.11 | 1.16 ± 0.03 | - | - | - |

**Supplemental Table S6.** Organic acids subcellular distribution. Data are presented as means ± SE ($n$ = 3). Values set in bold in *tdt* plants were determined by the Student's $t$ test to be significantly different ($P < 0.05$) from WT.

| Organic acids | nmol mg $FW^{-1}$ | | | Chloroplast (%) | | | Cytosol (%) | | | Vacuole (%) | | |
|---|---|---|---|---|---|---|---|---|---|---|---|---|
| | **WT** | ***tdt-1*** | ***tdt-2*** | **WT** | ***tdt-1*** | ***tdt-2*** | **WT** | ***tdt-1*** | ***tdt-2*** | **WT** | ***tdt-1*** | ***tdt-2*** |
| Glycerate | 49.4 ± 9.8 | 45.6 ± 10.0 | 58.5 ± 3.6 | 21.0 ± 8.7 | 40.0 ± 2.8 | 23.3 ± 3.1 | 45.3 ± 17.5 | 12.0 ± 9.8 | 65.3 ± 5.7 | 33.7 ± 2.9 | 48.0 ± 7.5 | 11.3 ± 2.8 |
| Pyruvate | 521.9 ± 89.7 | 379.5 ± 56.5 | 383.2 ± 7.3 | 9.7 ± 4.3 | 16.7 ± 2.4 | 14.7 ± 4.1 | 62.0 ± 7.8 | 15.3 ± 12.5 | 70.7 ± 6.4 | 28.3 ± 4.7 | 68.0 ± 12.5 | 14.7 ± 2.3 |
| Citrate | 4972.9 ± 217.5 | **8891.7 ± 378.5** | **11411.9 ± 387.7** | 0.0 ± 0.0 | 0.0 ± 0.0 | 1.0 ± 0.8 | 0.0 ± 0.0 | 1.7 ± 1.4 | 18.3 ± 12.2 | 100.0 ± 0.0 | 98.3 ± 1.4 | 80.7 ± 11.9 |
| Isocitrate | 1085.7 ± 588.6 | 708.3 ± 233.6 | 1827.8 ± 356.2 | 0.0 ± 0.0 | 0.0 ± 0.0 | 0.0 ± 0.0 | 0.0 ± 0.0 | 0.0 ± 0.0 | 0.0 ± 0.0 | 100.0 ± 0.0 | 100.0 ± 0.0 | 100.0 ± 0.0 |
| Aconitate | 985.9 ± 158.3 | 1155.3 ± 253.1 | 1631.5 ± 153.3 | 29.3 ± 0.7 | 18.0 ± 4.5 | 6.3 ± 5.2 | 7.0 ± 4.1 | 8.3 ± 6.8 | **56.3 ± 6.7** | 63.7 ± 4.8 | 73.7 ± 8.5 | **37.3 ± 1.5** |
| Succinate | 266.1 ± 44.4 | 230.1 ± 52.5 | 305.0 ± 17.6 | 14.7 ± 6.6 | 28.7 ± 4.4 | 30.7 ± 1.9 | 74.0 ± 8.2 | 33.7 ± 18.3 | 65.3 ± 3.5 | 11.3 ± 3.9 | 37.7 ± 14.3 | 4.0 ± 1.7 |
| Fumarate | 6042.1 ± 517.8 | 6333.2 ± 388.4 | 7677.0 ± 496.8 | 0.0 ± 0.0 | 0.3 ± 0.3 | 0.0 ± 0.0 | 0.0 ± 0.0 | 0.0 ± 0.0 | 2.3 ± 1.9 | 100.0 ± 0.0 | 99.7 ± 0.3 | 97.7 ± 1.9 |
| Malate | 3536.6 ± 103.9 | **1771.8 ± 46.4** | **1951.2 ± 119.3** | 2.7 ± 1.4 | 4.6 ± 3.8 | 4.6 ± 3.8 | 2.7 ± 2.2 | **38.4 ± 3.0** | **42.7 ± 1.7** | 94.7 ± 3.5 | **57.0 ± 7.1** | **52.7 ± 8.2** |

# Chapter 5

## Guard cell sucrose degradation promotes glycolysis and the TCA cycle during stomatal opening[1]

[1]*Submitted to Plant Physiology*

**Title:** Guard cell sucrose degradation promotes glycolysis and the TCA cycle during stomatal opening

**Authors:** David B. Medeiros[1,2], Leonardo Perez de Souza[1], Wagner L. Araújo[2], Danilo M. Daloso[3*], Alisdair R. Fernie[1]

[1]*Max-Planck-Institut für Molekulare Pflanzenphysiologie, Am Mühlenberg 1, 14476 Potsdam-Golm, Germany.*
[2]*Max-Planck Partner Group at the Departamento de Biologia Vegetal, Universidade Federal de Viçosa, 36570-900, Viçosa, Minas Gerais, Brazil.*
[3]*Departamento de Bioquímica e Biologia Molecular, Universidade Federal do Ceará, 60440-970, Fortaleza, Ceará, Brazil.*
*Corresponding author: daloso@ufc.br

**One sentence summary:** [U-$^{13}$C]-sucrose isotope labelling reveals that sucrose is a respiratory substrate, rather than an osmolyte, in Arabidopsis guard cells during the dark-to-light transition.

**Footnotes:**

**Author contribution:** D.B.M., D.M.D., and A.R.F. designed the research; D.B.M. performed the research; D.B.M.; D.M.D, and L.P.S. analysed the data; and D.B.M., D.M.D, A.R.F, and W.L.A. wrote the article.

**Funding information:** This work was supported by funding from the Max-Planck Society, the National Council for Scientific and Technological Development (CNPq-Brazil), and the Foundation for Research Assistance of the Minas Gerais State (FAPEMIG-Brazil). Scholarships granted by CNPq to L.P.S. and by FAPEMIG to D.B.M. (CRA-BDS-00020-16) are gratefully acknowledged.

**Abstract**

During the last decades sucrose has been thought to play an osmolytic role in stomatal opening. However, experimental evidence in support of this theory has remained fragmentary. Here, we used a combination of stomatal aperture assays coupled with kinetic [U-$^{13}$C]-sucrose isotope labelling experiments to define whether sucrose plays an osmolytic role during light-induced stomatal opening. Based on our own previous findings, we hypothesized that sucrose is used as a substrate rather than accumulates within guard cells. We show here that addition of sucrose in the medium did not enhance light-induced stomatal opening. By contrast, sucrose induces stomatal closure in a dose-dependent manner. [U-$^{13}$C]-sucrose isotope labelling experiments indicate that during light-induced stomatal opening sucrose is degraded, in contrast to what would be expected if the role of sucrose under this condition was osmolytic. Moreover, we also demonstrate that sucrose breakdown could be a mechanism to sustain glycolysis and the synthesis of tricarboxylic acid cycle-related metabolites in the light. Taken together, our results provide compelling evidence supporting the contention that, by contrast to what was previously thought, the role of sucrose during light-induced stomatal opening is not an osmolytic one. The results presented here, therefore, collectively allow us to redraw current models concerning the influence of sucrose during light-induced stomatal opening.

**Introduction**

Stomata, micro structures found in the leaf epidermal, are composed of two guard cells and a pore between them. The aperture of the stomatal pore simultaneously enables the influx of $CO_2$ to the leaf and the efflux of water to the environment (Hetherington and Woodward, 2003). The ratio between the $CO_2$ assimilated by photosynthesis ($A$) and the magnitude of the stomatal movement, measured as stomatal conductance ($g_s$), is known as intrinsic water use efficiency (WUEi) ($A/g_s$) and an important target for plant breeding (Condon et al., 2004; Gago et al., 2014; Lawson and Blatt, 2014; Flexas, 2016; Nunes-Nesi et al., 2016). The regulation of stomatal movement, i.e. the opening and closing of the stomatal pore, is therefore of paramount importance for the regulation of photosynthesis and water use efficiency (WUE). However, given the complexity of interacting regulatory endogenous and environmental factors, our knowledge of stomatal movements remains incomplete. Hence, there is a growing demand for studies which aim to understand guard cell function and how the surrounding cells and the external environment combine to influence stomatal movement.

More than a century of research indicates that stomatal movements are regulated by the osmotic potential of the surrounding guard cells (Lloyd, 1908; Imamura, 1943; Fischer,

1968). Turgid (low osmotic potential) and flaccid guard cells (high osmotic potential) induce stomatal opening and closure, respectively (Gao et al., 2005). Thus, the regulation of the osmotic potential through guard cell osmolyte accumulation and efflux is of fundamental significance in the control of stomatal movements. The accumulation of potassium ($K^+$) and its counter-ions chloride ($Cl^-$), nitrate ($NO_3^-$) and malate ($malate^{2-}$) is the best described model for the osmotic potential regulation of guard cells (Inoue and Kinoshita, 2017; Jezek and Blatt, 2017). An influx of $K^+$ to guard cells has been demonstrated to occur following blue light perception and stimulation of $H^+$ extrusion via $H^+$-ATPases (Hedrich, 2012). Although the signalling network downstream of the blue-light perception has been extensively studied in guard cells, the associated metabolic changes have only recently been revealed. Blue-light stimulates the breakdown of starch and lipid droplets in guard cells (Horrer et al., 2016; McLachlan *et al*., 2016). Despite still speculative, the authors suggest that as a mechanism to fuel mitochondrial metabolism in order to produce energy (ATP) via oxidative phosphorylation and/or for the accumulation of malate and other tricarboxylic acid (TCA) cycle-related metabolites. Similarly, sucrose breakdown has also been suggested as a mechanism to fuel the TCA cycle under dark-to-light transition (Daloso et al., 2015; Daloso et al., 2016b). However, although these mechanisms have been postulated to be required during stomatal opening, the fate of the C released from sucrose, starch and lipid breakdown still remains unclear. Understanding of which pathways are activated following the degradation of these storage molecules is therefore of fundamental importance in understanding how guard cell metabolism contributes to the regulation of the stomatal opening process.

On the basis of the osmolytic characteristics of sucrose coupled with the observed positive correlation between stomatal aperture and sucrose accumulation in guard cells (Talbott and Zeiger, 1993; Lu et al., 1995; Amodeo et al., 1996; Talbott and Zeiger, 1996), it has long been proposed to act as an osmolyte involved in stomatal opening. According to this model, sucrose is the main osmolyte during the afternoon period of the day, accumulating in replacement of the morning-accumulated $K^+$ (Talbott and Zeiger, 1998). These facts aside, the capacity of sucrose to induce stomatal opening has surprisingly not yet been directly reported. Moreover, recent evidences support the idea that sucrose can be degraded within guard cells during the dark-to-light transition in order to provide carbon skeleton for organic acid production (Daloso et al., 2015; Daloso et al., 2016b) and that high exogenous concentration of sucrose (100 mM) can induce stomatal closure in a mechanism mediated by both abscisic acid (ABA) and hexokinase (Kelly et al., 2013). On the basis of the latter findings, it has been proposed that hexokinase, a sugar-phosphorylating enzyme involved in sugar-sensing, is able to mediate stomatal closure by coordinating photosynthesis and transpiration in both

Arabidopsis and tomato (Kelly et al., 2013). Furthermore, overexpression of the Arabidopsis HXK1 (*At*HXK1) in citrus under the control of a guard cell-specific promoter, KST1, resulted in a reduced stomatal conductance and transpiration without impairing the rate of photosynthesis (Lugassi et al., 2015). Taken together, these results suggest that guard cell sucrose metabolism has a key role in the regulation of WUE and that sucrose likely plays a dual role on the regulation of the stomatal movements. Namely, its accumulation can induce stomatal closure whilst its degradation within guard cells may represent an important mechanism during stomatal opening (Daloso et al., 2016a). That said, a full understanding of the latter process is lacking and it is clear that guard cell sucrose metabolism needs to be better studied. Indeed, it is conceivable that such studies might pave the way for plant WUE improvement through genetic manipulation of guard cell metabolism.

Here, we took advantage of a protocol which enables the rapid isolation of dark-adapted guard cell enriched epidermal fragments in sufficient quantities to allow us to perform both stomatal aperture assays and metabolomic analyses (Daloso et al., 2015). To clarify the effect of exogenous sucrose addition on the stomatal aperture we further investigated the metabolic flux distribution by following the metabolic fate of $^{13}$C-sucrose during light-induced stomatal opening conditions. Based on the fact that sucrose seems to have an important role during both stomatal opening and closure (Kelly et al., 2013; Daloso et al., 2015; Li et al., 2015; Lugassi et al., 2015; Daloso et al., 2016b), we demonstrate that the role of sucrose during stomatal opening is dose-dependent whilst sucrose is degraded within guard cells during light-induced stomatal opening. Our results not only demonstrated that sucrose induces stomatal closure in a dose-dependent manner, but also indicates that sucrose breakdown occurs during light-induced stomatal opening. Furthermore, we also provide evidence that sucrose degradation induces glutamine biosynthesis during light-induced stomatal opening. These collected findings are discussed within the context of current models of the metabolic influence on stomatal movement.

## Results

### Sucrose-induced stomatal closure

Sucrose has long been proposed to act as an osmolyte during light-induced stomatal opening (Talbott and Zeiger, 1998). However, it has additionally recently been suggested that sucrose can induce stomatal closure at high concentration (100 mM; (Kelly et al., 2013). It seems likely that the effect of sucrose on stomatal aperture is dose-dependent. In order to test this hypothesis, we first checked the capacity of sucrose to induce stomatal closure in a concentration dependent manner. Detached leaves from dark-adapted Arabidopsis plants were

floated on opening buffer solution in the light for 2 h. This time was sufficient to induce stomatal opening. Following this, sucrose was added to the solution at diverse final concentrations and the stomatal aperture was determined after a further 2 h of incubation. In close agreement with our initial hypothesis, the effect of sucrose on stomatal aperture is dose-dependent. Whilst the addition of 0.1 mM and 1 mM of sucrose has no effect on stomatal aperture, the two highest concentrations tested (10 mM and 100 mM) significantly reduced stomatal aperture (Fig. 1). By contrast, no difference in stomatal aperture between the opening buffer and osmotic control (100 mM mannitol) solutions was observed suggesting that the effect of sucrose on stomatal aperture was not merely osmotic.

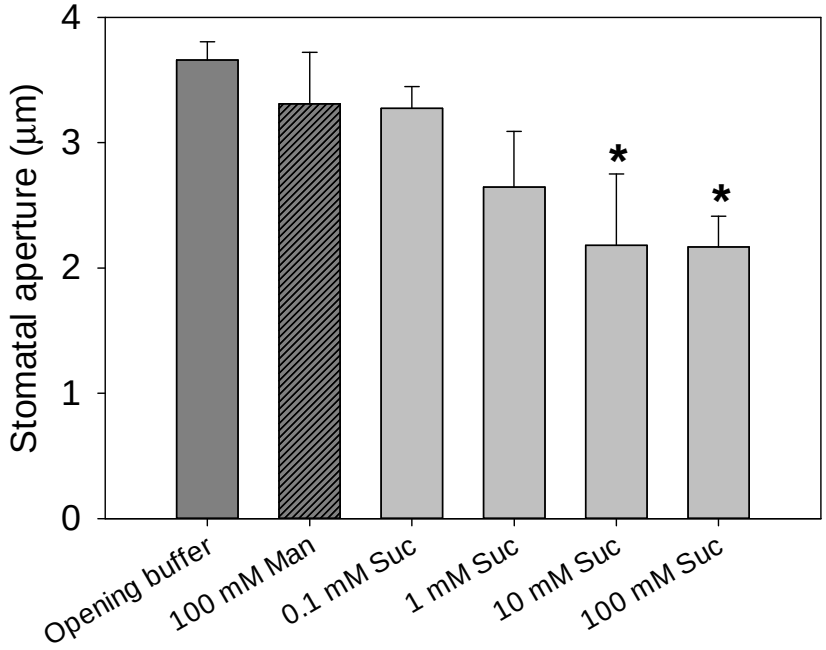


**Figure 1.** Sucrose-induced stomatal closure in 5-week-old Col-0 plants. Detached leaves (5$^{th}$ or 6$^{th}$ totally expanded) from dark-adapted Arabidopsis plants were floated on the opening buffer under light condition for 2 h. After, sucrose was added to the solution at different final concentration (0.1 mM, 1 mM, 10 mM, and 100mM) and the stomatal aperture determined after additional 2 h of incubation. The opening buffer was used as a control without sucrose and 100 mM mannitol as an osmotic control. Four leaves were used per treatment and around 20 stomata were visualized, totalizing at least 80 stomata per treatment. Asterisk indicates values statistically different comparing to the Opening buffer treatment by Student´s *t* test ($P < 0.05$). Values are presented as mean ± SE ($n = 4$).

**Can sucrose induce stomatal opening?**

We have observed that sucrose can induce stomatal closure in opened stomata. However, this result does not address the question whether sucrose can induce stomatal opening. In order to do so, we directly assessed the dark-to-light transition, simulating the circadian rhythm of stomatal movements. For this purpose, Arabidopsis leaves were harvested in the pre-dawn and incubated in different solutions in the dark or light for a period of 2 h,

whereafter the stomatal aperture was determined. The stomatal aperture was higher in all light treatments compared to the dark samples (Fig. 2). The largest stomatal aperture was observed in leaves on the opening buffer solution containing KCl (Fig. 2). We also observed an increase in stomatal aperture in leaves floated on opening buffer without KCl solution, compared to the dark treatment, albeit to a lesser extent than in the solution containing KCl (Fig. 2). Interestingly, comparing sucrose treatments with their control in the light, we observed no increase in stomatal aperture following the addition of sucrose (Fig. 2). By contrast, the addition of 100 mM sucrose minimized light-induced stomatal opening, reinforcing the idea that sucrose can induce stomatal closure at high concentration.

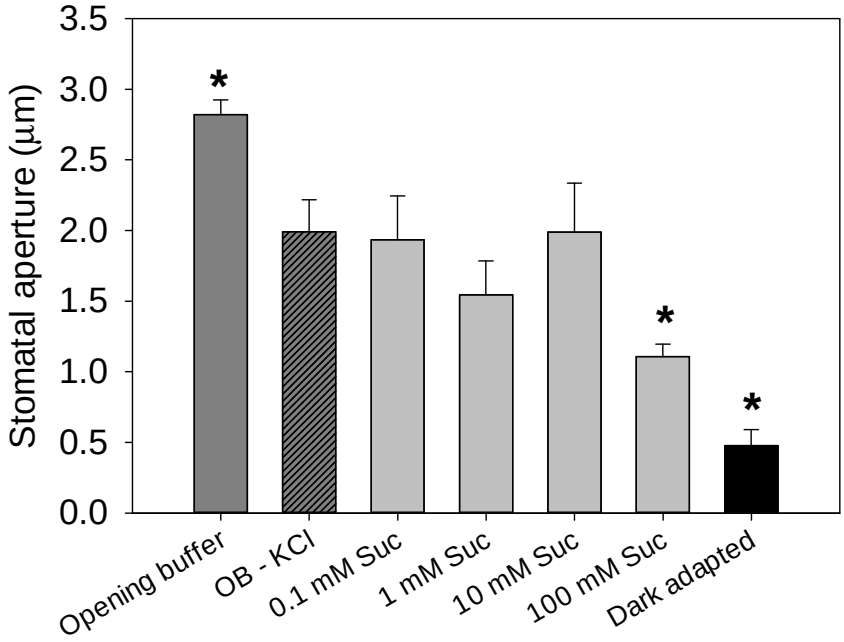


**Figure 2.** Sucrose-induced stomatal opening in 5-week-old Col-0 plants. Detached leaves (5$^{th}$ totally expanded) from dark-adapted Arabidopsis plants were floated under light condition for 2 h on the opening buffer (OB), OB without KCl (OB -KCl), and OB -KCl with different sucrose concentrations (0.1 mM, 1 mM, 10 mM, and 100 mM Suc). After 2 h of incubation the stomatal aperture was determined. All treatments were compared to the OB -KCl one since the solutions containing Suc were prepared using this buffer. Four leaves were used per treatment and around 20 stomata were visualized, totalizing at least 80 stomata per treatment. Asterisk indicates values statistically different comparing to OB -KCl treatment by Student´s *t* test ($P < 0.05$). Values are presented as mean ± SE ($n = 4$).

**Can the presence of sucrose improve light- and potassium-induced stomatal opening?**

Potassium is a well-known osmolyte that accumulates in guard cells during light-induced stomatal opening (Chen et al., 2012). It is also known that $K^+$ influx to guard cells depends on a proton gradient created at the plasma membrane by $H^+$-ATPases (Inoue et al., 2010). Thus, both light- and $K^+$-induced stomatal opening are characterized as ATP-dependent processes. Given this knowledge, we next tested whether sucrose, as a substrate for

glycolysis and mitochondrial metabolism, could increase the rate of stomatal opening following induction by light and $K^+$. detached leaves were incubated for 2h under light in three different opening buffer solutions containing 0, 0.1, and 100 mM of sucrose; whereafter the stomatal aperture was measured. The stomatal aperture was higher in all opening buffer solutions compared to the dark treatment (Fig. 3). However, it was significantly lower in the solution containing 100 mM of sucrose compared to opening buffer solution, whereas no differences were observed between opening buffer and the solution containing 0.1 mM of sucrose (Fig. 3). This strengthens the idea that the role of sucrose on stomatal movements is dose-dependent and further indicates that the addition of sucrose is not able to improve the light and $K^+$-induced stomatal opening.

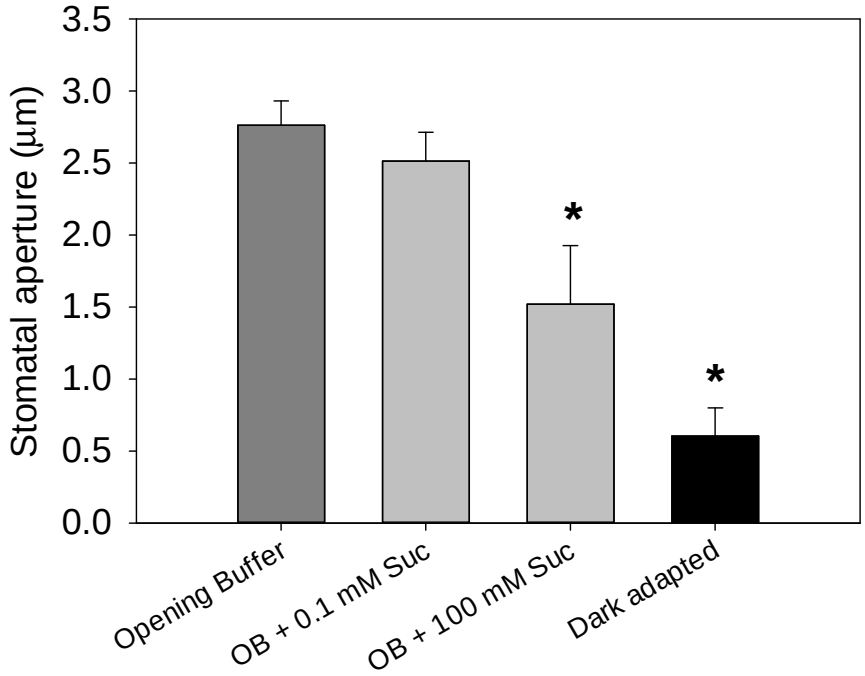


**Figure 3.** Sucrose-induced stomatal opening in 5-week-old Col-0 plants. Detached leaves (5$^{th}$ totally expanded) from dark-adapted Arabidopsis plants were floated under light condition for 2 h on the opening buffer (OB), OB with two sucrose concentrations (0.1 mM and 100 mM Suc). After 2 h of incubation the stomatal aperture was determined. Four leaves were used per treatment and around 20 stomata were visualized, totalizing at least 80 stomata per treatment. Asterisk indicates values statistically different comparing to OB treatment by Student´s *t* test ($P < 0.05$). Values are presented as mean ± SE ($n = 4$).

**What is the metabolic fate of sucrose during light-induced stomatal opening?**

We recently suggested that the role of sucrose in the regulation of guard cell movements is primarily energetic, rather than an osmolyte (Daloso et al., 2015; Daloso et al., 2016b; Antunes et al., 2017). However, it is important to highlight that our previous experiments were carried out using $^{13}C$-$NaHCO_3$. Despite these isotope experiments provided significant insight concerning the fate of the C fixed by guard cells during dark-to-light

transitions, they could not, in their own right, demonstrate which pathway is activated after sucrose breakdown. Thus, in order to better understand this process, we here directly evaluated the metabolic fate of [U-$^{13}$C]-sucrose under light-induced stomatal opening. We harvested guard cells-enriched epidermal fragments in the pre-dawn and incubated them in an opening buffer solution in the presence or absence of 0.1 mM $^{13}$C-sucrose in the light for 10, 30 or 60 min. We choose the concentration 0.1 mM of sucrose given that this concentration neither affects light- or $K^+$-induced stomatal opening nor it is able to induce stomatal closure (Fig. 3). At each point of the experiment samples were also harvested in order to measure the stomatal aperture and to ascertain whether the guard cells remained functional during the incubation time (a fact that was further supported by the continual increases in stomatal aperture over the incubation time; Supplemental Fig. S1).

On analysing the fate of the $^{13}$C-sucrose we observed a high total $^{13}$C-enrichment in fructose and glucose. Fructose was almost 100% labelled after 10 min whereas glucose labelling reached 80% after 10 min maintaining this proportion until 60 min (Fig. 4). Glucose labelling reflects the stability of the *m+1* and *m+2* isotopomers over time, while fructose presented increasing $^{13}$C-enrichement of the *m+3* ion over time (Supplemental Fig. S2). These labelling patterns suggest that the *m/z* 217 fragment of fructose was fully labelled while the *m/z* 160 fragment of glucose was not. It is important to mention, however, that we cannot rule out that other minor glucose isotopomers were labelled albeit below the level of detection. Glucose-1-phosphate (Glc-1P) displayed a peak of labelling at 10 min (24%) following which the total $^{13}$C-enrichment decreased (down to 15% at 60 min; Fig. 4). This decrease is explained by the isotopomers relative abundance analysis, which revealed that the full labelled *m+3* ion had a peak of labelling at 10 min, being reduced until 60 min (Supplemental Fig. S2).

Photorespiratory metabolites such as glycolate, serine, and glycine were also considerably labelled. Glycolate was clearly labelled over time, whilst serine presented a higher total $^{13}$C-enrichment only at 60 min compared to control samples. The total $^{13}$C-enrichement in glycine did not change over time within the treatments, being statistically higher in $^{13}$C-sucrose samples at 10 and 60 min compared to the control (Fig. 5). Relative isotopomers abundance analysis confirmed these results, since clear decreases and increases in *m+0* and *m+1* ions, respectively, were observed in glycolate, serine and glycine. No increase was observed in *m+2* ion of serine (Supplemental Fig. S3), suggesting that only a single $^{13}$C was incorporated into photorespiratory metabolites.

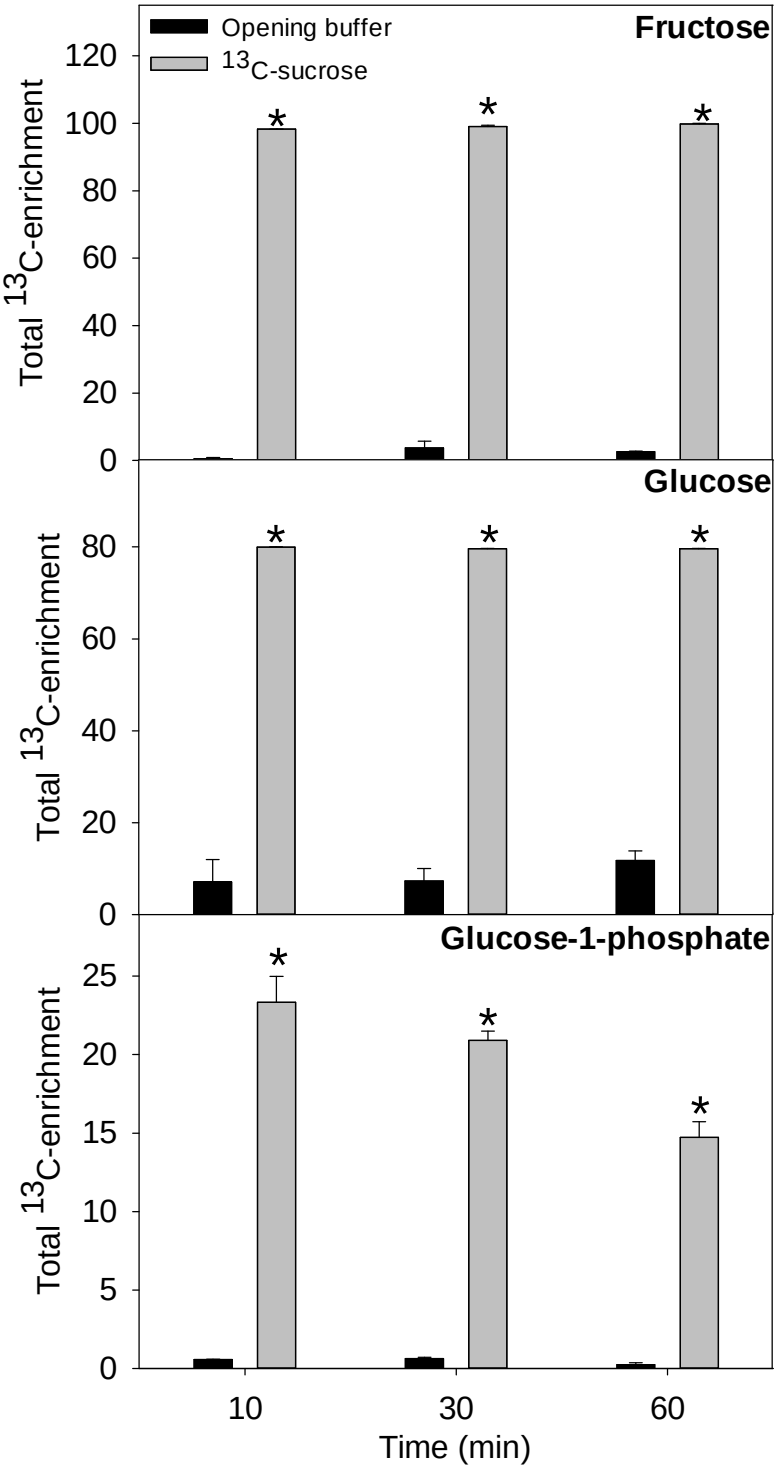


**Figure 4.** Total $^{13}C$ label enrichment into glucose, fructose and glucose-1-phosphate (G1P) following guard cell incubation. Dark-adapted guard cells were harvested in the pre-drawn and fed with [U$^{13}C$]-Sucrose in the opening buffer under light condition for 2h. The opening buffer without sucrose was used as control. At 10 min, 30 min, and 60 min of incubation the guard cells were sampled and the enrichment into the metabolites were determined. Values are presented as mean ± SE ($n$ = 4). An asterisk indicates that the values in the $^{13}C$-sucrose treatment were determined by the Student's t test to be significantly different ($P < 0.05$) from Opening buffer treatment.

Enhanced $^{13}$C-enrichment in glutamate and glutamine was also observed over time, reaching maxima of 25% in glutamate and 60% in glutamine after 60 min of incubation (Fig. 6A). Relative isotopomers abundance analysis suggests that glutamate was substantially labelled only at *m+1* and *m+2*. Decreases in the non-labelled glutamate *m+0* ion was simultaneous to the increases in glutamate *m+2*, which reached 22% following 60 min of incubation (Fig. 6B). By contrast, glutamine displayed $^{13}$C-incorporation in the *m+3* and *m+4* ions. The relative intensity of the non-labelled *m+0* ion being considerably lower for glutamine than glutamate. Moreover, the relative intensity of the fully-labelled glutamine *m+4* ion increased linearly over time while that of the *m+3* ion decreased from 10 to 60 min (Fig. 6B). This suggests that the $^{13}$C is continuously going to glutamine, which is confirmed by the relative content of this metabolite under $^{13}$C-sucrose supply (Supplemental Fig. S4), through glycolysis and part of the TCA cycle (Supplemental Fig. S5). These data provide further evidence that sucrose is used as a respiratory substrate for glycolysis and the TCA cycle, which in turn provides 2-oxoglutarate (2-OG) for glutamine biosynthesis (Fig. 7).

## Discussion

### Modifying the paradigmatic role of sucrose in guard cell regulation

In the vast majority of species sucrose is the main photoassimilate transported throughout the plant and performs a wide range of functions in different organs and tissues (Fettke and Fernie, 2015). Among these functions, it is noteworthy that sucrose is not only a storage compound, but can also act as a signaling molecule and represents a substrate for a wide range of metabolic pathways. Beyond these functions, sucrose is additionally a well-characterized osmolyte which can greatly contribute to the regulation of the cellular osmotic potential. On the basis of the latter property, but also due to an observed positive correlation between sucrose accumulation and stomatal aperture, the main function of sucrose in guard cell regulation was for decades assumed to be osmolytic (Zeiger, 1983; Tallman and Zeiger, 1988; Poffenroth et al., 1992; Talbott and Zeiger, 1993; Lu et al., 1995; Amodeo et al., 1996; Talbott and Zeiger, 1996; Lu et al., 1997; Talbott and Zeiger, 1998; Outlaw and De Vlieghere-He, 2001; Zeiger et al., 2002). However, experimental evidence supporting this role remains indirect and circumstantial. By using a combination of stomatal aperture assays and a kinetic analysis of $^{13}$C-sucrose feeding experiment, we here provide compelling evidence for the contention that the role of sucrose in guard cell regulation exceeds mere osmoregulation. Indeed, the data we present here suggest that, at least for stomatal opening, its role as an osmolyte is at best unimportant and could even be antagonistic to its role as substrate. Therefore, especially when considered together with other recent reports (Kelly et

al., 2013; Li et al., 2015; Lugassi et al., 2015; Gago et al., 2016), it seems reasonable to assume that a paradigm shift is required concerning how we view the role of sucrose in guard cell regulation.

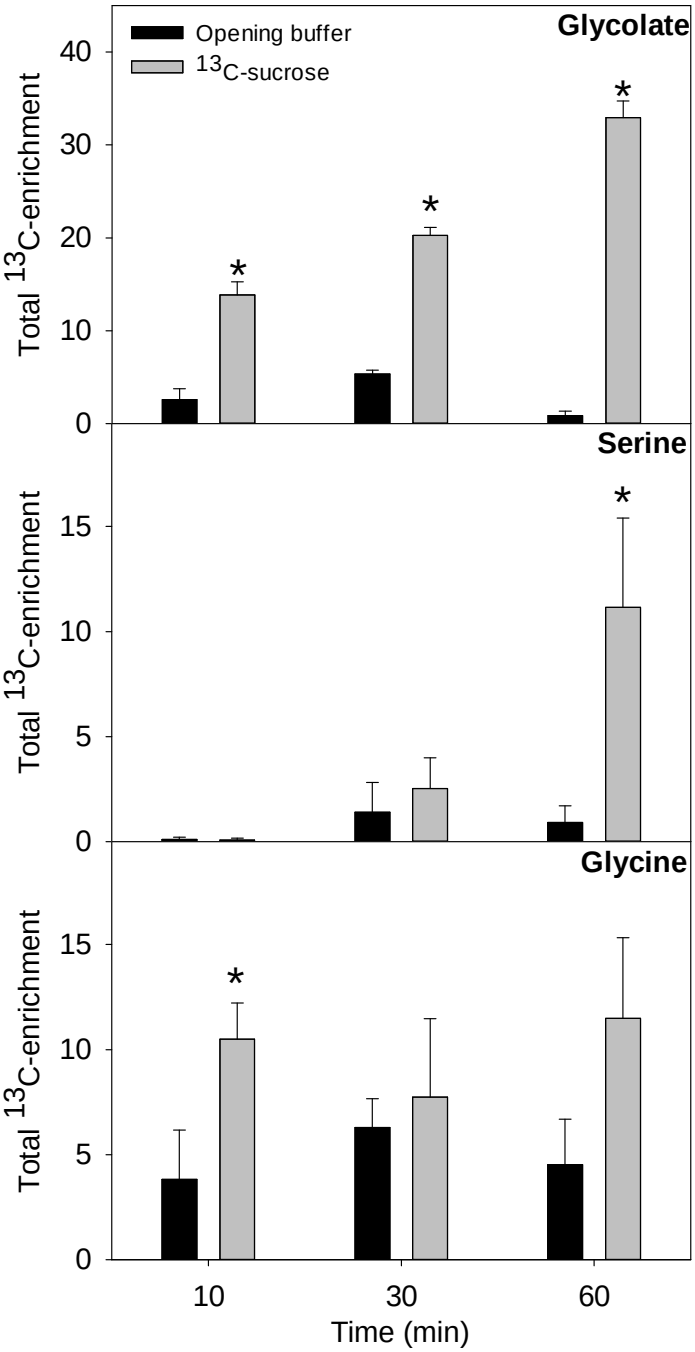


**Figure 5.** Total $^{13}C$ label enrichment into photorespiratory related metabolites following guard cell incubation. Dark-adapted guard cells were harvested in the pre-drawn and fed with [U$^{13}$C]-Sucrose in the opening buffer under light condition for 2h. The opening buffer without sucrose was used as control. At 10 min, 30 min, and 60 min of incubation the guard cells were sampled and the enrichment into the metabolites were determined. Values are presented as mean ± SE ($n$ = 4). An asterisk indicates that the values in the $^{13}C$-sucrose treatment were determined by the Student's t test to be significantly different ($P < 0.05$) from Opening buffer treatment.

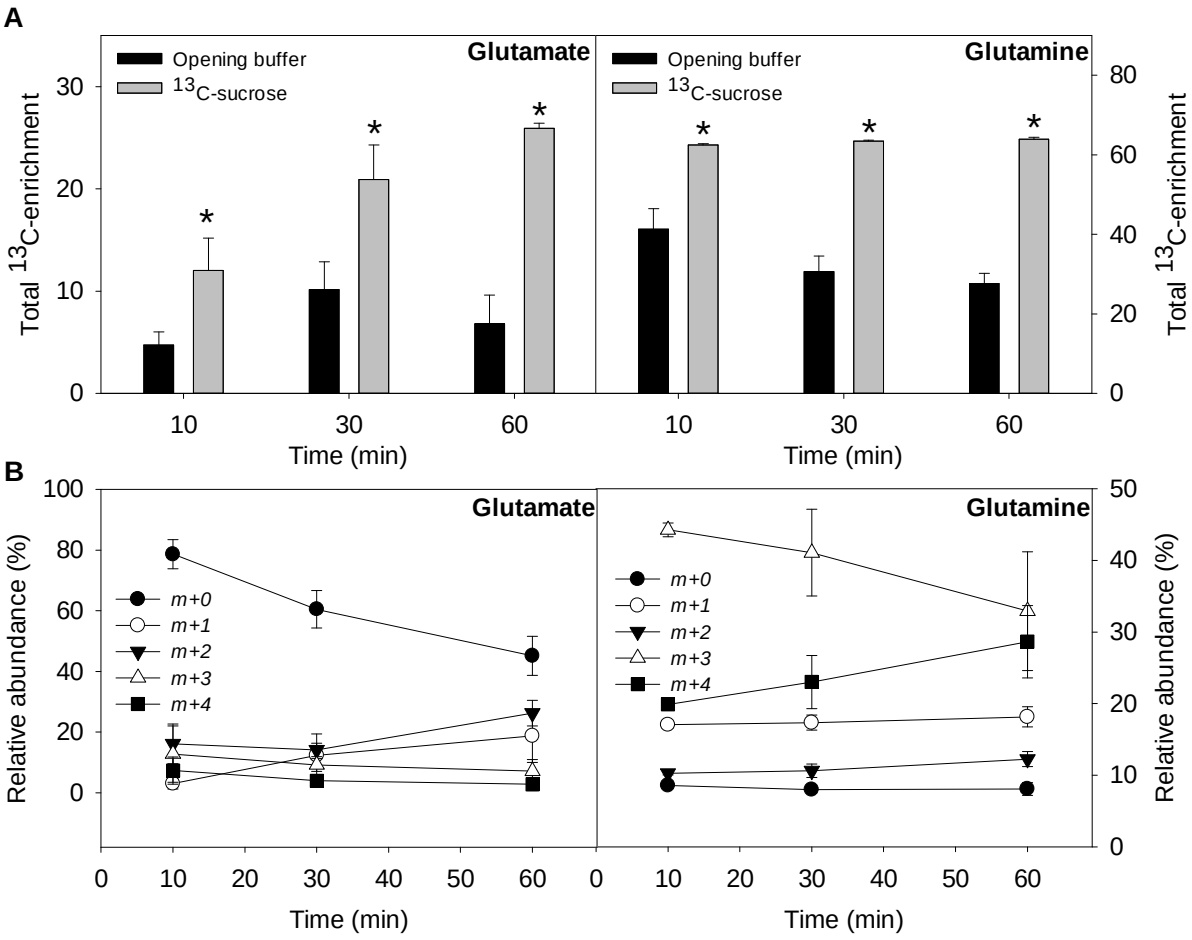


**Figure 6.** $^{13}C$ label enrichment of glutamate and glutamine. A, Total $^{13}C$ label enrichment into glutamate and glutamine. B, Relative abundance of mass isotopomers of following guard cell incubation. Dark-adapted guard cells were harvested in the pre-drawn and fed with [U$^{13}C$]-Sucrose in the opening buffer under light condition for 2h. The opening buffer without sucrose was used as control. At 10 min, 30 min, and 60 min of incubation the guard cells were sampled and the enrichment into the metabolites were determined. Values are presented as mean ± SE ($n$ = 4). An asterisk indicates that the values in the $^{13}C$-sucrose treatment were determined by the Student's t test to be significantly different ($P < 0.05$) from Opening buffer treatment.

**The dual role of sucrose during stomatal opening and closure**

Stomatal aperture assays carried out using different concentrations of sucrose indicate that the presence of sucrose at concentrations higher than 10 mM can induce stomatal closure under light conditions, whilst 100 mM of sucrose minimizes the magnitude of the light-induced stomatal opening. Interestingly, exogenous application of sucrose in concentrations below 10 mM does not change stomatal aperture. It is noteworthy that although concentrations lower than 10 mM of sucrose were not sufficient to induce stomatal closure, the stomata pore still opened during dark-to-light transition under these concentrations. Furthermore, the addition of 0.1 mM sucrose did not optimize light- or $K^+$-induced stomatal opening (Fig. 3). This indicates that in the presence of low concentrations of sucrose (< 10

mM) the stomatal pore opens in response to light but not in response to the availability of sucrose. Similar responses have previously been observed in isolated tobacco guard cells (Daloso et al., 2015). These data suggest that guard cells can both produce the energy and the osmolytes required to open the stomata autonomously or import these compounds from mesophyll cells and store them as starch or lipids, in the guard cell chloroplasts.

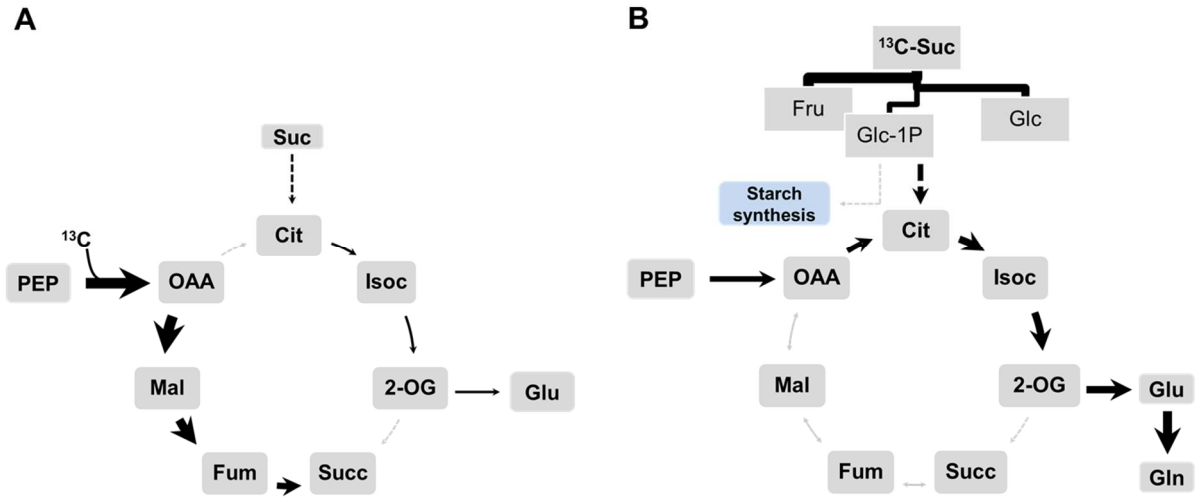


**Figure 7.** Schematic representation comparing $^{13}C$ redistribution observed in isotope feeding experiments using [$^{13}C$]-$NaHCO_3^-$ (A) and [U-$^{13}C$]-sucrose (B) in isolated guard cells under dark-to-light transition. Data from A are based on the results obtained previously (Daloso et al., 2015). Arrow thickness represents possible fluxes, although it is important to stress that metabolic fluxes is currently not feasible to determine in guard cells. Both experiments suggest that glycolysis and the TCA cycle are activated in the light. The experiment using $^{13}C$-$NaHCO_3^-$ indicates that the fluxes around PEPc are higher than those from glycolysis under this condition. This suggests a higher $CO_2$ fixation by PEPc rather than RubisCO. However, it is noteworthy that this may be result of the use of $^{13}C$-$NaHCO_3^-$ as substrate, which favors PEPc activity. By contrast, the experiment using $^{13}C$-sucrose suggests higher fluxes through glycolysis. Interestingly, both experiments showed that the Glu/Gln pathway is activated under light conditions, mainly when $^{13}C$-sucrose was used. Furthermore, the labelling found in Glu/Gln metabolites suggests a differential non-cyclic mode activity of the TCA cycle. Whilst $^{13}C$-$NaHCO_3^-$ favors the carbon flux through OAA, Mal, Fum and Succ, the $^{13}C$ coming from sucrose breakdown is used to sustain glycolysis and Gln biosynthesis via Cit, Isoc and 2-OG. Abbreviations: 2-OG, 2-oxoglutarate; Cit, citrate; Fum, fumarate; Fru, fructose; Glc, glucose; Glc-1-P, glucose1-phosphate; Gln, glutamine; Glu, glutamate; Isoc, isocitrate; Mal, malate; OAA, oxaloacetate; PEP, phospho*enol*pyruvate; Suc, sucrose; Succ, succinate.

A higher stomatal aperture was observed following incubation in lower concentrations of sucrose (Fig. 2), whilst addition of sucrose had no effect on light- and $K^+$-induced stomatal opening (Fig. 3). Taken together, these results provide strong evidence that the function of sucrose in the guard cell regulation is not solely osmolytic. However, it is noteworthy that transgenic plants exhibiting a guard cell specific decrease in the expression of the sucrose

transporter, *SUT1*, displayed substantial changes in the diurnal levels of *A*, $g_s$ and the accumulation of carbohydrate and $K^+$ within guard cells (Antunes et al., 2017). At the whole plant level, these transgenic plants displayed strong differences in whole plant transpiration, biomass accumulation and improved drought tolerance. Interestingly, when *SUT1* was knocked down specifically in guard cells the plants displayed lower $g_s$ than WT plants in the early morning (Antunes et al., 2017), period of the day in which the stomatal aperture seems to be mainly sustained by the accumulation of $K^+$ (Talbott and Zeiger, 1998). Therefore, although our results most likely exclude the possibility that sucrose is only an osmolyte under light-induced stomatal opening, it is important to stress that, as in other cell types, sucrose may display a wide range of functions in guard cells, beyond those related to osmotic potential regulation of the cell. Thus, it seems reasonable to assume that sucrose concentrations below 10 mM are seemingly not able to direct modify stomatal aperture. It is also important to stress that this fact does not mean that presence of sucrose is unimportant under these conditions. It likely seems that the role of sucrose in the regulation of stomatal movements is dose-dependent, in close agreement with our original hypothesis and with the idea that the differential accumulation of sucrose between the apoplastic space and within guard cells may act as key point that tightly connects photosynthesis to stomatal movements (Daloso et al., 2016a; Gago et al., 2016).

It has been previously proposed that the accumulation of sucrose in the apoplastic space may be a mechanism to induce stomatal closure in periods of high photosynthetic rate in phloem-loading species (Lu et al., 1995; Lu et al., 1997; Kang et al., 2007a; Kang et al., 2007b). Recent evidences also suggest that sucrose is sensed within guard cells and that the stomatal closure is mediated by ABA in a hexokinase-dependent manner (Kelly et al., 2013). It is important to highlight that both mechanisms could occur simultaneously. Initial characterization of sucrose flux through guard cell plasma membrane indicates that it may saturate at concentrations around 25 mM (Outlaw, 1995). Assuming that the import of sucrose to guard cells saturates at this concentration, it seems unlikely that 100 mM of sucrose (the concentration used by Kelly and co-workers) will be the concentration reached inside of guard cells, strengthening the idea that the sucrose-induced stomatal closure could be mediated by an osmotic effect in the apoplastic space (Lu et al., 1995; Lu et al., 1997; Kang et al., 2007a; Kang et al., 2007b) as well as by activating an ABA signalling network within guard cells (Kelly et al., 2013). Irrespective of the mechanism by which sucrose induces stomatal closure, it seems clear that sucrose has a pivotal role in the *A*-$g_s$ trade off regulation (Gago et al., 2016). The fact that only high concentrations of sucrose induce stomatal closure indicates that *in planta* this mechanism would occur only at high *A*. More importantly, it must have a strong

impact on WUE, since activating a mechanism to close the stomatal pore in periods of high *A* would certainly improve plant WUE by reducing water loss via transpiration in a non-carbon limited condition. Indeed, changes in *A*, $g_s$, and consequently WUE was observed in transgenic plants with altered guard cell sucrose metabolism (Antunes et al., 2012; Kelly et al., 2013; Lugassi et al., 2015; Daloso et al., 2016b; Antunes et al., 2017). That said, further characterization of transgenic plants containing altered guard cell sucrose metabolism will certainly improve our understanding on the role of sucrose in guard cell regulation and plant WUE.

**Metabolic flux distribution following $^{13}$C-sucrose supply**

Fructose and glucose, two of the three direct products of sucrose breakdown, were rapidly and clearly labelled, demonstrating that sucrose has been effectively degraded under our experimental conditions. This result is in accordance with previous feeding experiments suggestive of sucrose breakdown during dark-to-light transition (Daloso et al., 2015; Daloso et al., 2016b). Fructose was fully labelled whilst glucose was not, indicating that the degradation of sucrose is occurring by both sucrose synthase (SuSy) and invertase since an identical $^{13}$C-enrichment in the hexoses would be anticipated in case it was mediated only via invertase. This result strengthens the idea that both SuSy and invertase are important players in the control of sucrose metabolism in guard cells (Antunes et al., 2012; Ni, 2012; Daloso et al., 2016b), however, given that we do not have independent estimates of the rate of metabolism of glucose and fructose, we cannot quantitatively estimate the relative importance of either routes. That said, Glc-1P was also rapidly and clearly labelled (Fig. 4). Such a labelling kinetic for Glc-1P potentially confirms the occurrence of a considerable SuSy activity, given that UDP-glucose, a product of SuSy, is a substrate for Glc-1P synthesis via the activity of UDP-glucose pyrophosphorylase (UGPase) (Kleczkowski et al., 2004). However, it could alternatively be formed by phosphoglucomutase following phosphorylation of glucose produced after sucrose hydrolytic cleavage catalysed by invertase. Irrespective of its pedigree, the total $^{13}$C-enrichment in Glc-1P reaches around 25% at 10 min then decreases to 15% at 60 min. The analysis of relative isotopomer abundance corroborates with this observation, since the relative abundance of *m+3* decreases from 10 to 60 min, suggesting that Glc-1P is degraded over time (Fig. 4 and Supplemental Fig. S2). Glc-1P is a common substrate for glycolysis and starch metabolism, therefore its degradation could simultaneously activate these pathways (Zeeman et al., 2007; Stitt and Zeeman, 2012). However, it is important to mention that our experiment was carried out during the dark-to-light transition, simulating the circadian rhythm of the early morning stomatal aperture, a condition in which

starch is rapidly degraded and indeed not probably synthesized in guard cells (Tallman and Zeiger, 1988; Horrer et al., 2016; Santelia and Lawson, 2016; Antunes et al., 2017; Santelia and Lunn, 2017). Therefore, it strongly suggests that Glc-1P is used to sustain glycolysis rather than starch synthesis in the light. This idea is further supported by previous findings in which increased contents of fructose 2,6-biphosphate were observed in the dark-to-light transition (Hedrich et al., 1985) as well as by the fact that tricarboxylic acid (TCA) cycle-related metabolites, such as glutamate and glutamine, were highly labelled in our experiments (Fig. 6). In keeping with this, it has been demonstrated that a double mutant lacking the glycolytic enzyme phosphoglycerate mutase activity has lower blue light-induced stomatal aperture (Zhao and Assmann, 2011). Taken together, these data suggest that guard cell metabolism, unlike that of the mesophyll, prioritises activating glycolysis above starch or sucrose synthesis under light conditions (Fig. 7B). More importantly, our results provide evidence linking sucrose breakdown to glycolysis, TCA cycle and glutamine biosynthesis during dark-to-light transition via a mechanism which has not yet been described in stomatal physiology literature (discussed below).

In addition to the profound changes in photorespiratory and TCA cycle metabolites, significant differences in the $^{13}$C-enrichment or in the levels of glutamine or glutamate have also been observed during dark-to-light transition (Daloso et al., 2015; Daloso et al., 2016b). Here, substantial increases in the level of glutamine coupled with a clear $^{13}$C-enrichment in glutamate and glutamine were observed following $^{13}$C-sucrose breakdown, confirming that sucrose is used as a substrate for glycolysis and the TCA cycle. Interestingly, the total $^{13}$C-enrichment was higher in glutamine than glutamate and the relative abundance of the fully labelled *m+4* ion of glutamine increased over time, while the *m+4* ion from glutamate decreased, suggesting that glutamate is being catabolised to produce glutamine. Given that no $^{13}$C-enrichment in malate and fumarate was observed here (Supplemental Fig. S5), thus the only possibilities to explain the detection of full labelled glutamine are to assume that: (i) phospho*enol*pyruvate (PEP) is fully labelled by glycolysis, which produces full labelled pyruvate and acetyl CoA (AcCoA) and that two of these C are then incorporated into glutamate/glutamine (follow the black spheres from AcCoA in the schematic of Supplemental Fig S5); and (ii) the full labelled PEP is also converted to oxaloacetate (OAA). This reaction can produce three labelled C which are then incorporated into glutamine (follow the red spheres in the schematic of Supplemental Fig S5). These findings suggest that the TCA cycle is not working in the conventional cyclic manner under the conditions of the present study (Fig. 7B) and that the flux of C from sucrose breakdown differ from those observed after anaplerotic $CO_2$ fixation catalysed by phospho*enol*pyruvate carboxylase (PEPc) (Fig. 7A).

The non-cyclic mode of operation of the TCA cycle has been widely documented in different organs of the plant (Sweetlove et al., 2010), but our observations are pioneer in guard cells. However, further metabolic flux analyses are required to confirm the mode of operation of the TCA cycle in guard cells in the light.

It is important to highlight that increases in metabolic fluxes are not necessarily correlated with increases in the level of the metabolites (Williams et al., 2008). However, strong increases in the total $^{13}C$-enrichment and in the glutamine levels were observed here (Fig. 6A and Supplemental Fig. S4), strengthening the idea that the C from sucrose is used for glutamine biosynthesis during light and $K^+$-induced stomatal opening condition. The biological relevance of why the C from sucrose is used to produce glutamine under this condition remains to be elucidated. However, there is evidence showing that supplying sucrose exogenously increases the level of glutamine synthetase transcripts (Sahulka and Lisa, 1980), which may explain the increase in the level of glutamine observed here. It has also been shown that when glutamine is present in the medium cultured spinach cells decrease nitrate reductase (NR) activity (Shiraishi et al., 1992). Furthermore, it has been demonstrated that loss-of-function for both genes encoding NR (*NIA1* and *NIA2*) led to absence of ABA-inhibited $K^+$ inward current, ABA-enhanced slow anion currents and impaired key components of ABA signalling pathway in guard cells (Chen et al., 2016; Zhao et al., 2016). NR is a key enzyme for nitrogen metabolism regulating the level of N-compounds such as nitrate ($NO_3$) and nitric oxide (NO) (Chamizo-Ampudia et al., 2017). Transcriptomic analysis showed that the ABA signal is not transduced in guard cells of the double mutant *nia1nia2* (a mutant lacking NR activity) given up and down-regulation of negative and positive regulators of the ABA signalling network, respectively (Zhao et al., 2016). Thus, given that our feeding experiment was performed during light and $K^+$-induced stomatal opening condition, we propose that the C from sucrose to glutamine could be a mechanism to inhibit NR activity in order to: (i) maintain the levels of $NO_3^-$, a $K^+$ counter-ion (Guo et al., 2003); (ii) to inhibit the NO synthesis, a product of the NR activity and a well-known component of the ABA signalling network (Desikan et al., 2004; Wilson et al., 2008); and (iii) to repress the expression of ABA-responsive genes that positively regulate the ABA-induced stomatal closure (Chen et al., 2016; Zhao et al., 2016). However, considerable additional experimentation will be required in order to formally substantiate our hypothesis.

That said, collectively, our results provide evidence that the role of sucrose during light induced stomatal opening is not that of an osmolyte, as previously thought. This is supported by the fact that exogenous application of sucrose has no effect on light-induced stomatal opening and that the addition of sucrose at concentrations above of 10 mM even

induced stomatal closure. Instead of being an osmolyte, our data highlight that sucrose is used as a substrate for glycolysis, the TCA cycle and glutamine synthesis during the transition from dark to light. These findings thus suggest that different functionalities of sucrose are responsible for its role in stomatal opening and closure and suggest that further study of the reactions linking guard cell sucrose and glutamine should be a priority target for studies aiming at enhancing our understanding of guard cell metabolism.

## Material and methods

### Plant material and growth conditions

For all experiments described here we used wild type *Arabidopsis thaliana* Columbia-0 ecotype as plant material. Seeds were surface-sterilized and imbibed for 2 days at 4°C in the dark on 0.7% (w/v) agar plates containing half-strength Murashige and Skoog (MS) media (Sigma-Aldrich; pH 5.7). Seeds were subsequently germinated and grown at 22°C under short-day conditions (8 h light/16 h dark), 60% relative humidity with 150 µmol photons $m^{-2}$ $s^{-1}$. The $5^{th}$ or $6^{th}$ totally expanded leaves from 5-week-old plants were harvested and used for stomatal aperture assays. Whole rosettes grown in the same conditions were used for guard cell-enriched epidermal fragments isolation.

### Stomatal aperture assays

For sucrose-induced stomatal closure assays light-adapted leaves were floated on stomatal opening buffer containing 10 mM KCl, 50 µM $CaCl_2$ and 5 mM MES-Tris (pH 6.15) for 2 h under light (150 µmol $m^{-2}$ $s^{-1}$) in order to ensure fully open stomata. Then, opening buffer, mannitol (at a final concentration 100 mM) or sucrose at final concentrations of 0.1 mM, 1mM, 10 mM or 100 mM were added. After an additional 2 h of incubation the stomatal aperture was evaluated. For sucrose-induced stomatal opening assays dark-adapted leaves were floated on the opening buffer (in the presence or absence of KCl as indicated in the figure legends) or opening buffer containing sucrose to a final concentration of 0.1 mM, 1 mM, 10 mM or 100 mM and incubated under light (150 µmol $m^{-2}$ $s^{-1}$) for 2 h after which the stomatal aperture was evaluated. The leaves were gently dried and the adaxial epidermis was carefully fixed to autoclave tape. The abaxial surface of the leaves was, subsequently, peeled off following fixing and removal of an adhesive film (tesafilm® crystal clear, Tesa, Hamburg, Germany) and microscopic images were taken immediately (Azoulay-Shemer et al., 2015; Horrer et al., 2016). The stomatal aperture was also determined in dark-adapted leaves and used as a control. Four leaves from different plants were evaluated and the aperture of at least 20 stomata per leaf was measured resulting in a total of at least 80 stomata aperture

measurements per treatment. The images were taken with a digital camera (Axiocam MRc) attached to a microscope (Zeiss, model AX10, Jena, Germany). Subsequent measurements were derived from the images using the image processing package FIJI on the ImageJ software (Schindelin et al., 2012; Schindelin et al., 2015).

**Guard cell isolation for kinetic isotope labelling experiments**

A pool of guard cell-enriched epidermal fragments (hereafter simply referred as guard cells) was isolated following a protocol that was recently optimized for metabolite profiling analyses (Daloso et al., 2015). Briefly, guard cells were isolated in the pre-dawn by blending approximately 10 Arabidopsis rosettes per replicate in a Warring blender (Philips, RI 2044 B.V. International Philips, Amsterdam, The Netherlands), incorporating an internal filter to remove excess mesophyll cells, fibres and other cellular debris. All guard cell isolations were carried out in the dark in order to maintain closed stomata and simulate opening following the natural circadian rhythm.

**$^{13}$C-sucrose isotope kinetic labelling experiment**

The stomatal assays described above were essential in order to demonstrate that the effect of sucrose on stomatal opening/closure is concentration dependent. Having established this fact, we subsequently aimed to investigate the role of sucrose during light-induced stomatal opening. For this purpose, we decided to perform a $^{13}$C-sucrose isotope experiment by providing sucrose at a concentration of 0.1 mM. Guard cells were isolated, as described above, and subsequently transferred to the light and incubated in opening buffer solution (10 mM KCl, 50 μM $CaCl_2$ and 5 mM MES-Tris, pH 6.15) in the presence or absence of $^{13}$C-sucrose. Guard cell samples were rapidly harvested on a nylon membrane (220 μM) and snap-frozen in liquid nitrogen following 10, 30 and 60 min of light prior to storage at -80°C before subsequent metabolic analyses. A single sample per treatment was additionally taken in order to ascertain the stomatal aperture at each time point.

**GC-MS analysis**

The extraction of polar metabolites and their derivatisation was carried out exactly as described previously (Lisec et al., 2006). Briefly, approximately 30 mg of lyophilized guard cells were disrupted by shaking the cells in a tube together with metal balls. Extraction was subsequently performed in methanol, with shaking at 70 ºC for 1h, 60 μL of ribitol (0.2 mg $mL^{-1}$) was added as an internal standard. Following centrifugation, the supernatant was taken and the polar and apolar phases were separated by adding chloroform and water to the tube. A

new centrifugation was performed and 1 mL of the polar (upper) phase was taken and reduced to dryness for further derivatisation and analysed by gas chromatography coupled to time of flight mass spectrometry (GC-TOF-MS). For mass spectral analysis, the relative isotopomer abundance and the determination of the total $^{13}C$-enrichment was performed using Xcalibur® 2.1 software (Thermo Fisher Scientific, Waltham, MA, USA) and the CORRECTOR program (Huege et al., 2014) as described in previous guard cell isotope labelling studies (Daloso et al., 2015; Daloso et al., 2016b).

### Statistical analysis

Data were obtained from experiments using a completely randomized design. All data are expressed as the mean ± standard error (SE). Data were tested for significance ($P < 0.05$) differences using Student's *t* test. All statistical analyses were performed using the algorithm embedded in Microsoft Excel® (Microsoft, Seattle).

### Acknowledgements

The authors thank Prof. Dr. Thomas C.R. Williams and Prof. Dr. Werner C. Antunes for their helpful discussions concerning guard cell sucrose metabolism.

## LITERATURE CITED

**Amodeo G, Talbott LD, Zeiger E** (1996) Use of potassium and sucrose by onion guard cells during a daily cycle of osmoregulation. Plant Cell Physiol **37**: 575–579

**Antunes WC, de Menezes Daloso D, Pinheiro DP, Williams TCR, Loureiro ME** (2017) Guard cell-specific down-regulation of the sucrose transporter SUT1 leads to improved water use efficiency and reveals the interplay between carbohydrate metabolism and $K^+$ accumulation in the regulation of stomatal opening. Environ Exp Bot **135**: 73–85

**Antunes WC, Provart NJ, Williams TCR, Loureiro ME** (2012) Changes in stomatal function and water use efficiency in potato plants with altered sucrolytic activity. Plant, Cell Environ **35**: 747–759

**Chamizo-Ampudia A, Sanz-Luque E, Llamas A, Galvan A, Fernandez E** (2017) Nitrate reductase regulates plant nitric oxide homeostasis. Trends Plant Sci **22**: 163–174

**Chen C, Xiao YG, Li X, Ni M** (2012) Light-regulated stomatal aperture in Arabidopsis. Mol Plant **5**: 566–572

**Chen ZH, Wang Y, Wang JW, Babla M, Zhao C, Garcia-Mata C, Sani E, Differ C, Mak M, Hills A, et al** (2016) Nitrate reductase mutation alters potassium nutrition as well as nitric oxide-mediated control of guard cell ion channels in Arabidopsis. New Phytol **209**: 1456–1469

**Condon AG, Richards RA, Rebetzke GJ, Farquhar GD** (2004) Breeding for high water-use efficiency. J Exp Bot **55**: 2447–60

**Daloso DM, dos Anjos L, Fernie AR** (2016a) Roles of sucrose in guard cell regulation. New Phytol **211**: 809–818

**Daloso DM, Antunes WC, Pinheiro DP, Waquim JP, Araújo WL, Loureiro ME, Fernie AR, Williams TCR** (2015) Tobacco guard cells fix $CO_2$ by both Rubisco and PEPcase

while sucrose acts as a substrate during light-induced stomatal opening. Plant Cell Environ **38**: 2353–2371

**Daloso DM, Williams TCR, Antunes WC, Pinheiro DP, Müller C, Loureiro ME, Fernie AR** (2016b) Guard cell-specific upregulation of sucrose synthase 3 reveals that the role of sucrose in stomatal function is primarily energetic. New Phytol **209**: 1470–1483

**Desikan R, Cheung M, Bright J, Henson D, Hancock JT, Neill SJ** (2004) ABA , hydrogen peroxide and nitric oxide signalling in stomatal guard cells. **55**: 205–212

**Fettke J, Fernie AR** (2015) Intracellular and cell-to-apoplast compartmentation of carbohydrate metabolism. Trends Plant Sci **20**: 490–497

**Fischer RA** (1968) Stomatal opening: role of potassium uptake by guard cells. Science (80- ) **160**: 784–785

**Flexas J** (2016) Genetic improvement of leaf photosynthesis and intrinsic water use efficiency in C3 plants: why so much little success? Plant Sci **251:** 155-161

**Gago J, Daloso DM, Figueroa CM, Flexas J, Fernie AR, Nikoloski Z** (2016) Relationships of leaf net photosynthesis, stomatal conductance, and mesophyll conductance to primary plant metabolism: a multi-species meta-analysis approach. Plant Physiol **171**: 265-279

**Gago J, Douthe C, Florez-Sarasa I, Escalona JM, Galmes J, Fernie AR, Flexas J, Medrano H** (2014) Opportunities for improving leaf water use efficiency under climate change conditions. Plant Sci **226**: 108–119

**Gao X, Li C, Wei P, Zhang X, Chen J, Wang X** (2005) The dynamic changes of tonoplasts in guard cells are important for stomatal movement in *Vicia faba*. **139**: 1207–1216

**Guo F, Young J, Crawford NM** (2003) The nitrate transporter AtNRT1.1 (CHL1) functions in stomatal opening and contributes to drought susceptibility in Arabidopsis. **15**: 107–117

**Hedrich R** (2012) Ion channels in plants. Physiol Rev **92**: 1777–1811

**Hedrich R, Raschke K, Stitt M** (1985) A role for fructose 2,6-bisphosphate in regulating carbohydrate metabolism in guard cells. Plant Physiol **79**: 977–982

**Hetherington AM, Woodward FI** (2003) The role of stomata in sensing and driving environmental change. Nature **424**: 901–908

**Horrer D, Flütsch S, Pazmino D, Matthews JSA, Thalmann M, Nigro A, Leonhardt N, Lawson T, Santelia D** (2016) Blue light induces a distinct starch degradation pathway in guard cells for stomatal opening. Curr Biol **26**: 362–370

**Huege J, Goetze J, Dethloff F, Junker B, Kopka J** (2014) Quantification of stable isotope label in metabolites via mass Spectrometry. Methods Mol Biol **1056:** 213-223

**Imamura S** (1943) Untersuchungen uber den mechanismus der turgorschwandung der spaltoffnungesschliesszellen. Japanese J Bot **12**: 82–88

**Inoue S, Kinoshita T** (2017) Blue light regulation of stomatal opening and the plasma membrane $H^+$-ATPase. Plant Physiol doi: 10.1104/pp.17.00166

**Inoue S, Takemiya A, Shimazaki K** (2010) Phototropin signaling and stomatal opening as a model case. Curr Opin Plant Biol **13**: 587–593

**Jezek M, Blatt MR** (2017) The membrane transport system of the guard cell and its integration for stomatal dynamics. Plant Physiol doi: 10.1104/pp.16.01949

**Kang Y, Outlaw WH, Andersen PC, Fiore GB** (2007a) Guard-cell apoplastic sucrose concentration - A link between leaf photosynthesis and stomatal aperture size in the apoplastic phloem loader Vicia faba L. Plant Cell Environ **30**: 551–558

**Kang Y, Outlaw WH, Fiore GB, Riddle KA** (2007b) Guard cell apoplastic photosynthate accumulation corresponds to a phloem-loading mechanism. J Exp Bot **58**: 4061–4070

**Kelly G, Moshelion M, David-Schwartz R, Halperin O, Wallach R, Attia Z, Belausov E, Granot D** (2013) Hexokinase mediates stomatal closure. Plant J **75**: 977–988

**Kleczkowski L a, Geisler M, Ciereszko I, Johansson H** (2004) UDP-Glucose pyrophosphorylase. An old protein with new tricks. Plant Physiol **134**: 912–918

**Lawson T, Blatt MR** (2014) Stomatal size, speed, and responsiveness impact on

photosynthesis and water use efficiency. Plant Physiol **164**: 1556–1570

**Li Y, Xu S, Gao J, Pan S, Wang G** (2015) Glucose- and mannose-induced stomatal closure is mediated by ROS production, $Ca^{2+}$ and water channel in *Vicia faba*. Physiol Plant **156:** 252–261

**Lisec J, Schauer N, Kopka J, Willmitzer L, Fernie AR** (2006) Gas chromatography mass spectrometry–based metabolite profiling in plants. Nat Protoc **1**: 387–396

**Lloyd F** (1908) The physiology of stomata, 82nd ed. Carnegie Inst Washington Year Book, Washington

**Lu P, Outlaw Jr WH, Smith BG, Freed G a.** (1997) A new mechanism for the regulation of stomatal aperture size in intact leaves (accumulation of mesophyll-derived sucrose in the guard-cell wall of *Vicia faba*. Plant Physiol **114**: 109–118

**Lu P, Zhang SQ, Outlaw WH, Riddle KA** (1995) Sucrose: a solute that accumulates in the guard-cell apoplast and guard-cell symplast of open stomata. FEBS Lett **362**: 180–184

**Lugassi N, Kelly G, Fidel L, Yaniv Y, Attia Z, Levi A, Alchanatis V, Moshelion M, Raveh E, Carmi N, et al** (2015) Expression of Arabidopsis hexokinase in citrus guard cells controls stomatal aperture and reduces transpiration. Front Plant Sci **6**: 1114

**Ni DA** (2012) Role of vacuolar invertase in regulating Arabidopsis stomatal opening. Acta Physiol Plant **34**: 2449–2452

**Nunes-Nesi A, Nascimento V de L, de Oliveira Silva FM, Zsogon A, Araujo WL, Sulpice R** (2016) Natural genetic variation for morphological and molecular determinants of plant growth and yield. J Exp Bot **67:** 2989-3001

**Outlaw WH, De Vlieghere-He X** (2001) Transpiration rate. An important factor controlling the sucrose content of the guard cell apoplast of broad bean. Plant Physiol **126**: 1716–1724

**Outlaw WH Jr.** (1995) Sucrose and stomata: a full circle. in Carbon Partitioning and Sucrose-Sink Interactions in Plants. eds Madore MA, Lucus WJ (American Society of Plant Physiologists, Rockville, MD), pp 56–67.

**Poffenroth M, Green DB, Tallman G** (1992) Sugar concentrations in guard cells of *Vicia faba* illuminated with red or blue light : Analysis by high performance liquid chromatography. Plant Physiol **98**: 1460–1471

**Sahulka J, Lisa L** (1980) Effect of some disaccharides , hexoses and pentoses on nitrate reductase , glutamine synthetase and glutamate dehydrogenase in excised pea roots. Physiol Plant **50**: 32–36

**Santelia D, Lawson T** (2016) Rethinking guard cell metabolism. Plant Physiol **172:** 1371-1392

**Santelia D, Lunn JE** (2017) Transitory starch metabolism in guard cells: unique features for a unique function. Plant Physiol Press. doi: 10.1104/pp.17.00211

**Schindelin J, Arganda-Carreras I, Frise E, Kaynig V, Longair M, Pietzsch T, Preibisch S, Rueden C, Saalfeld S, Schmid B, et al** (2012) Fiji: an open-source platform for biological-image analysis. Nat Methods **9**: 676–682

**Schindelin J, Rueden CT, Hiner MC, Eliceiri KW** (2015) The ImageJ ecosystem: An open platform for biomedical image analysis. Mol Reprod Dev **82**: 518–529

**Shiraishi N, Sato T, Ogura N, Nakagawa H** (1992) Control by glutamine of the synthesis of nitrate reductase in cultured spinach cells. Plant Cell Physiol **33**: 727–731

**Stitt M, Zeeman SC** (2012) Starch turnover: Pathways, regulation and role in growth. Curr Opin Plant Biol **15**: 282–292

**Sweetlove LJ, Beard KFM, Nunes-Nesi A, Fernie AR, Ratcliffe RG** (2010) Not just a circle: Flux modes in the plant TCA cycle. Trends Plant Sci **15**: 462–470

**Talbott L, Zeiger E** (1998) The role of sucrose in guard cell osmoregulation. J Exp Bot **49**: 329–337

**Talbott LD, Zeiger E** (1993) Sugar and organic acid accumulation in guard cells of *Vicia faba* in response to red and blue light. Plant Physiol **102**: 1163–1169

**Talbott LD, Zeiger E** (1996) Central roles for potassium and sucrose in guard-cell osmoregulation. Plant Physiol **111**: 1051–1057

**Tallman G, Zeiger E** (1988) Light quality and osmoregulation in vicia guard cells: evidence for involvement of three metabolic pathways. Plant Physiol **88**: 887–895

**Williams TCR, Miguet L, Masakapalli SK, Kruger NJ, Sweetlove LJ, Ratcliffe RG** (2008) Metabolic network fluxes in heterotrophic Arabidopsis cells: stability of the flux distribution under different oxygenation conditions. Plant Physiol **148**: 704–718

**Wilson IAND, Neill SJ, Hancock JT** (2008) Nitric oxide synthesis and signalling in plants. 622–631

**Zeeman SC, Smith SM, Smith AM** (2007) The diurnal metabolism of leaf starch. Biochem J **401**: 13–28

**Zeiger E** (1983) The biology of stomatal guard cells. Annu Rev Plant Physiol **34**: 441–475

**Zeiger E, Talbott LD, Frechilla S, Srivastava A, Zhu J** (2002) The guard cell chloroplast: A perspective for the twenty-first century. New Phytol **153**: 415–424

**Zhao C, Cai S, Wang Y, Chen Z** (2016) Loss of nitrate reductases NIA1 and NIA2 impairs stomatal closure by altering genes of core ABA signaling components in Arabidopsis. Plant Signal Behav **11**: e1183088

**Zhao Z, Assmann SM** (2011) The glycolytic enzyme, phosphoglycerate mutase, has critical roles in stomatal movement, vegetative growth, and pollen production in Arabidopsis thaliana. J Exp Bot **62**: 5179–5189

**SUPPLEMENTAL DATA**

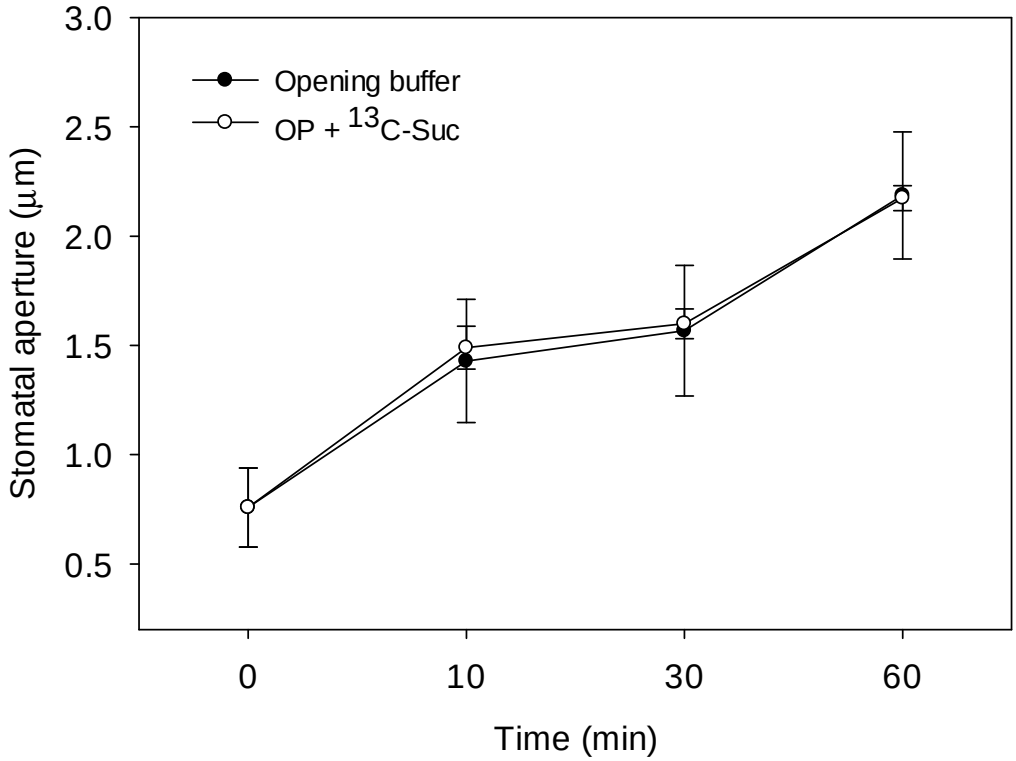


**Supplemental Fig. S1.** Stomatal aperture of Col-0 guard cells during dark-to-light transition. The stomatal aperture was measured as the width of the stomatal pore. Values are presented mean ± SE ($n$ = 20).

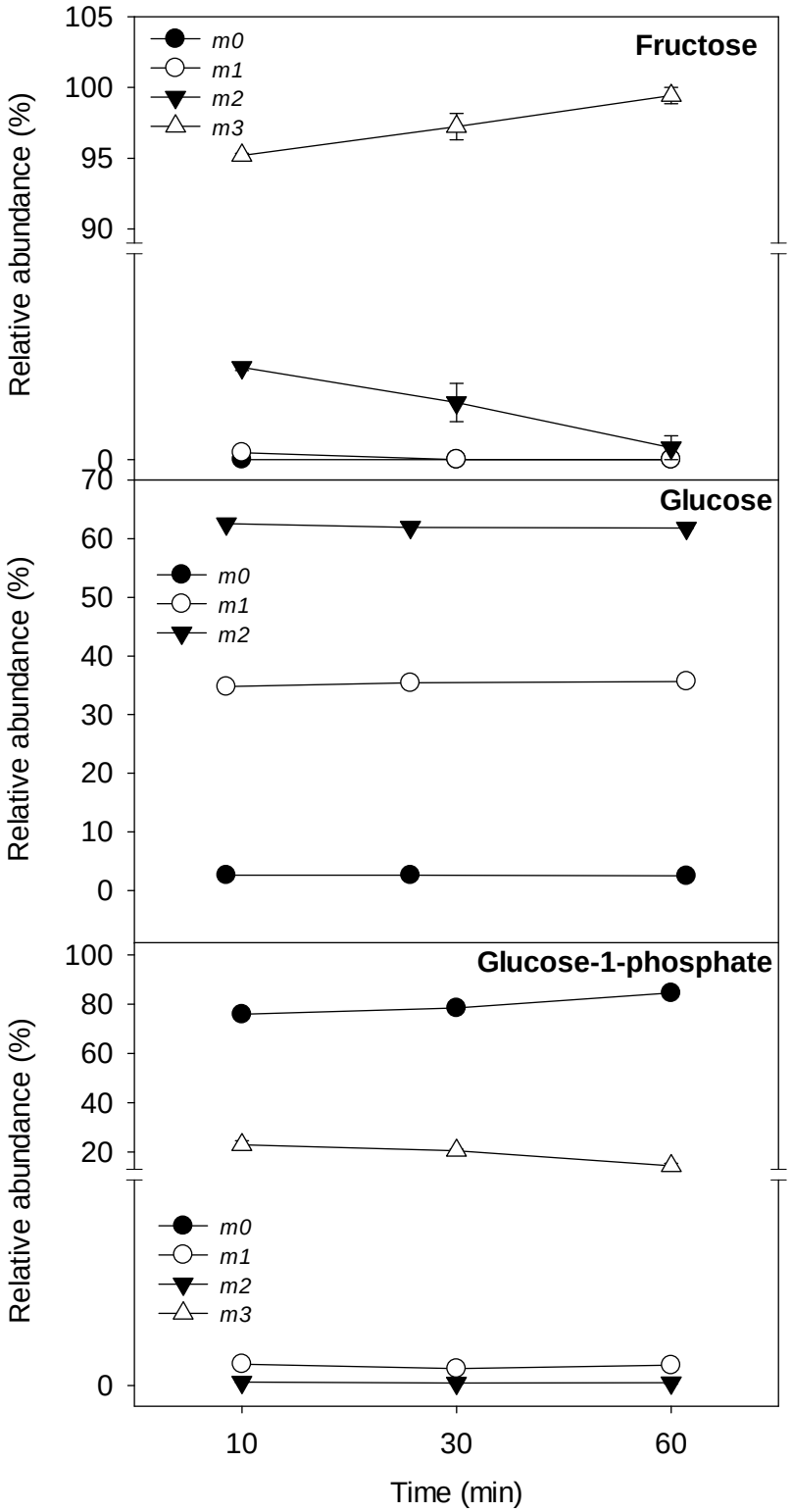


**Supplemental Fig. S2.** Relative abundance of mass isotopomers of glucose, fructose and glucose-1-phosphate (G1P) following guard cells incubation. Dark-adapted guard cells were harvested at pre-drawn and fed with [$U^{13}C$]-Sucrose in the opening buffer under light condition for 2h. At 10 min, 30 min, and 60 min of incubation the guard cells were sampled and the enrichment into the metabolites were determined. Values are presented as mean ± SE ($n = 4$).

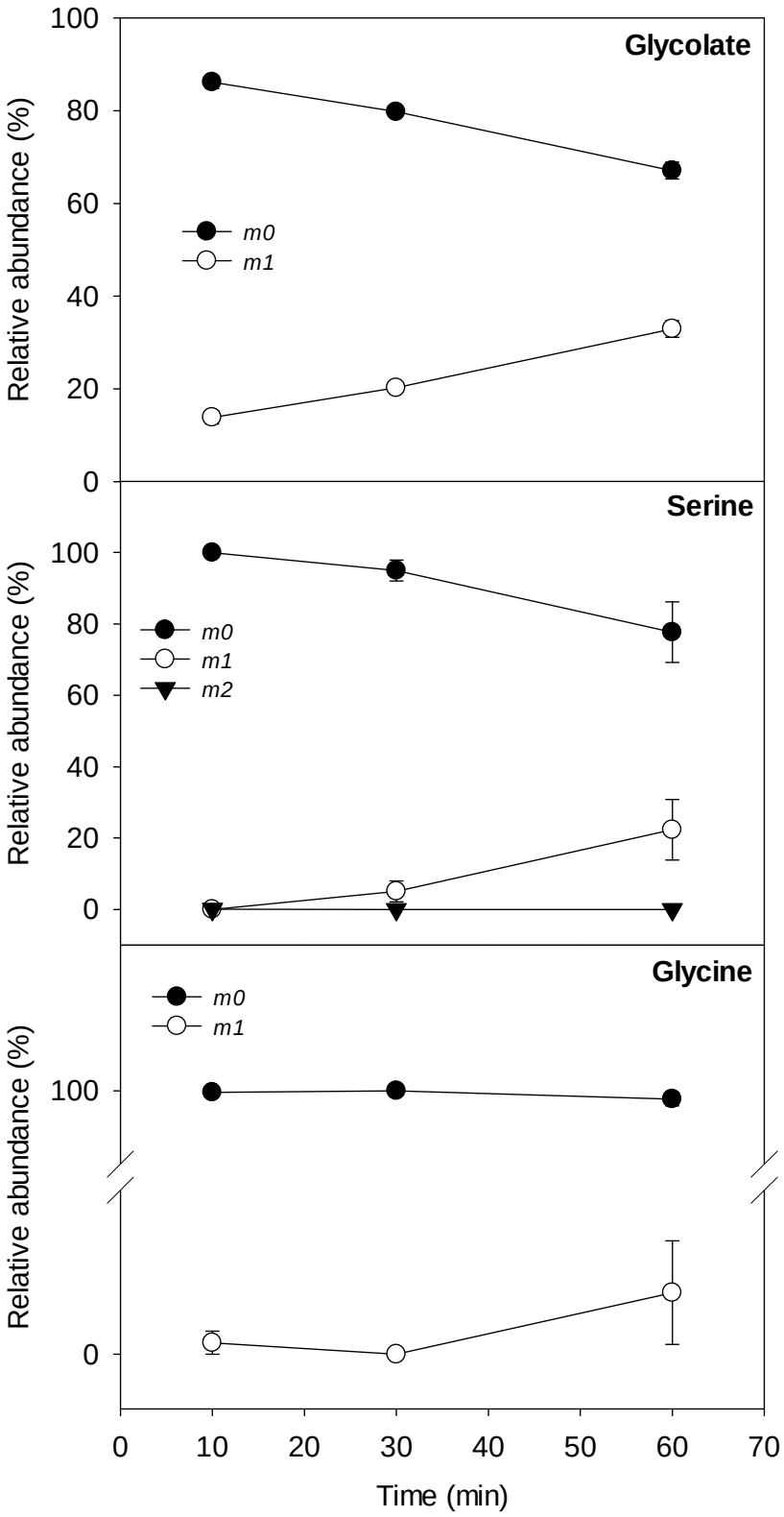


**Supplemental Fig. S3.** Relative abundance of mass isotopomers of photorespiratory related metabolites following guard cells incubation. Dark-adapted guard cells were harvested at pre-drawn and fed with [U$^{13}$C]-Sucrose in the opening buffer under light condition for 2h. At 10 min, 30 min, and 60 min of incubation the guard cells were sampled and the enrichment into the metabolites were determined. Values are presented as mean ± SE ($n$ = 4).

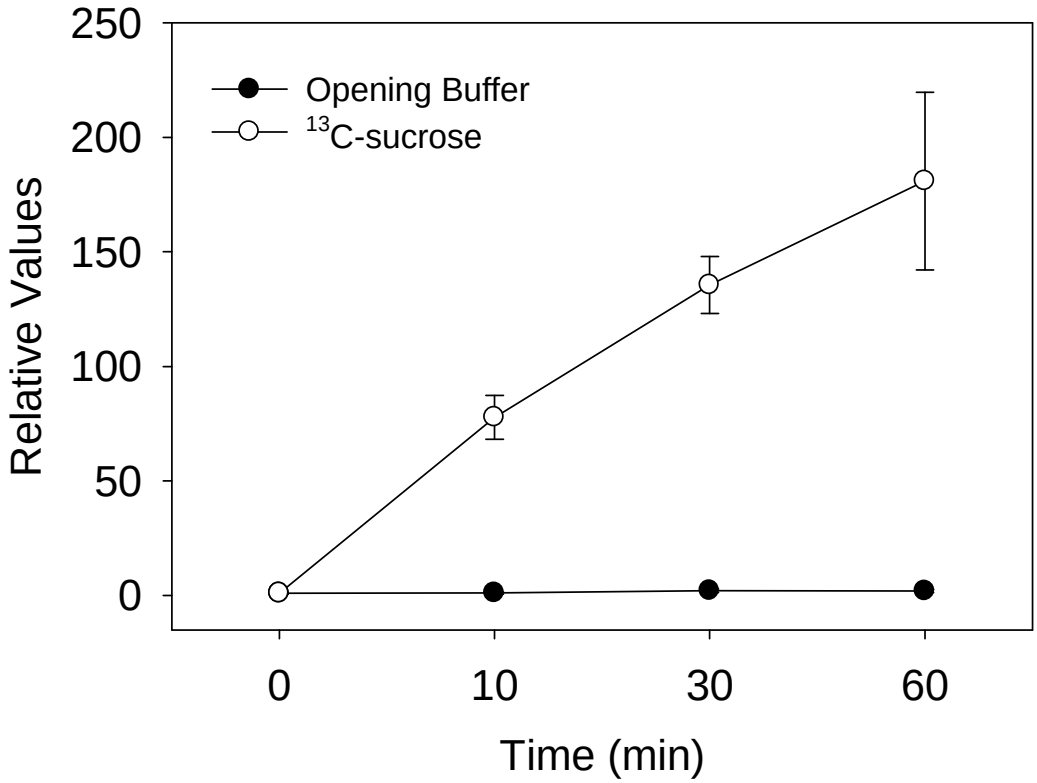


**Supplemental Fig. S4.** Relative glutamine content following guard cells incubation. Data are normalized with respect to the mean relative amount calculated for time point 0 min (dark-adapted guard cells). To allow statistical assessment, individual replicate from all the treatments and time points were normalized in the same way. Data are presented as means ± SD (n=4).

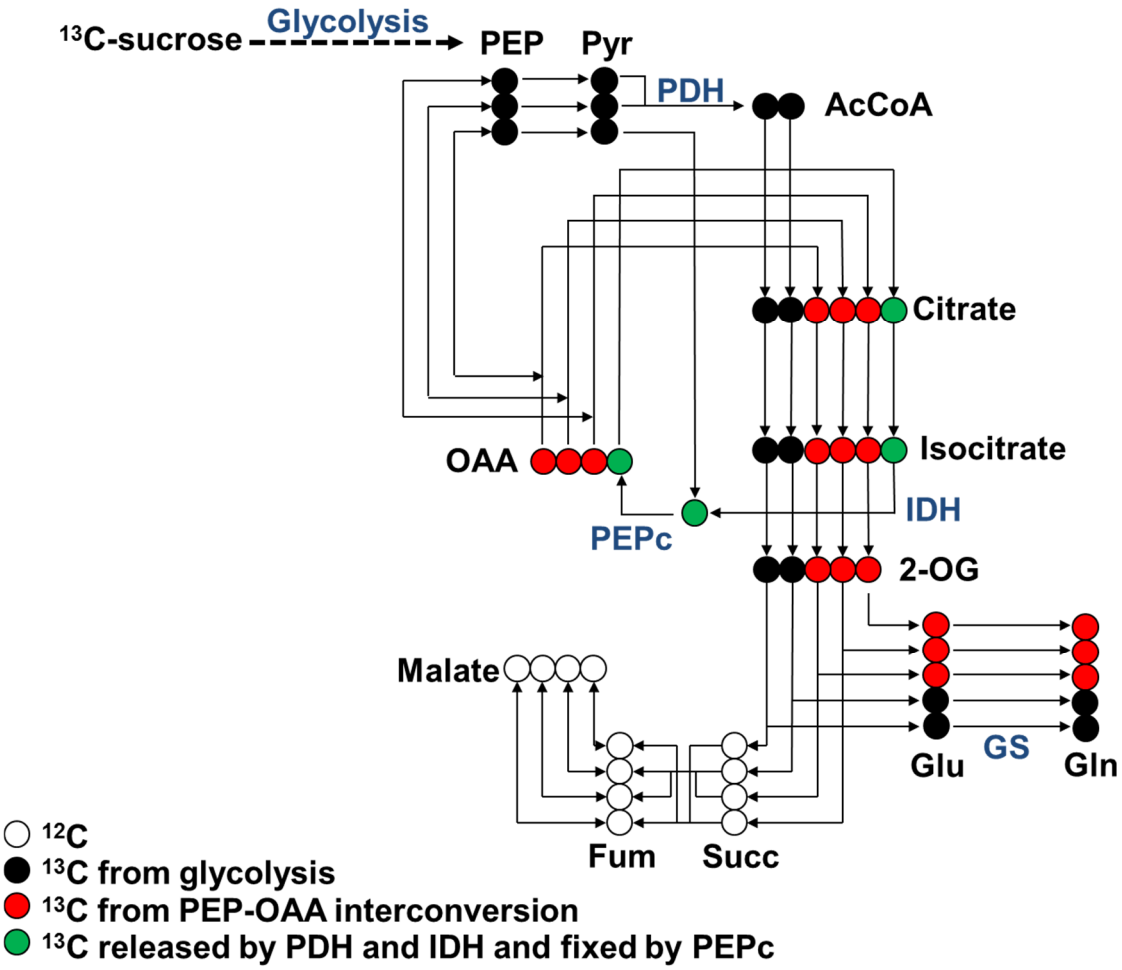


**Supplemental Fig. S5.** Schematic representation of stable isotope redistribution in guard cells during $^{13}$C-sucrose labelling kinetic assay. To detect full labelled glutamine, it is assumed, firstly, that PEP is fully labelled by glycolysis, producing full labelled pyruvate and AcCoa. This assumption is supported by the experimental data given that hexoses and Glc-1P were clearly labelled, indicating that the C from sucrose are used to sustain glycolysis and thus can produce full labelled PEP. Following this idea, two of these carbons can be incorporated into Glu and Gln (follow black spheres from AcCoA). Secondly, the full labelled PEP is also converted to OAA. This reaction can produce three labelled carbons (see red spheres) which are then incorporated into Gln. It is noteworthy that the PEPc fixation of the $CO_2$ released by PDH does not contribute to the $^{13}$C-enrichment observed in Gln, once this C is lost in the reaction catalysed by IDH. Enzymes are shown in blue. Abbreviations: 2-OG, 2-oxoglutarate; AcCoa, acetyl CoA; Fum, fumarate; Gln, glutamine; Glu, glutamate; GS, glutamine synthetase; IDH, isocitrate dehydrogenase; PEP, phospho*enol*pyruvate; PEPc, phospho*enol*pyruvate carboxylase; Pyr, pyruvate; PDH, pyruvate dehydrogenase; Succ, succinate.

# Chapter 6

# Concluding remarks

This thesis was largely focused on, first, obtaining a comprehensive picture of how and to which extent impairments in the organic acid accumulation might affect the stomatal movements and, second, providing experimental evidence supporting the role of sucrose as a substrate required during the light-induced stomatal opening. In attempt to reach these aims complementary experimental approaches were taken and the results obtained were divided in three independent research articles.

In chapter 3 it was clearly demonstrated that inefficient regulation of the stomatal closure via the repression of *At*QUAC1 culminates in higher growth and photosynthetic rates through increased $g_s$ and $g_m$, followed by changes in organic acids and sugars accumulation in the leaves. In the model we have proposed, the functional lack of AtQUAC1 lead to a misbalance in the uptake and release of malate in guard cells, which in turn keeps the stomata more open longer. Consequently, increases in $g_s$ and $g_m$ help to maintain higher photosynthesis. Moreover, carbon balance and metabolism are changed through increased levels of sugars, starch, organic acids, and dark respiration. Therefore, although the exact mechanism by which changes in organic acid transport induced simultaneous changes in both $g_s$ and $g_m$ remains as yet unclear, it seems reasonable to assume that the link is likely related to the suggested, but not yet completely known, metabolic signalling events connecting mesophyll photosynthetic activity and stomatal behaviour.

We went forward to better understand the link between organic acid accumulation and stomatal behaviour. Thus, in chapter 4, we took knockout lines for *AttDT* (encoding an organic acid vacuolar transporter) as a model because they were previously characterized by impaired malate and fumarate accumulation in the Arabidopsis vacuoles (Emmerlich et al., 2003; Hurth et al., 2005). In this work, we showed that accumulation of those organic acids is impaired throughout the entire diel cycle. Curiously, the citrate, fumarate, and malate concentration did not change in the apoplastic space. When evaluating the stomatal behaviour to different stimuli in *attdt* plants we did not observed any impact on the stomatal responses to ABA, organic acids, dark, light or high $CO_2$. Interestingly, the functional lack of *At*tDT strongly affected the cellular homeostasis in mesophyll cells by changes in the mitochondrial metabolism. For instance, levels of TCA cycle intermediates were highly altered in both leaves and guard cells and increases in both light and dark respiration were observed. Notably, these changes were not followed by any impact on photosynthetic behaviour in *attdt* plants. Thus, when the relative concentrations of the apoplastic and subcellular malate pools are considered, it is reasonable to suggest that the impact on mitochondrial metabolism is most likely due to increases in the carboxylates consumption within the cell, which seems to be a regulatory mechanism, since they cannot be properly stored into the vacuole.

Altogether the results from these complementary studies described above are highly exciting in a way that they highlight the importance of considering the different organic acid pools when evaluating stomatal responses. Moreover, it also increases the discussion on the fact that although a positive correlation between stomatal conductance, photosynthesis, and malate accumulation has been observed in a range of species (Gago et al., 2016), it is clear that there is no strict direct correlation among these traits, suggesting that their relationship is most likely modified in response to different internal or environmental conditions faced by plants during their life cycle.

In the third experimental approach described in this thesis, we took advantages of a protocol which enables the rapid isolation of dark-adapted guard cell-enriched epidermal fragments in sufficient quantities to allow us to perform both stomatal aperture assays and metabolomics analyses in an attempt to clarify the effect of exogenous sucrose application on the stomatal aperture. Further, we investigated the metabolic flux distribution by following the metabolic fate of $^{13}$C-sucrose during light-induced stomatal opening. Our results, detailed in chapter 5, not only demonstrated that sucrose induces stomatal closure in a dose-dependent manner, but also indicates that sucrose breakdown occurs during light-induced stomatal opening. Surprisingly, we also provide compelling evidence that sucrose breakdown induces glutamine biosynthesis during light-induced stomatal opening. These findings suggest that different functionalities of sucrose are responsible for its role during stomatal opening and closure and that the reactions linking guard cell sucrose and glutamine should be a priority target for future studies aiming at enhancing our understanding of guard cell metabolism, in general.

In this context, a growing body of evidence currently available have demonstrated a connection between ion channels activity, malate, sugars, and photosynthesis (Lawson et al., 2014; Gago et al., 2016), suggesting that genetic manipulation of these players should be further addressed in order to better understand the relationship between mesophyll and guard cells and in the end to obtain improvements in WUE. Importantly, it has been also suggested that guard cell metabolism is a key target and that it should be genetically engineered in order to understand not only the metabolism *per se* but also the interactions between guard cell metabolism and physiology with the surrounding cells (Lawson and Blatt, 2014). In line with that, the usage of specific guard cell promoters to manipulate guard cell metabolism or others stomatal traits presents itself as a powerful tool to dissect the guard cell function and in the end to improve WUE and yield (Lawson et al., 2014; Santelia and Lawson, 2016).

That being said it is clear that understanding stomatal behaviour and its regulatory network represents an important step towards the increase in WUE in land plants. It has been

clearly demonstrated that mesophyll and guard cell exhibit great differences in their gene expression, protein, and metabolite profiles (reviewed by Medeiros et al. (2015)). Beyond these differences, there are many controversies regarding the extent by which guard cells are influenced by the surrounding mesophyll cells and further studies are clearly required to better understand the connections between both cell types. The establishment of protocols to simultaneously and quickly isolate both mesophyll and guard cells from leaves without any previous isolation or microdissection procedures are urgently required. These protocols coupled with omics technologies would open new avenues to fully understand guard cells regulation.

During the recent years, we have witnessed an accumulation of experimental evidence concerning different aspects of stomatal behaviour. This is largely due to elegant studies of guard cells molecular physiology based on application of high-throughput technologies providing considerable amount of data regarding the guard cell transcriptome, proteome, and metabolome. Therefore, as discussed in Chapter 2, it seems reasonable to suggest that systems biology approach offers a comprehensive way to aid the elucidation of mechanisms governing stomatal function and the molecular hierarchies underpinning the stomata control, although the great challenge for the field is still obtaining a fuller comprehension about the stomatal movement regulation and its dynamic facing complex changing environments. Therefore, given the complexity of the networks governing stomatal movements and its interactions under variable internal and external conditions, a system approach, which simultaneously uses different high-throughput technologies to gather data and then integrates them within large-scale models of regulation, signalling, and metabolism can be helpful to better predict phenotypes under field conditions.

## LITERATURE CITED


**Emmerlich V, Linka N, Reinhold T, Hurth MA, Traub M, Martinoia E, Neuhaus HE** (2003) The plant homolog to the human sodium/dicarboxylic cotransporter is the vacuolar malate carrier. Proc Natl Acad Sci USA **100:** 11122-11126

**Gago J, Daloso DM, Figueroa CM, Flexas J, Fernie AR, Nikoloski Z** (2016) Relationships of leaf net photosynthesis, stomatal conductance, and mesophyll conductance to primary metabolism: a multispecies meta-analysis approach. Plant Physiol **171:** 265-279

**Hurth MA, Suh SJ, Kretzschmar T, Geis T, Bregante M, Gambale F, Martinoia E, Neuhaus HE** (2005) Impaired pH homeostasis in Arabidopsis lacking the vacuolar dicarboxylate transporter and analysis of carboxylic acid transport across the tonoplast. Plant Physiol **137:** 901-910

**Lawson T, Blatt MR** (2014) Stomatal size, speed, and responsiveness impact on photosynthesis and water use efficiency. Plant Physiol **164:** 1556-1570

**Lawson T, Simkin AJ, Kelly G, Granot D** (2014) Mesophyll photosynthesis and guard cell metabolism impacts on stomatal behaviour. New Phytol **203:** 1064-1081

**Medeiros DB, Daloso DM, Fernie AR, Nikoloski Z, Araújo WL** (2015) Utilizing systems biology to unravel stomatal function and the hierarchies underpinning its control. Plant Cell Environ **38:** 1457-1470

**Santelia D, Lawson T** (2016) Rethinking guard cell metabolism. Plant Physiol **172:** 1371-1392